Universidad de Oviedo

Doctoral Thesis

2-D STRANGE ATTRACTORS

IN UNFOLDINGS OF TANGENCIES OF 3-D DIFFEOMORPHISMS

Author:
Alejandro Marqués Lobeiras

Director:
José Ángel Rodríguez Méndez

PhD Programme in Mathematics and Statistics

Tesis doctoral
Programa oficial de doctorado en Matemáticas y Estadística
Universidad de Oviedo

Título: *Atractores extraños bidimensionales en despliegues de tangencias de difeomorfismos en dimensión tres*
Autor: Alejandro Marqués Lobeiras
Director: José Ángel Rodríguez Méndez
Año: 2024

Universidad de Oviedo

RESUMEN DEL CONTENIDO DE TESIS DOCTORAL

1.- Título de la Tesis	
Español: Atractores extraños bidimensionales en despliegues de tangencias de difeomorfismos en dimensión tres	Inglés: 2-D Strange Attractors in Unfoldings of Tangencies of 3-D Diffeomorphisms

2.- Autor	
Nombre: **Alejandro Marqués Lobeiras**	
Programa de Doctorado: Matemáticas y Estadística	
Órgano responsable: Centro Internacional de Posgrado	

RESUMEN (en español)

El principal objetivo de esta tesis es el estudio de la persistencia de atractores extraños bidimensionales en despliegues genéricos de tangencias homoclínicas de difeomorfismos tridimensionales. Para ello, analizamos la dinámica de la familia cuadrática bidimensional que se obtiene como la familia límite de las aplicaciones de retorno definidas en un entorno de una tangencia homoclínica generalizada desplegada genéricamente por familias biparamétricas de difeomorfismos tridimensionales que tienen un punto de silla disipativo con índice de estabilidad igual a uno. El principal interés de la dinámica de esta familia radica en la supuesta existencia de atractores extraños bidimensionales, tal y como fue observado numéricamente por Pumariño y Tatjer en 2007. Puesto que esta observación solo es posible si dichos atractores sobreviven para un conjunto de parámetros con medida de Lebesgue positiva, al menos se puede proclamar numéricamente que son persistentes.

Desde un punto de vista analítico, la prueba la persistencia de atractores extraños bidimensionales para la familia cuadrática bidimensional es de momento una tarea muy difícil. Al igual que en el caso unidimensional, la fuerte contracción que la órbita experimenta cerca de la recta crítica implica una adecuada exclusión de parámetros de forma que el resto tenga medida de Lebesgue positiva. Como una aproximación al problema dentro del marco de las aplicaciones lineales a trozos, en esta memoria iniciamos el estudio de la dinámica de una familia biparamétrica de *Expanding Baker Maps* que generaliza la familia uniparamétrica de *tiendas* bidimensionales introducida por Pumariño, Rodríguez, Tatjer y Vigil en 2014 y cuya dinámica es una buena aproximación de la dinámica de la familia cuadrática bidimensional a lo largo de una cierta curva de parámetros.

La dinámica de cada una de estas *Expanding Baker Maps* consiste en un pliegue, una rotación alrededor del origen y una expansión. Se prueba que posee un polígono compacto estrictamente invariante que contiene un atractor extraño bidimensional para parámetros de expansividad suficientemente pequeños. Estos atractores reproducen los mismos tipos topológicos que los observados numéricamente para la familia cuadrática bidimensional: atractores extraños convexos; atractores extraños conexos, pero no simplemente conexos; y atractores extraños no conexos, formados por múltiples piezas conexas. La ruptura de los atractores para dar lugar a atractores no conexos con un número creciente de piezas se prueba mediante un proceso de renormalización que permite también comprender cómo el número de atractores se puede duplicar (incluso indefinidamente) en algunos casos.

Muchas de las ideas que se desarrollan en el estudio de la familia biparamétrica de *Expanding Baker Maps* son de gran ayuda para entender dinámica de la familia cuadrática bidimensional y permiten, por ejemplo, construir recintos compactos invariantes donde tratar de probar analíticamente la persistencia de los posibles atractores extraños bidimensionales. Sin embargo, a pesar de las analogías entre los atractores extraños bidimensionales de ambas familias, la familia cuadrática bidimensional presenta dinámicas propias que no se observan para el caso de las *Expanding Baker Maps*. Entre estas diferencias cabe destacar la presencia de singularidades no hiperbólicas y las subsecuentes bifurcaciones locales en el caso de la familia cuadrática bidimensional. Así, además de atractores extraños bidimensionales, esta

familia presenta también órbitas periódicas atrayentes, curvas cerradas invariantes atrayentes y atractores extraños unidimensionales. En esta memoria se explica cómo estos últimos surgen al colisionar con los tres puntos de una órbita periódica de tipo silla las curvas cerradas que emergen de otra órbita periódica de periodo tres mediante una bifurcación de Hopf-Neimark-Sacker. Este hecho permite comprender fenómenos de competencia entre atractores que no habían sido señalados numéricamente antes.

RESUMEN (en Inglés)

The main objective of this thesis is the study of the persistence of 2-D strange attractors in generic unfoldings of homoclinic tangencies of 3-D diffeomorphisms. To that end, we analize the dynamics of the 2-D quadratic family obtained as the limit family of the return maps defined in a neighborhood of a generalized homoclinic tangency generically unfolded by two-parameter families of 3-D diffeomorphisms having a dissipative saddle fixed point with stability index equal to one. The main interest in the dynamics of this family lies in the presumed existence of 2-D strange attractors, as numerically observed by Pumariño and Tatjer in 2007. Since this observation is only possible if such attractors survive for parameter regions with positive Lebesgue measure, at least it can be numerically claimed that they are persistent.

From an analytical point of view, the proof of the persistence of 2-D strange attractors for the 2-D quadratic family is currently a very difficult task. As in the 1-D case, the strong contraction that the orbit undergoes near the critical line requires a suitable exclusion of parameters in such a way that the remaining has positive Lebesgue measure. As an approach to this problem in the piecewise linear setting, in this memoir we begin the study of a two-parameter family of Expanding Baker Maps that generalize the one-parameter family of 2-D tent maps introduced by Pumariño, Rodríguez, Tatjer and Vigil in 2014 whose dynamics is a good approximation of the dynamics of the 2-D quadratic family along a certain parameter curve.

The dynamics of each one of these Expanding Baker Maps consists of a fold, a rotation around the origin, and an expansion. We prove that they display a strictly invariant compact and convex polygon that contains a 2-D strange attractor for sufficiently small expansion rates. These strange attractors reproduce the same topological types as those numerically observed for the 2-D quadratic family: convex strange attractors; non-simply connected strange attractors; and disconnected strange attractors formed by multiples pieces. The splitting of these attractors giving rise to other ones formed by an increasing number of pieces is proved by a renormalization process that also permits to understand the (even infinite) doubling of attractors in some cases.

Many of the ideas carried out in the study of the two-parameter family of 2-D tent maps are of great help to understand the dynamics of the 2-D quadratic family and permit, for instance, to construct invariant compact sets where to prove the persistence of 2-D strange attractors. However, despite the similarities between the strange attractors of both families, the 2-D quadratic family exhibits proper dynamics not observed for the Expanding Baker Maps. Among these differences, it is worth mentioning the presence of nonhyperbolic singularities and the subsequent local bifurcations in the case of the former. Thus, besides 2-D strange attractors, the 2-D quadratic family displays attracting periodic orbits, attracting invariant closed curves, and 1-D strange attractors. We explain how these last ones emerge by the collision between the three points of a saddle periodic orbit and the closed curves coming from the other 3-periodic orbit by a Hopf—Neimark—Sacker bifurcation. This fact permits to understand competitions of attractors that had not been numerically checked before.

SR. PRESIDENTE DE LA COMISIÓN ACADÉMICA DEL PROGRAMA DE DOCTORADO EN MATEMÁTICAS Y ESTADÍSTICA

Contents

Agradecimientos

Esta tesis ha sido financiada parcialmente por el *Programa de ayudas Severo Ochoa para la formación en investigación y docencia del Principado de Asturias* (BP20-063) de la Consejería de Ciencia, Innovación y Universidad del Gobierno del Principado de Asturias y por el proyecto de I+D+i *Génesis de complejidad: dinámica discreta y continua* (MCI-21-PID2020-113052GB-I00) avalado por el Ministerio de Ciencia e Innovación del Gobierno de España.

A lo largo de estos años, son muchas las personas que han formado parte de mi vida y que, directa o indirectamente, han influido en el resultado de esta tesis. Aunque no voy a nombrarlas a todas, me gustaría mostrar mi agradecimiento por las que considero las más importantes.

A mi director, José Ángel Rodríguez. Nada de esto habría sido posible sin él. Solo tengo palabras de afecto y admiración.

A Enrique Vigil por estar ahí desde el principio de mi etapa doctoral. Por darme consejos, por encargarse de las publicaciones, por ayudarme con las figuras, la redacción de los *paper*, los programas...

A Antonio Pumariño por todo lo que he aprendido de él fruto de nuestras colaboraciones.

A Santiago Ibáñez por ayudarme con toda la burocracia relacionada con el proyecto y el grupo.

A José F. Alves por brindarme la oportunidad de hacer una estancia en Oporto y colaborar con él.

Por último, a mi madre, a quien le dedico este trabajo.

Introducción

En palabras del matemático René Thom: *Toute science est avant tout l'étude d'une phénomenologie*[1]. En último término, la ciencia tiene como objetivo la predicción o el control del comportamiento de los procesos que nos rodean. Los modelos matemáticos para el estudio de la evolución de los procesos son los *sistemas dinámicos*: iteración de aplicaciones o difeomorfismos, flujos asociados a campos de vectores o ecuaciones definidas en espacios de funciones (ecuaciones en derivadas parciales, por ejemplo). Durante la lectura de esta memoria será suficiente restringirse a sistemas de baja dimensión: campos, aplicaciones o difeomorfismos definidos en dimensión menor o igual que cuatro. Incluso en este contexto, los resultados obtenidos durante el último siglo han producido una revolución copernicana en el campo de los sistemas dinámicos.

Antecedentes históricos

Para empezar, consideremos, sin mayor complicación, un escenario sencillo en dimensión dos: una familia de difeomorfismos f_μ suficientemente regulares definidos sobre una superficie $\mathcal{M}$, todos ellos con un punto fijo hiperbólico P_μ de tipo silla con valores propios $|\lambda_{\mathrm{s}}^\mu| < 1 < |\lambda_{\mathrm{u}}^\mu|$. En cada punto P_μ se intersecan las dos variedades invariantes

$$W^{\mathrm{s}}(P_\mu) = \{Q \in \mathcal{M} : f_\mu^n(Q) \to P_\mu \text{ cuando } n \to \infty\}$$
$$W^{\mathrm{u}}(P_\mu) = \{Q \in \mathcal{M} : f_\mu^{-n}(Q) \to P_\mu \text{ cuando } n \to \infty\}$$

denominadas la *variedad estable* e *inestable* de P_μ, respectivamente. Estas variedades son tangentes en P_μ a los espacios propios generados por λ_{s}^μ y λ_{u}^μ, respectivamente.

A finales del siglo XIX, al tratar de estudiar la estabilidad del sistema solar, Poincaré [51] advirtió que las variedades invariantes de un punto de silla se pueden intersecar en un punto $Q_\mu \neq P_\mu$. Además, alertó de que la existencia de dicho punto, denominado *punto homoclínico*, fuerza la existencia de una infinidad de otros puntos homoclínicos, obligando así a las variedades a describir una complicada maralla. Un punto homoclínico Q_μ se dirá *transversal* si las variedades invariantes de P_μ se intersecan transversalmente en Q_μ, es decir,

$$\mathrm{T}_{Q_\mu} W^{\mathrm{s}}(P_\mu) \oplus \mathrm{T}_{Q_\mu} W^{\mathrm{u}}(P_\mu) = \mathrm{T}_{Q_\mu} \mathcal{M}$$

En caso contrario, el punto homoclínico Q_μ se dirá *tangencial*.

Tuvieron que pasar treinta años para que Birkhoff [7] probara que en un entorno $\mathcal{U}$ de un punto homoclínico transversal existe una infinidad de órbitas periódicas de periodos arbitrariamente grandes. Otros treinta años más tarde, Smale [65] probó la existencia en $\mathcal{U}$ de un recinto invariante hiperbólico no trivial para una de las aplicaciones más célebres en sistemas dinámicos: la *herradura* de Smale.

La aplicación herradura h supuso un hito en el estudio de los sistemas dinámicos. Se construye expansiva en una dirección y contractiva en la otra, de modo que su recinto

[1] *Paraboles et catastrophes : entretiens sur les mathématiques, la science et la philosophie* (1983)

compacto invariante Ω es el producto cartesiano de dos conjuntos de Cantor, sobre los cuales se introducen coordenadas definidas por una sucesión de dos símbolos. Cada punto de Ω se corresponde con una bisucesión

$$(\cdots a_{-n}\cdots a_{-2}a_{-1}, a_0a_1a_2\cdots a_n\cdots)$$

La imagen de una bisucesión bajo el *shift* de Bernouilli σ es el resultado de correr la coma un lugar a la derecha. Es bien conocido que la restricción de h a Ω es topológicamente conjugada a σ. Es inmediato concluir para σ, y por lo tanto para f por conjugación, la existencia de puntos periódicos de cualquier periodo. Más aún: se prueba también la existencia de una órbita densa que es expansiva en la dirección de expansión de h. Por consiguiente, sobre Ω, las desviaciones de las condiciones iniciales en la dirección de expansión serán incrementadas exponencialmente. Esta sensibilidad respecto a las condiciones inciales fue correctamente entendida como un rasgo de indeterminación o impredecibilidad. Por otra parte, los puntos homoclínicos transversales y las aplicaciones herradura asociadas son *robustos*, en el sentido de que continúan existiendo para familias de difeomorfismos C^1-próximas a f_μ.

Origen y significado del concepto de atractor extraño

La robustez de los puntos homoclínicos y, consecuentemente, de las aplicaciones herradura asociadas, así como la impredecibilidad que estas comportan, hicieron que en mucha literatura de los años setenta y posteriores se entendiera como comportamiento caótico la presencia de herraduras. Sin embargo, una objección se debe poner a esta interpretación debido a que la dinámica interna de Ω no es observable: carece de un conjunto significativo (abierto o con medida positiva) de condiciones iniciales

$$W^{\mathrm{s}}(\Omega) = \{P \in \mathcal{M} : \mathrm{dist}(h^n(P), \mathcal{M}) \to 0 \text{ cuando } n \to \infty\}$$

denominado el *conjunto estable* o *recinto de atracción* de Ω, cuyas iteraciones converjan a Ω. Esta deficiencia fue resuelta por Smale [65, 66] al construir un difeomorfismo del toro sólido $\mathbb{T}^2 = \mathbb{S}^1 \times \mathbb{D}^2$ sobre sí mismo, llamado el *solenoide*.

Definición (Atractores)**.** Un *atractor* de una aplicación T definida en una variedad diferenciable $\mathcal{M}$ es un conjunto compacto T-invariante que es transitivo y cuyo conjunto estable

$$W^{\mathrm{s}}(\mathcal{A}) = \{P \in \mathcal{M} : \mathrm{dist}(T^n(P), \mathcal{A}) \to 0 \text{ cuando } n \to \infty\}$$

tiene interior no vacío.

El solenoide tiene un recinto compacto invariante hiperbólico Ω cuya estructura local es homeomorfa al producto cartesiano de un conjunto de Cantor por un intervalo. Su estructura hiperbólica es también robusta y, en la dirección del intervalo, el solenoide es expansivo. Por consiguiente, presenta sensibilidad con respecto a las condiciones iniciales. Puesto que el conjunto estable de Ω es todo $\mathbb{T}^2$, la impredecibilidad de la dinámica es ahora observable. Recintos compactos invariantes como el del solenoide fueron denominados *atractores extraños* y su presencia fue propuesta como paradigma de los comportamientos caóticos.

El término atractor extraño fue acuñado por Ruelle y Takens [63] para referirse a aquellos atractores que, como el del solenoide, no eran ni puntos ni toros: ni tan siquiera tenían estructura de variedad diferenciable. Eran localmente el producto de una variedad por conjunto de Cantor y su dinámica interna era expansiva en alguna dirección: tienen algún exponente de Liapunov positivo.

Definición (Atractores extraños)**.** Un atractor de T es *extraño* si contiene una órbita densa $\{T^n(P_0) : n \in \mathbb{N}\}$ que presenta algún exponente de Liapunov positivo: existe un vector unitario v y una constante $c > 0$ tal que, para todo $n \in \mathbb{N}$,

$$\|\mathrm{D}T^n(P_0)v\| \geq \mathrm{e}^{cn}$$

La definición anterior garantiza la existencia de una dirección expansiva, pero no especifica cuántas hay. Aunque algunos autores definan los atractores extraños *multidimensionales* como aquellos que poseen múltiples direcciones expansivas, nosotros adoptaremos una versión más débil.

Definición (Atractores extraños multidimensionales)**.** Un atractor extraño tiene *dimensión* n si contiene una órbita densa con n exponentes de Liapunov cuya suma es positiva.

La presencia de atractores extraños robustos, como aquellos con estructura hiperbólica, fue considerada [63] como una mejor propuesta para explicar la naturaleza de la turbulencia que aquella dada con anterioridad mediante un crecimiento del número de frecuencias inconmesurables en un movimiento cuasiperiódico [37].

Definición (Atractores persistentes)**.** Sea $f_\mu \colon \mathcal{M} \to \mathcal{M}$ una familia de aplicaciones. Supóngase que f_{μ_0} tiene un atractor $\mathcal{A}_0$ para algún μ_0. El atractor $\mathcal{A}_0$ es *persistente* si, para todo $\delta > 0$, la aplicación f_μ tiene un atractor para todo valor de μ perteneciente a un conjunto $E \subseteq \mathcal{B}(\mu_0, \delta)$ con medida de Lebesgue positiva. El atractor $\mathcal{A}_0$ es *completamente persistente* si $E = \mathcal{B}(\mu_0, \delta)$ para algún $\delta > 0$.

Parafraseando a Ruelle y Takens [63, p. 171]: *An attractor of the type just described can therefore not be thrown away as non-generic pathology.* El camino para generar en flujos este tipo de atractores hiperbólicos tipo solenoide fue propuesto como una concatenación de *bifurcaciones de Hopf* [30, Th. 3.4.2] en dimensión mayor o igual que cuatro.

Abundancia de atractores: persistencia de atractores no hiperbólicos

Un escenario más simple que el propuesto por Ruelle y Takens [63] para la génesis de atractores extraños fue dado anteriormente por Lorenz [39] al analizar numéricamente el campo cuadrático

$$\begin{aligned} x' &= -\alpha x + \alpha y \\ y' &= \beta x - y - xz \\ z' &= \gamma z + xy \end{aligned}$$

con $(\alpha, \beta, \gamma) = (10, 28, -8/3)$. Este sistema surge de un truncamiento de la ecuación de Navier-Stokes. Sorprendentemente, bajo pequeñas perturbaciones, aparentemente consiguió un atractor completamente persistente, pero no estable: los atractores cercanos no son, en general, topológicamente equivalentes. En un escenario aún más simple, Hénon [31] encontró un atractor extraño posiblemente persistente, pero ciertamente no completamente persistente, para la familia de Hénon

$$H_{a,b}(x, y) = (1 - ax^2 + y, bx)$$

con $a = 1.4$ y $b = 0.3$. Por consiguiente, ninguno de los dos atractores es robusto y, por lo tanto, no son hiperbólicos. Pero ¿existen realmente atractores extraños no hiperbólicos?

La primera prueba analítica de la existencia de tales atractores fue dada por Benedicks y Carleson [5] para $H_{a,b}$ para valores positivos y suficientemente pequeños de b y valores de a en un conjunto con medida de Lebesgue positiva contenido en un intervalo $(2 - \delta, 2]$

para $\delta > 0$ suficientemente pequeño. Para el desarrollo de esta prueba fueron necesarios resultados previos de dinámica unidimensional.

Para valores positivos de b, la aplicación $H_{a,b}$ puede escribirse fácilmente como

$$H_{a,b}(x, y) = (1 - ax^2 + \sqrt{b}y, \sqrt{b}x)$$

Así, para todo $b > 0$ suficientemente pequeño, la familia de Hénon es una pequeña perturbación de

$$\Phi_a(x, y) = (1 - ax^2, 0)$$

Por lo tanto, la dinámica de Φ_a, y consecuentemente la dinámica de $H_{a,b}$ en el caso límite $b = 0$, se reduce al estudio de la dinámica de la familia cuadrática

$$T_a(x) = 1 - ax^2$$

La aplicación T_a es un ejemplo paradigmático de aplicación unimodal con derivada de Schwarz negativa. Estas aplicaciones unimodales fueron bien estudiadas. Véase, por ejemplo, De Melo y Van Strien [15].

Tras varios cambios adecuados de variables y parámetros, la familia cuadrática se transforma en

$$f_a(x) = ax(2 - x)$$

El intervalo $[0, 2]$ es f_a-invariante cuando $0 \leq a \leq 2$. Esta familia fue muy estudiada, no solo por servir como un modelo del crecimiento de una población, sino también porque genera una riqueza dinámica que se sigue de un proceso de *renormalización* descubierto independientemente por Feigenbaum [19, 20] y por Coullet y Tresser [12]. Este proceso de renormalización consiste, esencialmente, en la existencia de una sucesión a_n de valores del parámetro a y de una sucesión I_n de intervalos tales que la restricción del iterado $f_{a_n}^2$ al intervalo I_n coincide, salvo un reescalado, con la restricción de $f_{a_{n-1}}$ al intervalo I_{n-1}. Como una consecuencia de este hecho se sigue el bien conocido fenómeno de *duplicación de periodo* y, en cierta medida, la estructura fractal que se observa en la Figura 01 [15], donde se representa numéricamente la estructura del atractor de f_a para los distintos valores de a.

Existen ventanas de valores de a para los que el atractor es una órbita periódica de pequeño periodo. Sin embargo, para otros parámetros, el atractor luce como una órbita periódica de periodo muy largo o tal vez como un conjunto no finito: un posible atractor extraño. Tal atractor extraño existe ciertamente cuando $a = 2$. Más aún: se prueba que f_2 es conjugada a la correspondiente aplicación para $\bar{a} = 2$ de la familia de aplicaciones *tienda*

$$\lambda_{\bar{a}}(x) = \begin{cases} \bar{a}x & \text{if } 0 \leq x \leq 1 \\ \bar{a}(2 - x) & \text{if } 1 \leq x \leq 2 \end{cases}$$

El intervalo $I = [0, 2]$ también es $\lambda_{\bar{a}}$-invariante cuando $0 \leq \bar{a} \leq 2$. Más exactamente, el intervalo $I_{\bar{a}} = [\bar{a}(2 - \bar{a}), \bar{a}]$ es estrictamente $\lambda_{\bar{a}}$-invariante con $1 < \bar{a} \leq 2$. De hecho, el intervalo $I_{\bar{a}}$ es un atractor extraño cuando $\bar{a} \geq \sqrt{2}$, pues la órbita del punto crítico $x = 1$ es densa y expansiva en $I_{\bar{a}}$.

Para $\bar{a} = \sqrt{2}$, comienza un proceso de renormalización para la familia $\{\lambda_{\bar{a}}\}_{1<\bar{a}\leq\sqrt{2}}$. Para la sucesión $\bar{a}_n = 2^{1/2^n}$ existe un intervalo I_n tal que la restricción del iterado $\lambda_{\bar{a}_n}^2$ al intervalo I_n coincide, salvo un reescalado, con la restricción de $\lambda_{\bar{a}_{n-1}}$ al intervalo I_{n-1}. Este proceso de renormalización permite concluir que el atractor extraño $I_{\bar{a}}$ para $\sqrt{2} \leq a \leq 2$ se va rompiendo en un atractor extraño de 2^n componentes a medida que $\bar{a}$ cruza los valores $\bar{a}_n = 2^{1/2^n}$. Más aún, el proceso de renormalización visto para la familia f_a aporta una sucesión a_n para los cuales f_{a_n} es conjugada a $\lambda_{\bar{a}_n}$ para todo n. Por consiguiente, para esa sucesión de valores a_n la aplicación f_{a_n} presenta un atractor extraño con 2^n componentes conexas.

La familia $\lambda_{\bar{a}}$ presenta atractores extraños para $1 < a \leq 2$, que son, por lo tanto, persistentes. Sin embargo, la existencia de atractores extraños para la sucesión de valores del parámetros a_n para la familia f_a no permite afirmar que sean persistentes. La prueba de la persistencia fue dada por primera vez por Benedicks y Carleson [5] trabajando con la familia cuadrática para valores de a muy próximos a 2. Más exactamente, para todo $\delta > 0$ suficientemente pequeño existe un conjunto $E \subseteq (2-\delta, 2]$ con medida de Lebesgue positiva tal que, para todo $a \in E$, la aplicación T_a tiene un atractor extraño. Teniendo en mente el proceso de renormalización, esta persistencia se extiende a valores del parámetro a suficientemente próximos a la sucesión a_n.

A diferencia del caso de las aplicaciones *tienda* $\lambda_{\bar{a}}$, la prueba de la persistencia de los atractores extraños para la familia T_a presenta serias dificultades para conseguir la expansividad de la órbita del punto crítico $x = 1$. Cerca de este punto no hiperbólico, la derivada es casi nula y, por consiguiente, cada vez que la órbita retorne cerca de $x = 1$ puede perder toda la expansividad acumulada. Se hace entonces necesaria una adecuada exclusión de aquellos parámetros para los cuales la contracción cerca de $x = 1$ elimine la expansividad previamente acumulada. Esta exclusión permite conservar un conjunto de parámetros a con medida de Lebesgue positiva para los cuales la órbita tiene exponente de Liapunov positivo y, además, es densa en todo el intervalo $[1-a, 1]$. Esto permite concluir, para cada $a \in E$, la existencia de una medida invariante absolutamente continua μ_a con entropía positiva [15, Ch. V], tal y como había sido probado por Jakobson [34] con anterioridad a Benedicks y Carleson [5]. Frente a la impredecibilidad de la dinámica interna del atractor, esta medida informa de la distribución de las órbitas. Tiene soporte contenido en el atractor y es *estadísticamente estable*: su función de densidad depende con continuidad en L^1 con respecto al parámetro a.

La prueba de la persistencia de los atractores dada por Benedicks y Carleson [5] resultó ser fundamental para la prueba de la persistencia de atractores extraños [6] para la familia de Hénon. Como ya se dijo, la dinámica de T_a es una situación límite de la dinámica de $H_{a,b}$ para valores positivos y suficientemente pequeños de b. La familia de Hénon tiene un punto fijo P de tipo silla cuya variedad inestable se pliega una y otra vez sobre sí misma y permanece arbitrariamente próxima al intervalo $[1-a, 1]$ sobre el eje x. Es natural suponer entonces que la dinámica de $H_{a,b}$ sobre $W^{\mathrm{u}}(P)$ semeje la dinámica de T_a sobre $[1-a, 1]$. En efecto, se prueba que la clausura de $W^{\mathrm{u}}(P)$ es el atractor extraño de $H_{a,b}$ para todo $b > 0$ suficientemente pequeño y todo valor de a en un conjunto $E \subseteq (2-\delta, 2]$. Para ello, se hace necesaria de nuevo una exclusión de parámetros que controle la expansividad cerca de cada uno de los infinitos pliegues de $W^{\mathrm{u}}(P)$. A pesar de que esta exclusión de parámetros es más complicada y exhaustiva que la exclusión realizada para la familia cuadrática, se consigue probar que el nuevo conjunto E continúa teniendo medida de Lebesgue positiva. Nos referiremos al paralelismo entre la dinámica de la familia $H_{a,b}$ y su familia límite T_a diciendo que $H_{a,b}$ es un *buen despliegue* de T_a.

La familia de Hénon es una familia de difeomorfismos que presenta atractores extraños no hiperbólicos persistentes, pero ¿cuál es su presencia en el conjunto de los modelos dinámicos? En otras palabras: ¿existe un mecanismo genérico que conduzca a la existencia de atractores extraños no hiperbólicos persistentes? En esta dirección apuntaba Jacob Palis cuando conjeturó que familias uniparamétricas genéricas de difeomorfismos definidos sobre una superficie que despliegan para cada valor del parámetro una *tangencia homoclínica* presentan atractores extraños con probabilidad positiva. Por tangencia homoclínica debe ser entendido un punto homoclínico no transversal entre las variedades invariantes de un punto periódico del difeomorfismo en cuestión. Esta conjetura fue probada por Mora y Viana [44].

Teorema ([44, Th. A]). *Sea $(f_\mu)_\mu$ una familia uniparamétrica suficientemente regular de difeomorfismos sobre una superficie. Supóngase que f_0 presenta una tangencia homoclínica*

asociada a cierto punto periódico. Entonces, bajo condiciones genéricas (incluso abiertas y densas), existe un conjunto E de valores de μ cerca de $\mu = 0$ con medida de Lebesgue positiva tal que, para todo $\mu \in E$, el difeomorfismo f_μ presenta un atractor (o repulsor[2]) extraño cerca de la órbita de la tangencia.

La prueba de este resultado comienza considerando las aplicaciones de retorno de la familia $(f_\mu)_\mu$ en un entorno $\mathcal{V}$ de la tangencia homoclínica Q_0 de f_0. Sea $1 \leq r < \infty$ fijo. Bajo suposiciones genéricas (incluyendo la disipatividad de f_0 en P_0), se pueden encontrar renormalizaciones de f_μ que están arbitrariamente C^r próximas a la familia Φ_a. Esto significa que existen dominios (pequeños) $\mathcal{U}^n$ sobre la superficie que convergen al punto Q_0 de la órbita de tangencia, intervalos (pequeños) I^n que convergen a $\mu = 0$ en el espacio de parámetros y C^r coordenadas n-dependientes en $I^n \times \mathcal{U}^n$ con la siguiente propiedad: la expresión de $f^n{\restriction}_{I^n \times \mathcal{U}^n}$ en dichas coordenadas converge a la familia Φ_a en la topología C^r cuando $n \to \infty$. Véanse los detalles en Palis y Takens [48]. Esta convergencia verifica una serie de estimaciones dadas en el Teorema 2.1 [44] que son necesarias para poder aplicar las técnicas de Benedicks y Carleson [6] en la prueba de la existencia de atractores extraños para la familia $f^n{\restriction}_{I^n \times \mathcal{U}^n}$. Por este motivo, los autores se refieren a $f^n{\restriction}_{I^n \times \mathcal{U}^n}$, expresada en las nuevas coordenadas renormalizadas, como una familia tipo Hénon. En realidad, tal como ocurre con la familia de Hénon, la familia $f^n{\restriction}_{I^n \times \mathcal{U}^n}$ define un buen despliegue de su familia límite Φ_a, o, simplemente, de la familia cuadrática.

Los atractores probados por Mora y Viana [44] son infinitesimales en el sentido de que los dominios de renormalización han de estar arbitrariamente cerca del punto detangencia homoclínica. Otras renormalizaciones sin esta restricción fueron hechas para la sección transversal de una órbita de Shil'nikov en una familia de campos tridimensionales [52]. Después de esta renormalización, se obtiene una familia de difeomorfismos

$$T_{\lambda,a,b}(x, y) = (f_{\lambda,a} + \tfrac{1}{\lambda}\log(1 + \sqrt{b}y), \sqrt{b}(1 + \sqrt{b}y)\mathrm{e}^{\lambda x}\sin x)$$

cuya familia límite es la familia unimodal

$$f_{\lambda,a}(x) = \tfrac{1}{\lambda}\log a + x + \tfrac{1}{\lambda}\log\cos x$$

donde λ queda fijada al fijar el espectro del campo. Para la familia $f_{\lambda,a}$ se prueba la existencia de atractores extraños persistentes [52]. Luego, después de probar que la familia $T_{\lambda,a,b}$ es un buen despliegue de la familia $f_{\lambda,a}$, se aplican las ideas de Benedicks y Carleson [6] y de Mora y Viana [44] para concluir la existencia de atractores extraños persistentes de $f_{\lambda,a}$. Estos atractores no son infinitesimales y definen por suspensión atractores extraños persistentes para la familia de campos tridimensionales. Se muestra adicionalmente que las ideas de Benedicks y Carleson [6] se pueden extender a cualquier buen despliegue de una aplicación unimodal diferente de la familia cuadrática.

En busca de atractores extraños bidimensionales: la familia cuadrática bidimensional

Todos los atractores anteriormente mencionados tienen dimensión uno. Aparecen genéricamente al desplegar tangencias homoclínicas que involucran la variedad inestable unidimensional de un punto de silla disipativo. La prueba de su existencia está principalmente basada en procesos de renormalización definidos en un entorno de un punto de tangencia que son buenos despliegues de familias límite unidimensionales. Para estas familias se prueba previamente la persistencia de recintos compactos e invariantes que contienen una órbita densa con un exponente de Liapunov positivo.

[2] Un *repulsor* es un atractor de f_μ^{-1} cuando f_μ no es disipativo en P

El camino hacia la prueba de la persistencia de atractores extraños bidimensionales no seá probablemente muy diferente al seguido en el caso unidimensional, pero el incremento en la dimensión supondrá mayores dificultades y el problema está completamente abierto. La familia de difeomorfismos debe estar definida en una variedad de dimensión mayor o igual que tres. Solo así para algún valor del parámetro el correspondiente difeomorfismo puede presentar una tangencia homoclínica que involucre un variedad inestable de dimensión dos.

Sea f un difeomorfismo definido en una variedad diferenciable $\mathcal{M}$ de dimensión tres con un punto de silla P. Supóngase que $\mathrm{D}f(P)$ tiene valores propios reales $\lambda_{\mathrm{s}}, \lambda_{\mathrm{cu}}, \lambda_{\mathrm{u}}$ tales que

$$|\lambda_{\mathrm{s}}| < 1 < |\lambda_{\mathrm{cu}}| < |\lambda_{\mathrm{u}}|$$

En este caso, los siguientes hecho son bien conocidos:

1. La *variedad inestable fuerte* $W^{\mathrm{uu}}(P)$ de P yace sobre la variedad inestable de P y es tangente al espacio propio asociado a λ_{u} en P. Esta variedad es única, tiene la misma regularidad que f y tiene dimensión uno.

2. La variedad inestable de P está cubierta por las hojas de una *foliación inestable fuerte* $\mathcal{F}^{\mathrm{uu}}(P)$. Toda hoja ℓ^{uu} de $\mathcal{F}^{\mathrm{uu}}(P)$ es transversal al espacio propio asociado a λ_{cu}, y $W^{\mathrm{uu}}(P)$ es una de sus hojas.

3. La *variedad centro-estable* $W^{\mathrm{cs}}(P)$ de P es una variedad invariante que contiene a la variedad estable de P y toca el subespacio invariante de $\mathrm{T}_P\mathcal{M}$ asociado a λ_{s} y λ_{cu} en P. Esta variedad es en general de clase C^1 y no es única.

Supóngase además que existen una coordenadas linealizantes (x, y, z) de clase C^1 para f en un entorno $\mathcal{U}$ de P tales que $P = (0, 0, 0)$ y

$$f(x, y, z) = (\lambda_{\mathrm{cu}}, \lambda_{\mathrm{u}} y, \lambda_{\mathrm{s}} z)$$

para todo $(x, y, z) \in \mathcal{U}$. En $\mathcal{U}$, las variedades inestable y estable locales de P están dadas, respectivamente, por

$$W^{\mathrm{u}}_{\mathrm{loc}}(P) = \{(x, y, 0) : |x|, |y| < \delta\}$$

y

$$W^{\mathrm{s}}_{\mathrm{loc}}(P) = \{(0, 0, z) : |z| < \delta\}$$

para $\delta > 0$ suficientemente pequeño. Más aún, existe la foliación inestable fuerte local en la variedad inestable local tal que, para cualquier $\bar{\mathbf{x}} = (\bar{x}, \bar{y}, 0) \in W^{\mathrm{u}}_{\mathrm{loc}}(P)$, la hoja $\ell^{\mathrm{uu}}(\bar{\mathbf{x}})$ que contiene a $\bar{\mathbf{x}}$ viene dada por $\ell^{\mathrm{uu}}(\bar{\mathbf{x}}) = \{(\bar{x}, y, 0) : |y| < \delta\}$.

Supóngase que las variedades invariantes de P tienen una tangencia homoclínica cuadrática. Introducimos la definición de un tipo nuevo de bifurcación homoclínica de codimensión dos, que puede ser vista como una colisión entre una tangencia homoclínica cuadrática y una transversalidad homoclínica generalizada.

Definición (Tangencia homoclínica generalizada)**.** Se dice que el difeomorfismo f tiene una *tangencia homoclínica generalizada* (de tipo I del Caso B) en un punto

$$Q \in W^{\mathrm{s}}(P) \cap W^{\mathrm{u}}(P)$$

si se cumplen las siguientes condiciones:

(T_1) El punto fijo P es disipativo.

(T_2) Las variedades invariantes de P tienen una tangencia cuadrática en Q. Más aún, el punto Q no pertenece a la variedad inestable fuerte de P.

(T_3) La variedad estable de P es tangente a la hoja de $\mathcal{F}^{uu}$ que contiene a Q.

(T_4) La variedad centro-estable de P es transversal a la superficie definida por la variedad inestable de P en Q.

Observación. Para la tangencia cuadrática $Q \in \mathcal{M}$, consideramos la imagen $\overline{Q} = f^{n_0}(Q)$ para $n_0 \in \mathbb{N}$ grande. Sea $U(Q)$ el plano que contiene a $\overline{Q}$ y tal que $T_{\overline{Q}}U(\overline{Q})$ está generado, en coordenadas locales de P, por $(\partial/\partial x)_{\overline{Q}}, (\partial/\partial z)_{\overline{Q}} \in T_{\overline{Q}}\mathcal{M}$. Nótese que, por la coordenadas linealizantes elegidas, el plano $U(\overline{Q})$ en $T_{\overline{Q}}\mathcal{M}$ se corresponde con el fibrado centro-estable en Q. Así, la condición (T_4) se puede enunciar como sigue:

(T_4) El plano $U(\overline{Q})$ y la variedad inestable de P son transversales en $\overline{Q}$.

Bajo estas hipótesis, Tatjer probó [67, Prop. 4.5] que existe una familia biparamétrica de aplicaciones límite de retorno asociadas a la tangencia homoclínica generalizada, que vienen dadas por

$$\tilde{f}_{\tilde{a},\tilde{b}}(\tilde{x},\tilde{y},\tilde{z}) = (\tilde{z}, \tilde{a} + \tilde{b}\tilde{y} + \tilde{z}^2, \tilde{y})$$

Como era de esperar, tal y como ocurre en el despliegue de tangencias bidimensionales, estas aplicaciones límite de retorno no son lineales. Antes de tratar de probar la existencia de atractores extraños para la familia $\tilde{f}_{\tilde{a},\tilde{b}}$, nótese que, para cualquier par de parámetros $(\tilde{a},\tilde{b})$, todo punto en $\mathbb{R}^3$ *cae* tras una sola iteración de $\tilde{f}_{\tilde{a},\tilde{b}}$ en la superficie

$$\widetilde{\mathcal{C}}_{\tilde{a},\tilde{b}} = \{(\tilde{x},\tilde{y},\tilde{z}) \in \mathbb{R}^3 : \tilde{y} = \tilde{a} + \tilde{b}\tilde{z} + \tilde{x}^2\}$$

Por lo tanto, la superficie $\widetilde{\mathcal{C}}_{\tilde{a},\tilde{b}}$ es $\tilde{f}_{\tilde{a},\tilde{b}}$-invariante y es suficiente con estudiar la dinámica de la aplicación $\tilde{f}_{\tilde{a},\tilde{b}}$ en $\widetilde{\mathcal{C}}_{\tilde{a},\tilde{b}}$. Esto es, es suficiente con estudiar la dinámica de los endomorfismos bidimensionales

$$(g^{-1}_{\tilde{a},\tilde{b}} \circ \tilde{f}_{\tilde{a},\tilde{b}} \circ g_{\tilde{a},\tilde{b}})(\tilde{x},\tilde{z}) = (\tilde{z}, \tilde{a} + \tilde{b}\tilde{z} + \tilde{x}^2)$$

siendo $g_{\tilde{a},\tilde{b}}(\tilde{x},\tilde{z}) = (\tilde{x}, \tilde{a} + \tilde{b}\tilde{z} + \tilde{x}^2, \tilde{z})$ una parametrización de $\widetilde{\mathcal{C}}_{\tilde{a},\tilde{b}}$. Al aplicar el cambio de coordenadas

$$\mathbf{x} = \tilde{z} - \tilde{b}\tilde{x}, \quad \mathbf{y} = \tilde{x}$$

la anterior familia de endomorfismos se transforma en *la familia cuadrática bidimensional*:

$$T_{a,b}(\mathbf{x},\mathbf{y}) = (a + \mathbf{y}^2, \mathbf{x} + b\mathbf{y})$$

donde hemos escrito a, b en lugar de $\tilde{a}, \tilde{b}$ para evitar notación excesiva.

Del mismo modo que el estudio de la familia cuadrática fue fundamental para la prueba de la persistencia de atractores extraños unidimensionales, el estudio de la familia cuadrática bidimensional debería ser un primer paso hacia la prueba de la persistencia de atractores extraños bidimensionales.

Persistencia de atractores extraños bidimensionales en una familia uniparamétrica de aplicaciones *tienda* bidimensionales

Con vistas a probar analíticamente la existencia de atractores extraños bidimensionales para la familia cuadrática bidimensional, Pumariño y Tatjer [60] empezaron buscando valores de los parámetros para los que existen dominios invariantes.

Las situaciones más simples surgen para $b = 0$. En ese caso, el cuadrado

$$R_a = [a, a + a^2] \times [a, a + a^2]$$

es estrictamente $T_{a,0}$-invariante para todo $a \in [-2,-1]$. Más aún, el cuadrado R_a es un atractor extraño bidimensional [60, Prop. 3] para valores de a en un conjunto de medida de Lebesgue positiva contenido en $[-2,a_0]$ para un cierto $a_0 > -2$.

Aparte del caso $b = 0$, se construyeron triángulos curvilíneos invariantes para valores de los parámetros a lo largo de la curva

$$G = \{(-\tfrac{1}{4}s^3(s^3 - 2s^2 + 2s - 2), -s^2 + s) : 0 \le s \le 2\}$$

El punto $(-4,-2)$ pertenece a G para $s = 2$. Para $(a,b) = (-4,-2)$, el respectivo triángulo curvilíneo es invariante en el sentido estricto y la aplicación $T_{-4,-2}$ es conjugada a la aplicación afín a trozos no invertible

$$\Lambda(x,y) = \begin{cases} (x+y, x-y) & \text{if } (x,y) \in \mathcal{T}_0 \\ (2-x+y, 2-x-y) & \text{if } (x,y) \in \mathcal{T}_1 \end{cases}$$

definida en el triángulo $\mathcal{T} = \mathcal{T}_0 \cup \mathcal{T}_1$, donde

$$\mathcal{T}_0 = \{0 \le x \le 1,\ 0 \le y \le x\}, \quad \mathcal{T}_1 = \{1 \le x \le 2,\ 0 \le y \le 2-x\}$$

Como fue señalado [60, §2.3], la aplicación Λ presenta las mismas buenas propiedades que la aplicación *tienda* λ_2. En particular, las preimágenes consecutivas del segmento crítico $\{(x,y) \in \mathcal{T} : x = 1\}$ definen una sucesión de particiones (cuyo diámetro tiende a cero) de $\mathcal{T}$ que llevó a los autores a conjugar Λ a un *shift* de Bernouilli de dos símbolos. Además, para todo punto inicial $(x_0,y_0) \in \mathcal{T}$ cuya órbita nunca visita la recta crítica, el exponente de Liapunov de Λ a lo largo de la órbita de (x_0,y_0) es positivo (de hecho, es igual a $2^{-1}\log 2$) en toda dirección no nula. Finalmente, se puede construir con facilidad una medida invariante absolutamente continua y ergódica. Por conjugación, todos estos hechos se verifican para $T_{-4,-2}$. Estas fueron las principales razones por las que la aplicación Λ se llamó la *aplicación tienda bidimensional*.

Como un primer acercamiento al estudio general de la dinámica de $T_{a,b}$ a lo largo de la curva G, se introdujo [55] la familia de aplicaciones afines a trozos de $\mathcal{T}$ dada por

$$\Lambda_t(x,y) = \begin{cases} (t(x+y), t(x-y)) & \text{if } (x,y) \in \mathcal{T}_0 \\ (t(2-x+y), t(2-x-y)) & \text{if } (x,y) \in \mathcal{T}_1 \end{cases}$$

El triángulo $\mathcal{T}$ es Λ_t-invariante cuando $0 \le t \le 1$. Nótese que $\Lambda_1 = \Lambda$. Puesto que el parámetro t da esencialmente la expansividad, jugando el mismo papel que el parámetro $\bar{a}$ para la familia $\lambda_{\bar{a}}$, la familia Λ_t puede considerarse como una extensión natural de las aplicaciones *tienda* clásicas. Por eso, la familia $\{\Lambda_t\}_{0\le t\le 1}$ se llamó la *familia de aplicaciones tienda bidimensionales*.

La dinámica de la familia Λ_t es muy simple para $0 \le t \le \sqrt{2}/2$. Si $t < \sqrt{2}/2$, entonces el origen es el único punto fijo y es un atractor global de tipo nodo [55, Lem. 5.1]. Para $t = \sqrt{2}/2$, la aplicación $\Lambda_{\sqrt{2}/2}$ preserva el área y tiene un segmento de puntos fijos en $\mathcal{T}_0$, siendo el resto de puntos de $\mathcal{T}_0$ puntos periódicos de periodo dos.

Sin embargo, para $\sqrt{2}/2 < t \le 1$, la dinámica de Λ_t es verdaderamente rica. El origen es un nodo repulsor y aparece con otro punto fijo en $\mathcal{T}_1$, que es un foco repulsor. Además, los exponentes de Liapunov de cualquier punto que no pertenezca a ninguna preimagen del segmento crítico es igual a $\log\sqrt{2}t$ en toda dirección no nula, y todas las órbitas periódicas sin puntos críticos son repelentes. Más aún, la familia Λ_t presenta en este intervalo los mismos tipos topológicos de atractores extraños numéricos que la familia cuadrática bidimensional a lo largo de la curva G para $0 \le s \le 2$. A saber: atractores extraños convexos (para $\sqrt[3]{4}/2 \le t \le 1$); atractores extraños conexos, pero no simplemente conexos (para $\sqrt[5]{8}/2 \le t < \sqrt[3]{4}/2$); y atractores extraños no conexos, formados por múltiples piezas

conexas (parafor $\sqrt{2}/2 < t < \sqrt[5]{8}/2$). Esto fue lo que verdaderamente motivó el estudio de la dinámica de la familia Λ_t.

Una primera prueba analítica de la existencia de un atractor extraño convexo para Λ_t fue dado [56, Th. 1.1] para $\tau < t \leq 1$, donde

$$\tau = \frac{\sqrt{2}}{2}(1+\sqrt{2})^{\frac{1}{4}} \approx 0.882$$

Más aún, al igual que para Λ, se probó que el atractor soporta una única medida de probabilidad invariante y absolutamente continua para tales t, que además es ergódica. Por otro lado, la existencia de atractores extraños persistentes de varias piezas se probó a lo largo de varios trabajos [57, 58, 59]. Dicha prueba es una consecuencia de un proceso de renormalización que permite entender cómo conjuntos compactos invariantes conexos formados por una única pieza puede romperse dando lugar a otros formados por un número creciente de piezas. Entonces, por el Teorema 1.2 [59], se sigue que estos nuevos conjuntos compactos invariantes no conexos contienen atractores extraños formados por el mismo número de piezas. Más aún, se probó la coexistencia de números arbitrariamente grandes de atractores extraños [58, Th. B].

Para $\tau < t \leq 1$, es natural preguntarse si μ_t depende continuamente de la dinámica de Λ_t, es decir, si Λ_t es estadísticamente estable. En este caso, significa la continuidad de las densidades de μ_t con respecto a t en la norma L^1.

Alves, Pumariño y Vigil dieron condiciones suficientes para la estabilidad estadística de aplicaciones expansivas a trozos con distorsión acotada y ramas largas [3, Th. A] y, como corolario [3, Th. B], probaron la estabilidad estadística de la familia Λ_t. En realidad, se prueba que la familia de cierta iterada de Λ_t es estadísticamente estable. Después, Alves y Pumariño probaron la continuidad de la entropía de ciertas aplicaciones multidimensionales expansivas a trozos que admiten medidas de probabilidad invariantes, absolutamente continuas y ergódicas [2, Th. F], y de nuevo dedujeron la continuidad de la entropía para la familia Λ_t como corolario [2, Th. G].

Contribuciones de esta memoria

Como ya hemos avanzado, el objetivo último del proyecto de investigación en el que participa esta tesis doctoral es el estudio de la dinámica de la familia cuadrática bidimensional $T_{a,b}$. Esta familia se obtiene como la familia límite de las aplicaciones de retorno definidas en un entorno de una de las tangencias homoclínicas genéricas desplegadas por familias biparamétricas de difeomorfismos tridimensionales [67, Th. 1]. El principal interés de la dinámica de esta familia radica en la supuesta existencia de atractores extraños bidimensionales que fueron detectados numéricamente [60, 61]. Además de la prueba analítica de la persistencia de tales atractores, su génesis también debería ser entendida, así como la de sus atractores extraños unidimensionales numéricos [60].

Para la explicación de la existencia de atractores extraños unidimensionales, volveremos sobre los antecedentes comentados en esta introducción y, concretamente, sobre el resultado de Mora y Viana [44, Th. A] que prueba la persistencia de atractores extraños unidimensionales en despliegues genéricos de una tangencia homoclínica de difeomorfismos definidos sobre una superficie. La génesis de tales atractores también se explica a través de un análisis de las órbitas periódicas. En cuanto a la existencia de atractores extraños bidimensionales, primero tenemos que encontrar recintos compactos e invariantes donde poder probar la existencia de una órbita densa y expansiva. Como una primera aproximación a este problema, sustituimos la familia cuadrática bidimensional por una familia biparamétrica general de *Expanding Baker Map*.

Esta memoria se organiza como sigue. En el Capítulo 1 incluimos más detalle sobre el teorema principal de Tatjer [67, Th. 1] y el paso al límite de las aplicaciones de retorno

para obtener la familia $T_{a,b}$. Los resultados originales de este trabajo se encuentran en los Capítulos 2 y 3.

El Capítulo 2 se dedica al estudio de la familia biparamétrica $\Gamma_{a,\theta}$ de *Expanding Baker Map*, siendo $a > 1$ y $0 < \theta < \pi$ un parámetro de expansión y un ángulo de rotación, respectivamente. La familia Λ_t es un caso particular para $\theta = 3\pi/4$, y los correspondientes resultados [56, 57, 58, 59] son de gran ayuda en el caso general, especialmente si θ/π es un número racional. Como en ese caso, podemos construir recintos compactos estrictamente invariantes y probar que contienen atractores extraños bidimensionales adaptando unos pocos argumentos [59]. Se puede también iniciar un proceso de renormalización [57, 58] para esta familia general, explicando la ruptura e incluso la duplicación de atractores. Los resultados están recogidos en dos publicaciones recientes [42, 43].

El Capítulo 3 se dedica al análisis de la dinámica de la familia $T_{a,b}$. Empezamos con un estudio de las bifurcaciones locales, para lo que sacaremos provecho del análisis numérico por Pumariño y Tatjer [61], centrándonos en los puntos fijos y en las órbitas periódicas de periodos dos y tres. Como fue originalmente probado para familias de campos vectoriales [33, 16, 22], también se espera que toda la dinámica se pueda desplegar a partir de algunas de sus singularidades no hiperbólicas. Estas dinámicas serán órbitas periódicas atrayentes, curvas cerradas invariantes y atractores extraños unidimensionales. En particular, para $b = -1$ se encuentran dos familias de órbitas de periodo tres. Una de ellas es de tipo silla disipativa para valores de a para los que en la otra ocurre una bifurcación de Hopf-Neimark-Sacker. El crecimiento de las curvas cerradas que surgen de esta bifurcación colisionan con la órbita periódica de tipo silla generando una tangencia homoclínica. Este fenómeno ocurre para valores de los parámetros para los que también existe una órbita periódica atrayente. De esta manera se explica en la memoria un proceso que no había sido comprobado: la competencia de más de un atractor extraño.

Atractores extraños bidimensionales en una familia biparamétrica general de *Expanding Baker Map*

La dinámica de la aplicación *tienda* $\lambda_{\bar{a}} \colon [0,2] \to [0,2]$ consiste en doblar primero el intervalo $[0,2]$ por la mitad y después estirar el intervalo $[0,1]$ por un factor $\bar{a} > 1$ para obtener el intervalo $[0,\bar{a}]$. Similarmente, la aplicación *tienda* bidimensional $\Lambda_t \colon \mathcal{T} \to \mathcal{T}$ puede entenderse como la composición de la aplicación lineal definida por la matriz

$$\mathbf{A}_t = \begin{pmatrix} t & t \\ t & -t \end{pmatrix}$$

con el pliegue del triángulo $\mathcal{T}$ a lo largo del segmento crítico

$$\mathcal{C} = \{(x,y) \in \mathcal{T} : x = 1\}$$

sobre $\mathcal{T}_0$. Este pliegue puede definirse en todo $\mathbb{R}^2$ por

$$\mathcal{F}_{\mathcal{C},\mathcal{O}}(x,y) = \begin{cases} (x,y) & \text{if } x \leq 1 \\ (2-x,y) & \text{if } x \geq 1 \end{cases}$$

Si $t > \sqrt{2}/2$, entonces $\mathbf{A}_t$ es expansiva. Así, la familia Λ_t con $\sqrt{2}/2 < t \leq 1$ es un ejemplo de una clase de aplicaciones lineales a trozos, que llamaremos *Expanding Baker Map*, que generalizan esta dinámica: plegar un cierto dominio (posiblemente varias veces) y después expandir la región doblada resultante. Véase la Sección 2.1 para más detalles.

Recordemos que, para todo $t > \sqrt{2}/2$, la aplicación Λ_t tiene un foco repulsor P_t en $\mathcal{T}_1$ con coordenadas

$$(x_t, y_t) = \left(\frac{2t(2t+1)}{2t^2+2t+1}, \frac{2t}{2t^2+2t+1} \right)$$

Tras el cambio afín de coordenadas

$$X = \frac{x - x_t}{1 - x_t}, \quad Y = \frac{y - y_t}{x_t - 1}$$

la aplicación Λ_t se transforma en

$$\Gamma_{a,\theta} = \mathbf{A}_{a,\theta} \circ \mathcal{F}_{\mathcal{C},\mathcal{O}}$$

con $a = \sqrt{2}t$ y $\theta = 3\pi/4$, donde

$$\mathbf{A}_{a,\theta} = \begin{pmatrix} a\cos\theta & -a\sin\theta \\ a\sin\theta & a\cos\theta \end{pmatrix}$$

En estas coordenadas, el punto fijo P_t es el origen y $X = 1$ es de nuevo la recta crítica. Estudiaremos la familia general $\{\Gamma_{a,\theta}\}_{a,\theta}$ con $a > 1$ y $0 < \theta < \pi$. Nótese que la dinámica de $\Gamma_{a,0}$ y $\Gamma_{a,\pi}$ parecen unidimensionales, y $\Gamma_{a,\theta}$ es conjugada a $\Gamma_{a,-\theta}$ para todo $-\pi < \theta < 0$.

Primero probaremos la existencia de recintos $\mathcal{K}$ compactos estrictamente invariantes para $\Gamma_{a,\theta}$ y los divideremos en dos clases: de *primera clase* si $\mathcal{F}_{\mathcal{C},\mathcal{O}}(\mathcal{K}) \subseteq \mathcal{K}$, y de *segunda clase* en caso contrario. Los recintos estrictamente invariantes de primera clase serán un ejemplo de una clase mayor de conjuntos: los *autosemejantes*.

Definición (Recintos autosemejantes)**.** Un recinto $\mathcal{K} \subseteq \mathbb{R}^2$ es $\mathbf{A}_{a,\theta}$-*autosemejante* si

$$\mathbf{A}_{a,\theta}(\mathcal{K}_0) = \mathcal{K}$$

siendo $\mathcal{K}_0 = \mathcal{K} \cap \{x \leq 1\}$.

Así, un primer paso hacia la prueba de la existencia de recintos compactos y estrictamente invariantes es probar la existencia de recintos autosemejantes.

Teorema 1 (Existencia de conjuntos autosemejantes)**.** *Sea $0 < \theta < \pi$. Para todo $a > 1$, existe un polígono $\mathbf{A}_{a,\theta}$-autosemejante $\mathcal{K}_N$ de $N + 1$ lados con*

$$N = N(a, \theta) \geq 1 + \lfloor \pi/\theta \rfloor$$

que contiene todos los recintos $\mathbf{A}_{a,\theta}$-autosemejantes. Más aún, existe una sucesión no creciente a_j de valores de a con las siguientes propiedades:

(a) $a_j \geq 1$ *para todo* $j \in \mathbb{N}$

(b) Para todo $j \in \mathbb{N}$ *se cumple que* $a_{j+1} \leq a_j$ *con la igualdad verifcándose si y solo si* $a_j = 1$

(c) $\lim_{j\to\infty} a_j = 1$

(d) El conjunto $\{a_j\}_j$ *es finito si y solo si* $\theta/\pi \in \mathbb{Q}$

(e) La sucesión $N_j = N(a_j, \theta)$ *es creciente*

(f) Para todo $j \in \mathbb{N}$ *y todo* $a_j \leq a < a_{j-1}$ *se cumple que* $N(a, \theta) = N_j$

Puesto que $\mathbf{A}_{a,\theta}$ multiplica el área de todo recinto por un factor de a^2 y $\mathcal{F}_{\mathcal{C},\mathcal{O}}$ a lo sumo lo divide a la mitad, es claro que los recintos compactos y estrictamente invariantes con interior no vacío solo pueden existir para $a \leq \sqrt{2}$. Esta condición no es suficiente: existen valores de $a \leq \sqrt{2}$ para los que los polígonos autosemejantes del Teorema 1 no son estrictamente invariantes. Como dos ejemplos extremos, para $\theta = 2\pi/3$, estos polígonos son unos triángulos que no son estrictamente invariantes para ningún $a > 1$, mientras que, para $\theta = \pi/2$, son rectángulos estrictamente invariantes para todo $1 < a \leq \sqrt{2}$. De acuerdo con el siguiente resultado, excepto para $\theta = 2\pi/3$, estos polígonos autosemejantes son estrictamente invariantes para todo a suficientemente próximo a 1.

Teorema 2 (Existencia de polígonos estrictamente invariantes)**.** *Para todo* $\theta \in (0,\pi) \setminus \{2\pi/3\}$*, existe* $a_\theta > 1$ *tal que el polígono* $\mathbf{A}_{a,\theta}$*-autosemejante* $\mathcal{K}_N$ *es estrictamente* $\Gamma_{a,\theta}$*-invariante para todo* $a \in (1, a_\theta]$*. Para* $\theta = 2\pi/3$*, existe* $a_\theta > 1$ *tal que* $\Gamma_{a,\theta}^5(\mathcal{K}_2)$ *es un polígono estrictamente* $\Gamma_{a,\theta}$*-invariante de segunda clase para todo* $a \in (1, a_\theta]$*. Consecuentemente, para todo* $0 < \theta < \pi$ *y todo* $a \in (1, a_\theta]$*,*

$$\mathcal{K}_{a,\theta} = \bigcup_{n=1}^{\infty} \Gamma_{a,\theta}^n(\mathcal{K}_N)$$

es un polígono estrictamente $\Gamma_{a,\theta}$*-invariante.*

Para $\theta = 3\pi/4$, se probó [59] que $\mathcal{K}_{a,\theta}$ contiene un atractor extraño bidimensional que puede o bien coincidir con este (véase [56] para $(1+\sqrt{2})^{1/2} < a \leq \sqrt{2}$), o bien ser un atractor extraño bidimensional que se rompe en múltiples piezas o incluso contener un número arbitrariamente grande de atractores extraños [57, 58]. El siguiente resultado generaliza el Teorema 1.2 [59] y establece que el polígono $\mathcal{K}_{a,\theta}$ contiene algún atractor extraño bidimensional para todo $0 < \theta < \pi$.

Teorema 3. *Sea* $0 < \theta < \pi$*. Para todo* $a \in (1, a_\theta]$*, existe una familia finita* $\mathtt{A}_{a,\theta}$ *de atractores extraños bidimensionales de* $\Gamma_{a,\theta}$ *con interior no vacío que verifican las siguientes propiedades:*

(I) Todo atractor de $\Gamma_{a,\theta}$ *en* $\mathcal{K}_{a,\theta}$ *pertenece a* $\mathtt{A}_{a,\theta}$*.*

(II) Para cada $\mathcal{A} \in \mathtt{A}_{a,\theta}$ *existe una medida de probabilidad* μ *invariante, absolutamente continua y ergódica de* $\Gamma_{a,\theta}$ *soportada en* $\mathcal{A}$*.*

(III) Para cada $\mathcal{A} \in \mathtt{A}_{a,\theta}$ *existe un número natural* $\mathtt{b}$ *y una descomposición*

$$\mathcal{A} = \mathcal{X}_0 \cup \mathcal{X}_1 \cup \cdots \cup \mathcal{X}_{\mathtt{b}-1}$$

de $\mathcal{A}$ *de modo que* $\Gamma_{a,\theta}(\mathcal{X}_j) = \mathcal{X}_{j+1 \bmod \mathtt{b}}$ *para* $j = 0, \ldots, \mathtt{b}-1$*. La medida* μ *soportada en* $\mathcal{A}$ *es* mixing *(de periodo* $\mathtt{b}$*) y por lo tanto* $\Gamma_{a,\theta}^{\mathtt{b}}$ *es topológicamente* mixing *en todo* $\mathcal{X}_j$*.*

(IV) Si $\mathcal{A} \in \mathtt{A}_{a,\theta}$*, entonces* $\mathcal{A}$ *atrapa casi todo punto de* $W^s(\mathcal{A})$*. Es decir: para casi todo* $P \in W^s(\mathcal{A})$ *existe* $j \in \mathbb{N}$ *con* $\Gamma_{a,\theta}^j(P) \in \mathcal{A}$*. Más aún, el conjunto* $\bigcup_{\mathcal{A} \in \mathtt{A}_{a,b}} W^s(\mathcal{A})$ *recubre un conjunto de medida de Lebesgue total de* $\mathcal{K}_{a,\theta}$*.*

(V) Si $\mathcal{K}$ *es un recinto compacto y* $\Gamma_{a,\theta}$*-invariante con interior no vacío, entonces existe* $\mathcal{A} \in \mathtt{A}_{a,\theta}$ *tal que* $\mathcal{A} \subseteq \mathcal{K}$*. Más aún, si* $\mathcal{K}$ *y* $\mathcal{K}'$ *son dos conjuntos compactos y* $\Gamma_{a,\theta}$*-invariantes con interiores no vacíos y disjuntos, entonces existen* $\mathcal{A}, \mathcal{A}' \in \mathtt{A}_{a,\theta}$ *tales que* $\mathcal{A} \subseteq \mathcal{K}$ *y* $\mathcal{A}' \subseteq \mathcal{K}'$*.*

El Teorema 3 se probará de la misma forma que el Teorema 1.2 [59]. No obstante, tenemos que incluir ciertas consideraciones cruciales sobre la *multiplicidad ponderada* que debe ser comprobada para todo θ. Asimismo, cabe mencionar que la prueba del Teorema 3 se basa principalmente en la existencia de un recinto invariante de $\Gamma_{a,\theta}$, que fue dado en el Teorema 2, y de ahí la restricción en el intervalo de parámetros.

De ahora en adelante, consideraremos $\theta = 2\pi p/q \in (0,\pi)$ con $p, q \in \mathbb{N}$ y $\mathrm{mcd}(p,q) = 1$. Los siguientes resultados muestran cómo para todo a suficientemente próximo a 1, el polígono invariante $\mathcal{K}_{a,\theta}$ (y, consecuentemente, el atractor que contiene) se rompe en otro recinto invariante formado por q piezas.

Teorema 4 (Existencia de dominios restrictivos)**.** *Sea* $\theta = 2\pi p/q \in (0,\pi)$ *con* $p, q \in \mathbb{N}$ *y* $\mathrm{mcd}(p,q) = 1$*. Se verifican los siguientes enunciados:*

(a) *Existen* $a_1 = a_1(\theta) > 1$ *y un conjunto* $\mathcal{D} = \mathcal{D}(a,\theta) \subsetneq \mathcal{K}_{a,\theta}$ *tales que, para todo* $a \in (1, a_1)$*, se cumple que*

(I) $\Gamma^n_{a,\theta}(\mathcal{D}) \cap \mathcal{D} = \varnothing$ *para* $n = 1, \ldots, q-1$

(II) $\Gamma^q_{a,\theta}(\mathcal{D}) \subseteq \mathcal{D}$

(b) *Si* $q \geq 4$*, entonces la restricción de* $\Gamma^q_{a,\theta}$ *a* $\mathcal{D}$ *es una* Expanding Baker Map *de dos pliegues.*

Un conjunto que verifique las condiciones (I) y (II) se dice un *dominio restrictivo* de $\Gamma_{a,\theta}$. De acuerdo con el Teorema 4, la aplicación $\Gamma_{a,\theta}$ presenta un atractor extraño de al menos q piezas, cada una de ellas contenida en una de las diferentes iteradas disjuntas de $\mathcal{D}$. Nótese que del enunciado (a) se sigue que $\Gamma^n_{a,\theta}(\mathcal{D}) \cap \Gamma^m_{a,\theta}(\mathcal{D}) = \varnothing$ siempre que $n \neq m$. Como consecuencia de la prueba del Teorema 4 obtenemos el siguiente resultado.

Corolario 1. *Bajo las hipótesis del Teorema 4, el dominio restrictivo* $\mathcal{D}$ *se puede construir de modo que todo atractor de* $\Gamma_{a,\theta}$ *esté contenido en la órbita positiva de* $\mathcal{D}$*.*

Para valores de $a < a_1$ suficientemente próximos a 1, la restricción de $\Gamma^q_{a,\theta}$ a $\mathcal{D}$ tiene un foco inestable P con valores propios $a^q \mathrm{e}^{2\theta_1 \mathrm{i}}$, donde $\theta_1 = 2\pi/q$. La traslación de P al origen de coordenadas y un adecuado cambio de coordenadas permite expresar $\Gamma^q_{a,\theta}$ como la *Expanding Baker Map* de dos pliegues dada por

$$\Psi_{a,\theta} = \mathrm{EBM}(\mathcal{C}, \mathcal{L}_{a,\theta}, \mathcal{O}, \mathbf{A}_{a^q, 2\theta_1})$$

con

$$\mathcal{L}_{a,\theta} \equiv y = x \cot\theta_1 + \rho \csc\theta_1$$

donde $\rho = \rho(a,\theta)$ satisface $\lim_{a\to 1} \rho(a,\theta) = 1$. Sea $\mathbb{F}^k_{\sigma,\varphi}$ la familia de *Expanding Baker Map*

$$\Psi_{\sigma,\varphi} = \mathrm{EBM}(\mathcal{C}, \mathcal{L}_{\sigma,\varphi}, \mathcal{O}, \mathbf{A}^*)$$

verificando las siguientes condiciones:

(R_1) $\mathcal{C}$ es la recta crítica $x = 1$

(R_2) $\mathcal{L}_{\sigma,\varphi}$ es una recta que interseca $\mathcal{C}$ formando un ángulo de $0 < \varphi \leq 2\pi/5$ y cuya distancia a $\mathcal{O}$ es igual a σ.

(R_3) $\mathbf{A}^*(z) = a^q \mathrm{e}^{2\varphi \mathrm{i}} z$.

Así $\Psi_{a,\theta} \in \mathbb{F}^q_{a,\theta_1}$. Consideraremos que $\mathrm{EBM}(\mathcal{C}, \mathcal{O}, \mathbf{A}^*)$ está incluido en $\mathrm{EBM}(\mathcal{C}, \mathcal{L}_{\sigma,\varphi}, \mathcal{O}, \mathbf{A}^*)$, puesto que esto se cumple trivialmente si $\mathcal{L}_{\sigma,\varphi} = \mathcal{C}$ o $\mathcal{L}_{\sigma,\varphi}$ no interseca un cierto recinto invariante sobre el que se estudia la dinámica. Entonces, podemos enunciar un primer enunciado propio de renormalización.

Teorema 5 (Primera renormalización)**.** *Sea* $\theta = 2\pi p/q \in (0, \pi)$ *con* $p, q \in \mathbb{N}$ *y* $\mathrm{mcd}(p,q) = 1$*. Si* $q \geq 4$*, se verifican los siguientes enunciados:*

(a) *Si* q *es impar, entonces existe* $a_2 = a_2(\theta) \in (1, a_1)$ *tal que* $\Psi^q_{a,\theta}$ *tiene un dominio restrictivo* $\widehat{\mathcal{D}} = \widehat{\mathcal{D}}(a,\theta) \subsetneq \mathcal{D}$ *para todo* $a \in (1, a_2)$*.*

(b) *Si* $q = 2\nu$ *es par, entonces se cumple uno de los siguientes enunciados:*

(I) Si ν *es impar, entonces existe* $a_2 = a_2(\theta) \in (1, a_1)$ *tal que* $\Psi^\nu_{a,\theta}$ *tiene un dominio restrictivo* $\widehat{\mathcal{D}} = \widehat{\mathcal{D}}(a,\theta) \subsetneq \mathcal{D}$ *para todo* $a \in (1, a_2)$*.*

(II) Si ν es par, entonces existe $a_2 = a_2(\theta) \in (1, a_1)$ tal que $\Psi^{\nu}_{a,\theta}$ tiene dos dominios restrictivos disjuntos $\widehat{\mathcal{D}}^{\pm} = \widehat{\mathcal{D}}^{\pm}(a,\theta) \subsetneq \mathcal{D}$ para todo $a \in (1, a_2)$. Más aún, la restricción de $\Psi^{\nu}_{a,\theta}$ a cada uno de estos recintos pertenece a $\mathbb{F}^{\nu}_{a^q,\theta_1}$.

El enunciado (II) de (b) sigue cumpliéndose para $\Psi^{\nu/2}_{a,\theta}$ si ν es par, y sucesivamente para toda potencia $q = 2^s$ con $s \geq 2$. Por lo tanto, como consecuencia de los teoremas anteriores y el Teorema B [58] (véase el Lema 2.1.11 en el Capítulo 2), obtenemos el siguiente resultado.

Corolario 2 (Infinitas duplicaciones de atractores)**.** *Sea $\theta = 2\pi p/q \in (0, \pi)$ con $p, q \in \mathbb{N}$ y $\operatorname{mcd}(p, q) = 1$. Si $q = 2^s$ para algún $s \geq 2$, entonces existe una sucesión decreciente*

$$a_1(\theta) > a_2(\theta) > \cdots > a_n(\theta) > a_{n+1}(\theta) > \cdots > 1$$

tal que $\Gamma_{a,\theta}$ presenta 2^{n-1} atractores extraños simultáneamente para todo $a_{n+1}(\theta) \leq a < a_n(\theta)$ y todo $n \geq 1$.

Coexistencia de atractores en la familia cuadrática bidimensional

El comportamiento dinámico de la familia cuadrática bidimensional es más bien complicado, como fue numéricamente señalado por Pumariño y Tatjer [61]. En la Figura 1a se muestra una región $\mathcal{P}$ de parámetros (a_0, b_0) para los que se detectó numéricamente un recinto invariante de T_{a_0,b_0}. Esta región está coloreada según un análisis numérico de los exponentes de Liapunov:

- Región azul: Se corresponde con los valores de los parámetros para los que los dos exponentes de Liapunov son negativos (órbitas periódicas atrayentes)
- Región verde: Se corresponde con los valores de los parámetros para los que un exponente de Liapunov es cero (curvas cerradas atrayentes)
- Región roja: Se corresponde con los valores de los parámetros para los que la suma y el producto de los dos exponentes de Liapunov son negativos (atractores extraños unidimensionales)
- Región negra: Se corresponde con los valores de los parámetros para los que la suma de los dos exponentes de Liapunov es positiva (atractores extraños bidimensionales)

Como señalan los autores, la Figura 1a no muestra la posible coexistencia de atractores. Recojemos en la Figura 1b información adicional que indica la competición entre más de un atractor extraño, como ocurre con $\Gamma_{a,\theta}$.

A partir de la Figura 1b construimos la Figura 2 donde incluimos varios puntos significativos de $\mathcal{P}$ que nos ayudarán a ubicar los enunciados de los siguientes resultados. Así, el punto A es un punto de tangencia de las curvas $4a = (b-1)^2$ y $4a = 1 - 2b - 3b^2$ que delimitan, junto con la recta $4a = 2b - 3$, la región de parámetros (en azul) para los que existe un punto fijo atrayente. Este punto fijo será un foco si $64a + b^4 - 8b^3 + 8b^2 < 0$ y un nodo en caso contrario. La curva $64a + b^4 - 8b^3 + 8b^2 = 0$ interseca la recta $4a = 2b - 3$ en los puntos $B = (1/4, 2)$ y $D = (-7/4, -2)$. Para B, el único punto fijo $(1/2, 1/2)$ es una *singularidad de Bogdanov-Takens* (véase Broer *et al* [8]). Para D, el punto fijo $(-3/2, -1/2)$ tiene un valor propio doble igual a -1. Se prueba que este punto fijo es una singularidad unipotente de T^2_D, pero no de Bogdanov-Takens. A lo largo del segmento $\overline{BD}$ ocurre una bifurcación de Hopf-Neimark-Sacker que explica el nacimiento de curvas cerradas atrayentes.

Empezamos el Capítulo 3 con el estudio de los puntos fijos de $T_{a,b}$, que son los organizadores más simples de su dinámica.

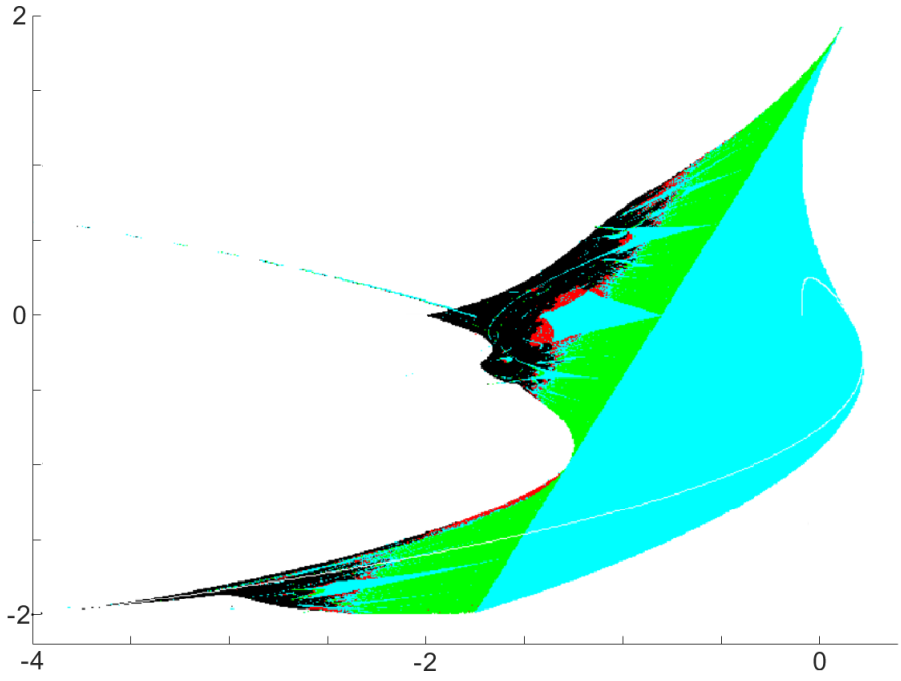

(a)

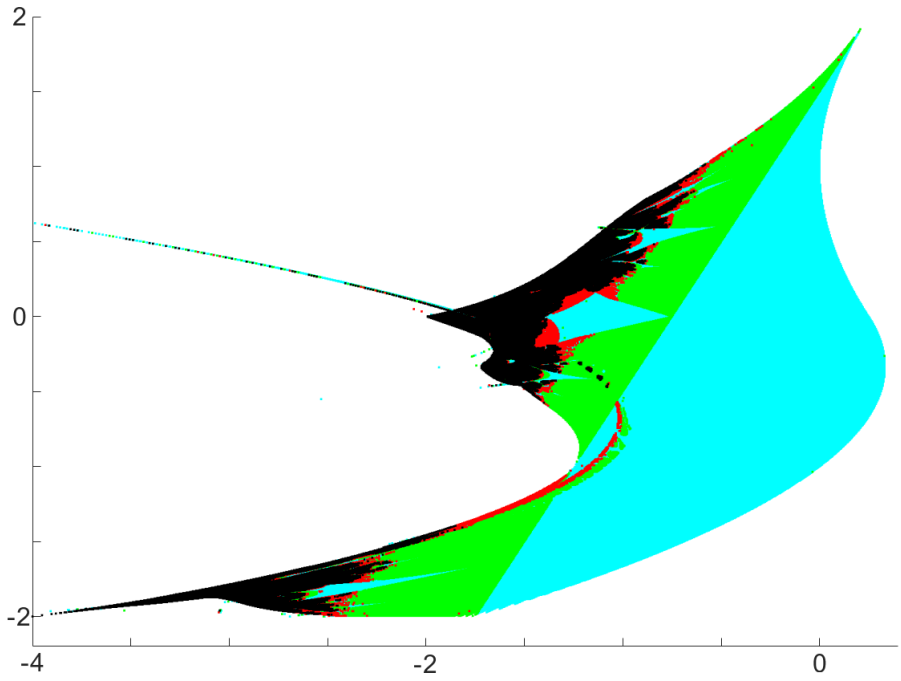

(b)

Figura 1: (a) Las regiones de parámetros originales [61, Fig. 1] coloreadas según el atractor numérico detectado; (b) Aparecen nuevos atractores compitiendo con los encontrados en (a)

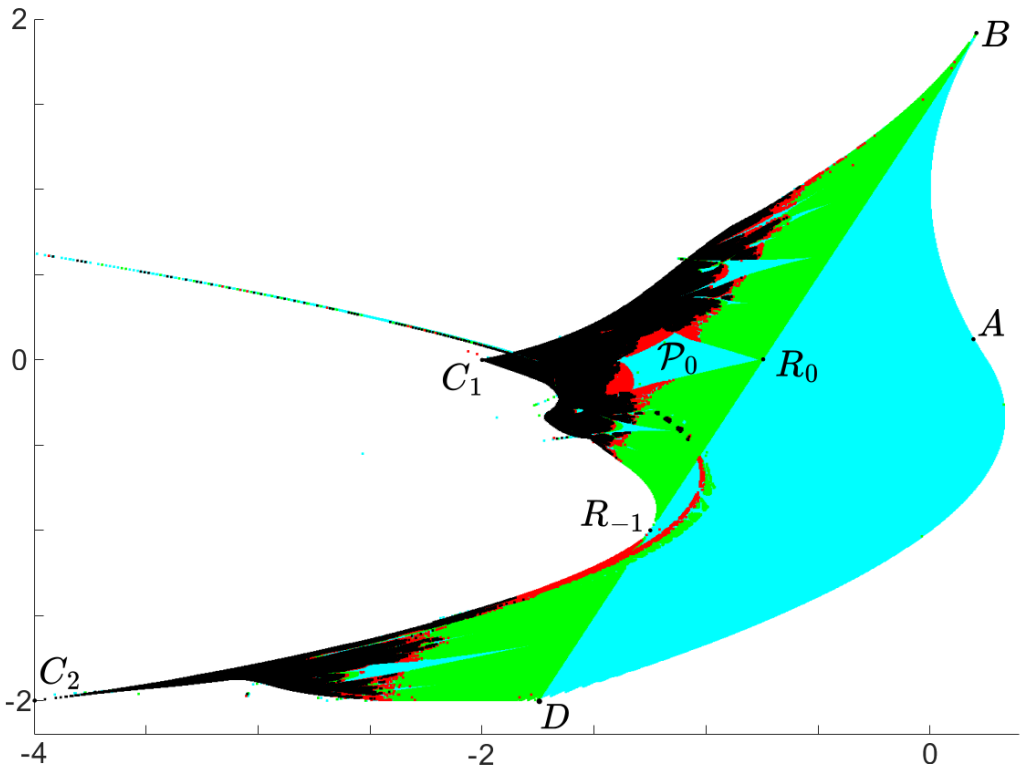

Figura 2: Puntos significativos del plano de parámetros (a, b): $A = (1/4, 0), B = (1/4, 2), C_1 = (-2, 0), C_2 = (-4, -2), D = (-7/4, -2), R_{-1} = (-5/4, -1), R_0 = (-3/4, 0)$

Teorema 6. *Los puntos fijos de la familia cuadrática bidimensional*

$$T_{a,b}(\mathbf{x}, \mathbf{y}) = (a + \mathbf{y}^2, \mathbf{x} + b\mathbf{y})$$

verifican los siguientes enunciados:

a) Si $4a > (b-1)^2$, *entonces* $T_{a,b}$ *no tiene puntos fijos. Más aún: ninguna órbita es acotada.*

b) Si $4a = (b-1)^2$, *entonces* $T_{a,b}$ *tiene un único punto fijo*

$$P^{(1)} = (\tfrac{1}{2}(1-b)^2, \tfrac{1}{2}(1-b))$$

con valores propios $b - 1$ *y* 1. *En particular, para* $(a, b) = (1/4, 2)$, *el punto fijo* $(1/2, -1/2)$ *es una singularidad de Bogdanov-Takens.*

c) Si $4a < (b-1)^2$, *entonces* $T_{a,b}$ *tiene dos puntos fijos diferentes:*

$$P^{(1),\pm} = ((1-b)\mathbf{y}^{\pm}, \mathbf{y}^{\pm}), \qquad \mathbf{y}^{\pm} = \tfrac{1}{2}(1-b) \pm \tfrac{1}{2}\sqrt{(b-1)^2 - 4a}$$

(I) El punto fijo $P^{(1),-}$ *es un foco si y solo si*

$$64a + b^4 - 8b^3 + 8b^2 < 0, \quad 4a \neq 2b - 3$$

Este foco es atrayente si $4a > 2b - 3$ *y repelente en otro caso. A lo largo del segmento*

$$4a = 2b - 3, \qquad -2 < b < 2$$

el punto fijo $P^{(1),-}$ *es un centro. Más aún, una bifurcación de Hopf-Neimark-Sacker ocurre en* $P^{(1),-}$ *para* $b \neq -1, 0$. *La curva* $64a + b^4 - 8b^3 + 8b^2 = 0$ *interseca el segmento* $4a = 2b - 3$ *en los puntos* $B = (1/4, 2)$ *y* $D = (-7/4, -2)$. *Para* $(a, b) = D$, *el punto fijo* $P^{(1),-}$ *tiene un valor propio doble igual a* -1. *Es una singularidad unipotente de* T^2_D, *pero no de Bogdanov-Takens.*
Si $64a + b^4 - 8b^3 + 8b^2 \geq 0$, *entonces* $P^{(1),-}$ *es un nodo si y solo si* $b \geq 0$ *o*

$$4a + 3b^2 + 2b - 1 < 0, \qquad b < 0$$

Este nodo es atrayente si $-2 < b < 2$ *y repelente en otro caso. Si*

$$4a + 3b^2 + 2b - 1 > 0, \qquad b < 0$$

entonces $P^{(1),-}$ *es un punto de silla que es disipativo si y solo si*

$$2b + 3 < 4a < 1 - 2b$$

(II) *El punto fijo* $P^{(1),+}$ *es un nodo repelente si* $b \leq 0$ *o*

$$4a + 3b^2 + 2b - 1 < 0, \qquad b > 0$$

Si

$$4a + 3b^2 + 2b - 1 > 0, \qquad b > 0$$

entonces $P^{(1),+}$ *es un punto de silla que es disipativo si y solo si* $4a > 1 - 2b$ *y*

$$4a < 2b - 3, \qquad b > 2$$

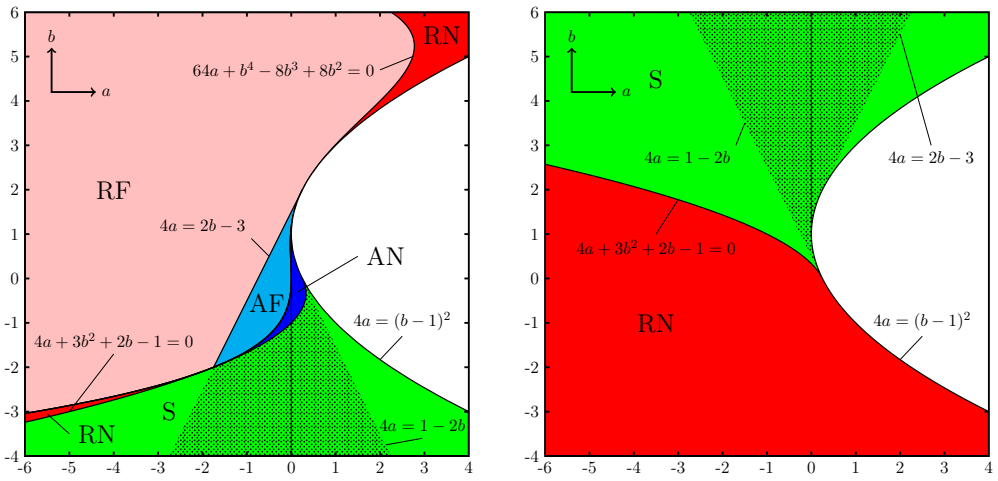

(a) (b)

Figura 3: (a) Configuración de la estabilidad de $P^{(1),-}$ en (a, b): AN (azul): nodo atrayente; RN (rojo): nodo repelente; AF (cian): foco atrayente; RF (rosa): foco repelente; S (verde): punto de silla, punteado: disipativo. A lo largo de $a = 0$ con $b \leq 1$, un valor propio es cero. (b) Configuración de la estabilidad de $P^{(1),+}$ en (a, b): RN (rojo): nodo repelente; S (verde): punto de silla, punteado: disipativo. A lo largo de $a = 0$ con $b \geq 1$, un valor propio es cero.

A la izquierda del segmento $\overline{BD}$, ninguno de los dos puntos fijos es atrayente. Sin embargo, podemos encontrar subregiones de $\mathcal{P}$ para las que se prueba la existencia de

órbitas periódicas atrayentes. Este es el caso de las región afilada $\mathcal{P}_0$ en azul que tiene su vértice R_0 en $\overline{BD}$. Véase la Figura 2. Ciertamente, el punto R_0, así como R_{-1}, se corresponde con valores de los parámetros para los que ciertas resonancias impiden la bifurcación de Hopf-Neimark-Sacker. Más aún, a la derecha de $\overline{BD}$ existen valores de los parámetros para los que, además del punto fijo atrayente, también existen órbitas periódicas atrayentes, curvas cerradas y atractores extraños unidimensionales. Esta coexistencia se puede explicar tras un estudio selectivo de la existencia de órbitas periódicas de periodo bajo.

Primero estudiaremos la existencia de órbitas 2-periódicas para concluir que ninguna es atrayente. Después, probaremos la existencia de órbitas 2^n-periódicas para $n \geq 2$ en la región $\mathcal{P}_0$. Mayor interés tendrá probar la existencia de órbitas 3-periódicas a lo largo de la recta $b = -1$, que corta transversalmente a $\mathcal{P}$ a través del punto R_{-1}. Para este caso, probaremos que dos familias de órbitas 3-periódicas pueden aparecer. Véase la Figura 4.

A partir de una de ellas se originan curvas cerradas atrayentes (véase la Figura 5) que colisionan con la otra órbita de tipo silla dando lugar a una órbita homoclínica, tal y como fue numéricamente comprobado en la Figura 6. Al desplegar estas tangencia homoclínicas tiene lugar la formación de atractores extraños unidimensionales [44]. Las transiciones se representan en la Figura 7 para $b = -1$ en un intervalo de valores de a.

Teorema 7. *Se cumplen los siguientes enunciados sobre las órbitas periódicas de la familia cuadrática bidimensional:*

1. *Existe una órbita* 2*-periódica si y solo si*

$$4a < 1 - 2b - 3b^2$$

En tal caso, es única. Más aún, es un nodo repelente si

$$4a < -3 - 6b - 5b^2$$

Si $4a > -3 - 6b - 5b^2$*, entonces es una órbita periódica de tipo silla que es disipativa si y solo si*

$$4a > -1 - 4b - 4b^2$$

y bien $-2 < b < 0$ *o bien* $4a < 1 - 4b - 4b^2$*.*

2. *Sea* $b = 0$*. Existe una sucesión decreciente*

$$-2 < \cdots < a_{n+1} < a_n < \cdots < a_3 < a_2 = -\tfrac{3}{4}$$

de valores de a *tal que existe una órbita* 2^n*-periódica atrayente para todo* $a_{n+1} < a < a_n$ *y todo* $n \geq 2$*.*

3. *Sea* $b = -1$*. Existe una órbita* 3*-periódica si y solo si* $a \leq -1$*. Más aún:*

   (a) *Si* $a = -1$ *o* $a = -5/4$*, entonces existe una única órbita* 3*-periódica* $\mathcal{P}^{(3)}$*. Si* $a = -1$*, entonces*

$$\mathcal{P}^{(3)} = \{(0,0), (-1,0), (-1,-1)\}$$

   con valores propios 0 *y* 1*. Si* $a = -5/4$*, entonces*

$$\mathcal{P}^{(3)} = \{(1, \tfrac{1}{2}), (-1, \tfrac{1}{2}), (-1, -\tfrac{3}{2})\}$$

   con valores propios $\pm \mathrm{i}\sqrt{3}$*.*

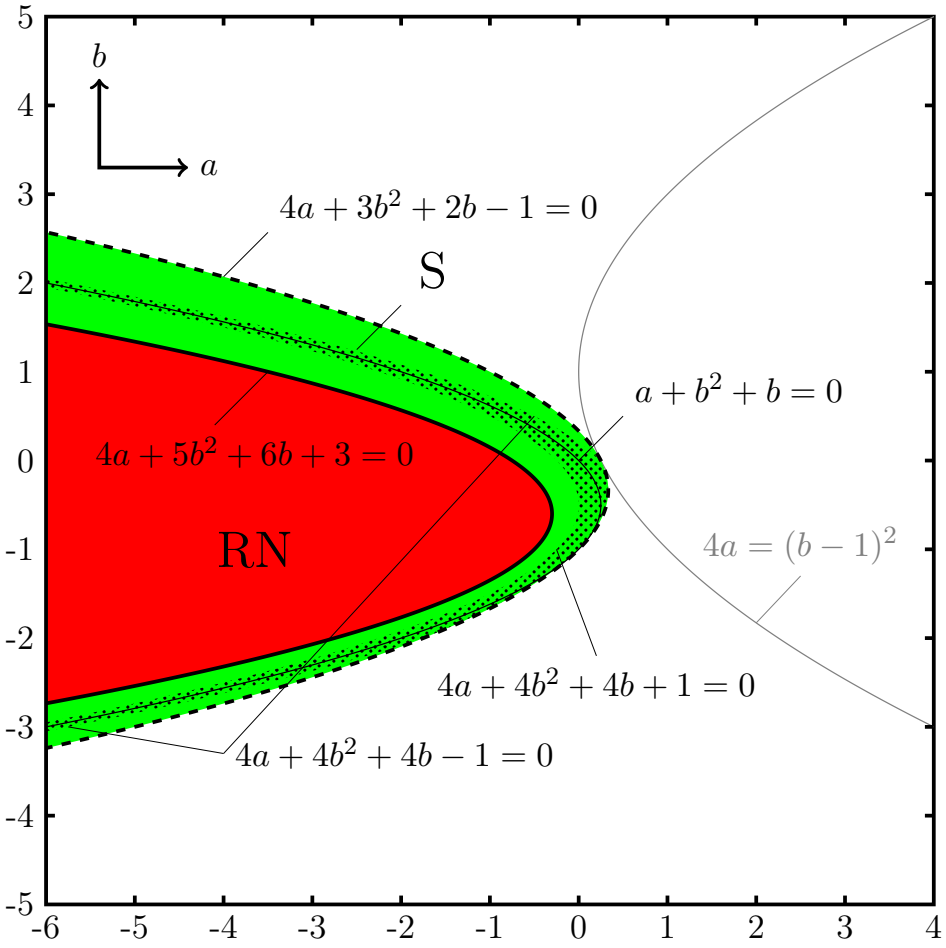

(a)

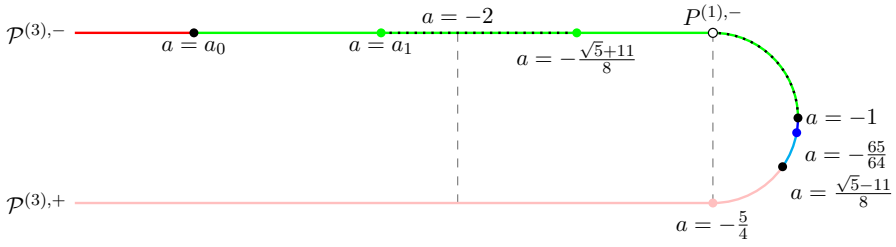

(b)

Figura 4: (a) Configuración de la estabilidad de la única órbita 2-periódica de $T_{a,b}$: RN (rojo): nodo repelente; S (verde): punto de silla, punteado: disipativo. A lo largo de $a + b^2 + b = 0$, un valor propio es cero. (b) Configuración de la estabilidad de las dos órbitas 3-periódicas $\mathcal{P}^{(3),\pm}$ de $T_{a,b}$ para $b = -1$: nodo atrayente (azul); nodo repelente (rojo); foco atrayente (cian); foco repelente (rosa); punto de silla (verde), punteado: disipativo. Para $a = -5/4$, la órbita $\mathcal{P}^{(3),-}$ colapsa con el punto fijo $P^{(1),-}$.

(b) *Si* $a \in (-\infty, -1) \setminus \{-5/4\}$, *entonces existen dos órbitas 3-periódicas* $\mathcal{P}^{(3),\pm}$ *diferentes.*

(I) *La órbita* $\mathcal{P}^{(3),-}$ *es de tipo silla disipativa si* $a > -5/4$. *Existe* $a_0 < -2$ *tal que* $\mathcal{P}^{(3),-}$ *es un nodo repelente si* $a < a_0$ *y una órbita periódica de tipo silla si* $a_0 < a < -5/4$, *que es disipativa si y solo si* $a_1 < a < -(11+\sqrt{5})/8$ *para algún* $a_0 < a_1 < -2$. *Para* $a = a_0$, *la órbita* $\mathcal{P}^{(3),-}$ *tiene un valor propio igual a* -1.

(II) *La órbita* $\mathcal{P}^{(3),+}$ *es un nodo atrayente si* $a \geq -65/64$. *Para* $a < -65/64$, *la órbita* $\mathcal{P}^{(3),+}$ *es un foco si y solo si* $a \neq (\sqrt{5}-11)/8$. *Este foco es atrayente si* $a > (\sqrt{5}-11)/8$ *y repelente en otro caso. Para* $a = (\sqrt{5}-11)/8$, *ocurre una bifurcación de Hopf-Neimark-Sacker.*

4. *Para cada* $n \in \mathbb{N}$, *existe un recinto compacto (que depende de* a *y* b*) con interior no vacío que contiene a todas la órbitas periódicas de periodo* n.

Antes de tratar de probar la persistencia de atractores extraños bidimensionales, observamos que la región en negro parece surgir tanto de C_1 como de C_2. Así, primero construiremos recintos compactos invariantes con interior no vacío para valores de los parámetros en regiones afiladas con vértices C_1 y C_2, respectivamente. Probaremos el siguiente resultado.

Teorema 8. *Cada* $(a^*, b^*) \in \{(-2, 0), (-4, -2)\}$ *es el vértice de una región afilada* $\mathcal{V}(a^*, b^*)$ *tal que, para todo* $(a, b) \in \mathcal{V}(a^*, b^*)$, *existe un recinto compacto y* $T_{a,b}$*-invariante con interior no vacío.*

Como consecuencia de la prueba del Teorema 8, obtenemos más información sobre la curva de parámetros $2a = b^3$. Una simulación numérica de los atractores a lo largo de esta curva recuerda a los obtenidos a lo largo de la curva G, aunque conseguimos aún más información en este caso.

Teorema 9. *Para valores de los parámetros a lo largo de la curva* $2a = b^3$, *se cumplen los siguientes enunciados:*

1) *Para* $b = -2$, *el triángulo curvilíneo* $\mathcal{K}$ *delimitado por las tres primeras iteradas de la recta crítica es estrictamente* $T_{-4,-2}$*-invariante. Más aún, es un atractor extraño bidimensional sobre el que la medida de Lebesgue es invariante y ergódica.*

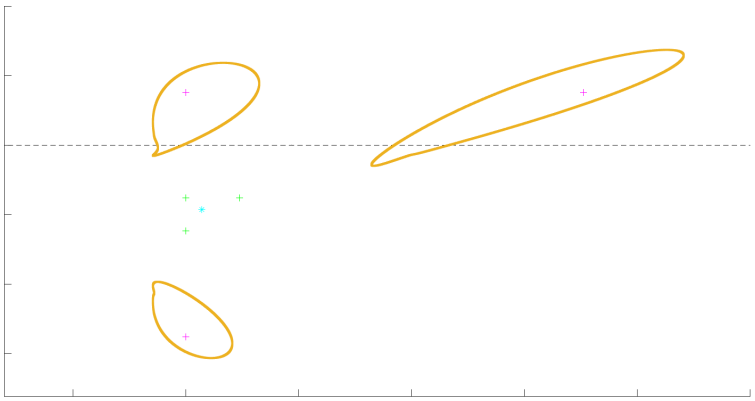

Figura 5: El foco 3-periódico repelente en magenta para $(a, b) = (-1.1145, -1)$ da lugar a tres ciclos límite que se aproximan a la órbita 3-periódica de tipo silla disipativa en verde, que a su vez se aproxima al foco fijo atrayente en cian

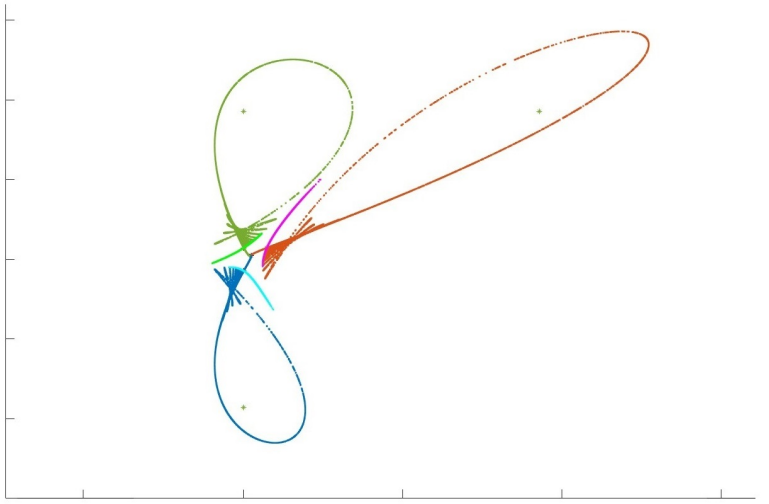

(a)

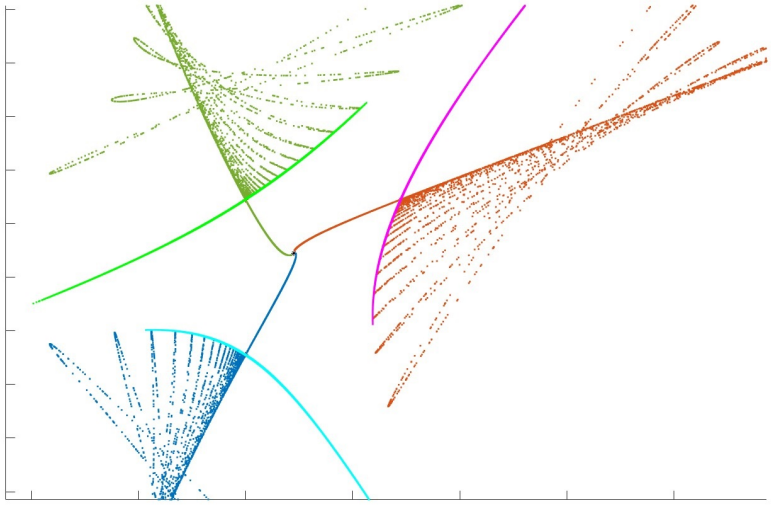

(b)

Figura 6: Tangencias homoclínicas desplegando atractores extraños unidimensionales para $(a, b) = (-1.18282, -1)$. (b) Ampliación de (a).

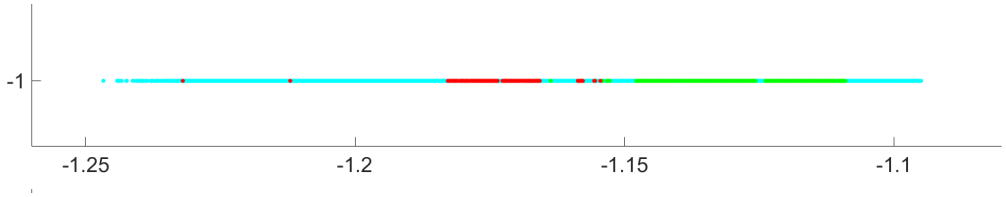

Figura 7: Diferentes transiciones para $b = -1$ con $a \in [-5/4, -1]$ coloreados como la Figura 1b

2) Si $b > -2$, entonces $\mathcal{K}$ es $T_{a,b}$-invariante, pero no en sentido estricto. Además, el triángulo curvilíneo $\mathcal{K}$ contiene al pentágono curvilíneo delimitado por las primeras cinco iteradas de la recta crítica, que es estrictamente $T_{a,b}$-invariante para todo $-2 < b < b_1$, para un cierto $b_1 > -2$.

3) Si $b < -2$, entonces no existen recintos compactos y estrictamente $T_{a,b}$-invariantes con interior no vacío.

Para $b > b_1$, esperamos que surjan polígonos curvilíneos estrictamente invariantes de un mayor número de lados.

Tras unos adecuados cambios de variables y parámetros, la aplicación $T_{a,b}$ puede escribirse como

$$F_{c,b}(x, y) = (y, cx(2 - x) + by)$$

donde

$$c = \tfrac{1}{2}(1 - b - \delta), \qquad \delta = \sqrt{(b-1)^2 - 4a}$$

Con frecuencia, esta nueva expresión será más útil para estudiar la dinámica. Más aún, la familia $F_{c,b}$ se puede expresar como la composición de un difeomorfismo con un pliegue. Esto permite comparar $F_{c,b}$ con $\Gamma_{a,\theta}$.

Problemas abiertos

A partir del estudio analítico y geométrico desarrollado a lo largo de esta memoria, surgen muchas cuestiones abiertas, todas ellas avaladas por la correspondiente experimentación numérica. Aparte de la prueba analítica de la persistencia de atractores extraños bidimensionales, la mayoría de los resultados de renormalización obtenidos para $\Gamma_{a,\theta}$ sugieren retos similares para una mejor descripción de la dinámica de $T_{a,b}$. De hecho, un proceso de renormalización completo para las *Expanding Baker Map* todavía no ha sido desarrollado. Además, algunos resultados sobre estabilidad estadística verificados por Λ_t tampoco han sido probados todavía. En esta breve sección final introductoria tratamos todos estos temas de investigación futura.

Minimalidad del dominio poligonal

Si el polígono estrictamente invariante $\mathcal{K}_{a,\theta}$ es minimal (es decir, no contiene ningún subconjunto compacto e invariante con interior no vacío aparte de sí mismo), entonces es un atractor por definición. En tal caso, dicho polígono contiene una órbita densa con dos exponentes de Liapunov positivos y, por lo tanto, es un atractor extraño bidimensional.

Sea $\mathcal{K}^*_{a,\theta} = \mathcal{K}_{a,\theta} \cap \{x \geq 1\}$. Los experimentos numéricos sugieren que $\mathcal{K}_{a,\theta}$ es minimal si y solo si $\mathcal{O} \in \mathcal{F}_{\mathcal{C},\mathcal{O}}(\mathcal{K}^*_{a,\theta})$, esto es, si y solo si $(2, 0) \in \mathcal{K}^*_{a,\theta}$. A medida que a decrece, el conjunto plegado $\mathcal{F}_{\mathcal{C},\mathcal{O}}(\mathcal{K}^*_{a,\theta})$ encoje y existe un valor a^* de a tal que $\mathcal{O} \in \mathcal{F}_{\mathcal{C},\mathcal{O}}(\mathcal{K}^*_{a,\theta})$ para $a = a^*$ y $\mathcal{O} \notin \mathcal{F}_{\mathcal{C},\mathcal{O}}(\mathcal{K}^*_{a,\theta})$ para todo $a < a^*$.

Conjetura. *Sea $0 < \theta < \pi$. El polígono estrictamente invariante $\mathcal{K}_{a,\theta}$ es minimal si y solo si $(2, 0) \in \mathcal{K}^*_{a,\theta}$.*

Para $\theta = 3\pi/4$, se prueba [54] que $(2, 0) \in \mathcal{K}^*_{a,\theta}$ si y solo si $a \geq \sqrt[6]{2}$. Más aún, se prueba [56] que $\mathcal{K}_{a,\theta}$ es transitivo para todo $(1+\sqrt{2})^{1/4} \leq a \leq \sqrt{2}$. La expansividad de $\Gamma_{a,\theta}$ para estos valores de a garantiza entonces que $\mathcal{K}_{a,\theta}$ es un atractor extraño. Para valores de a ligeramente más pequeños, se mostró numéricamente [54, 55] que el pentágono $\mathcal{K}_{a,\theta}$ pierde su minimalidad para contener otro atractor que es conexo, pero no simplemente conexo: tiene un agujero alrededor del origen. Este agujero se expande a medida que a decrece hasta

que el atractor se rompe en ocho piezas conexas para valores de a ligeramente menores que $a = \sqrt[10]{2}$. Esto motiva la siguiente conjetura.

Conjetura. *Sea $0 < \theta < \pi$. Sea $a_0' > 1$ el mínimo de los valores de a para los que $(2,0) \in \mathcal{K}_{a,\theta}$. Entonces, existe $a_0'' \in [1, a_0')$ tal que, para todo $a \in [a_0'', a_0')$, existe un entorno conexo $\mathcal{U}_{a,\theta}$ de $\mathcal{O}$ tal que $\mathcal{K}_{a,\theta} \setminus \mathcal{U}_{a,\theta}$ es estrictamente invariante y minimal (por lo tanto, un atractor extraño conexo, pero no simplemente conexo). Más aún, se cumple que $a_0'' = 1$ si y solo si θ/π es un número irracional.*

Los experimentos numéricos también parecen avalar esta conjetura. Véanse las Figuras 8, 9 y 10. Una aproximación numérica al caso irracional no es posible, por lo que solo se puede intentar probar analíticamente.

Renormalizaciones superiores: una sucesión de rupturas y duplicaciones de atractores

En el caso racional, conjeturamos que tiene lugar un proceso de ruptura y/o duplicación de atractores para una sucesión de valores de a en $(1, a_0'')$. Esto es de veras una ardua tarea que requiere controlar un complicado proceso de renormalización. Dado $\theta = 2\pi p/q \in (0, \pi)$ con $p, q \in \mathbb{N}$ y $\mathrm{mcd}(p,q) = 1$, hemos probado la existencia de dos rupturas consecutivas del recinto estrictamente invariante, y por lo tanto del atractor extraño que contiene, para $q \geq 4$ (una sola ruptura para $q = 3$). Sin embargo, cuando bien q es impar o bien q es par y $q/2$ impar, para el estudio de una posible tercera renormalización es necesario considerar una *Expanding Baker Map* de tres pliegues. Entonces, pararece natural preguntarse si el proceso de ruptura finaliza en algún punto o si se pueden llevar a cabo renormalizaciones superiores considerando *Expanding Baker Map* de más pliegues. Un posible incremento en el número de pliegues podría hacer este problema analíticamente intratable.

Después de la prueba del Teorema 5, podemos formular una primera conjetura en los siguientes términos.

Conjetura. *Para cada $m \in \{0, 1, \ldots, \infty\}$, sea S_m el m-ésimo nivel del orden de Sarkovskii:*

$$
\begin{aligned}
&S_0 : 3 \rhd 5 \rhd 7 \rhd 9 \rhd \cdots \\
&S_1 : 3 \times 2 \rhd 5 \times 2 \rhd 7 \times 2 \rhd \cdots \\
&\cdots \\
&S_m : 3 \times 2^m \rhd 5 \times 2^m \rhd 7 \times 2^m \rhd \cdots \\
&\cdots \\
&S_\infty : \cdots \rhd 2^n \rhd \cdots \rhd 2^3 \rhd 2^2 \rhd 2 \rhd 1
\end{aligned}
$$

Entonces, se verifican los siguientes enunciados:

(I) Para todo $q \in S_1 \cup S_0 \setminus \{3\}$ existe una sucesión infinita de ruptura de atractores.

(II) Para todo $q \in S_m$ con $2 \leq m < \infty$ existen $m-1$ duplicaciones seguidas de una sucesión infinita de ruptura de atractores.

(III) Para todo $q \in S_\infty \setminus \{1, 2\}$ existe una sucesión infinita de duplicación de atractores.

Sabemos por el Corolario 2 que el enunciado (III) es cierto. Numéricamente, algunas simulaciones en la Figura 8 muestran que para $q = 7$ cada una de las 49 piezas obtenidas para $a = 1.006$ se rompen otra vez en otras 7 piezas como se muestra para $a = 1.0006$. En la Figura 11 mostramos el caso $q = 24$ para $a = 1.0001$ en el que cada una de las 24 piezas del atractor inicial se ha roto en 12 piezas, después en 6, y finalmente en 3. En la Figura 12 mostramos para $q = 8$ la coexistencia de dos atractores extraños de 32 piezas para $a = 1.01$.

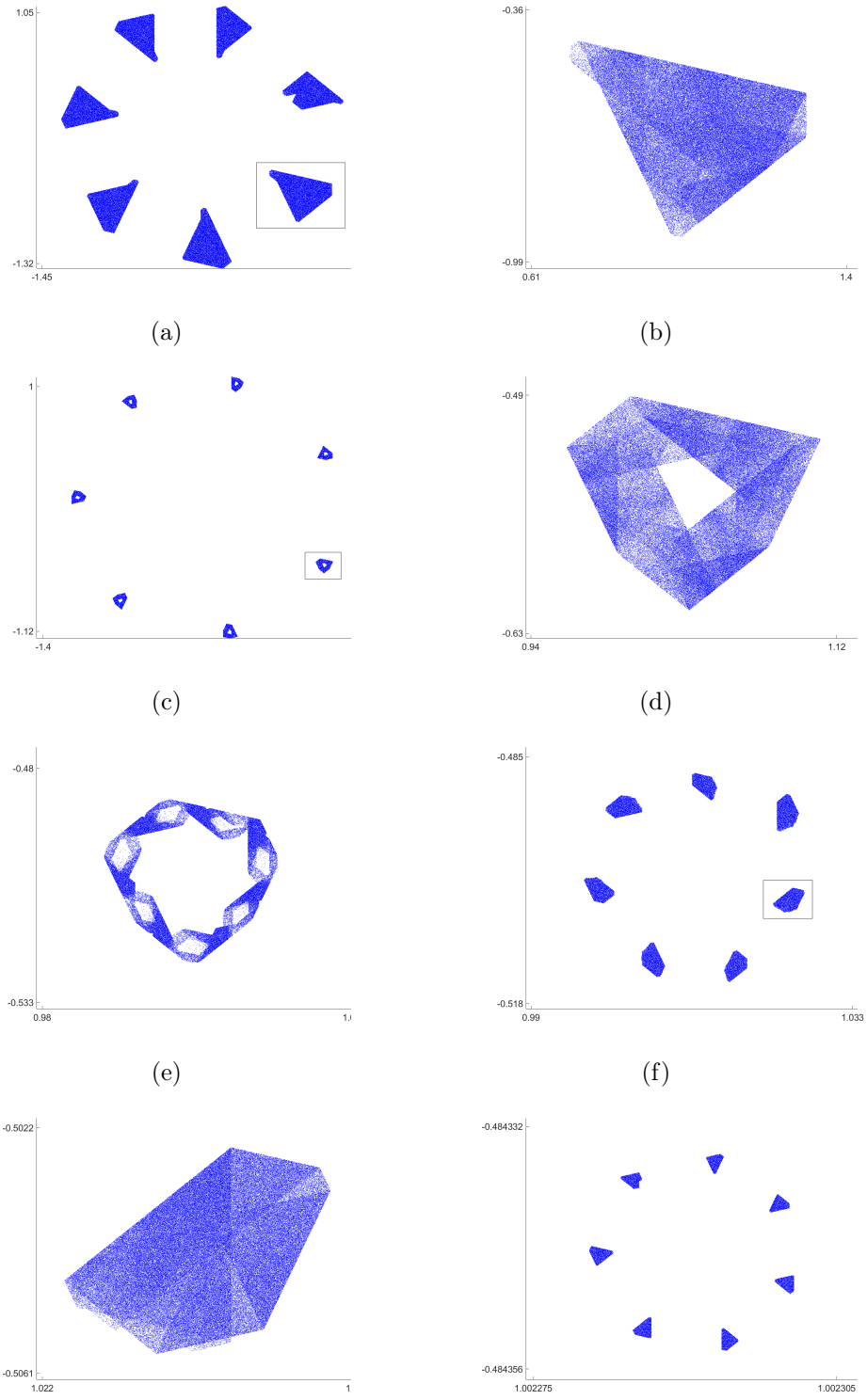

Figura 8: Simulación numérica para $\theta = 2\pi/7$ y valores decrecientes de a: (a) Un atractor de 7 piezas para $a = 1.05$; (b) Ampliación de una pieza en (a); (c) Un atractor de 7 piezas con agujeros para $a = 1.02$; (d) Ampliación de una pieza en (c); (e) Evolución de (d) antes de la ruptura; (f) Ruptura de (d) para $a = 1.006$; (g) Ampliación de una pieza en (f); (h) Ruptura de (g) para $a = 1.0006$.

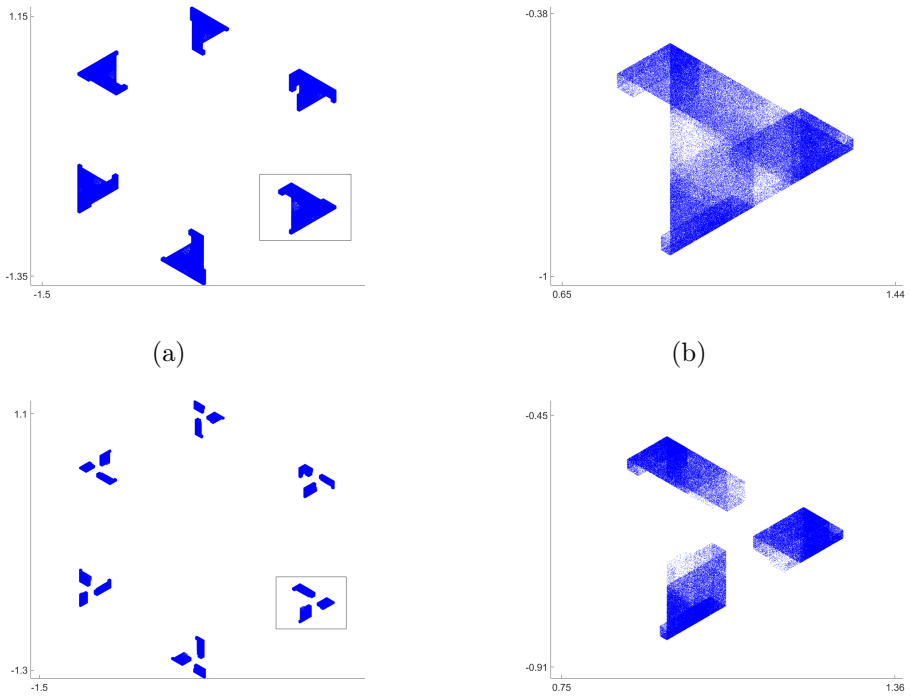

(a) (b)

(c) (d)

Figura 9: Simulación numérica para $\theta = 2\pi/6$ y valores decrecientes de a: (a) Un atractor de 6 piezas para $a = 1.05$; (b) Ampliación de una pieza en (a); (c) Ruptura de (b) para $a = 1.04$; (d) Ampliación de una pieza en (c).

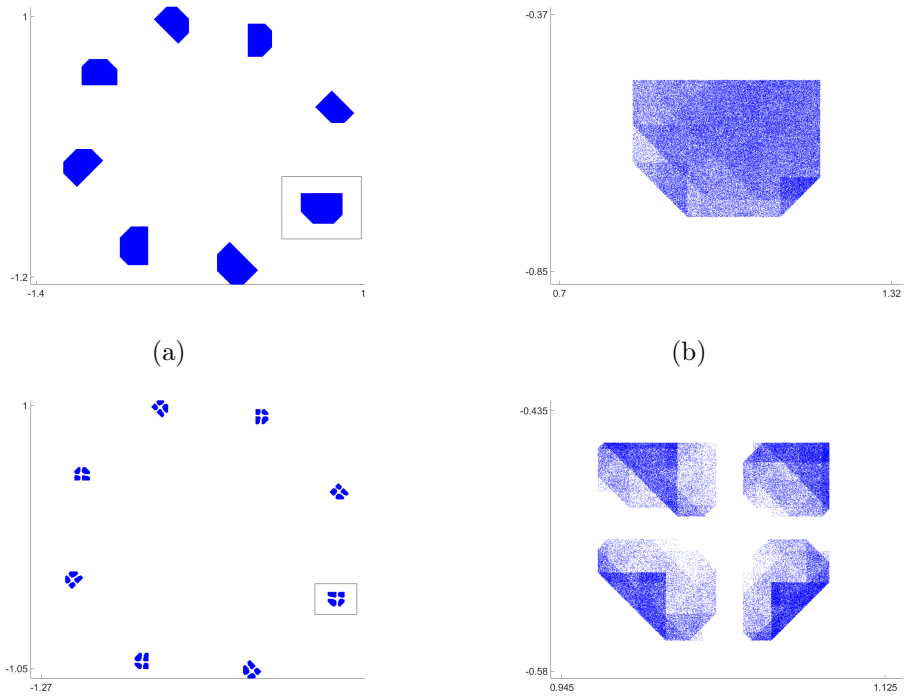

(a) (b)

(c) (d)

Figura 10: Simulación numérica para $\theta = 2\pi/8$ y valores decrecientes de a: (a) Un atractor de 8 piezas para $a = 1.05$; (b) Ampliación de una pieza en (a); (c) Ruptura de (b) para $a = 1.02$; (d) Ampliación de una pieza en (c).

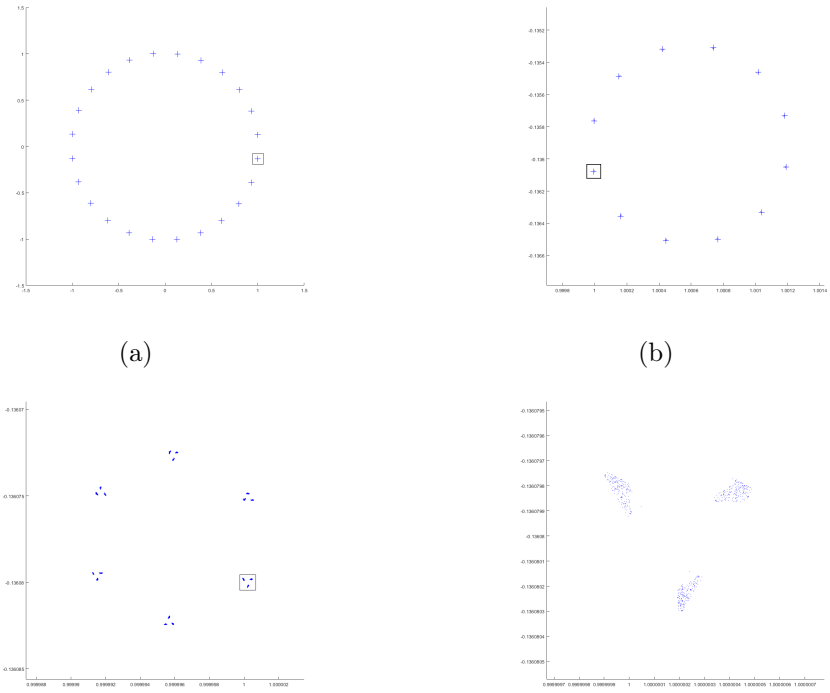

(a) (b)

(c) (d)

Figura 11: Simulación numérica para $\theta = 2\pi/24$ y $a = 1.0001$: (a) El atractor de $24 \times 12 \times 6 \times 3$ piezas; (b) Ampliación de una pieza en (a); (c) Ampliación de una pieza en (b); (d) Ampliación de una pieza en (c).

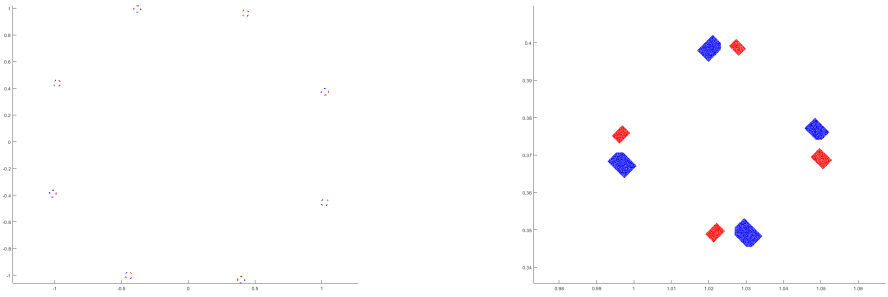

(a) (b)

Figura 12: Coexistencia de atractores para $\theta = 2\pi/8$: (a) Dos atractores de 32 piezas para $a = 1.01$; (b) Ampliación de 4 piezas de los dos atractores en (a).

Estabilidad estadística de la familia biparamétrica general de *Expanding Baker Map*

Fijemos $0 < \theta < \pi$ y tomemos a_θ del Teorema 2. De la misma definición de $\mathcal{K}_N$, se seguirá que $\mathcal{K}_{a_\theta,\theta}$ es $\Gamma_{a,\theta}$-invariante para todo $1 < a \leq a_\theta$. Por lo tanto, la familia uniparamétrica $\Gamma_{a,\theta}\colon \mathcal{K}_{a_\theta,\theta} \to \mathcal{K}_{a_\theta,\theta}$ con $a \in (1, a_\theta]$ está bien definida y podemos plantearnos cuestiones como la estabilidad estadística.

Conjecture. *Para todo $0 < \theta < \pi$, la familia $\{\Gamma_{a,\theta}\}_{1<a\leq a_\theta}$ es estadísticamente estable.*

El caso singular $q = 3$

Un estudio sobre todas las cuestiones anteriores, así como las particulares, debería llevarse a cabo para el ángulo $\theta = 2\pi/3$. Véase la Figura 13.

Conjetura. *Sea $\theta = 2\pi/3$. Entonces, existe $\tilde{a} > a_\theta$ tal que $\mathcal{K}_{a,\theta}$ es un polígono compacto si $a \leq \tilde{a}$ y $\mathcal{K}_{a,\theta} = \Gamma^2_{a,\theta}(\mathbb{R}^2)$ en caso contrario.*

Conjetura. *Sea $\theta = 2\pi/3$. Entonces, existe una sucesión infinita de ruptura de atractores.*

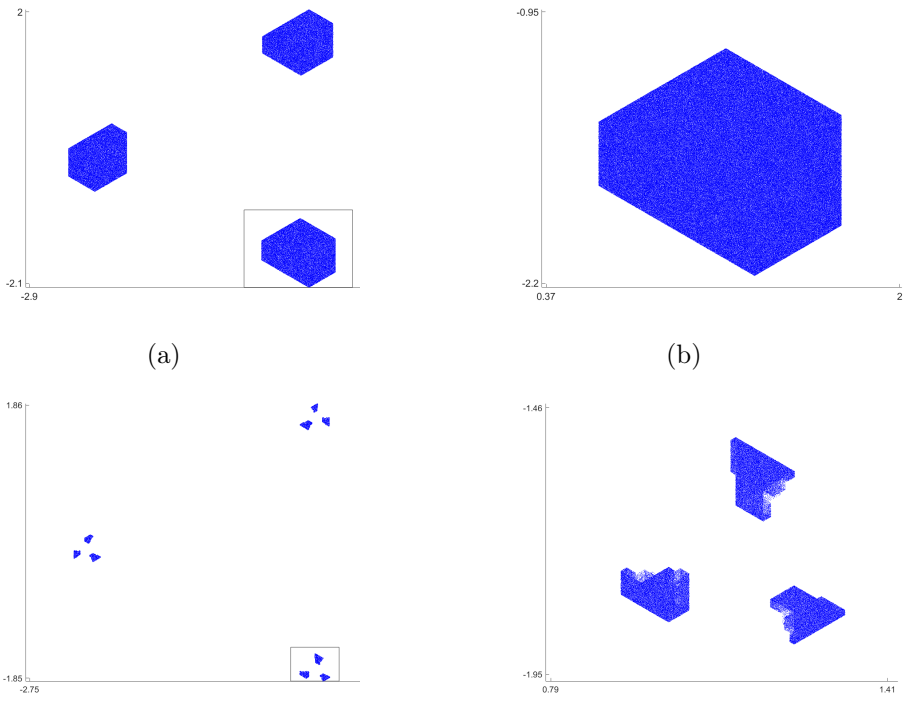

(a) (b)

(c) (d)

Figura 13: Simulación numérica para $\theta = 2\pi/3$ y valores decrecientes de a: (a) Un atractor de 3 piezas para $a = 1.1$; (b) Ampliación de una pieza en (a); (c) Ruptura de (b) para $a = 1.05$; (d) Ampliación de una pieza en (c).

Cálculo de todas las órbitas periódicas de periodo tres

La condición $b = 1$ simplifica el cálculo de las órbitas periódicas de periodo tres. La experimentación numérica confirma que la región de forma parabólica cuya frontera parece encajar con uno de los *pelos* de la región de parámetros $\mathcal{P}$ coincide con las región de existencia de todas dichas órbitas.

Conjetura. *La curva de la Figura 1b que pasa por* $(a, b) = (-1, -1)$ *y que coincide con el* pelo *mayoritariamente azul delimita la región de existencia de las órbitas periódicas de periodo tres.*

Puntos de densidad de atractores extraños bidimensionales

El estudio de la estabilidad de las órbitas periódicas, y muy especialmente la atención prestada a los casos no hiperbólicos, permite probar la existencia de tres de los cuatro tipos de atractores que habían sido detectados numéricamente en la Figura 1, a saber: órbitas periódicas atrayentes, curvas cerradas y atractores extraños unidimensionales. Sin embargo, la existencia de atractores extraños bidimensionales como los que fueron numéricamente detectados en la Figura 1 debe involucrar el carácter no inyectivo de las aplicaciones cuadráticas. Solo así un recinto $\mathcal{K}$ compacto e invariante puede contener a su imagen expandida, pero doblada. Esto es, la aplicación cuadrática bidimensional no puede ser inyectiva en el atractor extraño bidimensional. En otras palabras, el recinto $\mathcal{K}$ debe intersecar la recta crítica $y = 0$. Por esta razón, buscaremos aquí recintos $\mathcal{R}_{a,b}$ compactos e invariantes con interior no vacío que intersequen $y = 0$. Por supuesto, tales recintos $\mathcal{R}_{a,b}$ no son necesariamente atractores extraños bidimensionales. Es preciso que contengan una órbita densa con dos exponentes de Liapunov cuya suma sea positiva. Además, para que tal atractor extraño bidimensional sea observable, es necesario que sea persistente. Para el inicio de la prueba de la persistencia de tales atractores nos colocaremos en los puntos $C_1 = (-2, 0)$ y $C_2 = (-4, -2)$ sobre la frontera de $\mathcal{P}$, que son los vértices de las respectivas regiones afiladas en negro de valores de los parámetros para los que aparentemente existen (véase la Figura 2). Conjeturamos que estos puntos son *puntos de densidad* de atractores extraños bidimensionales persistentes.

Definición (Puntos de densidad)**.** Un *punto de densidad* de atractores (extraños) persistentes para una familia f_μ es un valor μ^* de μ para los que todo entorno de μ^* tiene un subconjunto E con medida de Lebesgue positiva que contiene a μ^* tal que f_μ presenta un atractor (extraño) para todo $\mu \in E$.

Probar que cualquiera de los puntos C_1 o C_2 son puntos de densidad de atractores extraños persistentes es una tarea muy difícil. En esta memoria, nos limitaremos a estudiar la existencia de posibles recintos compactos e invariantes con interior no vacío para un conjunto de parámetros próximos a C_1 y C_2, respectivamente. Si tales recintos son minimales (es decir, transitivos), entonces serán atractores. Para concluir que son atractores extraños bidimensionales, es necesario probar la existencia de una órbita densa con dos exponentes de Liapunov cuya suma sea positiva. Este es el escollo principal.

Conjetura. *Los puntos de parámetros* C_1 *y* C_2 *son puntos de densidad de atractores extraños bidimensionales persistentes.*

Acknowledgments

This thesis has been partially supported by the "Programa de ayudas Severo Ochoa para la formación en investigación y docencia del Principado de Asturias" (BP20-063) from the Department for Science, Innovation and Higher Education of the Government of the Principality of Asturias and the research project "Genesis of Complexity: discrete and continuous dynamics" (MCI-21-PID2020-113052GB-I00) funded by the Ministry of Science and Innovation of the Government of Spain.

Throughout these years, many are the people who have been part of my life and who, directly or indirectly, have influenced in the result of this thesis. I would like to convey my gratitude to those I deem to be the most important ones.

To my director, José Ángel Rodríguez. None of this could have been possible without him. I only have words of affection and admiration.

To Enrique Vigil for being there from the beginning of my doctoral years. For giving me advice, for taking care of the publishing, for helping me with the figures, the writing of the papers, the programs...

To Antonio Pumariño for all I have learned from him as a result of our collaborations.

To Santiago Ibáñez for helping me with all of the bureaucracy related to the project and the group.

To José F. Alves for giving me the opportunity to make a research stay at Porto and collaborate with him.

Lastly, to my mother, to whom I dedicate this work.

Introduction

In the words of mathematician René Thom, "Toute science est avant tout l'étude d'une phénomenologie[3]." Ultimately, science aims at predicting or controlling the behavior of the processes that surround us. The mathematical models for the evolution of the processes are the *dynamical systems*: iterations of maps or diffeomorphisms, or flows associated to vector fields or equations defined in functional spaces (e.g. partial differential equations.) For the reading of this memoir it will be enough to restrict to systems of low dimension: fields, maps, or diffeomorphisms defined in dimension less than or equal to four. Even in this context, the results obtained over the last century have produced a Copernican revolution in the field of dynamical systems.

Historical Background

To begin with, let us consider first an easy scenario in dimension two: a family f_μ of smooth diffeomorphisms defined on a surface $\mathcal{M}$, all of which having a hyperbolic saddle fixed point P_μ with eigenvalues $|\lambda_{\mathrm{s}}^\mu| < 1 < |\lambda_{\mathrm{u}}^\mu|$. The two invariant manifolds

$$W^{\mathrm{s}}(P_\mu) = \{Q \in \mathcal{M} : f_\mu^n(Q) \to P_\mu \text{ as } n \to \infty\}$$
$$W^{\mathrm{u}}(P_\mu) = \{Q \in \mathcal{M} : f_\mu^{-n}(Q) \to P_\mu \text{ as } n \to \infty\}$$

known as the *stable* and *unstable manifold* of P_μ, respectively, intersect at P_μ for each μ. These manifolds are tangent at P_μ to the eigenspaces generated by λ_{s}^μ and λ_{u}^μ, respectively.

By the end of the XIX century, upon his study of the stability of the solar system, Poincaré [51] noticed that the invariant manifolds of P_μ may intersect at a point $Q_\mu \neq P_\mu$. Moreover, he noticed that the existence of such point Q_μ, called a *homoclinic point*, implies the existence of an infinite number of other homoclinic points, thus forcing the invariant manifolds to describe a complicated mesh. A homoclinic point Q_μ is said to be *transversal* if the invariant manifolds of P_μ intersect transversally at Q_μ, that is,

$$\mathrm{T}_{Q_\mu} W^{\mathrm{s}}(P_\mu) \oplus \mathrm{T}_{Q_\mu} W^{\mathrm{u}}(P_\mu) = \mathrm{T}_{Q_\mu} \mathcal{M}$$

Otherwise, the homoclinic point Q_μ is said to be *tangential*.

It was not until thirty years later that Birkhoff [7] proved that in a neighborhood $\mathcal{U}$ of a transversal homoclinic point there exist infinitely many periodic orbits of arbitrarily large periods. Thirty years later, Smale [65] proved the existence in $\mathcal{U}$ of a nontrivial hyperbolic invariant set for one of the most well-known maps in dynamical systems: Smale's *horseshoe* map.

The horseshoe map h represented an important milestone in the field of dynamical systems. It is constructed expansive in one direction and contractive in the other one, in such a way that its invariant compact set Ω is the Cartesian product of two Cantor sets,

[3] "Paraboles et catastrophes : entretiens sur les mathématiques, la science et la philosophie" (1983)

on which coordinates defined by a two-symbol sequence are introduced. Each point in Ω corresponds with a bisequence

$$(\cdots a_{-n}\cdots a_{-2}a_{-1}, a_0a_1a_2\cdots a_n\cdots)$$

The image of this bisequence under the Bernouilli shift σ is the bisequence obtained by moving "," forward one position. It is well known that the restriction of h to Ω is topologically conjugate to σ, and it is immediate to conclude for σ, and therefore for h by conjugation, the existence of periodic points of any period. Moreover, it is also proved the existence of a dense orbit that is expansive in the expanding direction of the horseshoe map. Therefore, on Ω, the deviations of the initial conditions in the expanding direction will increase exponentially. This sensitivity with respect to the initial conditions was correctly understood as a sign of uncertainty. On the other hand, the associated transversal homoclinic points and horseshoe maps are *robust*, in the sense that they continue to exist for families of diffeomorphisms C^1-close to f_μ.

Origins and Meaning of the Concept of Strange Attractor

The robustness of homoclinic points and, consequently, of the associated horseshoe maps, as well as the uncertainty they entail, made the presence of horseshoes to be understood as a sign of chaos from the seventies onwards. However, an objection to this interpretation must be highlighted because the internal dynamics of Ω is not *observable*: it lacks a significant (open or with positive measure) set of initial conditions

$$W^{\mathrm{s}}(\Omega) = \{P \in \mathcal{M} : \mathrm{dist}(h^n(P), \mathcal{M}) \to 0 \text{ as } n \to \infty\}$$

known as the *stable set* or *basin of attraction* of Ω, whose iterations converge to Ω. This defficiency was overcome by Smale [65, 66] when he constructed a diffeomorphism of the solid torus $\mathbb{T}^2 = \mathbb{S}^1 \times \mathbb{D}^2$ onto itself, called the *solenoid*.

Definition (Attractors)**.** An *attractor* for a map T defined on a manifold $\mathcal{M}$ is a T-invariant compact set $\mathcal{A}$ that is transitive and whose stable set

$$W^{\mathrm{s}}(\mathcal{A}) = \{P \in \mathcal{M} : \mathrm{dist}(T^n(P), \mathcal{A}) \to 0 \text{ as } n \to \infty\}$$

has nonempty interior.

The solenoid has a hyperbolic invariant compact set Ω whose local structure is homeomorphic to the Cartesian product of a Cantor set by an interval. Its hyperbolic structure is also robust and the solenoid is expansive in the direction of the interval. Therefore, it exhibits sensitivity with respect to the initial conditions. Since the stable set of Ω is $\mathbb{T}^2$, the uncertainty of the dynamics is now observable. Invariant compact sets such as the solenoid's were called *strange attractors* and its presence was proposed as the paradigm of chaotic behaviors.

The term strange attractor was coined by Ruelle and Takens [63] to refer to those attractors that, such as the solenoid's, were neither points nor tori: not even did they have the structure of a smooth manifold. They were locally the Cartesian product of a manifold by a Cantor set and their internal dynamics was expansive in some direction: they had some positive Lyapunov exponent.

Definition (Strange attractors)**.** An attractor for T is *strange* if it contains a dense orbit $\{T^n(P_0) : n \in \mathbb{N}\}$ with some positive Lyapunov exponent: there exists a unit vector v and a constant $c > 0$ such that, for every $n \in \mathbb{N}$,

$$\|\mathrm{D}T^n(P_0)v\| \geq \mathrm{e}^{cn}$$

The above definition guarantees the existence of one expanding direction, but it does not specify how many there are. Although some authors define the *multidimensional* strange attractors as those having multiple expanding directions, we will adopt a weaker version.

Definition (Multidimensional strange attractors)**.** A strange attractor is *n-dimensional* if it contains a dense orbit with n Lyapunov exponents whose sum is positive.

The presence of *robust* strange attractors, such as those with a hyperbolic structure, was considered [63] as a better proposal to explain the nature of turbulence than the one given earlier by a growth of the number of unmeasurable frequencies in a quasi-periodic movement [37].

Definition (Persistent attractors)**.** Let $f_\mu \colon \mathcal{M} \to \mathcal{M}$ be a family of maps. Assume that f_{μ_0} has an attractor $\mathcal{A}_0$ for some μ_0. The attractor $\mathcal{A}_0$ is *persistent* if, for every $\delta > 0$, the map f_μ has an attractor for every μ-value belonging to a set $E \subseteq \mathcal{B}(\mu_0, \delta)$ with positive Lebesgue measure. The attractor $\mathcal{A}_0$ is *fully persistent* if $E = \mathcal{B}(\mu_0, \delta)$ for some $\delta > 0$.

Quoting Ruelle and Takens [63, p. 171], "An attractor of the type just described can therefore not be thrown away as non-generic pathology." The way to generate this type of solenoid-like hyperbolic attractors in flows was proposed as a concatenation of *Hopf bifurcations* [30, Th. 3.4.2] in dimension greater than or equal to four.

Abundance of Attractors: Persistence of Nonhyperbolic Attractors

A simpler scenario than the one proposed by Ruelle and Takens [63] for the genesis of strange attractors was earlier given by Lorenz [39] by numerically analysing the quadratic vector field

$$\begin{aligned} x' &= -\alpha x + \alpha y \\ y' &= \beta x - y - xz \\ z' &= \gamma z + xy \end{aligned}$$

for $(\alpha, \beta, \gamma) = (10, 28, -8/3)$. This system comes from the truncation of the Navier–Stokes equation. Surprisingly, under small perturbations, he seemed to get a fully persistent, but not stable, attractor: nearby attractors are in general not topologically equivalent. In an even simpler scenario, Hénon [31] found a possibly persistent (but certainly not fully persistent) strange attractor for the Hénon family

$$H_{a,b}(x, y) = (1 - ax^2 + y, bx)$$

with $a = 1.4$ and $b = 0.3$. Thus, neither of these attractors is robust and cannot therefore be hyperbolic. But, do there really exist nonhyperbolic strange attractors?

The first analytical proof of the existence of such attractors was given by Benedicks and Carleson [5] for $H_{a,b}$ for sufficiently small $b > 0$ and a-values belonging to a set with positive Lebesgue measure contained in an interval $(2 - \delta, 2]$ for sufficiently small $\delta > 0$. In order to develop this proof, certain previous results on 1-D dynamics were necessary.

For $b > 0$, the map $H_{a,b}$ can be easily written as

$$H_{a,b}(x, y) = (1 - ax^2 + \sqrt{b}y, \sqrt{b}x)$$

Thus, for sufficiently small $b > 0$, the Hénon family is a small perturbation of

$$\Phi_a(x, y) = (1 - ax^2, 0)$$

Therefore, the dynamics of Φ_a, and consequently the dynamics of $H_{a,b}$ in the limit case $b = 0$, reduces to the dynamics of the quadratic family

$$T_a(x) = 1 - ax^2$$

The map T_a is a paradigmatic example of a unimodal map with negative Schwarzian derivative. These unimodal maps were well studied. See, for instance, De Melo and Van Strien [15].

After several suitable changes of variable and parameter, the quadratic family transforms into

$$f_a(x) = ax(2 - x)$$

The interval $[0, 2]$ is f_a-invariant whenever $0 \leq a \leq 2$. The family $\{f_a\}_{a\in[0,2]}$ was very well studied because not only does it serve as a model of population growth, but also it generates a dynamical richness that follows after a renormalization process independently discovered by Feigenbaum [19, 20] and by Collet and Tresser [12]. This renormalization process essentially consists of the existence of a sequence of a-values a_n and a sequence of intervals I_n such that the restriction of the iterate $f_{a_n}^2$ to I_n coincides with the restriction of $f_{a_{n-1}}$ to I_{n-1} up to rescaling. As a consequence, the well-known phenomenon of period-doubling follows, as well as the fractal structure observed in Figure 01 [15], where it is numerically represented the structure of the attractor for f_a for different a-values.

There exist windows of a-values for which the attractor is a periodic orbit of low period. However, for other parameter values, the attractor looks like a periodic orbit of large period or perhaps an infinite set: a possible strange attractor. Such attractor certainly exists for $a = 2$. Even more: it is proved that f_2 is conjugate to the map for $\bar{a} = 2$ of the following tent maps family:

$$\lambda_{\bar{a}}(x) = \begin{cases} \bar{a}x & \text{if } 0 \leq x \leq 1 \\ \bar{a}(2 - x) & \text{if } 1 \leq x \leq 2 \end{cases}$$

The interval $I = [0, 2]$ is also $\lambda_{\bar{a}}$-invariant if $0 \leq \bar{a} \leq 2$. More precisely, the interval $I_{\bar{a}} = [\bar{a}(2 - \bar{a}), \bar{a}]$ is strictly $\lambda_{\bar{a}}$-invariant for $1 < \bar{a} \leq 2$ and is a strange attractor if $\bar{a} \geq \sqrt{2}$ since the orbit of $x = 1$ is dense and expansive in $I_{\bar{a}}$.

For $\bar{a} = \sqrt{2}$, a renormalization process begins for family $\{\lambda_{\bar{a}}\}_{1<\bar{a}\leq\sqrt{2}}$. For the sequence of $\bar{a}$-values $\bar{a}_n = 2^{1/2^n}$ there exists a interval I_n such that the restriction of the iterate $\lambda_{\bar{a}_n}^2$ to I_n coincides with the restriction of $\lambda_{\bar{a}_{n-1}}$ to I_{n-1} up to rescaling. This process of renormalization allows to conclude that the strange attractor $I_{\bar{a}}$ for $\sqrt{2} \leq \bar{a} \leq 2$ splits into a 2^n-piece strange attractor as a crosses the $\bar{a}$-values $\bar{a}_n$. Moreover, the renormalization process seen for family $\{f_a\}$ provides a sequence of a-values a_n for which f_{a_n} is conjugate to $\lambda_{\bar{a}}$ for all n. Therefore, for all $n \in \mathbb{N}$, the map f_{a_n} exhibits a 2^n-piece strange attractor.

The tent maps family $\lambda_{\bar{a}}$ displays strange attractors for $1 < \bar{a} \leq 2$ and, therefore, these attractors are persistent. However, the existence of strange attractors for the quadratic family f_a for a sequence of a-values do not imply their persistence. The proof was given for the first time by Benedicks and Carleson [5] working with family T_a for a-values very close to 2. More precisely, for every $\delta > 0$ sufficiently small there exists a set $E \subseteq (2 - \delta, 2]$ with positive Lebesgue measure such that T_a has a strange attractor for every $a \in E$. Keeping in mind this process of renormalization, this persistence is extended to a-values sufficiently close to the sequence a_n. Unlike the case for the tent maps $\lambda_{\bar{a}}$, the proof of the persistence of strange attractors for the quadratic family T_a shows serious difficulties to obtain the expansivity of the orbit of the critical point $x = 1$. Close to such nonhyperbolic point, the derivative almost vanishes and, therefore, every time the orbit returns close to $x = 1$ it may lose all the accumulated expansivity. Thus, an appropriate exclusion of parameters

becomes necessary for which the contraction close to $x = 1$ eliminates the previously accumulated expansivity. Such exclusion allows to conserve a set of a-values with positive Lebesgue measure for which the orbit has a positive Lyapunov exponent and, moreover, is dense in all the interval $[1-a, 1]$. This allows to conclude, for each $a \in E$, the existence of an absolutely continuous invariant measure μ_a with positive entropy [15, Ch. V] as was proved by Jakobson [34] before Benedicks and Carleson [5]. Before the uncertainty of the internal dynamics of the attractor, such measure informs about the distribution of the orbits. Its support is contained in the attractor and is *statistically stable*: its density depends continuously with respect to a in L^1.

The proof of the pesistence of the attractors provided by Benedicks and Carleson [5] turned out to be seminal for the proof of the persistence of strange attractors [6] for the Hénon family. As already mentioned, the dynamics of T_a is a limit situation of the dynamics of $H_{a,b}$ for sufficiently small $b > 0$. The Hénon family has a saddle fixed point P whose unstable manifold folds onto itself and remains arbitrarily close to the interval $[1-a, 1]$ on the x-axis. It is then natural to assume that the dynamics of $H_{a,b}$ on $W^{\mathrm{u}}(P)$ resembles the dynamics of T_a on $[1-a, 1]$. Indeed, it is proved that the closure of $W^{\mathrm{u}}(P)$ is the strange attractor of $H_{a,b}$ for sufficiently small b and a-values in a set $E \subseteq (2-\delta, 2]$. To that end, then again an exclusion of parameter becomes necessary to control the expansivity near each one of the infinitely many folds of $W^{\mathrm{u}}(P)$. Even though such exclusion of parameters is more complicated and exhaustive, they managed to prove that the new set E still has positive Lebesgue measure. We will refer to the parallelism between the dynamics of family $H_{a,b}$ and its limit family T_a by saying that family $H_{a,b}$ is a *good unfolding* of family T_a.

The Hénon family is a family of diffeomorphisms that exhibits persistent nonhyperbolic strange attractors, but what presence does it have in the set of the dynamical models? In other words: does there exists a generic mechanism leading to the existence of persistence nonhyperbolic strange attractors? In this direction did Jacob Palis point when he conjectured that generic one-parameter families of surface diffeomorphisms unfolding for any parameter value a homoclinic tangency have strange attractors with positive probability. By a homoclinic tangency we mean a nontransversal homoclinic point between the invariant manifolds of a saddle periodic point. This conjecture was proved by Mora and Viana [44].

Theorem ([44, Th. A]). *Let $(f_\mu)_\mu$ be a C^∞ one-parameter family of diffeomorphisms on a surface and suppose that f_0 has a homoclinic tangency associated to some periodic point p_0. Then, under generic (even open and dense) assumptions, there is a positive Lebesgue measure set E of parameter values near $\mu = 0$, such that for $\mu \in E$, the diffeomorphism f_μ exhibits a strange attractor, or repeller[4], near the orbit of tangency.*

The proof of this theorem begins by considering the return maps of family f_μ in a neighborhood $\mathcal{V}$ of the homoclinic point Q_{μ_0} of f_{μ_0}. Fix $1 \leq r < \infty$. Under generic assumptions (including the dissipativeness of P_{μ_0}), one can find renormalizations of f_μ which are arbitrarily C^r close to Φ_a. By this we mean that there are (small) domains $\mathcal{U}^n$ on the surface converging to the point Q_{μ_0} of the orbit of tangency, (small) intervals I^n converging to $\mu = 0$ in the parameter space and n-dependent C^r-coordinates on $I^n \times \mathcal{U}^n$ with the property that, as $n \to \infty$, the expression of $f^n{\restriction}_{I^n \times \mathcal{U}^n}$ in these coordinates converges to Φ_a in the C^r-topology. See details in Palis and Takens [48]. This convergence verifies a sequence of estimates given in Theorem 2.1 [44] which are necessary to apply the techniques of Benedicks and Carleson [6] in the proof of the existence of strange attractors for family $f^n{\restriction}_{I^n \times \mathcal{U}^n}$. For this reason, the authors refer to $f^n{\restriction}_{I^n \times \mathcal{U}^n}$, expressed in new renormalized coordinates, as a Hénon-like family. Actually, as happens for the Hénon

[4] A *repeller* is an attractor for f_μ^{-1} when f_μ is not dissipative at p.

family, family $f^n\restriction_{I^n\times\mathcal{U}^n}$ defines a good unfolding of its limit family Φ_a, or simply of the quadratic family.

The attractors shown by Mora and Viana [44] are infinitesimal in the sense that the renormalization domains must be arbitrarily close to the homoclinic tangency point. Other renormalizations without this restriction were made [52] for the transversal section of a Shilnikov orbit in a family of vector fields in $\mathbb{R}^3$. After this renormalization, the authors obtained a family of diffeomorphisms

$$T_{\lambda,a,b}(x,y) = (f_{\lambda,a} + \tfrac{1}{\lambda}\log(1+\sqrt{b}y), \sqrt{b}(1+\sqrt{b}y)\mathrm{e}^{\lambda x}\sin x)$$

whose limit family is the unimodal family

$$f_{\lambda,a}(x) = \tfrac{1}{\lambda}\log a + x + \tfrac{1}{\lambda}\log\cos x$$

where λ is fixed by fixing the spectrum of the field. For family $f_{\lambda,a}$ it is proved the existence of persistent strange attractors [52]. Then, after proving that family $T_{\lambda,a,b}$ is a good unfolding of family $f_{\lambda,a}$, they applied the ideas by Benedicks and Carleson [6] and Mora and Viana [44] to conclude the existence of persistent strange attractors for $T_{\lambda,a,b}$. Such attractors are not infinitesimal and define by suspension persistent strange attractors for the family of vector fields. Additionally, it is shown that the ideas by Benedicks and Carleson [6] can be extended to any good unfolding of a unimodal map other than the quadratic family.

In Search of 2-D Strange Attractors: the 2-D Quadratic Family

All the above-mentioned attractors have dimension one. They appear generically when unfolding the homoclinic tangencies that involve the 1-D unstable manifold of a dissipative saddle fixed point. The proof of their existence is mainly based on renormalization processes defined in a neighborhood of the tangency point that are good unfoldings of 1-D limit families. For these families it is previously proved the persistence of invariant compact sets containing a dense orbit with one positive Lyapunov exponent.

The path towards the proof of the persistence of 2-D strange attractors is not likely to be very different from the one followed in the 1-D case, but the increased dimension entails bigger difficulties and the problem is completely open. The family of diffeomorphisms must be defined on a manifold of dimension greater than or equal to three. That is the only way that, for some parameter value, the corresponding diffeomorphism may have a homoclinic tangency involving a 2-D unstable manifold of a saddle periodic point.

Let f be a diffeomorphism defined on a smooth 3-D manifold $\mathcal{M}$ with a saddle fixed point P. Assume that $\mathrm{D}f(P)$ has real eigenvalues $\lambda_{\mathrm{s}}, \lambda_{\mathrm{cu}}, \lambda_{\mathrm{u}}$ satisfying

$$|\lambda_{\mathrm{s}}| < 1 < |\lambda_{\mathrm{cu}}| < |\lambda_{\mathrm{u}}|$$

In this case, the following facts are well known:

1. The *strong unstable manifold* $W^{\mathrm{uu}}(P)$ of P lies on the unstable manifold of P and is tangent to the eigenspace associated to λ_{u} at P. This manifold is unique, as smooth as f and has dimension one.

2. The unstable manifold of P is foliated by leaves of a *strong unstable foliation* $\mathcal{F}^{\mathrm{uu}}(P)$. Every leaf ℓ^{uu} of $\mathcal{F}^{\mathrm{uu}}(P)$ is transverse to the eigenspace associated to λ_{cu}, and $W^{\mathrm{uu}}(P)$ is one of the leaves.

3. The *center-stable manifold* $W^{\mathrm{cs}}(P)$ of P is an invariant manifold containing the stable manifold of P and touching the invariant linear subspace of $\mathrm{T}_P\mathcal{M}$ associated to the eigenvalues λ_{s} and λ_{cu} at P. This manifold is (in general) C^1 smooth and it is not unique.

In addition, assume that there exist C^1 linearizing coordinates (x, y, z) for f on a neighborhood $\mathcal{U}$ of P such that $P = (0, 0, 0)$ and

$$f(x, y, z) = (\lambda_{\mathrm{cu}} x, \lambda_{\mathrm{u}} y, \lambda_{\mathrm{s}} z)$$

for all $(x, y, z) \in \mathcal{U}$. In $\mathcal{U}$, the local unstable and stable manifolds of P are respectively given by

$$W^{\mathrm{u}}_{\mathrm{loc}}(P) = \{(x, y, 0) : |x|, |y| < \delta\}$$

and

$$W^{\mathrm{s}}_{\mathrm{loc}}(P) = \{(0, 0, z) : |z| < \delta\}$$

for sufficiently small $\delta > 0$. Moreover, there exists the local strong unstable C^1 foliation $\mathcal{F}^{\mathrm{uu}}(P)$ in the local unstable manifold such that, for any $\bar{\mathbf{x}} = (\bar{x}, \bar{y}, 0) \in W^{\mathrm{u}}_{\mathrm{loc}}(P)$, the leaf $\ell^{\mathrm{uu}}(\bar{\mathbf{x}})$ containing $\bar{\mathbf{x}}$ is given by $\ell^{\mathrm{uu}}(\bar{\mathbf{x}}) = \{(\bar{x}, y, 0) : |y| < \delta\}$.

Suppose that the invariant manifolds of P have a quadratic homoclinic tangency. We introduce the definition of a new type of codimension two homoclinic bifurcation, which may be seen as a collision of a quadratic homoclinic tangency and a generalized homoclinic transversality.

Definition (Generalized homoclinic tangency)**.** We say that the diffeomorphism f has a *generalized homoclinic tangency* (of type I of Case B[5]) at a point

$$Q \in W^{\mathrm{s}}(P) \cap W^{\mathrm{u}}(P)$$

if the following conditions hold:

(T_1) The fixed point P is dissipative.

(T_2) The invariant manifolds of P have a quadratic tangency at Q. Moreover, the point Q does not belong to the strong unstable manifold of P.

(T_3) The stable manifold of P is tangent to the leaf of $\mathcal{F}^{\mathrm{uu}}(P)$ containing Q.

(T_4) The center-stable manifold of P is transverse to the surface defined by the unstable manifold of P at Q.

Remark. For the quadratic tangency point $Q \in \mathcal{M}$, we consider the forward image $\overline{Q} = f^{n_0}(Q)$ for a large $n_0 \in \mathbb{N}$. Let $U(Q)$ be the plane containing $\overline{Q}$ an such that $\mathrm{T}_{\overline{Q}} U(\overline{Q})$ is generated, in local coordinates of P, by $(\partial/\partial x)_{\overline{Q}}, (\partial/\partial z)_{\overline{Q}} \in \mathrm{T}_{\overline{Q}}\mathcal{M}$. Note that by the chosen linearizing coordinates on a neighborhood of P, the plane $U(\overline{Q})$ in $\mathrm{T}_{\overline{Q}}\mathcal{M}$ corresponds to the central-stable bundle at this tangent point. Thus, condition (T_4) may be stated as follows:

(T_4) The plane $U(\overline{Q})$ and the unstable manifold of P are transverse at $\overline{Q}$.

This concept is valid if we replace a fixed point by a periodic orbit.

Under these hypotheses, Tatjer proved [67, Prop. 4.5] that there exists a two-parameter family of limit return maps associated to the generalized homoclinic tangency, which are given by

$$\tilde{f}_{\tilde{a},\tilde{b}}(\tilde{x}, \tilde{y}, \tilde{z}) = (\tilde{z}, \tilde{a} + \tilde{b}\tilde{y} + \tilde{z}^2, \tilde{y})$$

As it was expected, as in the unfolding of two-dimensional tangencies, these limit return maps are not linear. Before any attempt to prove the existence of strange attractors for $\tilde{f}_{\tilde{a},\tilde{b}}$,

[5]There is another case (Case A) of generalized homoclinic tangency when the unstable invariant manifold if the fixed point has dimension one, but the fixed point is not sectionally dissipative

note that, for any parameter values $(\tilde{a},\tilde{b})$, every point in $\mathbb{R}^3$ *falls* by one iteration of $\tilde{f}_{\tilde{a},\tilde{b}}$ into the surface

$$\widetilde{\mathcal{C}}_{\tilde{a},\tilde{b}} = \{(\tilde{x},\tilde{y},\tilde{z}) \in \mathbb{R}^3 : \tilde{y} = \tilde{a} + \tilde{b}\tilde{z} + \tilde{x}^2\}$$

Therefore, the surface $\widetilde{\mathcal{C}}_{\tilde{a},\tilde{b}}$ is $\tilde{f}_{\tilde{a},\tilde{b}}$-invariant and it suffices to study the dynamics of $\tilde{f}_{\tilde{a},\tilde{b}}$ on $\widetilde{\mathcal{C}}_{\tilde{a},\tilde{b}}$. That is, it suffices to study the dynamics of the 2-D endomorphisms

$$(g^{-1}_{\tilde{a},\tilde{b}} \circ \tilde{f}_{\tilde{a},\tilde{b}} \circ g_{\tilde{a},\tilde{b}})(\tilde{x},\tilde{z}) = (\tilde{z}, \tilde{a} + \tilde{b}\tilde{z} + \tilde{x}^2)$$

being $g_{\tilde{a},\tilde{b}}(\tilde{x},\tilde{z}) = (\tilde{x}, \tilde{a} + \tilde{b}\tilde{z} + \tilde{x}^2, \tilde{z})$ a parametrization of $\widetilde{\mathcal{C}}_{\tilde{a},\tilde{b}}$. By performing the change of coordinates

$$\mathbf{x} = \tilde{z} - \tilde{b}\tilde{x}, \quad \mathbf{y} = \tilde{x}$$

the above family of endomorphisms transforms into the *2-D quadratic family*:

$$T_{a,b}(\mathbf{x},\mathbf{y}) = (a + \mathbf{y}^2, \mathbf{x} + b\mathbf{y})$$

where we have written a, b instead of $\tilde{a},\tilde{b}$ to avoid excessive notation.

As the study of the quadratic family was seminal for the proof of the persistence of 1-D strange attractors, the study of the 2-D quadratic family should be a first step towards the proof of the persistence of 2-D strange attractors.

Persistence of 2-D Strange Attractors in a One-Parameter Family of 2-D Tent Maps

With a view of analytically proving the existence of 2-D strange attractors for the 2-D quadratic family, Pumariño and Tatjer [60] began by searching for parameter values for which there exist invariant domains.

The most simple situations arise for $b = 0$. In that case, the square

$$R_a = [a, a + a^2] \times [a, a + a^2]$$

is strictly $T_{a,0}$-invariant for every $a \in [-2,-1]$. Moreover, the square R_a is a 2-D strange attractor [60, Prop. 3] for a-values in a positive Lebesgue measure set contained in $[-2, a_0]$ for some $a_0 > -2$.

Apart from the case $b = 0$, invariant curvilinear triangles were constructed for parameter values along the curve

$$G = \{(-\tfrac{1}{4}s^3(s^3 - 2s^2 + 2s - 2), -s^2 + s) : 0 \le s \le 2\}$$

The point $(-4,-2)$ belongs to G for $s = 2$. For $(a,b) = (-4,-2)$, the respective curvilinear triangle is invariant in the strict sense and map $T_{a,b}$ is conjugate to the non-invertible piecewise affine map

$$\Lambda(x,y) = \begin{cases} (x + y, x - y) & \text{if } (x,y) \in \mathcal{T}_0 \\ (2 - x + y, 2 - x - y) & \text{if } (x,y) \in \mathcal{T}_1 \end{cases}$$

defined on the triangle $\mathcal{T} = \mathcal{T}_0 \cup \mathcal{T}_1$, where

$$\mathcal{T}_0 = \{0 \le x \le 1,\ 0 \le y \le x\}, \quad \mathcal{T}_1 = \{1 \le x \le 2,\ 0 \le y \le 2 - x\}$$

As was pointed out [60, §2.3], the map Λ enjoys the same nice properties as λ_2. In particular, the consecutive pre-images of the critical segment $\{(x,y) \in \mathcal{T} : x = 1\}$ define a sequence of partitions (whose diameter tends to zero) of $\mathcal{T}$ leading the authors to conjugate Λ to a one-sided shift on two symbols. Moreover, for every initial point $(x_0,y_0) \in \mathcal{T}$

whose orbit never visits the critical line, the Lyapunov exponent of Λ along the orbit of (x_0, y_0) is positive (in fact, it is equal to $2^{-1}\log 2$) in all nonzero direction. Finally, an ergodic absolutely continuous invariant measure for Λ can be easily constructed. By conjugacy, all of these facts hold for $T_{-4,-2}$. These were the main reasons why Λ was called the *2-D tent map*.

As a first approach to the general study of the dynamics of $T_{a,b}$ along curve G, the family of piecewise affine maps of $\mathcal{T}$ given by

$$\Lambda_t(x,y) = \begin{cases} (t(x+y), t(x-y)) & \text{if } (x,y) \in \mathcal{T}_0 \\ (t(2-x+y), t(2-x-y)) & \text{if } (x,y) \in \mathcal{T}_1 \end{cases}$$

was introduced [55]. The triangle $\mathcal{T}$ is Λ_t-invariant if $0 \leq t \leq 1$ and $\Lambda_1 = \Lambda$. Since the parameter t essentially gives the expansion rate, playing the same role as the parameter $\bar{a}$ does for tent map family $\lambda_{\bar{a}}$, then family Λ_t can be considered a natural extension of the classical tent maps. That is why family Λ_t was called the *2-D tent maps family*.

The dynamics of family Λ_t is very simple for $0 \leq t \leq \sqrt{2}/2$. If $t < \sqrt{2}/2$, then the origin is the unique fixed point and is a global attractor of node type [55, Lem. 5.1]. For $t = \sqrt{2}/2$, the map $\Lambda_{\sqrt{2}/2}$ is area-preserving and has a segment of fixed points in $\mathcal{T}_0$, being the rest of points in $\mathcal{T}_0$ periodic points of period two.

However, for $\sqrt{2}/2 < t \leq 1$, the dynamics of Λ_t is verily rich. The origin is a repelling node and another fixed point appears in $\mathcal{T}_1$, which is a repelling focus. Also, the Lyapunov exponents of any point which does not belong to any pre-image of the critical segment in all nonzero direction is equal to $\log \sqrt{2}t$, and all the periodic orbits with no critical points are repelling. Moreover, family Λ_t exhibits in this interval the same topological types of numerical strange attractors as family $T_{a,b}$ along the curve G for $0 \leq s \leq 2$. Namely: convex strange attractors (for $\sqrt[3]{4}/2 \leq t \leq 1$); non-simply connected strange attractors (for $\sqrt[5]{8}/2 \leq t < \sqrt[3]{4}/2$); and disconnected strange attractors formed by numerous connected pieces (for $\sqrt{2}/2 < t < \sqrt[5]{8}/2$). This is what truly motivates the study of the dynamics of the family Λ_t.

A first analytical proof of the existence of a convex strange attractor for the family Λ_t was given [56, Th. 1.1] for $\tau < t \leq 1$, where

$$\tau = \tfrac{\sqrt{2}}{2}(1+\sqrt{2})^{\frac{1}{4}} \approx 0.882$$

Moreover, as was seen for Λ, it was also proved that the attractor supports a unique absolutely invariant probability measure μ_t for all such t, which is ergodic. On the other hand, the existence of persistent strange attractors with several pieces was proved through several papers [57, 58, 59]. The proof is a consequence of a renormalization procedure that permits to understand how connected invariant compact sets formed by a unique piece may split giving rise to other ones formed by an increasing number of pieces. Then, from Theorem 1.2 [59], it follows that these new disconnected invariant compact sets contain strange attractors formed by the same number of pieces. Moreover, it was proved the coexistence of arbitrarily large numbers of strange attractors [58, Th. B].

For $\tau < t \leq 1$, it is natural to wonder if μ_t depends continuously on the dynamics of the family Λ_t, i.e. if family Λ_t is statistically stable. In this case, this means continuity of the densities of μ_t with respect to t in the L^1-norm.

Alves, Pumariño, and Vigil gave sufficient conditions for the statistical stability of piecewise expanding maps with bounded distortion and long branches [3, Th. A] and, as a corollary [3, Th. B], they proved the statistical stability of the family Λ_t. Actually, it is proved that the family of a certain power of the map Λ_t is statistically stable. Then, Alves and Pumariño proved the continuity of the entropy of certain multidimensional piecewise expanding maps which admit ergodic absolutely continuous invariant probability

measures [2, Th. F], and again deduced the continuity of the entropy for the family Λ_t as a corollary [2, Th. G].

Contributions of This Memoir

As we have already stated, the ultimate goal of the research project this memoir takes part in is the study of the dynamics of the 2-D quadratic family $T_{a,b}$. This family is obtained as the limit family of the return maps defined in a neighborhood of a type of generic homoclinic tangency unfolded by two-parameter families of 3-D diffeomorphisms [67, Th. 1]. The main interest in the dynamics of this family lies in its numerically observed persistent 2-D strange attractors [60, 61]. Besides the analytical proof of the persistence of such attractors, their genesis should also be understood, as well as that of the numerical 1-D strange attractors [60].

In order to explain the existence of 1-D strange attractors, we will refer to the background from this Introduction and, concretely, to Mora and Viana [44, Th. A], which proves the persistence of 1-D strange attractors in generic unfoldings of a homoclinic tangency of surface diffeomorphisms. Also, the genesis of such attractors is explained by a periodic orbit analysis. As for the existence of 2-D strange attractors, we first have to find invariant compact sets where to prove the existence of an expansive dense orbit. As a first approach to this problem, we substitute family $T_{a,b}$ for a general two-parameter family of Expanding Baker Maps.

This memoir is organized as follows. In Chapter 1 we include more details on Tatjer's main theorem [67, Th. 1] and the limit step of the family of return maps to obtain the family $T_{a,b}$. The novel results of this memoir are found in Chapters 2 and 3.

Chapter 2 is devoted to the study of a general family $\Gamma_{a,\theta}$ of Expanding Baker Maps, being $a > 1$ and $0 < \theta < \pi$ an expasion rate and a rotation angle, respectively. The family Λ_t is a particular case for $\theta = 3\pi/4$, and the respective results [56, 57, 58, 59] are of help in this general case, especially if θ/π is a rational number. As in that case, we can construct strictly invariant compact sets and prove that they contain 2-D strange attractors adapting a few arguments [59]. A renormalization process [57, 58] can be started for this general family as well, explaining the splitting and even the doubling of attractors. The results are collected in two recent publications [42, 43].

Chapter 3 is devoted to the analysis of the dynamics of the family $T_{a,b}$. We begin with a study of the local bifurcations, for which we will take advantage of the numerical analysis by Pumariño and Tatjer [61], and focus on the fixed points and 2- and 3-periodic orbits. As was originally proved for families of vector fields [33, 16, 22], it is also expected that all the dynamics can be unfolded from some of its nonhyperbolic singularities. These dynamics will be attracting periodic orbits, attracting closed curves, and 1-D strange attractors. In particular, for $b = -1$ we find two families of 3-periodic orbits. One of them is of dissipative saddle type for a-values for which the other one undergoes a Hopf–Neimark–Sacker bifurcation. The growth of the closed curves originated from this bifurcation collide with the saddle periodic orbit thus generating a homoclinic tangency. This phenomenon occurs for parameter values for which an attracting periodic orbit coexists with them. Thus, we explain in this memoir a process that had not been checked: the competition between more than one strange attractor.

2-D Strange Attractors for a General Two-Parameter Family of Expanding Baker Maps

The dynamics of the tent map $\lambda_{\bar{a}}\colon [0,2] \to [0,2]$ consists of first folding the interval $[0,2]$ by the middle and then stretching the interval $[0,1]$ by a factor $\bar{a} > 1$ to obtain the

interval $[0, \bar{a}]$. Similarly, the 2-D tent map $\Lambda_t \colon \mathcal{T} \to \mathcal{T}$ can be thought of as the composition of the linear map defined by the matrix

$$\mathbf{A}_t = \begin{pmatrix} t & t \\ t & -t \end{pmatrix}$$

with the fold of the triangle $\mathcal{T}$ along the critical segment

$$\mathcal{C} = \{(x, y) \in \mathcal{T} : x = 1\}$$

onto $\mathcal{T}_0$. This fold can be defined in all $\mathbb{R}^2$ by

$$\mathcal{F}_{\mathcal{C},\mathcal{O}}(x, y) = \begin{cases} (x, y) & \text{if } x \leq 1 \\ (2 - x, y) & \text{if } x \geq 1 \end{cases}$$

If $t > \sqrt{2}/2$, then $\mathbf{A}_t$ is expanding. Thus, the family Λ_t with $\sqrt{2}/2 < t \leq 1$ is an example of a class of piecewise affine maps, which we will call *Expanding Baker Maps*, that generalize this dynamics: folding a certain domain (possibly several times) and then expanding the folded region. See Section 2.1 for more details.

Recall that, for all $\sqrt{2}/2 < t \leq 1$, the map Λ_t has a repelling focus P_t in $\mathcal{T}_1$, with coordinates

$$(x_t, y_t) = \left(\frac{2t(2t+1)}{2t^2 + 2t + 1}, \frac{2t}{2t^2 + 2t + 1} \right)$$

By performing the affine change of coordinates

$$X = \frac{x - x_t}{1 - x_t}, \quad Y = \frac{y - y_t}{x_t - 1}$$

the map Λ_t transforms into

$$\Gamma_{a,\theta} = \mathbf{A}_{a,\theta} \circ \mathcal{F}_{\mathcal{C},\mathcal{O}}$$

with $a = \sqrt{2}t$ and $\theta = 3\pi/4$, where

$$\mathbf{A}_{a,\theta} = \begin{pmatrix} a\cos\theta & -a\sin\theta \\ a\sin\theta & a\cos\theta \end{pmatrix}$$

In this coordinates, the fixed point P_t is the origin and $X = 1$ is again the critical line. We will study the general family $\{\Gamma_{a,\theta}\}_{a,\theta}$ with $a > 1$ and $0 < \theta < \pi$. Note that the dynamics of $\Gamma_{a,0}$ and $\Gamma_{a,\pi}$ look like one-dimensional, and $\Gamma_{a,\theta}$ is conjugate to $\Gamma_{a,-\theta}$ for all $-\pi < \theta < 0$.

We first prove the existence of strictly invariant compact sets $\mathcal{K}$ for $\Gamma_{a,\theta}$ and divide them into two classes: *first-rate* if $\mathcal{F}_{\mathcal{C},\mathcal{O}}(\mathcal{K}) \subseteq \mathcal{K}$, and *second-rate* otherwise. First-rate strictly invariant sets will be a particular case of a larger class, which we will call *self-similar sets*.

Definition (Self-similar sets)**.** A set $\mathcal{K} \subseteq \mathbb{R}^2$ is $\mathbf{A}_{a,\theta}$*-self-similar* if

$$\mathbf{A}_{a,\theta}(\mathcal{K}_0) = \mathcal{K}$$

being $\mathcal{K}_0 = \mathcal{K} \cap \{x \leq 1\}$.

Thus, a first step towards the proof of the existence of strictly invariant compact sets is the existence of self-similar sets.

Theorem 1 (Existence of self-similar polygons)**.** *Let $0 < \theta < \pi$. For every $a > 1$, there exists an $\mathbf{A}_{a,\theta}$-self-similar $(N+1)$-sided polygon $\mathcal{K}_N$ with*

$$N = N(a, \theta) \geq 1 + \lfloor \pi/\theta \rfloor$$

that contains all $\mathbf{A}_{a,\theta}$-self-similar sets. Moreover, there exists a nonincreasing sequence a_j of a-values with the following properties:

(a) $a_j \geq 1$ *for every* $j \in \mathbb{N}$

(b) *For any* $j \in \mathbb{N}$ *it holds that* $a_{j+1} \leq a_j$ *with equality holding if and only if* $a_j = 1$

(c) $\lim_{j\to\infty} a_j = 1$

(d) *The set* $\{a_j\}_j$ *is finite if and only if* $\theta/\pi \in \mathbb{Q}$

(e) *The sequence* $N_j = N(a_j, \theta)$ *is increasing*

(f) *For every* $j \in \mathbb{N}$ *and for all* $a_j \leq a < a_{j-1}$ *it holds that* $N(a, \theta) = N_j$

Since $\mathbf{A}_{a,\theta}$ multiplies the area of any set by a factor of a^2 and $\mathcal{F}_{\mathcal{C},\mathcal{O}}$ at most halves it, it is clear that strictly invariant compact sets with nonempty interior can only exist for $a \leq \sqrt{2}$. This condition is not sufficient: there exist a-values in $(1, \sqrt{2}]$ for which the self-similar polygons given in Theorem 1 are not strictly invariant. As an extreme example, for $\theta = 2\pi/3$, these polygons are triangles that are not strictly invariant for any $a > 1$, while, for $\theta = \pi/2$, they are strictly invariant rectangles for every $1 < a \leq \sqrt{2}$. According to the next result, except for $\theta = 2\pi/3$, these self-similar polygons become strictly invariant for every a sufficiently close to 1.

Theorem 2 (Existence of strictly invariant polygons)**.** *For every* $\theta \in (0, \pi) \setminus \{2\pi/3\}$, *there exists* $a_\theta > 1$ *such that the* $\mathbf{A}_{a,\theta}$*-self-similar polygon* $\mathcal{K}_N$ *is strictly* $\Gamma_{a,\theta}$*-invariant for every* $a \in (1, a_\theta]$. *For* $\theta = 2\pi/3$, *there exists* $a_\theta > 1$ *such that* $\Gamma^5_{a,\theta}(\mathcal{K}_2)$ *is a second-rate strictly* $\Gamma_{a,\theta}$*-invariant polygon for every* $a \in (1, a_\theta]$. *Consequently, for every* $0 < \theta < \pi$ *and every* $a \in (1, a_\theta]$,

$$\mathcal{K}_{a,\theta} = \bigcup_{n=1}^{\infty} \Gamma^n_{a,\theta}(\mathcal{K}_N)$$

is a strictly $\Gamma_{a,\theta}$*-invariant polygon.*

For $\theta = 3\pi/4$, it was proved [59] that $\mathcal{K}_{a,\theta}$ contains a 2-D strange attractor that may coincide with it (see [56] for $(1+\sqrt{2})^{1/4} < a \leq \sqrt{2}$), or it may be a 2-D strange attractor that splits into multiple pieces or even contain an arbitrarily large number of 2-D strange attractors [57, 58]. The following result generalizes Theorem 1.2 [59] and establishes that the set $\mathcal{K}_{a,\theta}$ contains some 2-D strange attractor for any $0 < \theta < \pi$.

Theorem 3 (Existence of 2-D strange attractors)**.** *Let* $0 < \theta < \pi$. *For every* $a \in (1, a_\theta]$, *there exists a finite family* $\mathtt{A}_{a,\theta}$ *of 2-D strange attractors for* $\Gamma_{a,\theta}$ *with nonempty interior verifying the following properties:*

(i) *Every attractor for* $\Gamma_{a,\theta}$ *in* $\mathcal{K}_{a,\theta}$ *belongs to* $\mathtt{A}_{a,\theta}$.

(ii) *For each* $\mathcal{A} \in \mathtt{A}_{a,\theta}$ *there exists an ergodic absolutely continuous invariant measure* μ *for* $\Gamma_{a,\theta}$ *supported on* $\mathcal{A}$.

(iii) *For each* $\mathcal{A} \in \mathtt{A}_{a,\theta}$ *there exists a natural number* $\mathtt{b}$ *and a decomposition*

$$\mathcal{A} = \mathcal{X}_0 \cup \mathcal{X}_1 \cup \cdots \cup \mathcal{X}_{\mathtt{b}-1}$$

of $\mathcal{A}$ *in such a way that* $\Gamma_{a,\theta}(\mathcal{X}_j) = \mathcal{X}_{j+1 \bmod \mathtt{b}}$ *for* $j = 0, \ldots, \mathtt{b}-1$. *The measure* μ *supported on* $\mathcal{A}$ *is mixing (up to the eventual period* $\mathtt{b}$*) and therefore* $\Gamma^{\mathtt{b}}_{a,\theta}$ *is topologically mixing on every* $\mathcal{X}_j$.

(iv) *If* $\mathcal{A} \in \mathtt{A}_{a,\theta}$, *then* $\mathcal{A}$ *traps almost every point in* $W^s(\mathcal{A})$, *i.e. for almost every point* $P \in W^s(\mathcal{A})$, *there exists* $j \in \mathbb{N}$ *with* $\Gamma^j_{a,\theta}(P) \in \mathcal{A}$. *Moreover, the set* $\bigcup_{\mathcal{A}\in\mathtt{A}_{a,b}} W^s(\mathcal{A})$ *covers a full Lebesgue measure set of* $\mathcal{K}_{a,\theta}$.

(v) If $\mathcal{K}$ is a compact $\Gamma_{a,\theta}$-invariant set with nonempty interior, then there exists $\mathcal{A} \in \mathtt{A}_{a,\theta}$ such that $\mathcal{A} \subseteq \mathcal{K}$. Moreover, if $\mathcal{K}$ and $\mathcal{K}'$ are two compact $\Gamma_{a,\theta}$-invariant sets with disjoint nonempty interiors, then there exist $\mathcal{A}, \mathcal{A}' \in \mathtt{A}_{a,\theta}$ with $\mathcal{A} \neq \mathcal{A}'$ such that $\mathcal{A} \subseteq \mathcal{K}$ and $\mathcal{A}' \subseteq \mathcal{K}'$.

Theorem 3 will be proved in the same way as Theorem 1.2 [59]. Nevertheless, we have to include certain crucial considerations on the *weighted multiplicity* which must be checked for all θ. Also, we point out that the proof of Theorem 3 mainly relies on the existence of an invariant set for $\Gamma_{a,\theta}$, which was given in Theorem 2, namely $\mathcal{K}_{a,\theta}$ (which is in fact strictly invariant), hence the restriction on the parameter interval.

From now on, we will consider $\theta = 2\pi p/q \in (0, \pi)$ with $p, q \in \mathbb{N}$ and $\gcd(p, q) = 1$. The following result shows how for a-values sufficiently close to 1 the strictly invariant polygon (and, consequently, the attractor it contains) splits into another invariant set formed by q pieces.

Theorem 4 (Existence of restrictive domains)**.** *Let $\theta = 2\pi p/q \in (0, \pi)$ with $p, q \in \mathbb{N}$ and $\gcd(p, q) = 1$. The following hold:*

(a) There exists $a_1 = a_1(\theta) > 1$ and a set $\mathcal{D} = \mathcal{D}(a, \theta) \subsetneq \mathcal{K}_{a,\theta}$ such that, for every $a \in (1, a_1)$, it holds that

(i) $\Gamma^n_{a,\theta}(\mathcal{D}) \cap \mathcal{D} = \varnothing$ for $n = 1, \ldots, q-1$

(ii) $\Gamma^q_{a,\theta}(\mathcal{D}) \subseteq \mathcal{D}$

(b) If $q \geq 4$, then the restriction of $\Gamma^q_{a,\theta}$ to $\mathcal{D}$ is a two-fold Expanding Baker Map.

A set verifying statements (i) and (ii) of (a) is said to be a *restrictive domain* of $\Gamma_{a,\theta}$. According to Theorem 4, the map $\Gamma_{a,\theta}$ displays a strange attractor with at least q pieces, each of which contained in a different $\Gamma^n_{a,\theta}(\mathcal{D})$ with $n = 0, 1, \ldots, q-1$. Note that from statement (a) it follows that $\Gamma^n_{a,\theta}(\mathcal{D}) \cap \Gamma^m_{a,\theta}(\mathcal{D}) = \varnothing$ whenever $n \neq m$. As a consequence of the proof of Theorem 4 we obtain the following result.

Corollary 1. *Under the hypotheses of Theorem 4, the set $\mathcal{D}$ can be constructed in such a way that every attractor for $\Gamma_{a,\theta}$ is contained in the forward orbit of $\mathcal{D}$.*

For values of $a < a_1$ sufficiently close to 1, the restriction of $\Gamma^q_{a,\theta}$ to $\mathcal{D}$ has an unstable focus P with eigenvalues $a^q \mathrm{e}^{2\theta_1 \mathrm{i}}$ with $\theta_1 = 2\pi/q$. The translation of P to the origin of coordinates and a suitable change in coordinates allows to express $\Gamma^q_{a,\theta}$ as the two-fold Expanding Baker Map

$$\Psi_{a,\theta} = \mathrm{EBM}(\mathcal{C}, \mathcal{L}_{a,\theta}, \mathcal{O}, \mathbf{A}_{a^q, 2\theta_1})$$

with

$$\mathcal{L}_{a,\theta} \equiv y = x \cot\theta_1 + \rho \csc\theta_1$$

where $\rho = \rho(a, \theta)$ satisfies $\lim_{a \to 1} \rho(a, \theta) = 1$. Let $\mathbb{F}^k_{\sigma,\varphi}$ be the family of Expanding Baker Maps

$$\Psi_{\sigma,\varphi} = \mathrm{EBM}(\mathcal{C}, \mathcal{L}_{\sigma,\varphi}, \mathcal{O}, \mathbf{A}^*)$$

satisfying the following conditions:

(R_1) $\mathcal{C}$ is the critical line $x = 1$

(R_2) $\mathcal{L}_{\sigma,\varphi}$ is a line that crosses $\mathcal{C}$ at an angle $0 < \varphi \leq 2\pi/5$ and its distance to $\mathcal{O}$ is equal to σ.

(R_3) $\mathbf{A}^*(z) = a^q \mathrm{e}^{2\varphi \mathrm{i}} z$.

Hence $\Psi_{a,\theta} \in \mathbb{F}^q_{a,\theta_1}$. We will consider $\mathrm{EBM}(\mathcal{C}, \mathcal{O}, \mathbf{A}^*)$ to be included in $\mathrm{EBM}(\mathcal{C}, \mathcal{L}_{\sigma,\varphi}, \mathcal{O}, \mathbf{A}^*)$, since this trivially holds when $\mathcal{L}_{\sigma,\varphi} = \mathcal{C}$ or $\mathcal{L}_{\sigma,\varphi}$ does not intersect a certain invariant set on which the dynamics is studied. Then we can state a first proper result on renormalization:

Theorem 5 (First renormalization)**.** *Let $\theta = 2\pi p/q \in (0, \pi)$ with $p, q \in \mathbb{N}$ and $\gcd(p, q) = 1$. If $q \geq 4$, then the following statements hold:*

(a) If q is odd, then there exists $a_2 = a_2(\theta) \in (1, a_1)$ such that $\Psi^q_{a,\theta}$ has a restrictive domain $\widehat{\mathcal{D}} = \widehat{\mathcal{D}}(a, \theta) \subsetneq \mathcal{D}$ for every $a \in (1, a_2)$.

(b) If $q = 2\nu$ is even, then one of the following statements hold:

(i) If ν is odd, there exists $a_2 = a_2(\theta) \in (1, a_1)$ such that $\Psi^\nu_{a,\theta}$ has a restrictive domain $\widehat{\mathcal{D}} = \widehat{\mathcal{D}}(a, \theta) \subsetneq \mathcal{D}$ for every $a \in (1, a_2)$.

(ii) If ν is even, there exists $a_2 = a_2(\theta) \in (1, a_1)$ such that $\Psi^\nu_{a,\theta}$ has two disjoint restrictive domains $\widehat{\mathcal{D}}^{\pm} = \widehat{\mathcal{D}}^{\pm}(a, \theta) \subsetneq \mathcal{D}$ for every $a \in (1, a_2)$. Moreover, the restriction of $\Psi^\nu_{a,\theta}$ to each one of these domains belongs to $\mathbb{F}^\nu_{a^q,\theta_1}$.

Statement (ii) of (b) still holds for $\Psi^{\nu/2}_{a,\theta}$ provided that ν is even, and successively for any power $q = 2^s$ with $s \geq 2$. Therefore, as we have stated above, as a consequence of the previous Theorems and Theorem B [58] (see Lemma 2.1.11 in Chapter 2) we obtain the following result.

Corollary 2 (Infinitely many doublings of attractors)**.** *Let $\theta = 2\pi p/q \in (0, \pi)$ with $p, q \in \mathbb{N}$ and $\gcd(p, q) = 1$. If $q = 2^s$ for some $s \geq 2$, then there exists a decreasing sequence*

$$a_1(\theta) > a_2(s) > \cdots > a_n(s) > a_{n+1}(s) > \cdots > 1$$

such that $\Gamma_{a,\theta}$ exhibits 2^{n-1} strange attractors simultaneously for every $a_{n+1}(s) \leq a < a_n(s)$ and every $n \geq 1$.

Coexistence of Attractors in the 2-D Quadratic Family

The dynamical behavior of the 2-D quadratic family is rather complicated as was numerically pointed out by Pumariño and Tatjer [61]. In Figure 14a, a region $\mathcal{P}$ of parameter values (a_0, b_0) for which an invariant domain for T_{a_0,b_0} is numerically detected was plotted. This region is colored according to a numerical analysis of Lyapunov exponents:

— Blue region: It corresponds to the parameter values for which the two Lyapunov exponents are negative (attracting periodic orbits)

— Green region: It corresponds to the parameter values for which one Lyapunov exponent is zero (attracting closed curves)

— Red region: It corresponds to the parameter values for which the sum and the product of the two Lyapunov exponents are negative (1-D strange attractors)

— Black region: It corresponds to the parameter values for which the sum of the two Lyapunov exponents is positive (2-D strange attractors)

As the authors point out, Figure 14a does not show the possible coexistence of attractors. In Figure 14b we gather additional information that indicates the competition between more than one attractor, as happens for $\Gamma_{a,\theta}$.

From Figure 14b we construct Figure 15 where we include significant points that will help us locate the statements of the following results. First, the point A is a tangency

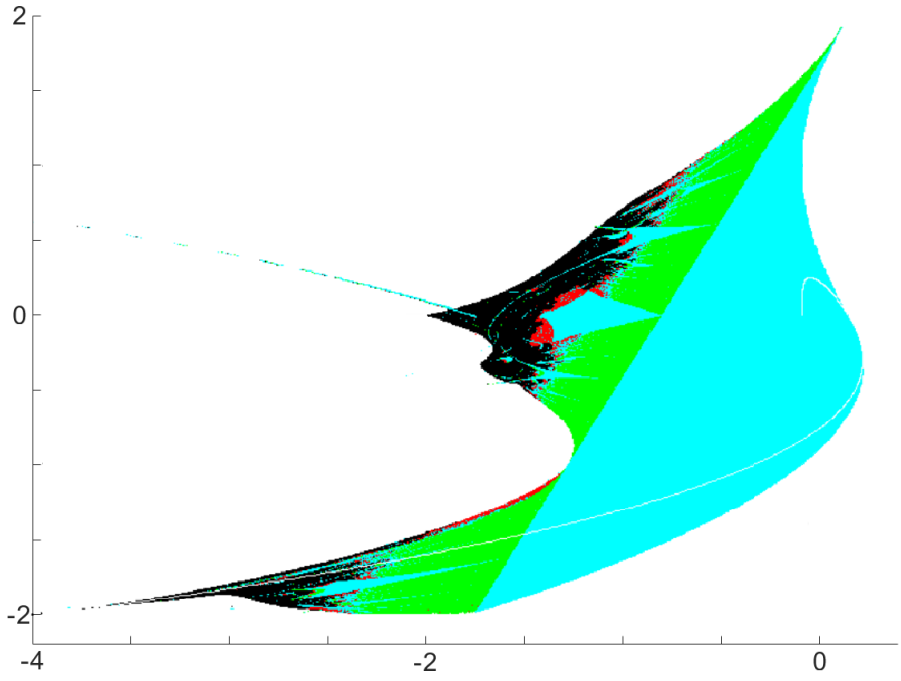

(a)

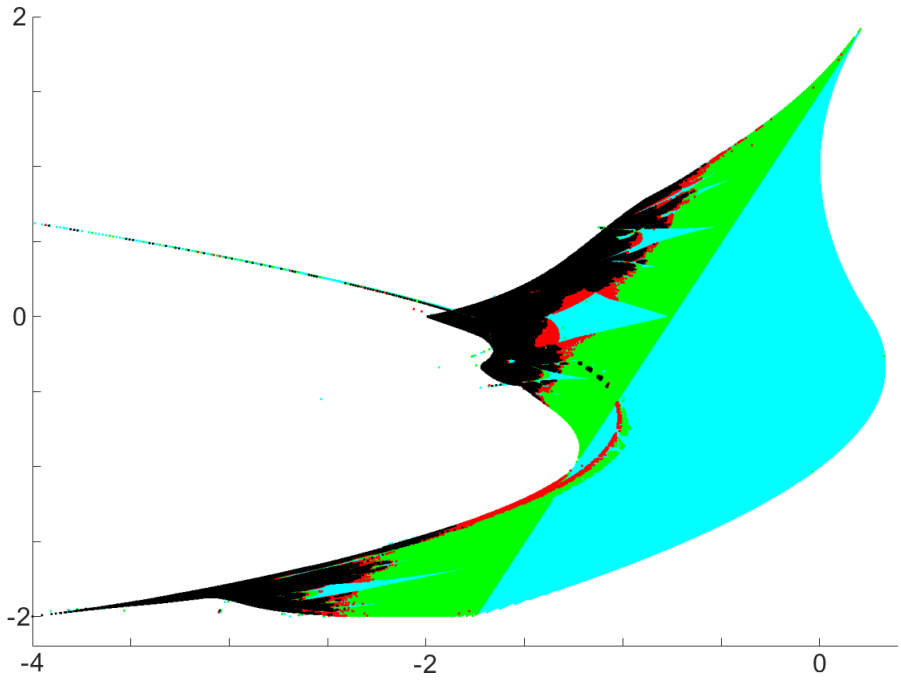

(b)

Figure 14: (a) Original parameter regions [61, Fig. 1] colored by the type of the attractor numerically detected; (b) New attractors appear in competition with those found in (a)

point of the curves $4a = (b-1)^2$ and $4a = 1 - 2b - 3b^2$ that limit, together with the line $4a = 2b - 3$, the parameter region for which there exists an attracting fixed point. In this region, the fixed point will be a focus if $64a + b^4 - 8b^3 + 8b^2 < 0$ and a node otherwise. The curve $64a + b^4 - 8b^3 + 8b^2 = 0$ intersects the line $4a = 2b - 3$ at the points $B = (1/4, 2)$ and $D = (-7/4, -2)$. For B, the unique fixed point $(1/2, 1/2)$ is a *Bogdanov–Takens singularity* (see Broer *et al* [8]). For D, the fixed point $(-3/2, -1/2)$ has double eigenvalue equal to -1. It is proved that it is a unipotent fixed point of T_D^2, but not a Bogdanov–Takens singularity. Along the segment $\overline{BD}$, a Hopf–Neimark–Sacker bifurcation occurs that explains the birth of attracting closed curves.

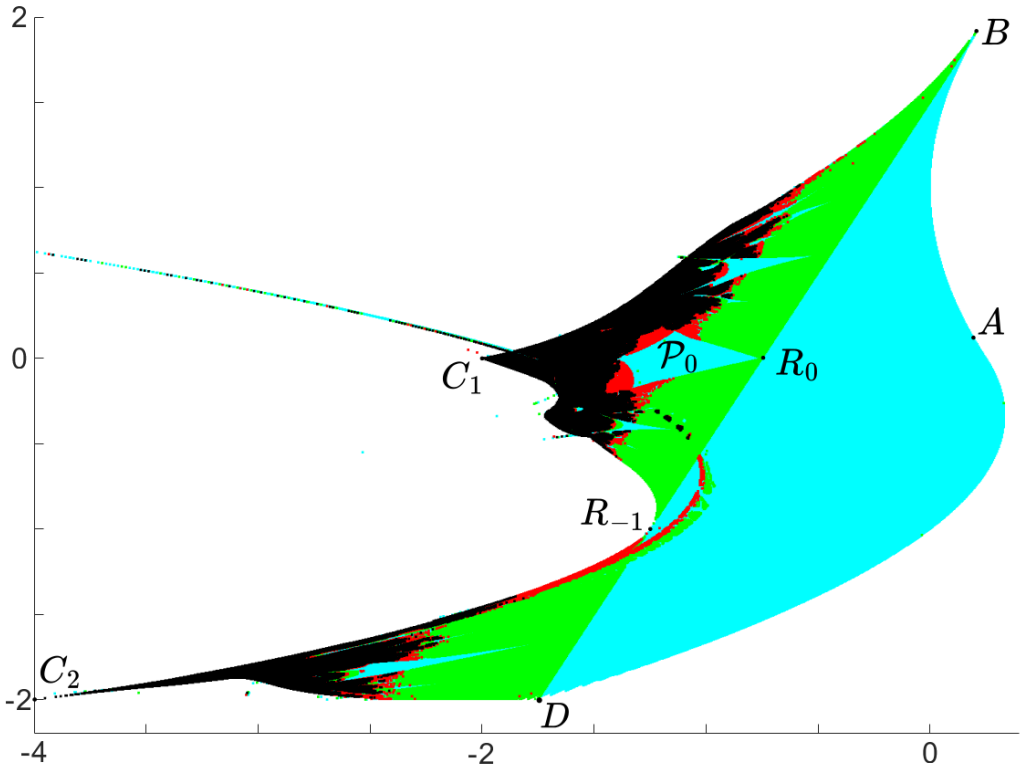

Figure 15: Significant points in the parameter plane (a, b): $A = (1/4, 0), B = (1/4, 2), C_1 = (-2, 0), C_2 = (-4, -2), D = (-7/4, -2), R_{-1} = (-5/4, -1), R_0 = (-3/4, 0)$

We start Chapter 3 with the study of the fixed points of family $T_{a,b}$, which are the simplest organizers of its dynamics. See Figure 16.

Theorem 6. *The fixed points of the quadratic family*

$$T_{a,b}(\mathbf{x}, \mathbf{y}) = (a + \mathbf{y}^2, \mathbf{x} + b\mathbf{y})$$

verify the following statements:

a) If $4a > (b-1)^2$, then $T_{a,b}$ has no fixed points. Moreover, there is no bounded orbit.

b) If $4a = (b-1)^2$, then $T_{a,b}$ has a unique fixed point

$$P^{(1)} = (\tfrac{1}{2}(1-b)^2, \tfrac{1}{2}(1-b))$$

with eigenvalues $b-1$ and 1. In particular, for $(a, b) = (1/4, 2)$, the fixed point $(1/2, -1/2)$ is a Bogdanov–Takens singularity.

c) If $4a < (b-1)^2$*, then* $T_{a,b}$ *has two different fixed points:*

$$P^{(1),\pm} = ((1-b)\mathbf{y}^{\pm}, \mathbf{y}^{\pm}), \qquad \mathbf{y}^{\pm} = \tfrac{1}{2}(1-b) \pm \tfrac{1}{2}\sqrt{(b-1)^2 - 4a}$$

i) The fixed point $P^{(1),-}$ *is a focus if and only if*

$$64a + b^4 - 8b^3 + 8b^2 < 0, \quad 4a \neq 2b - 3$$

This focus is attracting if $4a > 2b - 3$ *and repelling otherwhise. Along the segment*

$$4a = 2b - 3, \qquad -2 < b < 2$$

the fixed point $P^{(1),-}$ *is a center. Moreover, a Hopf–Neimark–Sacker bifurcation occurs at* $P^{(1),-}$ *for* $b \neq -1, 0$*. The curve* $64a + b^4 - 8b^3 + 8b^2 = 0$ *intersects the segment* $4a = 2b - 3$ *at the points* $B = (1/4, 2)$ *and* $D = (-7/4, -2)$*. For* $(a, b) = D$*, the fixed point* $P^{(1),-}$ *has double eigenvalue equal to* -1*. It is a unipotent singularity of* T_D^2*, but not Bogdanov–Takens.*
If $64a + b^4 - 8b^3 + 8b^2 \geq 0$*, then* $P^{(1),-}$ *is a node if and only if either* $b \geq 0$ *or*

$$4a + 3b^2 + 2b - 1 < 0, \qquad b < 0$$

This node is attracting if $-2 < b < 2$ *and repelling otherwise. If*

$$4a + 3b^2 + 2b - 1 > 0, \qquad b < 0$$

then $P^{(1),-}$ *is a saddle fixed point that is dissipative if and only if*

$$2b + 3 < 4a < 1 - 2b$$

ii) The fixed point $P^{(1),+}$ *is a repelling node if either* $b \leq 0$ *or*

$$4a + 3b^2 + 2b - 1 < 0, \qquad b > 0$$

If

$$4a + 3b^2 + 2b - 1 > 0, \qquad b > 0$$

then $P^{(1),+}$ *is a saddle fixed point that is dissipative if and only if* $4a > 1 - 2b$ *and*

$$4a < 2b - 3, \qquad b > 2$$

On the left-hand side of the segment $\overline{BD}$, neither of the two fixed points is attracting. However, we can find subregions in $\mathcal{P}$ for which the existence of attracting periodic orbits is proved. This is the case for the sharp region $\mathcal{P}_0$ in blue that has its vertex R_0 on $\overline{BD}$. See Figure 15. Certainly, the point R_0, as well as R_{-1}, corresponds to parameter values for which certain resonances prevent the Neimark–Sacker bifurcation. Moreover, on the right-hand side of $\overline{BD}$ there exist parameter values for which, besides the attracting fixed point, there also exist attracting periodic orbits, closed curves, and 1-D strange attractors. This coexistence will be explained after a selective study on the existence of periodic orbits of low period for the 2-D quadratic family.

We will first study the existence of 2-periodic orbits to conclude that there are no attracting ones. Afterwards, we will prove the existence of attracting 2^n-periodic orbits for $n \geq 2$ in the region $\mathcal{P}_0$, more precisely along the line $b = 0$. Of greater interest will be to prove the existence of 3-periodic orbits along the line $b = -1$, which transversally cuts $\mathcal{P}$ through the point R_{-1}. For this case, we will prove that two families of 3-periodic orbits appear. See Figure 17.

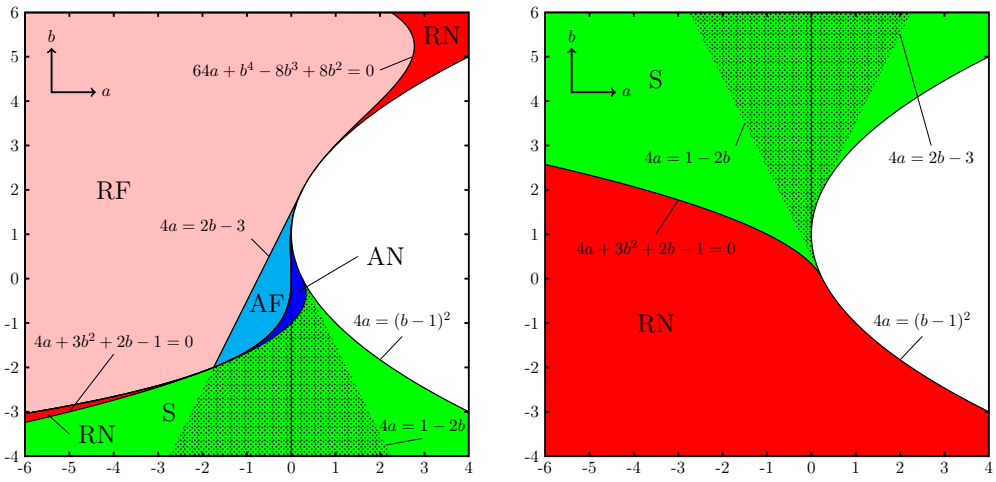

(a) (b)

Figure 16: (a) Stability configuration of the fixed point $P^{(1),-}$ in (a, b): AN (blue): attracting node; RN (red): repelling node; AF (cyan): attracting focus; RF (pink): repelling focus; S (green): saddle fixed point, dotted: dissipative. Along $a = 0$ with $b \leq 1$, one eigenvalue is zero. (b) Stability configuration of the fixed point $P^{(1),+}$ in (a, b): RN (red): repelling node; S (green): saddle fixed point, dotted: dissipative. Along $a = 0$ with $b \geq 1$, one eigenvalue is zero.

From one of them, attracting closed curves are originated (see Figure 18) that collide with the other orbit of saddle type giving rise to a homoclinic orbit as numerically checked in Figure 19. By unfolding these homoclinic tangencies the formation of 1-D strange attractors will take place [44]. The transitions are represented in Figure 20 for $b = -1$ in an interval of a-values.

Theorem 7. *The following statements on the periodic orbits of*

$$T_{a,b}(\mathbf{x}, \mathbf{y}) = (a + \mathbf{y}^2, \mathbf{x} + b\mathbf{y})$$

hold:

1. *There exists a 2-periodic orbit if and only if*

$$4a < 1 - 2b - 3b^2$$

In such case, it is unique. Moreover, it is a repelling node if

$$4a < -3 - 6b - 5b^2$$

If $4a > -3 - 6b - 5b^2$, then it is a saddle periodic orbit that is dissipative if and only if

$$4a > -1 - 4b - 4b^2$$

and either $-2 < b < 0$ or $4a < 1 - 4b - 4b^2$.

2. *Let $b = 0$. There exists a decreasing sequence*

$$-2 < \cdots < a_{n+1} < a_n < \cdots < a_3 < a_2 = -\tfrac{3}{4}$$

of a-values such that there exists an attracting 2^n-periodic orbit for every $a_{n+1} < a < a_n$ and $n \geq 2$.

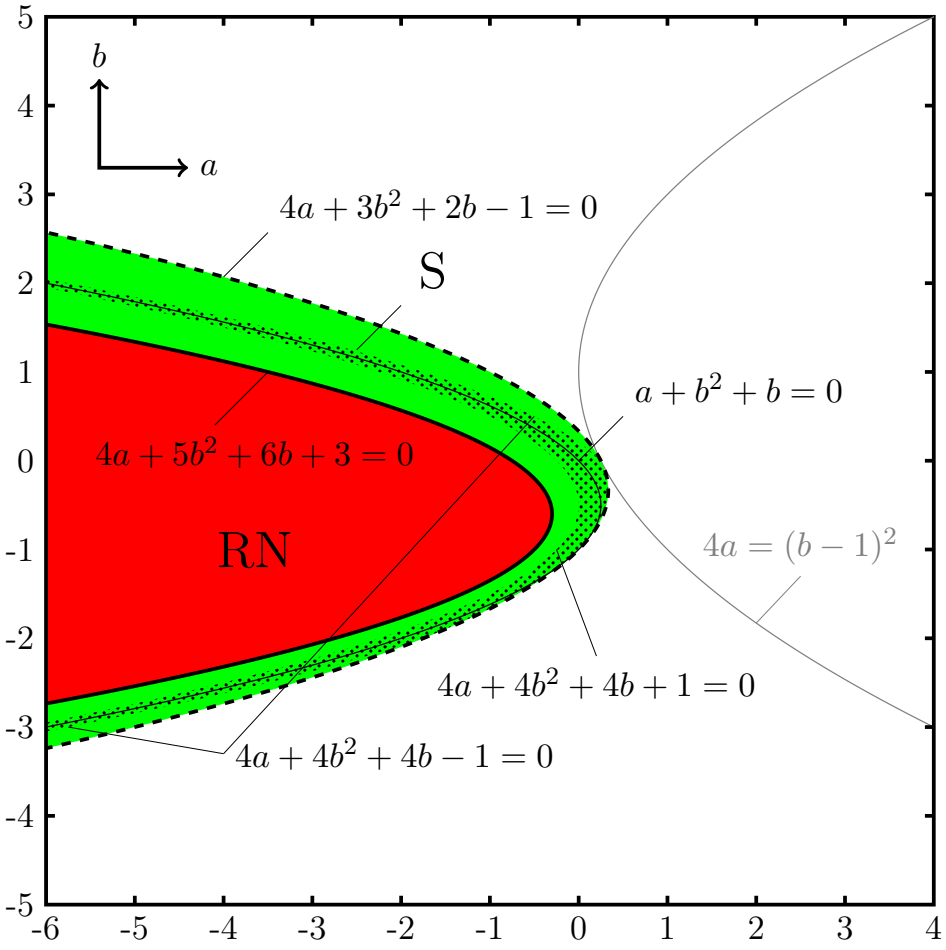

(a)

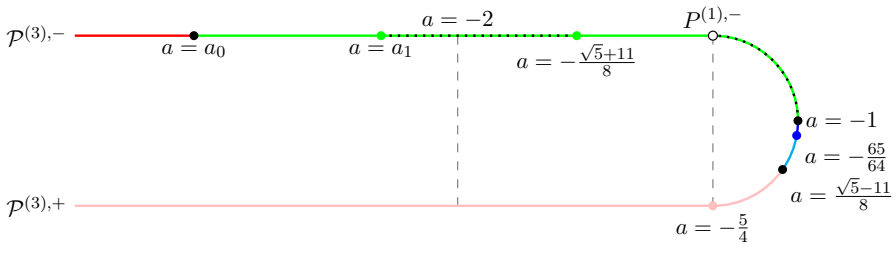

(b)

Figure 17: (a) Stability configuration of the unique 2-periodic orbit of $T_{a,b}$: RN (red): repelling node; S (green): saddle fixed point, dotted: dissipative. Along $a + b^2 + b = 0$, one eigenvalue is zero. (b) Stability configuration of the two 3-periodic orbits $\mathcal{P}^{(3),\pm}$ of $T_{a,b}$ for $b = -1$: attracting node (blue); repelling node (red); attracting focus (cyan); repelling focus (pink); saddle fixed point (green), dotted: dissipative. For $a = -5/4$, the orbit $\mathcal{P}^{(3),-}$ collapses to the fixed point $P^{(1),-}$.

3. *Let $b = -1$. There exists a 3-periodic orbit if and only if $a \leq -1$. Moreover:*

   (a) *If $a = -1$ or $a = -5/4$, then there exists a unique 3-periodic orbit $\mathcal{P}^{(3)}$. If $a = -1$, then*

   $$\mathcal{P}^{(3)} = \{(0,0), (-1,0), (-1,-1)\}$$

   with eigenvalues 0 and 1. If $a = -5/4$, then

   $$\mathcal{P}^{(3)} = \{(1, \tfrac{1}{2}), (-1, \tfrac{1}{2}), (-1, -\tfrac{3}{2})\}$$

   with eigenvalues $\pm \mathrm{i}\sqrt{3}$.

   (b) *If $a \in (-\infty, -1) \setminus \{-5/4\}$, then there exist two different 3-periodic orbits $\mathcal{P}^{(3),\pm}$.*

      i) *The orbit $\mathcal{P}^{(3),-}$ is a dissipative saddle periodic orbit if $a > -5/4$. There exists $a_0 < -2$ such that $\mathcal{P}^{(3),-}$ is a repelling node if $a < a_0$ and a saddle periodic orbit if $a_0 < a < -5/4$, which is dissipative if and only if $a_1 < a < -(11+\sqrt{5})/8$ for some $a_0 < a_1 < -2$. For $a = a_0$, the orbit $\mathcal{P}^{(3),-}$ has one eigenvalue equal to -1.*

      ii) *The orbit $\mathcal{P}^{(3),+}$ is an attracting node if $a \geq -65/64$. For $a < -65/64$, the orbit $\mathcal{P}^{(3),+}$ is a focus if and only if $a \neq (\sqrt{5} - 11)/8$. This focus is attracting if $a > (\sqrt{5}-11)/8$ and repelling otherwise. For $a = (\sqrt{5}-11)/8$, a Hopf–Neimark–Sacker bifurcation occurs at $\mathcal{P}^{(3),+}$.*

4. *For each $n \in \mathbb{N}$, there exists a compact set (depending on a and b) with nonempty interior containing all the n-periodic orbits.*

Before trying to prove the persistence of 2-D strange attractors, we observe that the black region seems to spring from both C_1 and C_2. Thus, we first construct invariant compact sets with nonempty interior for parameter values in sharp regions with vertices C_1 and C_2, respectively. We will prove the following result.

Theorem 8. *Each $(a^*, b^*) \in \{(-2,0), (-4,-2)\}$ is the vertex of a sharp region $\mathcal{V}(a^*, b^*)$ such that, for every $(a,b) \in \mathcal{V}(a^*, b^*)$, there exists a $T_{a,b}$-invariant compact set with nonempty interior.*

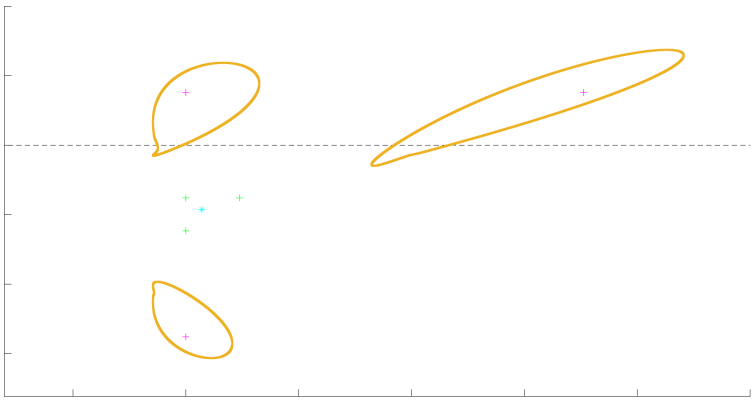

Figure 18: The repelling 3-periodic focus in magenta for $(a,b) = (-1.1145, -1)$ gives rise to three limit cycles that get closer to the dissipative saddle 3-periodic orbit in green, closer itself to the attracting fixed focus in cyan

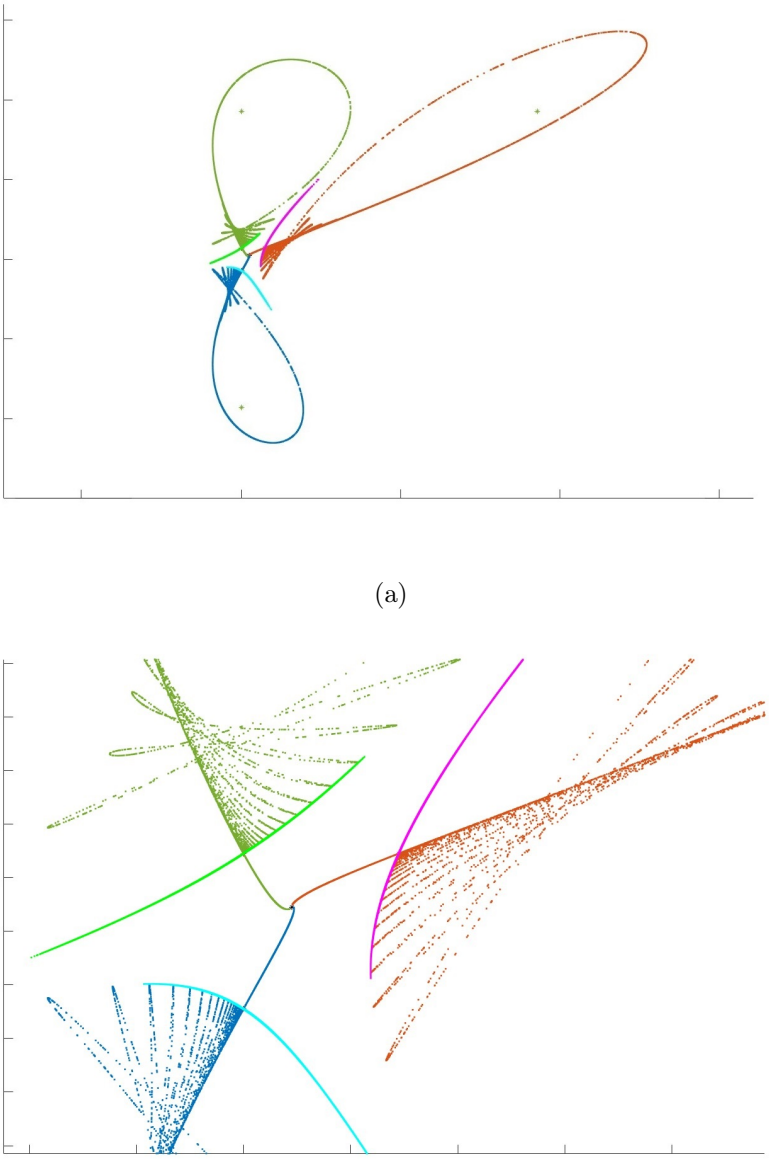

(a)

(b)

Figure 19: (a) Homoclinic tangencies unfolding 1-D strange attractors for $(a, b) = (-1.18282, -1)$. (b) Amplification of (a).

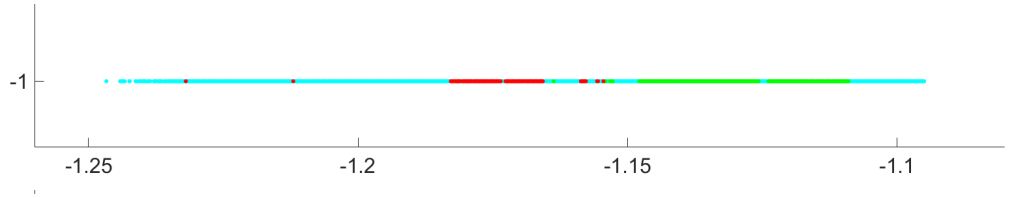

Figure 20: Different transitions for $b = -1$ with $a \in [-5/4, -1]$ colored as Figure 14b

As a consequence of the proof of Theorem 8 we obtain more information for the parameter curve $2a = b^3$. A numerical simulation of the attractors along this curve reminds of the ones obtained along curve G, though we get even more information along the former.

Theorem 9. *For parameter values along the curve $2a = b^3$, the following hold:*

1) *If $b = -2$, the curvilinear triangle $\mathcal{K}$ limited by the first three iterates of the critical line is strictly $T_{-4,-2}$-invariant. Moreover, it is a strange attractor on which the Lebesgue measure is invariant and ergodic.*

2) *If $b > -2$, the triangle $\mathcal{K}$ is $T_{a,b}$-invariant, but not in a strict sense. This triangle contains the curvilinear pentagon limited by the first five iterates of the critical line, which is strictly $T_{a,b}$-invariant for all $-2 < b < b_1$, for some $b_1 > -2$.*

3) *If $b < -2$, then there exists no strictly $T_{a,b}$-invariant compact set with nonempty interior.*

For $b > b_1$, we expect strictly invariant curvilinear polygons of a larger number of sides to appear.

After performing suitable changes of variables and parameters, the family $T_{a,b}$ can be written as

$$F_{c,b}(x, y) = (y, cx(2 - x) + by)$$

where

$$c = \tfrac{1}{2}(1 - b - \delta), \qquad \delta = \sqrt{(b-1)^2 - 4a}$$

Frequently, this new expression will be more useful to study the dynamics. Moreover, the family $F_{c,b}$ can be expressed as the composition of a diffeomorphism with a fold. This allows to compare $F_{c,b}$ with $\Gamma_{a,\theta}$.

Open Problems

From the analytic and geometric study carried out throughout this memoir many open questions come up, all of which supported by the corresponding numerical experimentation. Apart from the analytic proof for the persistence of 2-D strange attractors, most of the renormalization results obtained for $\Gamma_{a,\theta}$ suggest similar challenges for a better description of the dynamics of $T_{a,b}$. In fact, a complete renormalization process for the former has not been developed yet. Also, some results on statistical stability verified for Λ_t have not been proved yet either. In this brief final introductory section we bring about all these topics for future research.

Minimality of the Polygonal Domain

If the strictly invariant compact polygon $\mathcal{K}_{a,\theta}$ is minimal (i.e. contains no invariant compact set with nonempty interior different from itself), then it is an attractor by definition. In that case, such polygon contains a dense orbit with two positive Lyapunov exponents and, therefore, it will be a 2-D strange attractor.

Let $\mathcal{K}^*_{a,\theta} = \mathcal{K}_{a,\theta} \cap \{x \geq 1\}$. Numerical experiments suggest that $\mathcal{K}_{a,\theta}$ is minimal if and only if $\mathcal{O} \in \mathcal{F}_{\mathcal{C},\mathcal{O}}(\mathcal{K}^*_{a,\theta})$, that is, if and only if $(2, 0) \in \mathcal{K}^*_{a,\theta}$. As a decreases, the folded set $\mathcal{F}_{\mathcal{C},\mathcal{O}}(\mathcal{K}^*_{a,\theta})$ shrinks and there is an a-value a^* such that $\mathcal{O} \in \mathcal{F}_{\mathcal{C},\mathcal{O}}(\mathcal{K}^*_{a,\theta})$ for $a = a^*$ and $\mathcal{O} \notin \mathcal{F}_{\mathcal{C},\mathcal{O}}(\mathcal{K}^*_{a,\theta})$ for all $a < a^*$.

Conjecture. *Let $0 < \theta < \pi$. The strictly invariant polygon $\mathcal{K}_{a,\theta}$ is minimal if and only if $(2, 0) \in \mathcal{K}^*_{a,\theta}$.*

For $\theta = 3\pi/4$, it is proved [54] that $(2,0) \in \mathcal{K}^*_{a,\theta}$ if and only if $a \geq \sqrt[6]{2}$. Moreover, it is proved [56] that $\mathcal{K}_{a,\theta}$ is transitive for all $(1+\sqrt{2})^{1/4} \leq a \leq \sqrt{2}$. The expansivity of $\Gamma_{a,\theta}$ for these a-values guarantees then that $\mathcal{K}_{a,\theta}$ is a strange attractor. For slightly smaller a-values, it was numerically shown [54, 55] that the pentagon $\mathcal{K}_{a,\theta}$ loses its minimality to contain another attractor that is connected, but not simply connected: a hole around $\mathcal{O}$ appears. This hole expands as a decreases until the attractor splits into eight connected pieces for a-values slightly smaller than $a = \sqrt[10]{2}$. This motivates the following conjecture.

Conjecture. *Let $0 < \theta < \pi$. Let $a_0' > 1$ be the minimum of the a-values for which $(2,0) \in \mathcal{K}_{a,\theta}$. Then, there exists $a_0'' \in [1, a_0')$ such that, for every $a \in [a_0'', a_0')$, there exists a connected neighborhood $\mathcal{U}_{a,\theta}$ of $\mathcal{O}$ such that $\mathcal{K}_{a,\theta} \setminus \mathcal{U}_{a,\theta}$ is strictly invariant and minimal (hence a non-simply connected strange attractor). Moreover, it holds that $a_0'' = 1$ if and only if θ/π is an irrational number.*

Numerical experiments also seem to support this conjecture. See Figures 21, 22, and 23. A numerical approach to the irrational case is not possible, so that it can only be analytically tackled.

Further Renormalizations: A Sequence of Splittings and Doublings of Attractors

In the rational case, we conjecture that a process of splitting and/or doubling of attractors occurs for a sequence of a-values in $(1, a_0'')$. This is actually a hard task that requires to control a complicated process of renormalization. Given $\theta = 2\pi p/q \in (0,\pi)$ with $p, q \in \mathbb{N}$ and $\gcd(p,q) = 1$, we have proved the existence of two consecutive splittings of the strictly invariant set, and therefore of the strange attractor it contains, for $q \geq 4$ (one splitting for $q = 3$.) However, when q is odd or $q = 2\nu$ with ν odd, for the study of a possible third splitting it is necessary to consider a three-fold Expanding Baker Map. Then, it seems natural to ask whether the splitting process finishes at that point or further renormalizations can be carried out considering Expanding Baker Maps of more folds. A possible increasing number of folds could make this problem analytically unmanageable.

After the proof of Theorem 5, we can formulate a first conjecture in the following terms.

Conjetura. *For each $m \in \{0, 1, \ldots, \infty\}$, let S_m be the mth level of the Sarkovskii ordering:*

$$
\begin{aligned}
&S_0 : 3 \rhd 5 \rhd 7 \rhd 9 \rhd \cdots \\
&S_1 : 3 \times 2 \rhd 5 \times 2 \rhd 7 \times 2 \rhd \cdots \\
&\cdots \\
&S_m : 3 \times 2^m \rhd 5 \times 2^m \rhd 7 \times 2^m \rhd \cdots \\
&\cdots \\
&S_\infty : \cdots \rhd 2^n \rhd \cdots \rhd 2^3 \rhd 2^2 \rhd 2 \rhd 1
\end{aligned}
$$

Then, the following hold:

i) For every $q \in S_1 \cup S_0 \setminus \{3\}$ there exists an infinite sequence of splitting of attractors.

ii) For every $q \in S_m$ with $2 \leq m < \infty$ there exist $m-1$ doublings followed by an infinite sequence of splittings of attractors.

iii) For every $q \in S_\infty \setminus \{1, 2\}$ there exists an infinite sequence of doublings of attractors.

We know by Corollary 2 that statement iii) holds. Numerically, some simulations in Figure 21 show that for $q = 7$ each one of the 49 pieces obtained for $a = 1.006$ split again

into another 7 pieces as is shown for $a = 1.0006$. In Figure 24 we show the case $q = 24$ for $a = 1.0001$ in which each one of the 24 pieces of the initial attractor has split into 12, then into 6, and finally into 3. In Figure 25 we show for $q = 8$ the coexistence of two 32-piece strange attractors for $a = 1.01$.

Statistical Stability of the General Two-Parameter Family Expanding Baker Maps

Fix $0 < \theta < \pi$, and take a_θ from Theorem 2. From the very definition of $\mathcal{K}_N$, it will follow that $\mathcal{K}_{a_\theta,\theta}$ is $\Gamma_{a,\theta}$-invariant for all $1 < a \leq a_\theta$. Therefore, the one-parameter family $\Gamma_{a,\theta} \colon \mathcal{K}_{a_\theta,\theta} \to \mathcal{K}_{a_\theta,\theta}$ with $a \in (1, a_\theta]$ is well defined and we can consider questions such as the statistical stability.

Conjecture. *For every $0 < \theta < \pi$, the family $\{\Gamma_{a,\theta}\}_{1<a\leq a_\theta}$ is statistically stable.*

The Singular Case $q = 3$

A study on all the previous questions, as well as the particular ones, should be carry out for the angle $\theta = 2\pi/3$. See Figure 26.

Conjecture. *Let $\theta = 2\pi/3$. Then, there exists $\tilde{a} > a_\theta$ such that $\mathcal{K}_{a,\theta}$ is a compact polygon if $a \leq \tilde{a}$ and $\mathcal{K}_{a,\theta} = \Gamma^2_{a,\theta}(\mathbb{R}^2)$ otherwise.*

Conjecture. *Let $\theta = 2\pi/3$. Then, there exists an infinite sequence of splitting of attractors.*

Calculation of All the Three-Periodic Orbits

The assumption $b = -1$ simplifies the calculation of the 3-periodic orbits. Numerical experimention confirms that the parabolic-like region whose boundary seems to match one of the "hairs" of the parameter region $\mathcal{P}$ coincides with the region of existence of all such orbits.

Conjecture. *The curve from Figure 14b going through $(a, b) = (-1, -1)$ that matches the mostly blue "hair" limits the region of existence of the 3-periodic orbits.*

Points of Density of 2-D Strange Attractors

The study of the stability of the periodic orbits of $T_{a,b}$, and especially the attention paid to the nonhyperbolic cases, allows to prove the existence of three out of the four types of attractors that had been numerically detected in Figure 14, namely: attracting periodic orbits, closed curves, and 1-D strange attractors. However, the existence of 2-D strange attractors such as the ones numerically detected in Figure 14 must involve the non-injective character of the quadratic maps. That is the only way an invariant compact set $\mathcal{K}$ can contain its expanded image, yet folded. That is, on the 2-D strange attractor, the map $T_{a,b}$ cannot be injective. In other words, the set $\mathcal{K}$ must cut the critical line $y = 0$. For this reason, here we will search for invariant compact sets $\mathcal{R}_{a,b}$ with nonempty interior intersecting the critical line $y = 0$. Of course, such compact set $\mathcal{R}_{a,b}$ is not necessarily a 2-D strange attractor. It is precise that it contains a dense orbit with two positive Lyapunov exponents. Moreover, in order that such 2-D strange attractor can be observable, it is necessary that it be persistent. For the beginning of the proof of the persistence of 2-D strange attractors we will place ourselves at the points $C_1 = (-2, 0)$ and $C_2 = (-4, -2)$ on the boundary of $\mathcal{P}$, which are vertices of the respective sharp regions of the parameter values for which 2-D strange attractors seem to appear (see Figure 15). We conjecture that these points are *points of density* of persistent 2-D strange attractors.

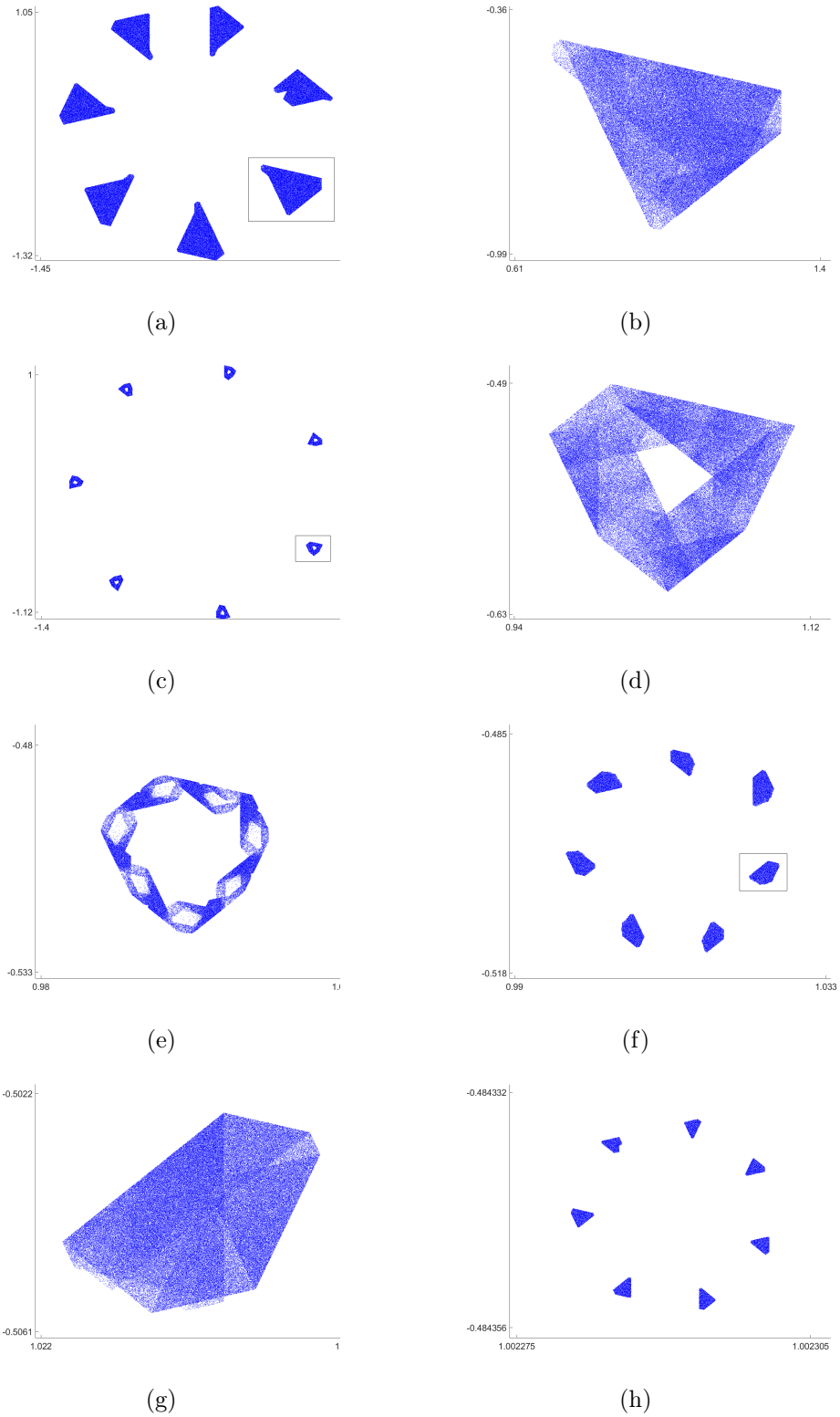

Figure 21: Numerical simulation for $\theta = 2\pi/7$ and decreasing values of a: (a) 7-piece attractor for $a = 1.05$; (b) Amplification of a piece in (a); (c) 7-piece attractor for $a = 1.02$; (d) Amplification of a not simply connected piece in (c); (e) Evolution of (d) before the splitting; (f) Splitting of (d) for $a = 1.006$; (g) Amplification of a piece in (f); (h) Splitting of (g) for $a = 1.0006$.

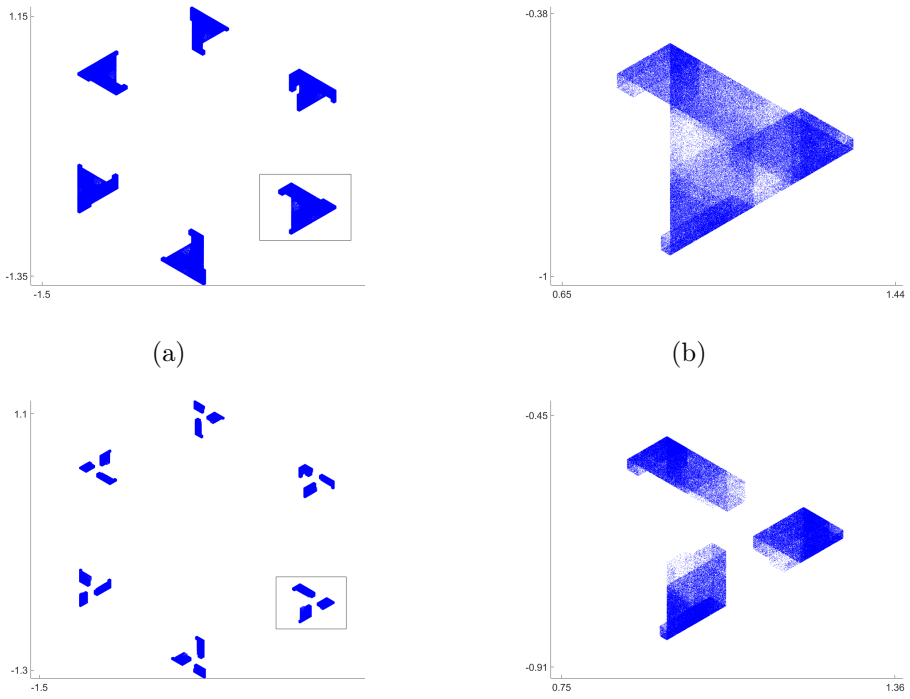

Figure 22: Numerical simulation for $\theta = 2\pi/6$ and decreasing values of a: (a) 6-piece attractor for $a = 1.05$; (b) Amplification of a piece in (a); (c) Splitting of (b) for $a = 1.04$; (d) Amplification of a piece in (c).

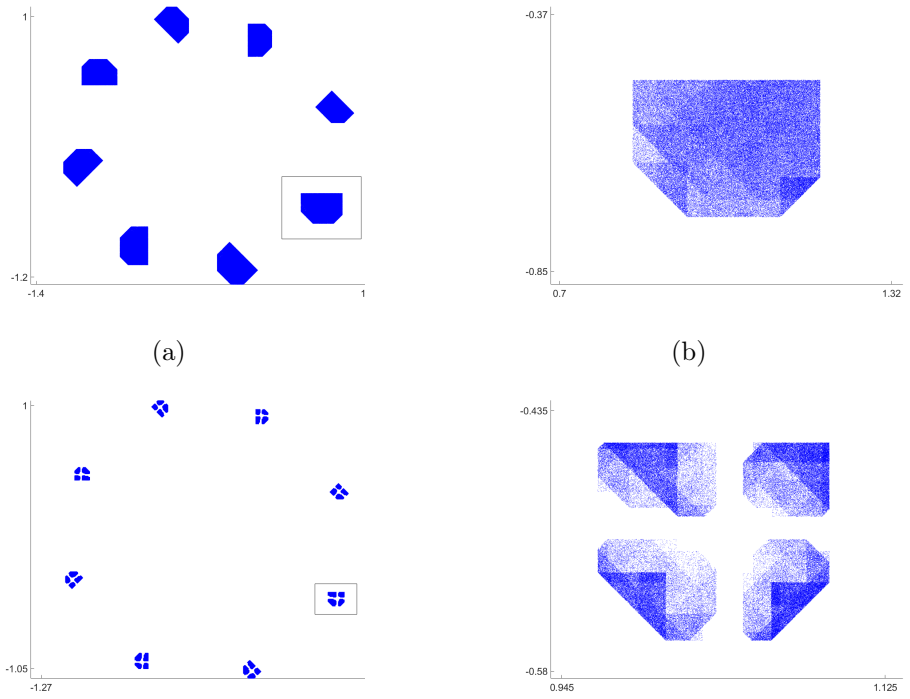

Figure 23: Numerical simulation for $\theta = 2\pi/8$ and decreasing values of a: (a) 8-piece attractor for $a = 1.05$; (b) Amplification of a piece in (a); (c) Splitting of (b) for $a = 1.02$; (d) Amplification of a piece in (c).

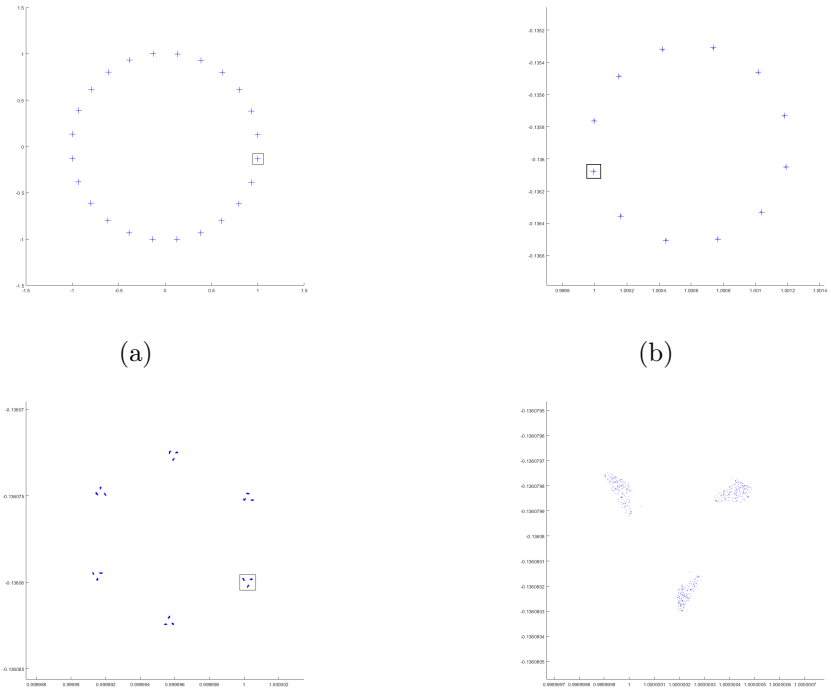

(a) (b)

(c) (d)

Figure 24: Numerical simulation for $\theta = 2\pi/24$ and $a = 1.0001$: (a) The $(24 \times 12 \times 6 \times 3)$-piece attractor; (b) Amplification of a piece in (a); (c) Amplification of a piece in (b); (d) Amplification of a piece in (c).

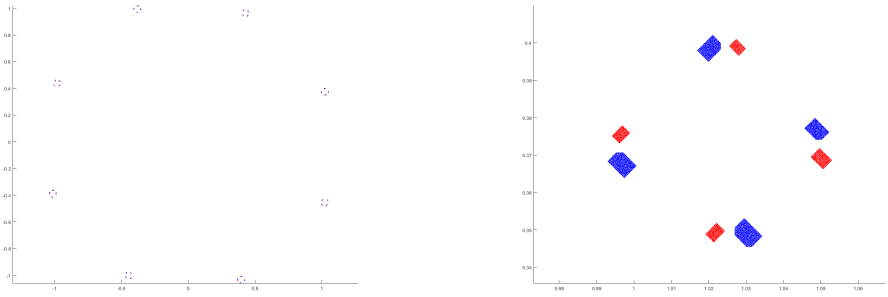

(a) (b)

Figure 25: Coexistence of attractors for $\theta = 2\pi/8$: (a) Two 32-piece attractors for $a = 1.01$; (b) Amplification of 4 pieces of the two attractors in (a).

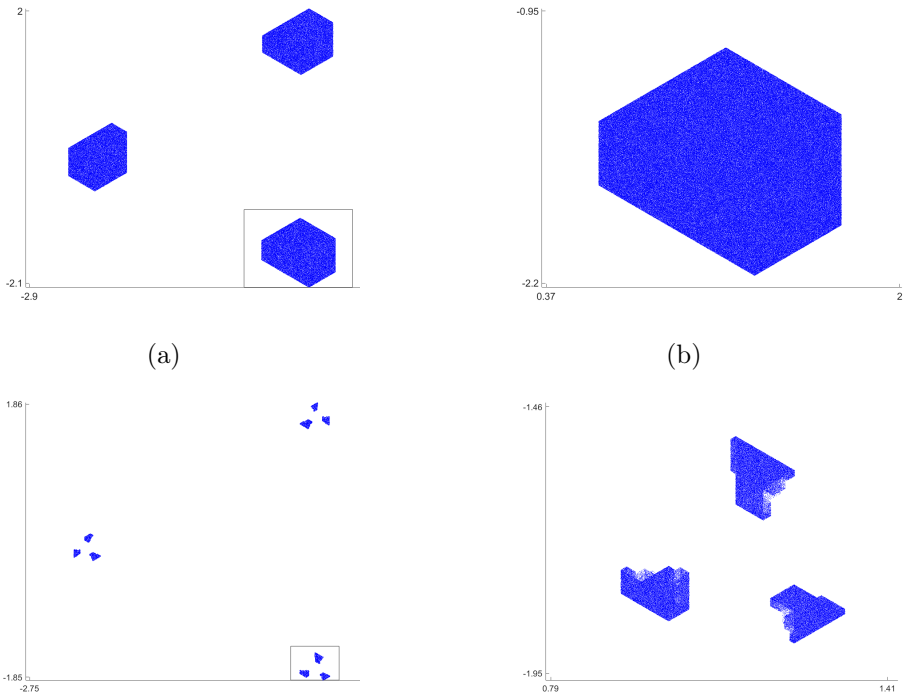

(a) (b)

(c) (d)

Figure 26: Numerical simulation for $\theta = 2\pi/3$ and decreasing values of a: (a) 3-piece attractor for $a = 1.1$; (b) Amplification of a piece in (a); (c) Splitting of (b) for $a = 1.05$; (d) Amplification of a piece in (c).

Definition (Points of density)**.** A *point of density* of persistent (strange) attractors for a family f_μ of diffeomorphisms is a μ-value μ^* for which every neighborhood of μ^* has a subset E containing μ^* with positive Lebesgue measure such that f_μ has a (strange) attractor for every $\mu \in E$.

Proving that any of the points C_1 or C_2 are points of density of persistent strange attractors is a very difficult task. In this thesis, we limit ourselves to studying the existence of possible invariant compact sets $\mathcal{R}_{a,b}$ with nonempty interior for an open set of parameter values close to both C_1 and C_2. If these invariant compact sets are minimal (transitive), then they will be attractors. To conclude that they are 2-D strange attractors, it is necessary to prove the existence of a dense orbit in $\mathcal{R}_{a,b}$ with two positive Lyapunov exponents (or at least whose sum is positive). This is the main stumbling block.

Conjecture. *The parameter points C_1 and C_2 are points of density of persistent 2-D strange attractors.*

Chapter 1

The 2-D Quadratic Family as a Limit Return Maps Family in the Unfolding of a 3-D Generalized Homoclinic Tangency

We include this chapter in this memoir to give a proper presentation of the 2-D quadratic family $T_{a,b}$. We briefly describe Tatjer's main theorem [67, Th. 1] that explains how to obtain the two-parameter quadratic family

$$\tilde{f}_{\tilde{a},\tilde{b}}(\tilde{x},\tilde{y},\tilde{z}) = (\tilde{z}, \tilde{a} + \tilde{b}\tilde{y} + \tilde{z}^2, \tilde{y})$$

as the limit return maps of a two-parameter family of 3-D diffeomorphisms generically unfolding a certain case of generalized homoclinic tangency.

In Section 1.1 we give a background on the homoclinic scenario in dimension-two, introducing important notions such as the limit return maps of a family of diffeomorphisms near a homoclinic orbit. We focus on the three-dimensional case in Section 1.2 reviewing Tatjer's work [67] and defining the generalized homoclinic tangency. In Section 1.3 we introduce the family $T_{a,b}$.

1.1 Introduction: 2-D Homoclinic Dynamics

From the time of Poincaré, homoclinic scenarios have been usually identified with the presence of a rich amount of complicated dynamics. Especially from the sixties to the present day, a great effort has been done in order to clarify all the possible chaotic behaviors emerging when a *homoclinic tangency* is unfolded in the two-dimensional setting. By this unfolding we mean the creation of homoclinic orbits associated to a periodic saddle fixed point. More concretely, assume the presence of a periodic saddle fixed point of a diffeomorphism on a surface whose invariant manifolds intersect at some homoclinic point. A natural question in this scenario is: How does the existence of this homoclinic point affect to the dynamics? Or, more precisely: How does the dynamics change after a homoclinic orbit is created?

1.1.1 Limit Return Maps Near Homoclinic Orbits

Most of the results concerning this problem start at the same point: By using the existence of *limit return maps* associated to the unfolding of a two-dimensional homoclinic tangency.

Definition 1.1.1 (Limit return maps)**.** Let $\{F_a\}_{a\in V}$ be a smooth family of diffeomorphisms in some d-dimensional manifold $\mathcal{M}$ depending on a parameter $a \in V$, where V is an open subset of $\mathbb{R}^k$. Suppose that for $a = a_0$ there exists a homoclinic orbit O_0 of some dissipative fixed point. We say that $\{F_a\}_{a\in V}$ has a family of *limit return maps* associated to the homoclinic orbit O_0 in the C^l-topology if there exist a point of the orbit Q and a natural number N such that, for any positive integer $n \geq N$, there exist reparametrizations

$$a = M_n(\tilde{a})$$

and $\tilde{a}$-dependent coordinate transformations

$$x = \Psi_{n,\tilde{a}}(\tilde{x})$$

satisfying the following properties:

1) For each compact set $\mathcal{K}$ in the $(\tilde{a}, \tilde{x})$-space, the images of $\mathcal{K}$ under the maps

$$(\tilde{a}, \tilde{x}) \mapsto (M_n(\tilde{a}), \Psi_{n,\tilde{a}}(\tilde{x}))$$

converge in the (a, x)-space to (a_0, Q) as $n \to \infty$

2) The domains of the maps

$$(\tilde{a}, \tilde{x}) \mapsto (\tilde{a}, (\Psi^{-1}_{n,\tilde{a}} \circ F^n_{M_n(\tilde{a})} \circ \Psi_{n,\tilde{a}}))$$

converge to all of $\mathbb{R}^{d+k}$ as $n \to \infty$, and the maps converge in the C^l topology to some map of the form

$$(\tilde{a}, \tilde{x}) \mapsto (\tilde{a}, \widetilde{F}_{\tilde{a}}(\tilde{x}))$$

In such case, the map $\widetilde{F}_{\tilde{a}}$ will be called a *limit return map* and $\{\widetilde{F}_{\tilde{a}}\}_{\tilde{a}\in\mathbb{R}^k}$ a family of limit return maps associated to the homoclinic orbit O_0.

In a few words: limit return maps explain the asymptotic behavior of high iterates of the diffeomorphism when it is restricted to certain neighborhoods of the homoclinic orbit.

Under generic assumptions, in the *dissipative* case, that is, if the eigenvalues λ_1, λ_2 associated to the homoclinic orbit satisfy $|\lambda_1\lambda_2| < 1$, then the family of limit return maps can be written as

$$(\tilde{x}_1, \tilde{x}_2) \mapsto (\tilde{a} - \tilde{x}_1^2, 0)$$

For $\tilde{a} > 1$, this family of endomorphisms is completely equivalent to the following one:

$$\widetilde{F}_{\tilde{a}}(\tilde{x}_1, \tilde{x}_2) = (1 - \tilde{a}\tilde{x}_1^2, 0) \tag{1.1}$$

This means that a convenient (high) power of F_a restricted to certain neighborhood near the homoclinic point is conjugate to a (small) perturbation of the well-known quadratic family $f_a(x) = 1 - ax^2$.

Let us mention that family (1.1) also works as a family of limit return maps in higher-dimensional settings. For instance, under the assumption of *sectionally dissipativeness*, that is, if $\dim \mathcal{M} = d$ and $F_a \colon \mathcal{M} \to \mathcal{M}$ unfolds a homoclinic tangency associated to a homoclinic orbit whose eigenvalues $\lambda_1, \lambda_2, \ldots, \lambda_d$ satisfy

$$|\lambda_1| < |\lambda_2| < \ldots < |\lambda_{d-1}| < 1 < |\lambda_d|, \quad |\lambda_{d-1}\lambda_d| < 1$$

then it is proved that the respective family of limit return maps is given by

$$\widetilde{F}_{\tilde{a}}(\tilde{x}_1, \tilde{x}_2, \ldots, \tilde{x}_d) = (1 - \tilde{a}\tilde{x}_1^2, 0, \ldots, 0)$$

1.1.2 Existence of Strange Attractors in Unfoldings of Surface Diffeomorphisms

Let $\mathcal{M}$ be a two-dimensional manifold and let us consider one-parameter families of diffeomorphisms $f_\mu \colon \mathcal{M} \to \mathcal{M}$ such that f_{μ_0} has a homoclinic point Q_{μ_0} associated to a hyperbolic saddle P_{μ_0}. Moreover, for $\mu = \mu_0$, we assume that the invariant manifolds of P_{μ_0} display a quadratic tangency at Q_{μ_0}. It is said that the family $\{f_\mu\}$ *generically unfolds the homoclinic tangency* if, for $\mu < \mu_0$ the invariant manifolds of the saddle fixed point P_μ (the analytic continuation of P_{μ_0}) have no intersections and for $\mu > \mu_0$, there exist transverse homoclinic points associated to P_μ. See Figure 1.1.

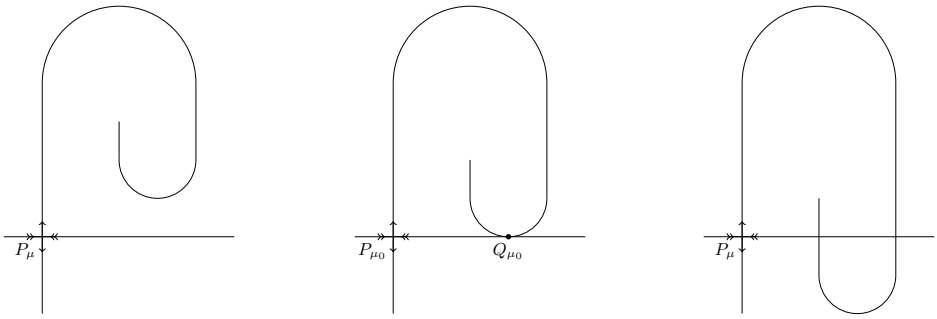

(a) (b) (c)

Figure 1.1: Unfolding of a quadratic tangency: (a) $\mu < \mu_0$ (b) $\mu = \mu_0$ (c) $\mu > \mu_0$

One of the main purposes during the past four decades is to determine the prevalence or not of hyperbolic dynamics for $\mu > \mu_0$. One of the main results in this sense was provided by Mora and Viana [44]. This result guarantees the existence of physically persistent (that is, persistent in the sense of probability measure) strange attractors when a generic homoclinic tangency associated to a dissipative periodic point is unfolded in dimension-two. In this sense, we point out that a deep study [5, 34] of the chaotic behavior of the quadratic family f_a for a positive Lebesgue measure set of parameters was made and, moreover, the techniques and results in those papers were extensively used [44].

Theorem ([44, Th. A, adapted]). *Let $\{f_\mu\}_\mu$ be a generic family of diffeomorphisms on a surface, unfolding a homoclinic tangency of f_{μ_0}. Suppose that f_{μ_0} is area dissipative at the saddle point involved in the tangency. Then, there exists a positive measure set of μ-values for which f_μ has strange attractors of Hénon type.*

Recall that the Hénon family is a small perturbation of family (1.1) for sufficiently small $b > 0$. This is why the strange attractors from Theorem A [44] are called Hénon-like attractors: They appear in the dynamics of small perturbations of family (1.1).

We must point out that the above important result, as well as many other interesting ones (e.g. the results by Colli [13], Newhouse [46], Yorke–Alligood [70], or Palis–Yoccoz [49]), is strongly based on the existence of families of limit return maps associated to the unfolding of the homoclinic tangency.

1.2 Limit Return Maps for 3-D Diffeomorphisms

The results by Mora and Viana [44] have been stated in the two-dimensional scenario, and it is natural to wonder if a similar result prevails in higher dimensions. In particular, we are especially interested in proving the existence and persistence of two-dimensional strange attractors when certain classes of 3-D homoclinic tangencies are unfolded. As one can see

in [60, 61], numerical evidence shows us that many different strange attractors arise in this case, to the contrary of the two-dimensional scenario, where only Hénon-like attractors are expected. Nevertheless, we are going to develop a similar programme as the one needed in the lower-dimensional case. More precisely, the starting point will be again the existence of limit return maps associated to the unfolding of these three-dimensional tangencies.

1.2.1 Preliminaries

We begin by stating several elementary dynamical definitions.

Definition 1.2.1 (Fixed points)**.** Let $\mathcal{M}$ be an d-dimensional smooth manifold and let $F\colon \mathcal{M} \to \mathcal{M}$ be a diffeomorphism. Let $P \in \mathcal{M}$ be a fixed point of F, and let $\lambda_1, \dots, \lambda_d$ be the eigenvalues of $\mathrm{D}F(P)$. Then:

- We say that P is *dissipative* if the product of the eigenvalues is less than 1 in absolute value.
- We say that P is *sectionally dissipative* is P is dissipative and $|\lambda_i \lambda_j| < 1$ for all $i, j = 1, \dots, d$ such that $i \neq j$.
- The *index of stability* of P is the number of eigenvalues whose absolute values is less than 1.
- We say that P is a *saddle* if $|\lambda_i| \neq 1$ for all $i = 1, \dots, d$ and its index of stability is different from 0 and d.

By the Stable Manifold Theorem [47], given a saddle fixed point, we can consider the *invariant manifolds*.

Definition 1.2.2 (Invariant manifolds)**.** Let $\mathcal{M}$ be a d-dimensional smooth manifold and let $F\colon \mathcal{M} \to \mathcal{M}$ be a diffeomorphism. Let $P \in \mathcal{M}$ be a saddle fixed point of F. The *stable invariant manifold* of F is

$$W^{\mathrm{s}}(F, P) = \{Q \in \mathcal{M} : \lim_{n \to \infty} F^n(Q) = P\}$$

The *unstable invariant manifold* is $W^{\mathrm{u}}(F, P) = W^{\mathrm{s}}(F^{-1}, P)$.

Apart from fixed points, there are other invariant objects we are interested in. Given a smooth submanifold $\mathcal{N}$ of $\mathcal{M}$, we denote by $L_i(\mathcal{N})$ the pairs (P, L) of points $P \in \mathcal{N}$ and i-dimensional linear subspaces L of $\mathrm{T}_P\mathcal{M}$ such that $\mathrm{T}_P\mathcal{N} \cap L \neq \{0\}$. Also, denote by E^{cu} (respectively, E^{ss}) the invariant linear subspace of $\mathrm{T}_P\mathcal{M}$ associated to the eigenvalues λ_2 and λ_3 (respectively, λ_1). Let $F_1\colon L_1(W^{\mathrm{s}}(P)) \to L_1(W^{\mathrm{s}}(P))$ and $F_2\colon L_2(W^{\mathrm{u}}(P)) \to L_2(W^{\mathrm{u}}(P))$ be the maps induced by f on the respective spaces.

It is easy to check that (P, E^{ss}) is a fixed point of F_1 with eigenvalues λ_1, λ_2, and $\lambda_2\lambda_1^{-1}$. Therefore, the corresponding unstable manifold $W^{\mathrm{s}}(P, E^{\mathrm{ss}})$ has dimension two since $|\lambda_1| < |\lambda_2| < 1 < |\lambda_2\lambda_1^{-1}|$. On the other hand, (P, E^{cu}) is a fixed point of F_2 with eigenvalues λ_3 and $\lambda_1\lambda_2^{-1}$, so $W^{\mathrm{u}}(P, E^{\mathrm{cu}})$ has dimension one.

Using these invariant manifolds, we can give the following definitions.

Definition 1.2.3 (Strong invariant manifolds, invariant tangent bundles)**.** Suppose that f is as before and P is a saddle fixed point.

- If $|\lambda_1| < |\lambda_2| < 1 < |\lambda_3|$, the foliation $\mathcal{F}^{\mathrm{ss}}(P)$ induced by $W^{\mathrm{s}}(P, E^{\mathrm{ss}})$ is called the *strong stable manifold* of P. Moreover, the *unstable invariant tangent bundle* of P is the vector bundle $W^{\mathrm{u}}(P, E^{\mathrm{cu}})$.
- If $|\lambda_1| < 1 < |\lambda_2| < |\lambda_3|$, the *strong unstable foliation* of P, denoted by $\mathcal{F}^{\mathrm{uu}}(P)$ is the strong stable foliation of P with respect to f^{-1} and the *stable invariant tangent bundle* of P is the unstable invariant tangent bundle of P with respect to f^{-1}.

1.2.2 The Linearization Assumption

The *linearization assumption* is a generic (open and dense) condition for families of 3-D diffeomorphisms having saddle fixed points that simplifies the study of families of such diffeomorphisms.

Definition 1.2.4 (The linearization assumption)**.** Let $\{f_a\}_{a\in V}$ be a family of 3-D diffeomorphisms. Assume that f_a has a saddle fixed point $P(a)$ for all $a \in V$, and the eigenvalues $\lambda_1, \lambda_2, \lambda_3$ of $P(a)$ satisfy $|\lambda_1| < |\lambda_2| < |\lambda_3|$. We say that $\{f_a\}_{a\in V}$ satisfies the *linearization assumption* with respect to the map of fixed points $p(a)$ if there exists an open (unbounded) set $U \subseteq \mathbb{R}^{3+k}$ and a C^s $(s \geq 3)$ map $\mathbf{x}\colon U \to \mathcal{M}$ such that:

1. $\Lambda(U) = U$, where
$$\Lambda(t_1, t_2, t_3, a) = (\lambda_1 t_1, \lambda_2 t_2, \lambda_3 t_3, a)$$
for $(t_1, t_2, t_3, a) \in \mathbb{R}^{3+k}$
2. U is either a neighbourhood of
$$\{(t_1, t_2, t_3) : (t_1^2 + t_2^2)t_3 = 0\} \times V$$
if $|\lambda_1| < |\lambda_2| < 1$ and $|\lambda_3| > 1$ or a neighbourhood of
$$\{(t_1, t_2, t_3) : (t_2^2 + t_3^2)t_1 = 0\} \times V$$
if $|\lambda_1| < 1 < |\lambda_2| < |\lambda_3|$
3. $\mathbf{x}(0, 0, 0, a) = p(a)$ for all $a \in V$
4. $\mathbf{x}(\lambda_1 t_1, \lambda_2 t_2, \lambda_3 t_3, a) = f_a(\mathbf{x}(t_1, t_2, t_3, a))$ for $(t_1, t_2, t_3, a) \in U$

If the family $\{f_a\}_{a\in V}$ is linearizable, the invariant manifolds have natural parametrizations. If $|\lambda_1| < |\lambda_2| < 1 < |\lambda_3|$, then

$$W^{\mathrm{s}}(P(a)) = \{Q \in \mathcal{K} : Q = \mathbf{x}(t_1, t_2, 0, a) \text{ for some } (t_1, t_2) \in \mathbb{R}^2\}$$
$$W^{\mathrm{u}}(P(a)) = \{Q \in \mathcal{K} : Q = \mathbf{x}(0, 0, t_3, a) \text{ for some } t_3 \in \mathbb{R}\}$$

The leaves of the strong stable foliation of $P(a)$ are parametrized by the maps $\mathbf{x}(t, \bar{t}_2, 0, a)$ with t a real parameter small enough and $\bar{t}_2$ a small constant. Moreover, the fiber of the unstable tanent vector bundle at a point $\mathbf{x}(0, 0, t_3, a)$ of $W^{\mathrm{u}}(P(a))$ is generated by the vectors $\mathrm{D}_2\mathbf{x}(0, 0, t_3, a)$ and $\mathrm{D}_3\mathbf{x}(0, 0, t_3, a)$, tangent to $W^{\mathrm{u}}(P(a))$.

On the other hand, if $|\lambda_1| < 1 < |\lambda_2| < |\lambda_3|$, the leaves of $\mathcal{F}^{\mathrm{uu}}(P(a))$ are parametrized by $\mathbf{x}(0, \bar{t}_2, t, a)$ and the fiber of the stable vector bundle at $\mathbf{x}(t_1, 0, 0, a)$ is generated by the vectors $\mathrm{D}_1\mathbf{x}(t_1, 0, 0, a)$ and $\mathrm{D}_2\mathbf{x}(t_1, 0, 0, a)$.

Remark 1.2.5. Without loss of generality, when we take a family $\{f_a\}_{a\in V}$ of diffeomorphisms satisfying the linearizaton assumption, we can suppose that $\mathcal{M} = \mathbb{R}^3$ and $P(a) = 0$ for all $a \in V$. Moreover, consider the sets

$$A_1 = \{(t_1, t_2, t_3) \in \mathbb{R}^3 : (t_1^2 + t_2^2)t_3 = 0\} \times V$$
$$A_2 = \{(t_1, t_2, t_3) \in \mathbb{R}^3 : (t_2^2 + t_3^2)t_1 = 0\} \times V$$
$$B_1 = \{(t_1, t_2, 0) \in \mathbb{R}^3 : t_1^2 + t_2^2 \leq 3\}$$
$$B_2 = \{(t_1, 0, 0) \in \mathbb{R}^3 : |t_1| \leq 3\}$$

The linearization assumption allows us to suppose (via a change of coordinates and a reparametrization if necessary) that if $|\lambda_1| < |\lambda_2| < 1 < |\lambda_3|$ (respectively, $|\lambda_1| < 1 < |\lambda_2| < |\lambda_3|$) there exists a C^k map $(k \geq 3)$ $\mathbf{x}_f$ defined on a neighborhood U_f of A_1 (respectively, A_2) such that:

1. if $(t_1, t_2, t_3, a) \in U_f$, then $(\lambda_1 t_1, \lambda_2 t_2, \lambda_3 t_3) \in U_f$ and

$$f_a(\mathbf{x}_f(t_1, t_2, t_3)) = \mathbf{x}_f(\lambda_1 t_1, \lambda_2 t_2, \lambda_3 t_3, a)$$

2. for some neighborhood $U_{1,f}$ of B_1 (respectively, B_2) the map $\mathbf{x}_f(\cdot, \cdot, \cdot, a)$ restricted to $U_{1,f}$ is the identity for all $a \in V$.

1.2.3 Unfolding of 3-D Homoclinic Tangencies: the Generalized Homoclinic Tangency

In this subsection we study the unfolding of homoclinic tangencies of 3-D diffeomorphisms and define the *generalized homoclinic tangency*. We first give the definition of the generic unfolding of a quadratic tangecy between a curve and a surface in dimension-three in order to define a homoclinic quadratic tangency unfolding generically. Then, we state the generalized transversality between a curve and a foliated surface that defines the generalized homoclinic transversality. This type of transversality describes the generalized (quadratic) homoclinic tangency (Definition 1.2.14). In all cases we write the conditions of generic unfolding that are needed for the proof of Tatjer's main theorem (see Subsection 1.2.5).

Definition 1.2.6 (Quadratic tangency)**.** Let $\{\mathcal{C}_a\}_{a \in V}$ be a smooth family of smooth regular curves $\mathcal{C}_a \subseteq \mathbb{R}^3$, and let $\{\mathcal{S}_a\}_{a \in V}$ be a smooth family of smooth regular surfaces $\mathcal{S}_a \subseteq \mathbb{R}^3$ depending on a parameter $a \in V \subseteq \mathbb{R}$, where V is an open subset, such that, for $a = a_0$, the curve $\mathcal{C}_a$ and the surface $\mathcal{S}_a$ intersect at a point $P_0 \in \mathbb{R}^3$. We say that $\mathcal{C}_a$ and $\mathcal{S}_a$ have a *quadratic tangency* at P_0 (or a contact of order 1) which unfolds generically with a at $a = a_0$ if there exists some smooth change of variables such that, in the new variables,

- $P_0 = (0, 0, 0)$
- $S_a = \{(x, y, z) \in U : z = 0\}$, where U is a neighbourhood of $0 \in \mathbb{R}^3$
- C_a is represented by the parametrized curve $\gamma(t, a) = (x(t, a), y(t, a), z(t, a))$

and the following properties hold:

1. $z(0, a_0) = 0$
2. $D_1 z(0, a_0) = 0$
3. $D_{11} z(0, a_0) \neq 0$
4. $D_2 z(0, a_0) \neq 0$

In order to define quadratic tangencies between invariant manifolds (quadratic homoclinic tangencies), we will add a generic condition. It concerns the position of an orbit inside a two-dimensional invariant manifold.

Definition 1.2.7 (General position)**.** Let f be a 3-D diffeomorphism defined on a neighbourhood of a hyperbolic saddle fixed point P, with eigenvalues λ_1, λ_2 and λ_3, which are supposed to be real and different in absolute value. We denote by Λ the linear map $\Lambda(t_1, t_2, t_3) = (\lambda_1 t_1, \lambda_2 t_2, \lambda_3 t_3)$. Let W and $\widetilde{W} \subseteq W$ be, respectively, the two-dimensional (stable or unstable) invariant manifolds of P, and the strong stable or unstable manifolds contained in W. We say that $Q \in W$ is *in general position* if $Q \notin \widetilde{W}$ and there exists some smooth conjugacy F between f and Λ such that the orbit of $F(q)$, corresponding to the map Λ, has at least one point out of the coordinate axes.

In many cases, the condition for an orbit to be in general position is equivalent to being in the two-dimensional stable or unstable invariant manifold, but not in the corresponding strong (stable or unstable) one-dimensional manifold.

Definition 1.2.8 (Quadratic homoclinic tangency)**.** We say that $\{f_a\}_{a\in V}$ has a *quadratic homoclinic tangency* at

$$Q \in W^{\mathrm{s}}(P(a_0)) \cap W^{\mathrm{u}}(P(a_0))$$

unfolding generically with a at $a = a_0$ if the manifolds $W^{\mathrm{u}}(P(a))$ and $W^{\mathrm{s}}(P(a))$ have a quadratic tangency at Q with unfolds generically at $a = a_0$, and Q is in general position.

Definition 1.2.9 (Foliated surfaces)**.** Let $\mathcal{S} \subseteq \mathbb{R}^3$ be a surface and let $\Phi = \{\mathcal{L}_\alpha\}_{\alpha\in A}$, where A is a set of indices, be a partition of $\mathcal{S}$ into disjoint sets called *leaves*. The partition Ψ is called a *foliation* if there is a parametrization $\mathbf{x}\colon I \times J \subseteq \mathbb{R}^2 \to \mathbb{R}^3$ of $\mathcal{S}$ such that $\mathcal{L}_\alpha = \mathbf{x}(I \times \{c_\alpha\})$, where I and J are open intervals, $\mathcal{S} = \mathbf{x}(I \times J)$, and c_α is a constant for each $\alpha \in A$. We call the pair $(\mathcal{S}, \Phi)$ a *foliated surface*.

In order to define the *generalized transversality*, we take a family of foliated surfaces $\{(\mathcal{S}_a, \Phi_a)\}$, where V is an open set of $\mathbb{R}$, and a family of vector bundles $\{\mathcal{V}_a\}_{a\in V}$ whose zero section is a curve $\gamma = \gamma(t, a)$ and with fibers that are tangent planes to the curve. We can associate to each fiber of the bundle a vector

$$v_a(t) = v(t, a) \in \mathrm{T}_{\gamma_a(t)}\mathbb{R}^3 \setminus \mathrm{T}_{\gamma_a(t)}\gamma_a$$

such that v is a smooth map, in such a way that $v_a(t)$ and $\dot\gamma(a)$ generate the fiber. In this situation, we say that the family of vector fields $\{v_a\}_{a\in V}$ along the family of curves $\{\gamma_a\}_{a\in V}$ is associated to the family of tangent vector bundles $\{\mathcal{V}_a\}_{a\in V}$.

This definition means that, at the point P of generalized transversality, the corresponding surface and curve have a transversal intersection, and that the fiber of the vector bundle and the leaf of the foliation at P are tangent. This latter property is lost when we change the value of the parameter.

Definition 1.2.10 (Generalized transversal intersection)**.** We say that $\{(\mathcal{S}_a, \Phi_a)\}_{a\in V}$ and $\{\mathcal{V}_a\}_{a\in V}$ have a *generalized transversal intersection* at $P \in \mathcal{S}_{a_0}$ which unfolds generically with a at $a = a_0 \in V$ if, in some coordinate system for which the leaves of the foliation are the straight lines $z = 0$, $y = c$, the following properties are satisfied:

1. $P = \gamma(0, a_0)$
2. $z(0, a_0) = 0$
3. $\mathrm{D}_1 z(0, a_0) \neq 0$
4. $T(t, a) = v_2(t, a)\mathrm{D}_1 z(t, a) - v_3(t, a)\mathrm{D}_1 y(t, a) = 0$ implies $T(0, a_0) = 0$
5. $\mathrm{D}_1 z(0, a_0)\mathrm{D}_2 T(0, a_0) - \mathrm{D}_2 z(0, a_0)\mathrm{D}_1 T(0, a_0) \neq 0$

Here $v = (v_1, v_2, v_3)$ is a family of vector fields associated to the family of vector bundles and we write $\gamma(t, a) = (x(t, a), y(t, a), z(t, a))$.

Definition 1.2.11 (Generalized homoclinic transversality)**.** We say that $\{f_a\}_{a\in V}$ has a *generalized homoclinic transversality* at

$$Q \in W^{\mathrm{s}}(P(a_0)) \cap W^{\mathrm{u}}(P(a_0))$$

unfolding generically with a at $a = a_0$ if:

1. When $|\lambda_2| < 1$, the family of foliated surfaces

$$\{W^{\mathrm{s}}(P(a)), \mathcal{F}^{\mathrm{ss}}(P(a))\}_{a\in V}$$

and the family of invariant tangent vector bundles

$$\{W^{\mathrm{u}}(P(a)), E^{\mathrm{cu}}(P(a))\}_{a\in V}$$

have a generalized transversal intersection at Q, which unfolds generically with a at $a = a_0$. Moreover, the point $Q \in W^{\mathrm{s}}(P(a_0))$ is in general position.

2. When $|\lambda_2| < 1$, the invariant manifolds of $P(a)$ with respect to the family $\{f_a^{-1}\}_{a\in V}$ have a generalized homoclinic transversality at Q unfolding generically with a at $a = a_0$.

As before, we first study a new type of tangency between a two-parameter family of foliated surfaces $\{(\mathcal{S}_{a,b}, \Phi_{a,b})\}_{(a,b)\in V}$, and a two-parameter family of vector bundles $\{\mathcal{V}_{a,b}\}_{(a,b)\in V}$ having a regular parametrized curve

$$\gamma_{a,b} = \gamma_{a,b}(t) = (x(t,a,b), y(t,a,b), z(t,a,b))$$

as a zero section and tangent planes to $\gamma_{a,b}(t)$ as fibers. Here, $V \subseteq \mathbb{R}^2$ is an open neighbourhood of $(a,b) = (a_0,b_0)$. Recall that a smooth family of vector fields $\{v_{a,b}\}_{(a,b)\in V}$ associated to $\{\mathcal{V}_{a,b}\}_{(a,b)\in V}$ satisfies that, for all t,

$$v_{a,b}(t) = (v_1(t,a,b), v_2(t,a,b), v_3(t,a,b))$$

and $\dot{\gamma}_{a,b}(t)$ generate the corresponding fiber of $\mathcal{V}_{a,b}$.

Definition 1.2.12 (Generalized tangency of type I)**.** We say that $\{(\mathcal{S}_{a,b}, \Phi_{a,b})\}_{(a,b)\in V}$ and $\{\mathcal{V}_{a,b}\}_{(a,b)\in V}$ have a *generalized tangency of type I* at $P_0 = \gamma_{a_0,b_0}(t_0) \in \mathcal{S}_{a_0,b_0}$, which unfolds generically with (a,b) at (a_0,b_0) if there exist:

(a) a coordinate system (x,y,z) for which $\mathcal{S}_{a,b}$ is the plane $z = 0$ and the leaves of the foliation are the straight lines $z = 0, y = c$

(b) a two-parameter family of vector fields $\{v_{a,b}\}_{(a,b)\in V}$ associated to $\{\mathcal{V}_{a,b}\}_{(a,b)\in V}$ such that

   (a) $z(t_0,a_0,b_0) = 0$, $\mathrm{D}_1 z(t_0,a_0,b_0) = 0$, $\mathrm{D}_1 y(t_0,a_0,b_0) = 0$

   (b) $\mathrm{D}_{11}(t_0,a_0,b_0) \neq 0$, $v_3(t_0,a_0,b_0) \neq 0$

   (c) The determinant

$$\begin{vmatrix} 0 & \mathrm{D}_2 z(t_0,a_0,b_0) & \mathrm{D}_3 z(t_0,a_0,b_0) \\ \mathrm{D}_{11} z(t_0,a_0,b_0) & \mathrm{D}_{12} z(t_0,a_0,b_0) & \mathrm{D}_{13} z(t_0,a_0,b_0) \\ \mathrm{D}_{11} y(t_0,a_0,b_0) & \mathrm{D}_{12} y(t_0,a_0,b_0) & \mathrm{D}_{13} y(t_0,a_0,b_0) \end{vmatrix}$$

   is nonzero

   (d) $\mathrm{D}_{11} y(t_0,a_0,b_0) v_3(t_0,a_0,b_0) - \mathrm{D}_{11} z(t_0,a_0,b_0) v_2(t_0,a_0,b_0) \neq 0$

Definition 1.2.13 (Generalized tangency of type II)**.** We say that $\{(\mathcal{S}_{a,b}, \Phi_{a,b})\}_{(a,b)\in V}$ and $\{\mathcal{V}_{a,b}\}_{(a,b)\in V}$ have a *generalized tangency of type II* at $P_0 = \gamma_{a_0,b_0}(t_0) \in \mathcal{S}_{a_0,b_0}$, which unfolds generically with (a,b) at (a_0,b_0) if there exist:

(a) a coordinate system (x,y,z) for which $\mathcal{S}_{a,b}$ is the plane $z = 0$ and the leaves of the foliation are the straight lines $z = 0, y = c$

(b) a two-parameter family of vector fields $\{v_{a,b}\}_{(a,b)\in V}$ associated to $\{\mathcal{V}_{a,b}\}_{(a,b)\in V}$ such that

(a) $z(t_0, a_0, b_0) = 0$, $\mathrm{D}_1 z(t_0, a_0, b_0) = 0$, $v_3(t_0, a_0, b_0) = 0$

(b) $\mathrm{D}_{11}(t_0, a_0, b_0) \neq 0$, $\mathrm{D}_1 y(t_0, a_0, b_0) \neq 0$

(c) The determinant

$$\begin{vmatrix} 0 & \mathrm{D}_2 z(t_0, a_0, b_0) & \mathrm{D}_3 z(t_0, a_0, b_0) \\ \mathrm{D}_{11} z(t_0, a_0, b_0) & \mathrm{D}_{12} z(t_0, a_0, b_0) & \mathrm{D}_{13} z(t_0, a_0, b_0) \\ \mathrm{D}_1 v_3(t_0, a_0, b_0) & \mathrm{D}_2 v_3(t_0, a_0, b_0) & \mathrm{D}_3 v_3(t_0, a_0, b_0) \end{vmatrix}$$

is nonzero

(d) $\mathrm{D}_1 y(t_0, a_0, b_0)\mathrm{D}_1 v_3(t_0, a_0, b_0) - \mathrm{D}_{11} z(t_0, a_0, b_0) v_2(t_0, a_0, b_0) \neq 0$

Let $\{f_{a,b}\}_{(a,b)\in V}$, where V is an open set of $\mathbb{R}^2$, be a smooth two-parameter family of three-dimensional diffeomorphisms having a saddle fixed point $p = p(a, b)$ for $(a, b) \in V$ with real eigenvalues $|\lambda_1| < |\lambda_2| < |\lambda_3|$.

Definition 1.2.14 (Generalized homoclinic tangency)**.** We say that $\{f_{a,b}\}_{(a,b)\in V}$ has a *generalized (quadratic) homoclinic tangency of type I* (respectively, *of type II*) at

$$Q \in W^{\mathrm{s}}(P(a_0, b_0)) \cap W^{\mathrm{u}}(P(a_0, b_0))$$

unfolding generically with (a, b) at $(a, b) = (a_0, b_0)$ if:

1. When $|\lambda_2| < 1$, the family of foliated surfaces

$$\{W^{\mathrm{s}}(P(a, b)), \mathcal{F}^{\mathrm{ss}}(P(a, b))\}_{(a,b)\in V}$$

and the family of invariant tangent vector bundles

$$\{(W^{\mathrm{u}}(P(a, b)), E^{\mathrm{cu}}(P(a, b))\}_{(a,b)\in V}$$

have a generalized tangency of type I (respectively, of type II) at Q which unfolds generically with (a, b) at $(a, b) = (a_0, b_0)$. Moreover, the point Q is in general position.

2. When $|\lambda_2| > 1$, the invariant manifolds of $P(a, b)$ with respect to the family $\{f_{a,b}^{-1}\}_{(a,b)\in V}$ have a generalized quadratic homoclinic tangency of type I (respectively, of type II) at Q unfolding generically with (a, b) at $(a, b) = (a_0, b_0)$.

1.2.4 Bifurcations of periodic points

The Bogdanov–Takens bifurcation will play the role in the third-dimensional case that the saddle-node bifurcation did in the second-dimensional one. Tatjer's main theorem is written in terms of this bifurcation.

Definition 1.2.15. We say that $\{f_{a,b}\}_{(a,b)\in V}$ has a *Bogdanov–Takens bifurcation* at P_0 which unfolds generically with (a, b) at (a_0, b_0) if via a smooth change of variables and a reparametrization, we can obtain the family of maps

$$(u, v) \mapsto (u + v, v + \mu + u^2 + v(\nu + \tilde{\gamma}u) + \tilde{c}v^2 + \tilde{r}^3(u, v))$$

where P_0 is transformed into $(0, 0)$, $\mu = \mu(a, b)$ and $\nu = \nu(a, b)$ are the new parameters such that $(\mu(a_0, b_0), \nu(a_0, b_0)) = (0, 0)$ and $|\partial(\mu, \nu)/\partial(a, b)|$ is nonzero when $(a, b) = (a_0, b_0)$, $\tilde{\gamma}$ and $\tilde{c}$ are functions of (a, b) such that $\tilde{\gamma}(a_0, b_0) \neq 2$. Moreover, $\tilde{r}_3 = \tilde{r}_3(u, v, a, b)$ is a smooth function whose Taylor expansion around $(u, v) = (0, 0)$, for each fixed (a, b), begins at degree 3.

1.2.5 Tatjer's Results

Tatjer's main theorem [67] describes the dynamical behavior of a two-parameter family of 3-D diffeomorphisms having a generalized homoclinic tangency in several situations (see Subsection 1.2.3), none of which the corresponding fixed point is sectionally dissipative.

Theorem ([67, Th. 1, adapted]). *Let $\{f_{a,b}\}_{a,b}$ be a two-parameter family of 3-D diffeomorphisms having a hyperbolic dissipative fixed point P_0 for $(a,b)=(0,0)$ with eigenvalues λ_1, λ_2 and λ_3. Assume that either of the following cases hold:*

- *Case A:* $|\lambda_1| < |\lambda_2| < 1$, $|\lambda_3| > 1$, $|\lambda_1\lambda_3| < 1$, $|\lambda_2\lambda_3| > 1$
- *Case B:* $|\lambda_1| < 1$, $|\lambda_3| > |\lambda_2| > 1$

Moreover, suppose that the invariant manifolds of P_0 have a generalized homoclinic tangency which unfolds generically and the family $f_{a,b}$ satisfies the linearization assumption. Then:

1. *For n large enough there are values of the parameter (a_n, b_n) for which the map $f_{a,b}$ undergoes a generic n periodic Bogdanov–Takens bifurcation. Moreover, $(a_n, b_n) \to (0,0)$ when $n \to \infty$.*

2. *There exists a family of limit return maps $\{\tilde{f}_{\tilde{a},\tilde{b}}\}_{(\tilde{a},\tilde{b})\in\mathbb{R}^2}$ associated to the generalized homoclinic tangency, such that:*

   (a) *In Case A,*
   $$\tilde{f}_{\tilde{a},\tilde{b}}(\tilde{x},\tilde{y},\tilde{z}) = (\tilde{z}, \tilde{b}\tilde{z}, \tilde{a} + \tilde{y} + \tilde{z}^2)$$
   or
   $$\tilde{f}_{\tilde{a},\tilde{b}}(\tilde{x},\tilde{y},\tilde{z}) = (0, \tilde{z}, \tilde{a} + \tilde{b}\tilde{y} + \tilde{z}^2)$$
   depending on the type of generalized homoclinic tangency (I or II, respectively).

   (b) *In Case B,*
   $$\tilde{f}_{\tilde{a},\tilde{b}}(\tilde{x},\tilde{y},\tilde{z}) = (\tilde{z}, \tilde{a} + \tilde{b}\tilde{y} + \tilde{z}^2, \tilde{y})$$

3. *$(a,b) = (0,0)$ is in the closure of the set of parameter values for which there exist differentiable invariant circles. In Case A, the circles can be of attracting or saddle type (attracting or repelling inside the centre manifold), depending on the geometry of the tangency. In Case B, the circles are always attracting.*

4. *$(a,b) = (0,0)$ is in the closure of the set of parameter values for which there are attracting periodic orbits.*

5. *There is a set E of paremeter values such that its intersection with any neighbourhood of $(0,0)$ has positive Lebesgue measure, and for $(a,b) \in E$ the diffeomorphism $f_{a,b}$ exhibits a strange attractor near the orbit of the tangency.*

6. *There are open sets $U \subset \mathbb{R}^2$ arbitrarily near $(0,0)$ such that for a generic $(a,b) \in U$ the map $f_{a,b}$ has infinitely many sinks.*

Remark 1.2.16. The two quadratic maps from Case A are conjugate if $\tilde{b} \neq 0$. When $\tilde{b} = 0$, they are not conjugate, but if we restrict the first map to the plane $\tilde{y} = 0$ and the second to $\tilde{x} = 0$, we obtain the same two-dimensional map. These restrictions are logistic maps in both cases.

This result describes in different situations the dynamics of the above family $f_{a,b}$ having a generalized homoclinic tangency at a point Q when $(a,b) = (0,0)$. Assumed generic linearization conditions, a suitable renormalization can be used to define return maps for $f_{a,b}$ in a neighbourhood of Q. At first glance, one can see that the limit return maps from Case A are essentially the Hénon map. The non-invertible quadratic map from Case B are the natural setting in which topologically two-dimensional strange attractors must show up.

1.3 The 2-D Quadratic Family

Let $\{f_{a,b}\}_{(a,b)\in V}$ be a family of diffeomorphisms defined in $\mathbb{R}^3$, where V is an open subset of $\mathbb{R}^2$. Suppose that $P(a,b)$ is a saddle fixed point of $f_{a,b}$ for all $(a,b) \in V$, and the eigenvalues of $\mathrm{D}f_{a,b}$ at $P_{a,b}$ satisfy $|\lambda_1| < 1 < |\lambda_2| < |\lambda_3|$. Moreover:

1. The fixed point $P(a,b)$ is dissipative for all $(a,b) \in V$.
2. The invariant manifolds of P_{a_0,b_0} have a generalized homoclinic tangency which unfolds generically with (a,b). See Subsection 1.2.3.
3. The family $\{f_{a,b}\}_{(a,b)\in V}$ satisfies the linearization assumption (see Subsection 1.2.2).

Theorem 1.2.5 ensures the existence of a family of limit return maps defined by

$$\tilde{f}_{\tilde{a},\tilde{b}}(\tilde{x},\tilde{y},\tilde{z}) = (\tilde{z}, \tilde{a} + \tilde{b}\tilde{y} + \tilde{z}^2, \tilde{y}) \tag{1.2}$$

associated to $\{f_{a,b}\}_{a,b}$. It is easy to see that every point in $\mathbb{R}^3$ *falls* by one iteration of the map $\tilde{f}_{\tilde{a},\tilde{b}}$ into the surface

$$\widetilde{\mathcal{C}}_{\tilde{a},\tilde{b}} = \{(\tilde{x},\tilde{y},\tilde{z}) : \tilde{y} = \tilde{a} + \tilde{b}\tilde{z} + \tilde{x}^2\}$$

Therefore, the surface $\widetilde{\mathcal{C}}_{\tilde{a},\tilde{b}}$ is $\tilde{f}_{\tilde{a},\tilde{b}}$-invariant and it is enough to study the dynamics of these maps on $\widetilde{\mathcal{C}}_{\tilde{a},\tilde{b}}$. That is, it is enough to study the dynamics of the 2-D endomorphisms

$$(g^{-1}_{\tilde{a},\tilde{b}} \circ \tilde{f}_{\tilde{a},\tilde{b}} \circ g_{\tilde{a},\tilde{b}})(\tilde{x},\tilde{z}) = (\tilde{z}, \tilde{a} + \tilde{b}\tilde{z} + \tilde{x}^2)$$

being $g_{\tilde{a},\tilde{b}}(\tilde{x},\tilde{z}) = (\tilde{x}, \tilde{a} + \tilde{b}\tilde{z} + \tilde{x}^2, \tilde{z})$ a parametrization of $\widetilde{\mathcal{C}}_{\tilde{a},\tilde{b}}$. Lastly, we take that change of coordinates

$$x = \tilde{z} - \tilde{b}\tilde{x}, \quad y = \tilde{x}$$

in order to write the above family of transformations as

$$T_{a,b}(x,y) = (a + y^2, x + by)$$

As it was expected, as in the unfolding of two-dimensional tangencies, these limit return maps are not linear. However, for special values of the parameters $a = -4$ and $b = -2$, the respective limit return map is conjugate to a piecewise affine map defined on a certain triangle. The same holds in the lower-dimensional case, i.e. when $\dim \mathcal{M} = 2$, the limit return map $f_2(x) = 1-2x^2$ is also conjugate to the piecewise affine map $\lambda_2(x) = 1-2|x|$ and this fact is also useful to obtain [44, Th. A]. Both f_2 and λ_2 present *sensitivity* with respect to initial conditions: A map $f\colon I \to I$ defined on an interval I is said to have *sensitivity with respect to initial conditions* if there exists $\varepsilon > 0$ such that for every $x \in I$ and for any neighborhood U of x, there exists $y \in U$ and $n \in \mathbb{N}$ with $|f^n(x) - f^n(y)| > \varepsilon$.

As was pointed out [11, p. 145], the desire to compare maps with sensitivity to simple maps (piecewise affine maps) has a long history for the diffeomorphisms of the circle. In the

case of transformations defined on intervals let us firstly recall a result of Milnor–Thurston which asserts that every continuous piecewise monotone map with positive topological entropy is semiconjugate to a continuous piecewise linear map with constant slope and with the same entropy. We refer the reader to a previous result of Parry [50] and [15, Sec. 8, Ch. II], where this kind of results are extensively treated. Furthermore, from [11, Th. II.7.12], if $f_a(x) = 1 - ax^2$ has no stable periodic orbits and no restrictive central points, then there exists $a' \in (\sqrt{2}, 2]$ such that f_a and $\lambda_{a'}(x) = 1 - a'|x|$ are conjugate.

Hence, one of the main purposes of this thesis is to perform a family of two-dimensional tent maps playing the same role as λ_a does for the lower-dimensional case. This family of two-dimensional tent maps is constructed in Chapter 2. Every one of the members of this family are Expanding Baker Maps.

Let us finish this chapter by pointing out that the family $T_{a,b}$ of limit return maps was earlier introduced in a series of papers by Gonchenko, Shilnikov, and Turaev [25, 26, 27, 28]. In these papers, the authors studied parameter families X_μ of dynamical systems unfolding a homoclinic tangency in any dimension bigger than two. In those cases, they obtained two-parameter families of limit return maps, but one of the parameters depends on the multipliers of the involved saddle periodic orbit. However, we are going to deal with two-parameter families of diffeomorphisms defined in a 3-D manifold unfolding a generalized homoclinic tangency and, as a consequence, in our case both parameters a and b in the definition of $T_{a,b}$ depend on the geometry of the tangency.

Chapter 2

Dynamics of a General Two-Parameter Family of Expanding Baker Maps as an Approximation for the Dynamics of the 2-D Quadratic Family: Existence of 2-D Strange Attractors

In this chapter, we prove the existence of 2-D strange attractors for a general two-parameter family $\Gamma_{a,\theta}$ of Expanding Baker Maps. For any $0 < \theta < \pi$, the map $\Gamma_{a,\theta}$ has a strictly invariant polygon $\mathcal{K}_{a,\theta}$ for every a sufficiently close to 1. Moreover, the restriction of $\Gamma_{a,\theta}$ to $\mathcal{K}_{a,\theta}$ admits finitely many absolutely continuous invariant probability measures $\mu_1, \ldots, \mu_{\texttt{tsu}}$ whose supports are 2-D strange attractors. These attractors undergo a process of splitting and/or doubling as a decreases to 1.

We begin by defining the Expanding Baker Maps and studying their properties in Section 2.1. Then, we construct the strictly invariant polygon $\mathcal{K}_{a,\theta}$ in Section 2.2. In Section 2.3 we prove that the supports of $\mu_1, \ldots, \mu_{\texttt{tsu}}$ are 2-D strange attractors. Finally, in Sections 2.4 and 2.5 we study the process of splitting and doubling of such attractors.

2.1 Expanding Baker Maps

The dynamics of the *Expanding Baker Maps* resembles the way a baker kneads bread dough, folding their domain into itself (possibly several times) and then expanding the resulting folded region. They consist of a sequence of *good folds* and a suitable *expanding linear map*.

Definition 2.1.1 (Folds)**.** Let $\mathcal{K}$ be a set with nonempty interior. Let $\mathcal{L}$ be a line in $\mathbb{R}^2$ such that $\mathcal{L} \cap \operatorname{int} \mathcal{K} \neq \varnothing$. Then, the line $\mathcal{L}$ splits $\mathcal{K}$ into two subsets $\mathcal{K}_0$ and $\mathcal{K}_1$ such that $\mathcal{K}_0 \cup \mathcal{K}_1 = \mathcal{K}$ and $\mathcal{K}_0 \cap \mathcal{K}_1 = \mathcal{L} \cap \mathcal{K}$. Let $P \in \mathcal{K}_0 \setminus \mathcal{L}$. The *fold* of $\mathcal{K}$ with respect to $\mathcal{L}$ onto P is the map given by

$$\mathcal{F}_{\mathcal{L},P}(Q) = \begin{cases} Q & \text{if } Q \in \mathcal{K}_0 \\ \widetilde{Q} & \text{if } Q \in \mathcal{K}_1 \end{cases}$$

where $\widetilde{Q}$ denotes the symmetric point of Q with respect to $\mathcal{L}$.

Definition 2.1.2 (Good folds)**.** A fold $\mathcal{F}_{\mathcal{L},P}\colon \mathcal{K} \to \mathbb{R}^2$ is *good* if $\mathcal{F}_{\mathcal{L},P}(\mathcal{K}) \subseteq \mathcal{K}$, i.e. if $\mathcal{F}_{\mathcal{L},P}(\mathcal{K}) = \mathcal{K}_0$.

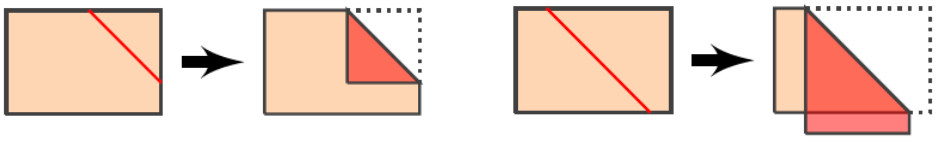

(a) (b)

Figure 2.1: Examples of folds: (a) A good fold; (b) A bad fold

Applying a good fold $\mathcal{F}_{\mathcal{L}^0,P}\colon \mathcal{K} \to \mathcal{K}_0$ allows us to fold $\mathcal{K}$ into itself again by folding $\mathcal{K}_0$ with a good fold $\mathcal{F}_{\mathcal{L}^1,P}\colon \mathcal{K}_0 \to \mathcal{K}_{00}$ for some line $\mathcal{L}^1$ such that $\mathcal{L}^1 \cap \operatorname{int} \mathcal{K}_0 \neq \varnothing$ and $P \notin \mathcal{L}^1$. This way, we can successively define a finite sequence of good folds with general term

$$\mathcal{F}_{\mathcal{L}^k,P}\colon \mathcal{K}_{(0)^k} \to \mathcal{K}_{(0)^{k+1}}, \qquad k = 0, \dots, n$$

where $(0)^k = 0 \dots 0$ (k times) if $k > 0$ and $(0)^0 = \varnothing$. See Figure 2.2.

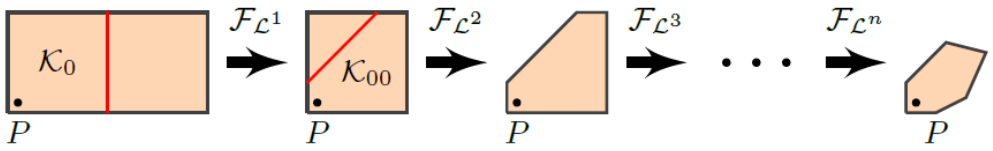

Figure 2.2: A sequence of good folds

The final ingredient to define the Expanding Baker Maps is the linear expansion.

Definition 2.1.3 (Expanding linear maps)**.** A linear map $\mathbf{A}\colon \mathbb{R}^2 \to \mathbb{R}^2$ is *expanding* if $|\det \mathbf{A}| > 1$.

Definition 2.1.4 (Expanding Baker Maps)**.** An *Expanding Baker Map* on a set $\mathcal{K}$ with nonempty interior is a map $\Gamma\colon \mathcal{K} \to \mathcal{K}$ of the form

$$\Gamma = \tau_P \circ \mathbf{A} \circ \tau_P^{-1} \circ \mathcal{F}_{\mathcal{L}^n,P} \circ \cdots \circ \mathcal{F}_{\mathcal{L}^0,P}$$

for some finite sequence $\mathcal{F}_{\mathcal{L}^0,P}, \dots, \mathcal{F}_{\mathcal{L}^n,P}$ of good folds for $\mathcal{K}$ and some expanding linear map $\mathbf{A}\colon \mathbb{R}^2 \to \mathbb{R}^2$ such that

$$\tau_P \circ \mathbf{A} \circ \tau_P^{-1}(\mathcal{K}_{(0)^{n+1}}) \subseteq \mathcal{K}$$

being τ_P the translation to the point P. The map Γ is referred to as the Expanding Baker Map on $\mathcal{K}$ associated to the lines $\mathcal{L}^0, \dots, \mathcal{L}^n$, the point P, and the map $\mathbf{A}$, and is denoted by

$$\Gamma = \mathrm{EBM}(\mathcal{K}, \mathcal{L}^0, \dots, \mathcal{L}^n, P, \mathbf{A})$$

Example 2.1.5 ([55]). For all $\sqrt{2} < t \leq 1$, the piecewise affine map

$$\Lambda_t(x,y) = \begin{cases} (t(x+y), t(x-y)) & \text{if } (x,y) \in \mathcal{T}_0 \\ (t(2-x+y), t(2-x-y)) & \text{if } (x,y) \in \mathcal{T}_1 \end{cases}$$

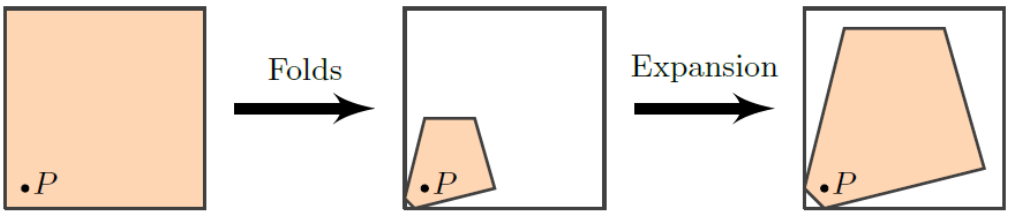

Figure 2.3: The dynamics of an Expanding Baker Map

defined on the triangle $\mathcal{T} = \mathcal{T}_0 \cup \mathcal{T}_1$, where

$$\mathcal{T}_0 = \{0 \le x \le 1, 0 \le y \le x\}, \quad \mathcal{T}_1 = \{1 \le x \le 2, 0 \le y \le 2 - x\}$$

can be written as the Expanding Baker Map

$$\Lambda_t = \mathrm{EBM}(\mathcal{T}, \mathcal{C}, \mathcal{O}, \mathbf{A}_t)$$

where

$$\mathbf{A}_t = \begin{pmatrix} t & t \\ t & -t \end{pmatrix}$$

We will usually take $\mathcal{K} = \mathbb{R}^2$ or $\mathcal{K}$ a compact and convex polygonal domain and P as the origin of coordinates $\mathcal{O} = (0, 0)$. The linear map $\mathbf{A}$ will be of the type

$$\mathbf{A}_{a,\theta} = \begin{pmatrix} a\cos\theta & -a\sin\theta \\ a\sin\theta & a\cos\theta \end{pmatrix}, \qquad a > 1, \quad 0 < \theta < \pi \tag{2.1}$$

The following lemma will be useful in Section 2.4 to obtain Expanding Baker Maps of multiple folds.

Lemma 2.1.6. *Let $\mathcal{L}$ be a line in $\mathbb{R}^2$ not passing through $\mathcal{O}$. Let Π_0 and Π_1 be the two half-planes limited by $\mathcal{L}$, with $\mathcal{O} \in \operatorname{int}\Pi_0$. Let $\mathcal{L}_- = \mathbf{A}_{a,\theta}^{-1}(\mathcal{L})$. Then,*

$$\mathcal{F}_{\mathcal{L},\mathcal{O}} \circ \mathbf{A}_{a,\theta}(Q) = \mathbf{A}_{a,\theta} \circ \mathcal{F}_{\mathcal{L}_-,\mathcal{O}}(Q)$$

for all $Q \in \Pi_0$ such that $\mathcal{F}_{\mathcal{L}_-,\mathcal{O}}(Q) \in \Pi_0$.

Proof. Let Π_{00} and Π_{01} be the two subsets into which Π_0 is divided by $\mathcal{L}_- \cap \Pi_0$, with $\mathcal{O} \in \operatorname{int}\Pi_{00}$. Then, we have that $\mathbf{A}_{a,\theta}(\Pi_{00}) \subseteq \Pi_0$ and $\mathbf{A}_{a,\theta}(\Pi_{01}) \subseteq \Pi_1$. For $Q \in \Pi_{00}$, it holds that $\mathcal{F}_{\mathcal{L}_-,\mathcal{O}}(Q) = Q$ and $\mathbf{A}_{a,\theta}(Q) \in \Pi_0$. Thus,

$$\mathcal{F}_{\mathcal{L},\mathcal{O}} \circ \mathbf{A}_{a,\theta}(Q) = \mathbf{A}_{a,\theta}(Q) = \mathbf{A}_{a,\theta} \circ \mathcal{F}_{\mathcal{L}_-,\mathcal{O}}(Q)$$

Now, let $Q \in \Pi_{01}$ and assume that $\mathcal{F}_{\mathcal{L}_-,\mathcal{O}}(Q) \in \Pi_0$. By definition, the pair of points Q and $\mathcal{F}_{\mathcal{L}_-,\mathcal{O}}(Q)$ are symmetric with respect to $\mathcal{L}_-$, and so are $\mathbf{A}_{a,\theta}(Q)$ and $\mathbf{A}_{a,\theta} \circ \mathcal{F}_{\mathcal{L}_-,\mathcal{O}}(Q)$ with respect to $\mathbf{A}_{a,\theta}(\mathcal{L}_-) = \mathcal{L}$ because of the orthogonality of the rotation matrix $a^{-1}\mathbf{A}_{a,\theta}$. Since $A_{a,\theta}(Q) \in \Pi_1$, then

$$\mathcal{F}_{\mathcal{L},\mathcal{O}} \circ \mathbf{A}_{a,\theta}(Q) = \mathbf{A}_{a,\theta} \circ \mathcal{F}_{\mathcal{L}_-,\mathcal{O}}(Q) \qquad \square$$

Definition 2.1.7 (Restrictive domains)**.** A *restrictive domain* for a map $\Gamma\colon \mathcal{K} \to \mathcal{K}$ is a subset $\mathcal{D} \neq \mathcal{K}$ with nonempty interior for which there exists a (necessarily unique) natural number $r = r(\mathcal{D}) \ge 2$ such that

- $\Gamma^k(\mathcal{D}) \cap \mathcal{D} = \varnothing$ for $k = 1, \dots, r-1$
- $\Gamma^r(\mathcal{D}) \subseteq \mathcal{D}$

Apart from several extensions to higher dimensions (see [4, 23, 40], among others), the notion of renormalization comes from the one-dimensional framework: A map f belonging to some family $\mathbb{F}$ (for instance, the family of unimodal maps defined on an interval) is said to be *renormalizable* if there exists a restrictive domain $\mathcal{D}$ such that the restriction of f^r to $\mathcal{D}$ is, up to an affine change of coordinates, a member of $\mathbb{F}$. In this sense, the concept of renormalizable Expanding Baker Map arises.

Definition 2.1.8 (Renormalization)**.** An Expanding Baker Map $\Gamma\colon \mathcal{K} \to \mathcal{K}$ is *renormalizable* if there exists a restrictive domain $\mathcal{D}$ for Γ such that $\Gamma^r\colon \mathcal{D} \to \mathcal{D}$ is an Expanding Baker Map on $\mathcal{K}$ by performing a certain affine change of coordinates Ξ such that $\Xi(\mathcal{D}) = \mathcal{K}$.

Example 2.1.9 ([57, Th. 4.2])*.* For $\sqrt{2}/2 < t < \sqrt[5]{8}/2$, the Expanding Baker Map Λ_t from Example 2.1.5 is renormalizable with $r = 8$.

Definition 2.1.10 (Further renormalizations)**.** An Expanding Baker Map $\Gamma = \Gamma_0\colon \mathcal{K} \to \mathcal{K}$ is:

- *n times renormalizable* (with $n \in \mathbb{N}$) if for every $k \in \{1, \dots, n-1, n\}$ there exists a restrictive domain $\mathcal{D}_k$ for Γ_{k-1} such that

  $$\Gamma_k = \Gamma_{k-1}^{r_k}\colon \mathcal{D}_k \to \mathcal{D}_k, \qquad r_k = r(\mathcal{D}_k)$$

  is an Expanding Baker Map on $\mathcal{K}$ by performing a certain affine change of coordinates Ξ_k such that $\Xi_k(\mathcal{D}_k) = \mathcal{K}$.
- *infinitely many times renormalizable* if it is n times renormalizable for all $n \in \mathbb{N}$.

The following result for the map $\Gamma_{a,\theta}$ with $\theta = \pi/2$ will be useful in Sections 2.4 and 2.5.

Lemma 2.1.11 ([58, Lem. 2.2, adapted])**.** *Let $\theta = \pi/2$. The following statements hold:*

(a) For every $a \in (\sqrt[4]{2}, \sqrt{2}]$, the map $\Gamma_{a,\theta}$ has a strongly topologically mixing strange attractor with two positive Lyapunov exponents.

(b) For every $n \geq 2$ and every $a \in (2^{1/2^{n+1}}, 2^{1/2^n}]$, the map $\Gamma_{a,\theta}$ is n times renormalizable and displays 2^n strange attractors with two positive Lyapunov exponents.

2.2 Existence of Strictly Invariant Sets: Proof of Theorems 1 and 2

The aim of this section is to find strictly invariant sets for the general family

$$\Gamma_{a,\theta} = \mathrm{EBM}(\mathbb{R}^2, \mathcal{C}, \mathcal{O}, \mathbf{A}_{a,\theta}), \qquad a > 1, \quad 0 < \theta < \pi \tag{2.2}$$

where $\mathcal{C} \equiv x = 1$ is the critical line and $\mathbf{A}_{a,\theta}$ is the expanding linear map given by matrix (2.1). Recall that the attractors of $\Gamma_{a,\theta}$, provided that they exist, as well as their respective stable sets and their closure, are strictly $\Gamma_{a,\theta}$-invariant. Moreover, attractors are compact and minimal (i.e. containing no nonempty compact strictly invariant set different from themselves), while the closure of their respective stable sets are maximal (i.e. contained in no strictly invariant set different from themselves).

Since $\mathbf{A}_{a,\theta}$ multiplies the area of any set by a factor of a^2 and $\mathcal{F}_{\mathcal{C},\mathcal{O}}$ at most halves it, then strictly $\Gamma_{a,\theta}$-invariant compact sets $\mathcal{K}$ with nonempty interior can only exist for

$a \leq \sqrt{2}$. We will distinguish two types of such sets: if $\mathcal{F}_{\mathcal{C},\mathcal{O}}(\mathcal{K}) \subseteq \mathcal{K}$, we will say that $\mathcal{K}$ is *first-rate*, and *second-rate* otherwise.

First-rate strictly invariant sets are a particular case of another type of sets, called *self-similar* sets. We will construct a polygon $\mathcal{R}_N$ whose image $\mathcal{K}_N$ is a self-similar polygon, which becomes (first-rate) strictly invariant for a sufficiently close to 1 for all $\theta \neq 2\pi/3$. For $\theta = 2\pi/3$, we provide some examples of second-rate strictly invariant sets from the respective polygon.

2.2.1 Existence of Self-Similar Sets: The Polygon $\mathcal{K}_N$

Connected sets intersecting the critical line which are *self-similar* can be recovered from their left-hand part by rotation and expansion.

Definition 2.2.1 (Self-similar sets)**.** A set $\mathcal{K} \subseteq \mathbb{R}^2$ is $\mathbf{A}_{a,\theta}$*-self-similar* if

$$\mathbf{A}_{a,\theta}(\mathcal{K} \cap \Pi_0) = \mathcal{K}$$

where $\Pi_0 = \{x \leq 1\}$.

Arguing by induction, we will prove that every $\mathbf{A}_{a,\theta}$-self-similar set is contained in the $\mathbf{A}_{a,\theta}$-image of the intersection of the sets

$$\mathcal{R}_n = \Pi_n \cap \Pi_{n-1} \cap \cdots \cap \Pi_0$$

constructed from the $\mathbf{A}_{a,\theta}$-iterates Π_n of Π_0. These are half-planes containing the origin and limited by the $\mathbf{A}_{a,\theta}$-iterates $\mathcal{L}_n$ of the critical line $\mathcal{L}_0 = \mathcal{C}$, implicitly given by

$$\mathcal{L}_n \equiv x \cos n\theta + y \sin n\theta = a^n \tag{2.3}$$

Proposition 2.2.2. *Let $0 < \theta < \pi$. For every $a > 1$, the sequence of (possibly unbounded) closed convex polygons inductively defined by*

$$\mathcal{R}_n = \begin{cases} \mathbf{A}_{a,\theta}(\mathcal{R}_{n-1}) \cap \Pi_0 & \text{if } n > 0 \\ \Pi_0 & \text{if } n = 0 \end{cases}$$

is nonincreasing (with respect to inclusion) and bounded below by the closed unit disc. Moreover, for any n it holds that $\mathcal{R}_n = \mathcal{R}_{n+1}$ if and only if $\mathcal{L}_{n+1} \cap \operatorname{int} \mathcal{R}_n = \varnothing$.

Remark 2.2.3. If $\mathcal{R}_n = \mathcal{R}_{n+1}$ for some n, then $\mathcal{R}_n = \mathcal{R}_{n+j}$ for all j.

Proof. It is clear by definition that $\mathcal{R}_0 \supseteq \mathcal{R}_1$. Proceeding by induction, if we assume that $\mathcal{R}_{n-1} \supseteq \mathcal{R}_n$, then

$$\mathcal{R}_n = \mathbf{A}_{a,\theta}(\mathcal{R}_{n-1}) \cap \mathcal{R}_0 \supseteq \mathbf{A}_{a,\theta}(\mathcal{R}_n) \cap \mathcal{R}_0 = \mathcal{R}_{n+1}$$

and therefore $\{\mathcal{R}_n\}_n$ is a nonincreasing sequence. Now, let $\overline{\mathbb{D}}$ be the closed unit disc. This disc is clearly contained in $\mathcal{R}_0$, and $\mathbf{A}_{a,\theta}(\overline{\mathbb{D}})$ is the closed disc centered at the origin of radius $a > 1$. Proceeding again by induction, if we assume that $\overline{\mathbb{D}} \subseteq \mathcal{R}_n$, then

$$\overline{\mathbb{D}} = \mathbf{A}_{a,\theta}(\overline{\mathbb{D}}) \cap \overline{\mathbb{D}} \subseteq \mathbf{A}_{a,\theta}(\mathcal{R}_n) \cap \mathcal{R}_0 = \mathcal{R}_{n+1}$$

and therefore $\overline{\mathbb{D}} \subseteq \bigcap_{n=0}^{\infty} \mathcal{R}_n$. Now, let $n \in \mathbb{N} \cup \{0\}$. By construction, it readily follows that $\mathcal{R}_n = \mathcal{R}_{n+1}$ if and only if $\mathcal{R}_n \subseteq \Pi_{n+1}$. If $\mathcal{L}_{n+1} \cap \operatorname{int} \mathcal{R}_n = \varnothing$, then $\operatorname{int} \mathcal{R}_n$ is contained in Π_{n+1} because $\mathcal{O} \in \Pi_{n+1} \cap \operatorname{int} \mathcal{R}_n$. Since $\mathcal{R}_n$ is a closed convex set with nonempty interior, then $\mathcal{R}_n = \overline{\operatorname{int} \mathcal{R}_n} \subseteq \Pi_{n+1}$. Conversely, if $\mathcal{R}_n \subseteq \Pi_{n+1}$, then $\operatorname{int} \mathcal{R}_n \subseteq \operatorname{int} \Pi_{n+1}$ and therefore

$$\mathcal{L}_{n+1} \cap \operatorname{int} \mathcal{R}_n \subseteq \mathcal{L}_{n+1} \cap \operatorname{int} \Pi_{n+1} = \varnothing \qquad \square$$

The next lemma will be used to prove that the sequence $\mathcal{R}_n$ is eventually constant from and provide a lower bound.

Lemma 2.2.4. *Let $0 < \theta < \pi$. Let $N_\theta = 1 + \lfloor \pi/\theta \rfloor$, where $\lfloor \cdot \rfloor$ denotes the floor function. Then,*

(i) $2 \leq N_\theta < 2\pi/\theta$ *and* $\sin N_\theta\theta < 0$

(ii) $N_\theta = \min\{n \in \mathbb{N} : \theta > \pi/n\}$

(iii) $\mathcal{R}_{N_\theta}$ *is bounded*

Proof. Immediate from the definition of the floor function since

$$\theta \leq (N_\theta - 1)\theta \leq \pi < N_\theta\theta \leq \pi + \theta$$ □

Theorem 2.2.5. *Let $0 < \theta < \pi$. For every $a > 1$, the set $\{n \in \mathbb{N} : \mathcal{R}_n = \mathcal{R}_{n+1}\}$ is nonempty and inductive. Let*

$$N = \inf\{n \in \mathbb{N} : \mathcal{R}_n = \mathcal{R}_{n+1}\}$$

Then, it holds that $N_\theta \leq N < \infty$ and

$$\mathcal{R}_N = \bigcap_{n=0}^{\infty} \Pi_n, \quad \mathcal{K}_N = \bigcap_{n=1}^{\infty} \Pi_n$$

are compact and convex $(N+1)$-sided polygons. Moreover, the polygon $\mathcal{K}_N$ is the maximal self-similar set. In particular, if $\mathcal{K}_N$ is strictly $\Gamma_{a,\theta}$-invariant, then $\mathcal{K}_N$ is the maximal first-rate strictly $\Gamma_{a,\theta}$-invariant set.

Proof. Assume by contradiction that $\mathcal{R}_n \supsetneq \mathcal{R}_{n+1}$ for all $n \in \mathbb{N}$. By Proposition 2.2.2, for each $n \in \mathbb{N}$ we can choose a point $P_n \in \mathcal{L}_{n+1} \cap \mathcal{R}_n$. The sequence $\{P_n\}_{n \geq N_\theta}$ is contained in the polygon $\mathcal{R}_{N_\theta}$ because of the monoticity, which is compact by Lemma 2.2.4, and therefore it has a convergent subsequence $\{P_{n_k}\}$. Now, for all $k \in \mathbb{N}$ the distance between P_{n_k} and $\mathcal{O}$ is greater than or equal to a^{n_k+1} because $P_{n_k} \in \mathcal{L}_{n_k+1}$, from whence we deduce that the sequence $\{P_{n_k}\}$ is divergent. We have arrived at a contradiction, and therefore the set $\{n : \mathcal{R}_n = \mathcal{R}_{n+1}\}$ is nonempty and its infimum N is a natural number by the well-ordering principle. Consequently, by Remark 2.2.3 we have that $\bigcap_{n=0}^{\infty} \mathcal{R}_n = \mathcal{R}_N$.

On the other hand, it holds that $N \geq N_\theta$ because otherwise $\mathcal{R}_{N_\theta} = \mathcal{R}_N$ would be unbounded, which is a contradiction.

Now,

$$\mathcal{K}_N \cap \mathcal{R}_N = \mathcal{R}_{N+1} = \mathcal{R}_N$$

and therefore $\mathcal{R}_N$ is contained in $\mathcal{K}_N$. Let $\mathcal{K}$ be a $A_{a,\theta}$-self-similar set, and let $\mathcal{K}_0 = \mathcal{K} \cap \Pi_0$. It is clear that $\mathcal{K}_0 \subseteq \Pi_0$. Proceeding by induction, if we assume that $\mathcal{K}_0 \subseteq \Pi_n$, then

$$\mathcal{K}_0 \subseteq \mathcal{K} \subseteq \mathbf{A}_{a,\theta}(\Pi_n) = \Pi_{n+1}$$

Thus, we have that $\mathcal{K}_0 \subseteq \mathcal{R}_N$, and therefore $\mathcal{K} \subseteq \mathcal{K}_N$. □

Corollary 2.2.6. *Every first-rate strictly invariant set is bounded.*

Remark 2.2.7. The definition of the natural number N given in Theorem 2.2.5 can be extended to the limit case $a = 1$. It is easy to check that

$$N(1,\theta) = \inf\{n \in \mathbb{N} : \cos(n+1)\theta = 1\}$$

Write $\theta = 2\pi\beta$. If $\beta = p/q \in \mathbb{Q}$ with $\gcd(p,q) = 1$, then $N(1,\theta) = q-1$ and $\mathcal{R}_{q-1}$ is a regular q-sided polygon centered at $\mathcal{O}$ with one vertex at $(1,0)$. On the other hand, if β is an irrational number, then $N(1,\theta) = \infty$ and $\mathcal{R}_\infty$ is the closed unit disc.

The limit case $a = 1$ is of little interest to us since $\mathcal{R}_N$ is strictly $\Gamma_{1,\theta}$-invariant for all θ, but cannot be a strange attractor. However, in the rational case, the natural number $N(1,\theta)$ proves to be useful as it is a nontrivial upper bound for N because $\mathcal{L}_{N(1,\theta)+1} \cap \operatorname{int} \mathcal{R}_{N(1,\theta)} = \varnothing$ for every $a > 1$.

Example 2.2.8. For $\theta = 2\pi/3$, it holds that $N = 2$ for every $a \geq 1$. The self-similar triangle $\mathcal{K}_2$ is strictly invariant if and only if $a = 1$. For $\theta = \pi/2$, it holds that $N = 3$ for every $a \geq 1$. The self-similar rectangle $\mathcal{K}_3$ is strictly invariant if and only if $a \leq \sqrt{2}$. For $\theta = 3\pi/4$, it holds that

$$N = \begin{cases} 2 & \text{if } a \geq \sqrt{2} \\ 4 & \text{if } a_2 \leq a < \sqrt{2} \\ 7 & \text{if } 1 \leq a < a_2 \end{cases}$$

being $a_2 \approx 1.092$ the unique real root of $\sqrt{2}a^5 - a^2 - 1$. The self-similar polygon $\mathcal{K}_N$ is strictly invariant if and only if $a \leq \sqrt{2}$.

In the following proposition we gather some basic facts about the orbit of the self-similar polygon $\mathcal{K}_N$.

Proposition 2.2.9. *Let $0 < \theta < \pi$. For every $a > 1$, the polygon $\mathcal{K}_N$ is contained in $\Gamma_{a,\theta}(\mathcal{K}_N)$. In particular, if $\mathcal{K}_N$ is not strictly $\Gamma_{a,\theta}$-invariant, then $\bigcup_{n=1}^{\infty} \Gamma_{a,\theta}^n(\mathcal{K}_N)$ is second-rate strictly $\Gamma_{a,\theta}$-invariant.*

Proof. Immediate from the fact that $\mathcal{R}_N \subseteq \mathcal{F}_{\mathcal{C},\mathcal{O}}(\mathcal{K}_N)$. Since $\mathcal{K}_N \subseteq \Gamma_{a,\theta}(\mathcal{K}_N)$, then the sequence of the iterates of $\mathcal{K}_N$ is nondecreasing with respect to inclusion. Therefore, it is clear that $\bigcup_{n=1}^{\infty} \Gamma_{a,\theta}^n(\mathcal{K}_N)$ is strictly invariant. If $\mathcal{K}_N$ is not strictly invariant, then $\mathcal{K}_N$ is strictly contained in $\Gamma_{a,\theta}(\mathcal{K}_N)$ and consequently in $\bigcup_{n=1}^{\infty} \Gamma_{a,\theta}^n(\mathcal{K}_N)$. As $\mathcal{K}_N$ contains all the first-rate strictly invariant sets, we deduce that $\bigcup_{n=1}^{\infty} \Gamma_{a,\theta}^n(\mathcal{K}_N)$ is second-rate. □

For each $0 < \theta < \pi$, let

$$\mathcal{K}_{a,\theta} = \bigcup_{n=1}^{\infty} \Gamma_{a,\theta}^n(\mathcal{K}_N), \qquad a > 1 \tag{2.4}$$

From Proposition 2.2.9 it follows that $\mathcal{K}_{a,\theta}$ is strictly $\Gamma_{a,\theta}$-invariant for every θ. If $\mathcal{K}_N$ is strictly $\Gamma_{a,\theta}$-invariant, then trivially $\mathcal{K}_{a,\theta} = \mathcal{K}_N$. Otherwise, the set $\mathcal{K}_{a,\theta}$ is second-rate and may not be bounded. We will prove that $\mathcal{K}_N$ is strictly $\Gamma_{a,\theta}$-invariant for all a sufficiently close to 1 if $\theta \neq 2\pi/3$. For $\theta = 2\pi/3$, the triangle $\mathcal{K}_2$ is not strictly $\Gamma_{a,\theta}$-invariant for any $a > 1$ and we will see that $\mathcal{K}_{a,\theta}$ is a (compact) polygon for every a sufficiently close to 1.

2.2.2 Geometry of the Polygons $\mathcal{R}_N$ and $\mathcal{K}_N$

In order to geometrically deduce the (strict) invariance of $\mathcal{K}_N$, we will introduce now the following notation on the vertices of $\mathcal{R}_N$ and their orbits.

Recall that $\mathcal{R}_N$ and $\mathcal{K}_N$ from Theorem 2.2.5 are the $(N+1)$-sided convex polygon limited by the lines $\mathcal{L}_0, \mathcal{L}_1, \ldots, \mathcal{L}_N$ and $\mathcal{L}_1, \mathcal{L}_2, \ldots, \mathcal{L}_{N+1}$, respectively. The lines $\mathcal{L}_n$ are the iterates of the critical line and are given in equation (2.3).

A line $\mathcal{L}_n$ is vertical if and only if $\sin n\theta = 0$. Otherwise, its slope is equal to $-\cot n\theta$. In addition, two lines $\mathcal{L}_n$ and $\mathcal{L}_m$ are parallel if and only if $\sin(n-m)\theta = 0$. Otherwise, they intersect at the point

$$V_{n,m} = (x_{n,m}, y_{n,m}) \tag{2.5}$$

with

$$\begin{aligned} x_{n,m} &= (a^m \sin n\theta - a^n \sin m\theta) \csc(n-m)\theta \\ y_{n,m} &= (a^m \cos n\theta - a^n \cos m\theta) \csc(m-n)\theta \end{aligned}$$

Note that $\mathbf{A}_{a,\theta}^{\ell}(V_{n,m}) = V_{n+\ell,m+\ell}$ for every $\ell \geq 0$ whenever $V_{n,m}$ exists.

We introduce now the following notation on the vertices and their orbits:

- V_0^+ and V_0^- denote the upper and lower vertices of $\mathcal{R}_N$ on $\mathcal{L}_0$, respectively, see Figure 2.4.
- n^+ and n^- denote the unique natural numbers such that $V_0^+ = V_{0,n^+}$ and $V_0^- = V_{0,n^-}$. Note that $n^\pm \in \{1, 2, \ldots, N\}$. Moreover, $\sin n^+\theta > 0$ and $\sin n^-\theta < 0$ since $y_0^+ > 0$ and $y_0^- < 0$, respectively, see (2.5).
- $\mathcal{V}_0^+$ and $\mathcal{V}_0^-$ denote the $\mathbf{A}_{a,\theta}$-orbits on $\mathcal{R}_N$ of V_0^+ and V_0^-, respectively. These orbits lie on the boundary $\partial\mathcal{R}_N$ of $\mathcal{R}_N$ and consist of a finite number of points.
- ℓ^+ and ℓ^- denote the lengths of $\mathcal{V}_0^+$ and $\mathcal{V}_0^-$, respectively. Note that $\ell^\pm \in \{1, 2, \ldots, N+1\}$. Moreover, $\mathcal{V}_0^\pm = \{V_{\ell,\ell+n^\pm} : \ell = 0, \ldots, \ell^\pm - 1\}$.

These numbers will play a crucial role in what follows.

Example 2.2.10. If $N < 2\pi/\theta$, the $N+1$ vertices of $\mathcal{R}_N$ and $\mathcal{K}_N$ are

$$V_{0,1}, V_{1,2}, \ldots, V_{N-1,N}, V_{0,N}$$

and

$$V_{1,2}, \ldots, V_{N-1,N}, V_{N,N+1}, V_{1,N+1}$$

respectively. Hence $n^+ = \ell^- = 1$ and $n^- = \ell^+ = N$. See Figure 2.4.

The following result describes the dynamics of the vertices of $\mathcal{R}_N$. We will prove it later.

Proposition 2.2.11. *Let $0 < \theta < \pi$. For every $a > 1$, the $N+1$ vertices of $\mathcal{R}_N$ are $\mathcal{V}_0^+ \cup \mathcal{V}_0^-$. Moreover, exactly one of the following three statements holds:*

(a) $\mathcal{L}_{N+1} \cap \partial\mathcal{R}_N = \varnothing$ *and* $\mathcal{V}_0^+ \cap \mathcal{V}_0^- = \varnothing$

(b) $\mathcal{L}_{N+1} \cap \partial\mathcal{R}_N = \{V_0^+\}$ *and* $\mathcal{V}_0^+ \cup \mathcal{V}_0^- = \mathcal{V}_0^-$

(c) $\mathcal{L}_{N+1} \cap \partial\mathcal{R}_N = \{V_0^-\}$ *and* $\mathcal{V}_0^+ \cup \mathcal{V}_0^- = \mathcal{V}_0^+$

According to Proposition 2.2.11, essentially only two scenarios can take place:

(i) If the line $\mathcal{L}_{N+1}$ comes into contact with $\mathcal{R}_N$ at either V_0^+ or V_0^-, then the orbit of the contact vertex V_0^σ, with $\sigma = +$ or $\sigma = -$, is strictly contained in the orbit of the other one, which therefore runs through all the vertices of $\mathcal{R}_N$.

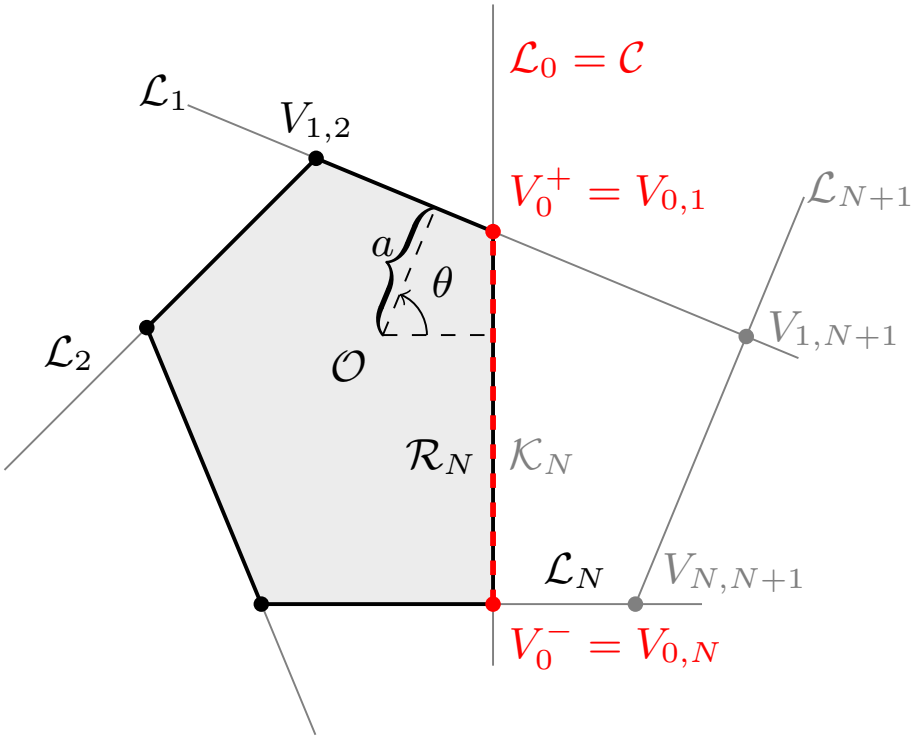

Figure 2.4: The polygons $\mathcal{R}_N$ and $\mathcal{K}_N$ with $N = 4$ for $a = 1.25$ and $\theta = 3\pi/8$

(ii) If the line $\mathcal{L}_{N+1}$ does not intersect $\mathcal{R}_N$ at all, then V_0^+ or V_0^- have disjoint orbits whose union consist of all the vertices of $\mathcal{R}_N$.

Note that, if the line $\mathcal{L}_{N+1}$ does not intersect $\mathcal{R}_N$, the structure of $\mathcal{R}_N$ is persistent in the sense that the corresponding perturbed polygon $\mathcal{R}_{N(\tilde{a},\theta)}(\tilde{a},\theta)$ with $\tilde{a} = a + \varepsilon$ for every sufficiently small $|\varepsilon|$ is essentially the same as $\mathcal{R}_N$. In particular, they have the same number of sides, i.e. $N(\tilde{a},\theta) = N(a,\theta)$. Otherwise, this is not so for $\varepsilon < 0$, where a bifurcation occurs on the boundary of $\mathcal{R}_N$: each and every vertex in the orbit of the contact vertex V_0^σ bifurcates into two new ones giving rise to a polygon with $N(a) + \ell^\sigma(a) + 1$ sides (see Figures 2.5 and 2.6). We will carry out a study of this bifurcation process later.

We can first consider the nonexpansive case $a = 1$ when θ/π is a rational number in order to understand this process. Assume that $\theta = 2\pi p/q \in (0,\pi)$ with $p, q \in \mathbb{N}$ and $\gcd(p,q) = 1$. Then, from Remark 2.2.7 we know that $N = q - 1$ and $\mathcal{R}_N$ is a regular polygon limited by the lines $\mathcal{L}_0 = \mathcal{L}_q, \mathcal{L}_1, \mathcal{L}_2, \ldots, \mathcal{L}_{q-1}$, which are tangent to the unit circle at $\mathrm{e}^{n\theta_1 \mathrm{i}}$ with $\theta_1 = 2\pi/q$ for $n = 0, 1, \ldots, q-1$. Let $r, s \in \{1, \ldots, q-1\}$ be such that $r\theta = \theta_1 \mod 2\pi$ and $s\theta = 2\pi - \theta_1 \mod 2\pi$. If $a = 1 + \varepsilon$ with $\varepsilon > 0$, then the line $\mathcal{L}_q$ is the vertical line $x = (1+\varepsilon)^q > 1$. By considering ε small enough in such a way that the abscissa of the intersection point of $\mathcal{L}_r$ and $\mathcal{L}_s$ is greater than or equal to $(1+\varepsilon)^q$, then $\mathcal{R}_N$ continues to be a polygon with q sides limited by the lines $\mathcal{L}_0, \mathcal{L}_1, \mathcal{L}_2, \ldots, \mathcal{L}_{q-1}$. Otherwise, the polygon $\mathcal{R}_N$ has $N + 1 < q$ sides. In fact, the number of sides of $\mathcal{R}_N$ remains constant or decreases as a increases until $\mathcal{R}_N$ becomes a primary polygon according to the following definition.

Definition 2.2.12 (Primary polygons)**.** A polygon $\mathcal{R}_N$ is *primary* if $N = N_\theta$, i.e. if $\mathcal{R}_N$ has $N_\theta + 1$ sides.

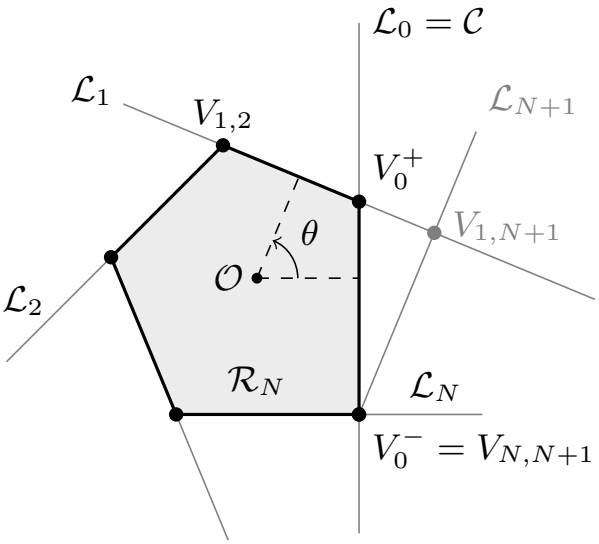

(a)

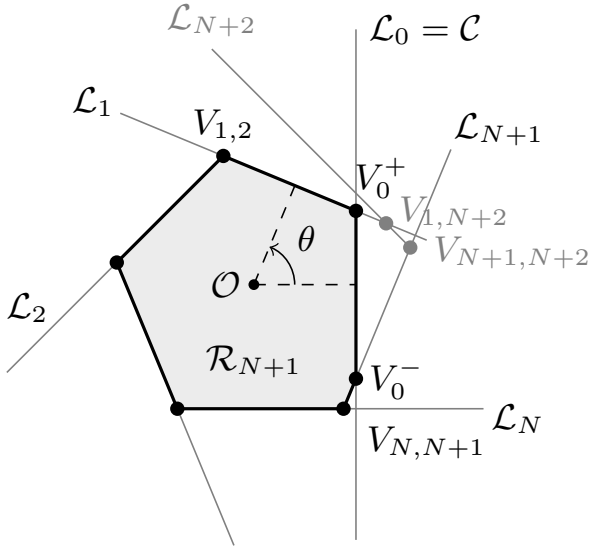

(b)

Figure 2.5: Bifurcation from V_0^- for $\theta = 3\pi/8$: (a) the polygon $\mathcal{R}_4$ for $a = 1.074\ldots$; (b) the polygon $\mathcal{R}_5$ for a slightly less than $1.074\ldots$

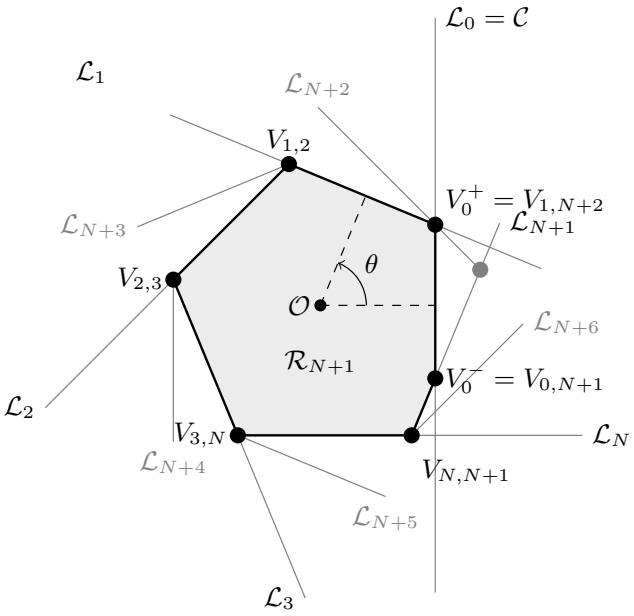

(a)

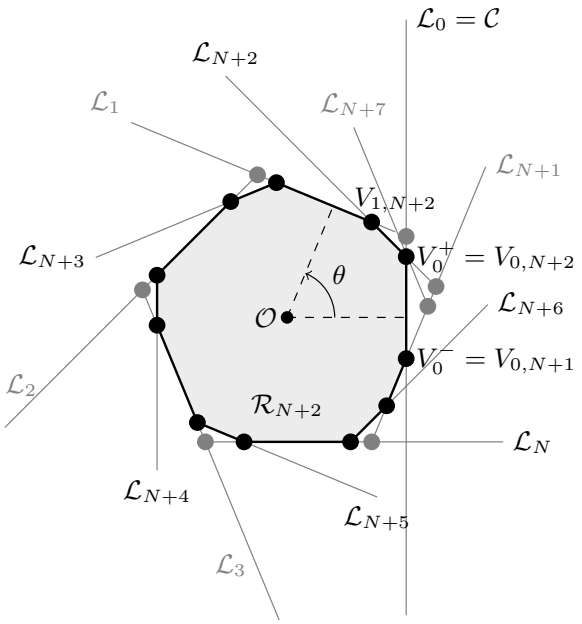

(b)

Figure 2.6: Bifurcation from V_0^+ for $\theta = 3\pi/8$: (a) the polygon $\mathcal{R}_5$ for $a = 1.031\ldots$; (b) the polygon $\mathcal{R}_{10}$ for a slightly less than $1.031\ldots$

A primary polygon has the minimum number of sides $N_\theta + 1$ and is clearly obtained for a large enough. As a decreases towards 1, the number of sides $N + 1$ increases to q if $\theta = 2\pi p/q$ or tends to infinity if θ/π is an irrational number.

Fixed $0 < \theta < \pi$, we will study next the variation of N with respect to a. According to the construction of $\mathcal{R}_N$ it is clear that $N = N(a, \theta)$ remains constant until a certain value of a for which the line $\mathcal{L}_{N+1}$ intersects $\mathcal{R}_N$ at a vertex $V_0^+(a, \theta)$ or $V_0^-(a, \theta)$ on the line $\mathcal{L}_0$. These values of a for which the natural number N changes we will be called the *bifurcation values*. Just to clarify these ideas, for each θ let us consider the map

$$a \in [1, \infty) \mapsto N(a, \theta) \in \mathbb{N} \tag{2.6}$$

We will indirectly prove that this map is nonincreasing and piecewise constant. Of course, its points of discontinuity will be precisely the bifurcation values associated to θ. We advance that each bifurcation sequence will be decreasingly convergent to 1 for every θ. We will meet two different situations:

(i) If $\theta/\pi \in \mathbb{Q}$, then the set of points of discontinuity of map (2.6) is finite. In this case, the bifurcation sequence is eventually constant equal to 1.

(ii) If $\theta/\pi \notin \mathbb{Q}$, then the set of points of discontinuity of map (2.6) is countably infinite and accumulates at 1.

Of course, the irrational case shows much more dynamical richness that the rational one, nonetheless keeping in mind that map (2.6) is always nonincreasing. In both cases, and once the value of θ is fixed, the domain of definition of this map can be decomposed as the (finite or infinite) disjoint union of intervals on which it will be continuous (i.e. constant). Our aim is to determine, at once, the bifurcation sequence and the value of map (2.6) on such intervals.

The proof of Proposition 2.2.11 will be straightforward by the following lemma:

Lemma 2.2.13. *Let $0 < \theta < \pi$. For every $a > 1$, the following statements hold:*

(a) If $V_{n,m}$ is a vertex of $\mathcal{R}_N$, then either $|n - m| = n^+$ or $|n - m| = n^-$.

(b) If $V_{n,m}$ is a vertex of $\mathcal{R}_N$, then $V_{n+1,m+1}$ is a vertex of $\mathcal{R}_N$ if and only if $x_{n+1,m+1} \leq 1$.

(c) $\ell^\pm = \min\{\ell \in \mathbb{N} : x_{\ell,\ell+n^\pm} > 1\}$.

(d) $\mathcal{V}_0^\pm \subseteq \mathcal{V}_0^\mp$ if and only if $V_0^\pm \in \mathcal{V}_0^\mp$.

(e) $\mathcal{V}_0^+ \cap \mathcal{V}_0^- \neq \varnothing$ if and only if either $V_0^+ \in \mathcal{O}_0^-$ or $V_0^- \in \mathcal{O}_0^+$.

(f) $\mathcal{L}_{N+1} \cap \partial\mathcal{R}_N \neq \varnothing$ if and only if either $V_0^+ \in \mathcal{L}_{N+1}$ or $V_0^- \in \mathcal{L}_{N+1}$.

(g) If $V_0^\pm \in \mathcal{L}_{N+1}$, then $V_0^\pm \in \mathcal{V}_0^\mp$.

(h) If $\mathcal{L}_{N+1} \cap \partial\mathcal{R}_N = \varnothing$, then $\mathcal{V}_0^+ \cap \mathcal{V}_0^- = \varnothing$.

Proof. We perform the proof item by item:

(a) Assume, without loss of generality, that $n < m$. Since $V_{0,m-n} = \mathbf{A}_{a,\theta}^{-n}(V_{n,m})$, then

$$\begin{pmatrix} x_{0,m-n} \\ y_{0,m-n} \end{pmatrix} = \begin{pmatrix} a^{-n}\cos n\theta & a^{-n}\sin n\theta \\ -a^{-n}\sin n\theta & a^{-n}\cos n\theta \end{pmatrix} \begin{pmatrix} x_{n,m} \\ y_{n,m} \end{pmatrix}$$

By Theorem 2.2.5, for all $1 \leq k \leq N$,

$$(x_{0,m-n}, y_{0,m-n}) \begin{pmatrix} \cos k\theta \\ \sin k\theta \end{pmatrix} = (x_{n,m}, y_{n,m}) \begin{pmatrix} a^{-n} \cos(n+k)\theta \\ a^{-n} \sin(n+k)\theta \end{pmatrix} \leq a^k$$

and therefore $V_{0,m-n} \in \mathcal{R}_N$.

(b) If $V_{n+1,m+1}$ is a vertex of $\mathcal{R}_N$, then clearly $x_{n+1,m+1} \leq 1$. Conversely, if $x_{n+1,m+1} \leq 1$, then for $V_{n+1,m+1}$ to belong to $\mathcal{R}_N$ we need to prove that $V_{n+1,m+1} \in \Pi_k$ for all $k \in \{1, 2, \ldots, N\}$. Since $V_{n+1,m+1} = \mathbf{A}_{a,\theta}(V_{n,m})$, then

$$\begin{pmatrix} x_{n+1,m+1} \\ y_{n+1,m+1} \end{pmatrix} = \begin{pmatrix} a\cos\theta & -a\sin\theta \\ a\sin\theta & a\cos\theta \end{pmatrix} \begin{pmatrix} x_{n,m} \\ y_{n,m} \end{pmatrix}$$

and therefore

$$(x_{n+1,m+1}, y_{n+1,m+1}) \begin{pmatrix} \cos k\theta \\ \sin k\theta \end{pmatrix} = (x_{n,m}, y_{n,m}) \begin{pmatrix} a\cos(k-1)\theta \\ a\sin(k-1)\theta \end{pmatrix} \leq a^k$$

for all k, and therefore $V_{n+1,m+1} \in \mathcal{R}_N$.

(c) This is a direct consequence of statement (b).

(d) Assume that $V_0^{\pm} \in \mathcal{V}_0^{\mp}$, i.e. there exists $k \in \mathbb{N}$ such that $V_0^{\pm} = \mathbf{A}_{a,\theta}^k(V_0^{\mp})$. Then,

$$\partial\mathcal{R}_N \ni \mathbf{A}_{a,\theta}^{\ell}(V_0^{\pm}) = \mathbf{A}_{a,\theta}^{\ell+k}(V_0^{\mp}) \in \mathcal{V}_0^{\mp}$$

for all $0 \leq \ell < \ell^{\pm}$, and therefore $\mathcal{V}_0^{\pm} \subseteq \mathcal{V}_0^{\mp}$.

(e) There exists a vertex $V_{n,m}$ of $\mathcal{R}_N$ and $\ell_1 \neq \ell_2 \in \mathbb{N}$ such that $V_{n,m} = \mathbf{A}_{a,\theta}^{\ell_1}(V_0^+) = \mathbf{A}_{a,\theta}^{\ell_2}(V_0^-)$. If $\ell_1 < \ell_2$, then $V_0^+ = \mathbf{A}_{a,\theta}^{\ell_2-\ell_1}(V_0^-) \in \mathcal{V}_0^-$, and therefore $\mathcal{V}_0^+ \subseteq \mathcal{V}_0^-$. Otherwise, we have that $V_0^- = \mathbf{A}_{a,\theta}^{\ell_1-\ell_2}(V_0^+) \in \mathcal{V}_0^+$, and therefore $\mathcal{V}_0^- \subseteq \mathcal{V}_0^+$.

(f) There exists a vertex $V_{n,m}$ of $\mathcal{R}_N$ with $n < m \leq N$ such that

$$V_{n,N+1} = V_{n,m} = V_{m,N+1}$$

Assume for contradiction that $n \geq 1$. Then, since $N+1-n \leq N$, it holds that $N+1 = m$ because $V_{0,N+1-n} = V_{0,m-n} \in \partial\mathcal{R}_N$. This is a contradiction and therefore $n = 0$ and $V_{n,m}$ is either the upper or lower vertex of $\mathcal{R}_N$ on $\mathcal{C}$.

(g) If $V_0^{\pm} \in \mathcal{L}_{N+1}$, then $V_0^{\pm} = V_{N+1,n^{\pm}} = \mathbf{A}_{a,\theta}^{n^{\pm}}(V_{0,N+1-n^{\pm}})$, so necessarily $V_{0,N+1-n^{\pm}} = V_0^{\mp}$ because $n^{\pm} \geq 1$ and therefore $V_0^{\pm} = \mathbf{A}_{a,\theta}^{n^{\pm}}(V_{0^{\mp}})$.

(h) Assume by contradiction and without loss of generality that $V_0^- \in \mathcal{V}_0^+$, i.e. there exists ℓ such that $V_{0,n^-} = V_{\ell,\ell+n^+}$. Then,

$$V_{0,n^-} = V_{0,\ell} = V_{0,\ell+n^+}$$

Since $\mathcal{L}_{N+1} \cap \partial\mathcal{R}_N = \varnothing$, then $\ell + n^+ \leq N$, and therefore $\ell = \ell + n^+$ and therefore $n^+ = 0$, a contradiction. □

Proof of Proposition 2.2.11. Let $V_{n,m}$ be a vertex of $\mathcal{R}_N$ with $n < m$. Then, either $V_{0,m-n} = V_0^+$ or $V_{0,m-n} = V_0^-$, and therefore either $V_{n,m} = \mathbf{A}_{a,\theta}^n(V_0^+)$ or $V_{n,m} = \mathbf{A}_{a,\theta}^n(V_0^-)$, and therefore $V_{m,n} \in \mathcal{V}_0^+ \cup \mathcal{V}_0^-$. The rest is obvious by Lemma 2.2.13. □

2.2.3 The Bifurcation Sequence

For each fixed angle $0 < \theta < \pi$, the respective bifurcations (if any) occur at those values $a_j = a_j(\theta)$ for which the line $\mathcal{L}_{N_j+1}$ contains either of the vertices V_{0,n_j^+} or V_{0,n_j^-} that the polygon $\mathcal{R}_{N_j}$ has on the critical line $\mathcal{L}_0 = \mathcal{C}$. For a slightly less than a_j, another polygon with $N_{j+1}+1$ sides appears, where $N_{j+1} = N_j + \ell_j^+$ or $N_{j+1} = N_j + \ell_j^-$ depending on whether the contact takes place at V_{0,n_j^+} or V_{0,n_j^-}, respectively. Recall that ℓ_j^+ and ℓ_j^- denote the lengths of the orbits of V_{0,n_j^+} and V_{0,n_j^-}, respectively. Therefore, in order to determine the sequence of bifurcation values a_j in an iterative way, we define the 6-tuple

$$\mathcal{A}_j = (a_j, N_j, n_j^+, n_j^-, \ell_j^+, \ell_j^-)$$

that we call a *bifurcation stair-step*. Each $\mathcal{A}_j$ is a tag representing a (N_j+1)-sided bounded polygon that becomes a $(N_{j+1}+1)$-sided bounded polygon for a slightly less than a_j.

The largest bifurcation value a_1 is associated to the primary polygon $\mathcal{R}_{N_\theta}$. For this polygon it holds that $N_1 = N_\theta$, $n_1^+ = \ell_1^- = 1$ and $n_1^- = \ell_1^+ = N_\theta$. See Example 2.2.10. Therefore, the first bifurcation stair-step is

$$\mathcal{A}_1 = (a_1, N_\theta, 1, N_\theta, N_\theta, 1)$$

where a_1 depends on the sign σ_1 of $\sin(N_\theta+1)\theta$ in the following way:

- If $\sigma_1 = 0$, then the line $\mathcal{L}_{N_\theta+1}$ is vertical for all $a \geq 1$. Therefore no bifurcation occurs and $a_1 = 1$. Note that $\sigma_1 = 0$ if and only if $\theta \in \{\pi/2, 2\pi/3\}$.

- If $\sigma_1 = +1$, the upper vertex, see equation (2.5), is

  $$V_{0,1}(a_1) = (1, (a_1 - \cos\theta)\csc\theta)$$

  and the line $\mathcal{L}_{N_\theta+1}(a_1)$ is given, see equation (2.3), by

  $$x\cos(N_\theta+1)\theta + y\sin(N_\theta+1)\theta = a_1^{N_\theta+1}$$

  Since $V_{0,1}(a_1) \in \mathcal{L}_{N_\theta+1}(a_1)$, then

  $$a_1^{N_\theta+1}\sin\theta - a_1\sin(N_\theta+1)\theta + \sin N_\theta\theta = 0 \tag{2.7}$$

- If $\sigma_1 = -1$, the lower vertex, see equation (2.5), is

  $$V_{0,N_\theta}(a_1) = (1, (a_1^{N_\theta} - \cos N_\theta\theta)\csc N_\theta\theta)$$

  Since $V_{0,N_\theta}(a_1) \in \mathcal{L}_{N_\theta+1}(a_1)$, then

  $$a_1^{N_\theta+1}\sin N_\theta\theta - a_1^{N_\theta}\sin(N_\theta+1)\theta + \sin\theta = 0 \tag{2.8}$$

Equations (2.7) and (2.8) can be seen as polynomials of the form

$$p_1^+(a) = a^{r_1+s_1}\sin r_1\theta - a^{r_1}\sin(r_1+s_1)\theta + \sin s_1\theta$$
$$p_1^-(a) = a^{r_1+s_1}\sin s_1\theta - a^{s_1}\sin(r_1+s_1)\theta + \sin r_1\theta$$

where $r_1 = 1$ and $s_1 = N_\theta$. In the following lemma we prove that these polynomials have unique positive roots denoted by a_1^+ and a_1^-, respectively. Then, it holds that $a_1 = \max\{a_1^+, a_1^-\}$.

Lemma 2.2.14. *Let $0 < \theta < \pi$, and let $r, s \in \mathbb{N}$ such that $\sin r\theta > 0$ and $\sin s\theta < 0$. Then, the polynomials*

$$p^+(a) = a^{r+s} \sin r\theta - a^r \sin(r+s)\theta + \sin s\theta$$
$$p^-(a) = a^{r+s} \sin s\theta - a^s \sin(r+s)\theta + \sin r\theta$$

have unique positive roots a^+ and a^-, respectively. Moreover, the roots a^+ and a^- are simple and $a^+ \cdot a^- = 1$.

Proof. The existence and uniqueness of a^+ and a^- are guaranteed by Descartes' rule of signs as $\sin r\theta > 0$ and $\sin s\theta < 0$. Moreover, since $p^-(a)$ is the reciprocal polynomial of $p^+(a)$, then $a^- = 1/a^+$ by uniqueness. □

The construction of the bifurcation sequence is iteratively obtained from $\mathcal{A}_1$ according to the following result. For each $j \in \mathbb{N}$, let us denote by σ_j the sign of $\sin(N_j + 1)\theta$.

Proposition 2.2.15. *For every $j \in \mathbb{N}$, given*

$$\mathcal{A}_j = (a_j, N_j, n_j^+, n_j^-, \ell_j^+, \ell_j^-)$$

the next bifurcation stair-step

$$\mathcal{A}_{j+1} = (a_{j+1}, N_{j+1}, n_{j+1}^+, n_{j+1}^-, \ell_{j+1}^+, \ell_{j+1}^-)$$

is obtained applying the following rule:

(a) Case $\sigma_j = +1$:

$$N_{j+1} = N_j + \ell_j^+, \qquad n_{j+1}^+ = \ell_{j+1}^- = N_j + 1, \qquad n_{j+1}^- = n_j^-, \qquad \ell_{j+1}^+ = \ell_j^+$$

(b) Case $\sigma_j = -1$:

$$N_{j+1} = N_j + \ell_j^-, \qquad n_{j+1}^+ = n_j^+, \qquad n_{j+1}^- = \ell_{j+1}^+ = N_j + 1, \qquad \ell_{j+1}^- = \ell_j^-$$

(c) Case $\sigma_j = 0$:

$$N_{j+1} = N_j, \qquad n_{j+1}^+ = n_j^+, \qquad n_{j+1}^- = n_j^-, \qquad \ell_{j+1}^+ = \ell_j^+, \qquad \ell_{j+1}^- = \ell_j^-$$

In order to obtain a_{j+1}, if $\sigma_{j+1} = 0$, then $a_{j+1} = 1$. Otherwise, the bifurcation value a_{j+1} is the unique positive root of the polynomial

$$p_{j+1}^+(a) = a^{N_{j+1}+1} \sin n_{j+1}^+\theta - a^{n_{j+1}^+} \sin(N_{j+1} + 1)\theta + \sin n_{j+1}^-\theta$$

if $\sigma_{j+1} = +1$, or of

$$p_{j+1}^-(a) = a^{N_{j+1}+1} \sin n_{j+1}^-\theta - a^{n_{j+1}^-} \sin(N_{j+1} + 1)\theta + \sin n_{j+1}^+\theta$$

if $\sigma_{j+1} = -1$, respectively.

Proof. If $\sigma_j = 0$, then $\mathcal{L}_{N_j+1}$ is vertical for all $1 \leq a < a_{j-1}$, and therefore no other bifurcation occurs. Therefore, all parameters of $\mathcal{A}_j$ remain constant and $a_j = 1$. If $\sigma_j \neq 0$, then from our geometric discussion in the previous subsection we deduce the values of the entries of $\mathcal{A}_{j+1}$. In this case, if $\sigma_{j+1} = +1$, then the upper vertex, see equation (2.5),

$$V_0^+(a_{j+1}) = (1, (a_{j+1}^{n_{j+1}^+} - \cos n_{j+1}^+\theta)\csc n_{j+1}^+\theta) \tag{2.9}$$

belongs to the line $\mathcal{L}_{N_{j+1}+1}(a_{j+1})$, whose equation, see (2.3), is

$$x\cos(N_{j+1}+1)\theta + y\sin(N_{j+1}+1)\theta = a_{j+1}^{N_{j+1}+1} \tag{2.10}$$

From a direct substitution of equation (2.9) into (2.10) we obtain $p_{j+1}^+(a_{j+1}) = 0$. Similarly, if $\sigma_{j+1} = -1$, then the lower vertex, see equation (2.5),

$$V_0^-(a_{j+1}) = (1, (a_{j+1}^{n_{j+1}^-} - \cos n_{j+1}^-\theta)\csc n_{j+1}^-\theta) \tag{2.11}$$

belongs to the line $\mathcal{L}_{N_{j+1}+1}(a_{j+1})$. From a direct substitution of equation (2.11) into (2.10) we obtain $p_{j+1}^-(a_{j+1}) = 0$. The uniqueness of the positive roots of $p_{j+1}^+(a)$ and $p_{j+1}^-(a)$ is due to Lemma 2.2.14. □

The result that we prove next contains Theorem 1.

Theorem 2.2.16. *For each $0 < \theta < \pi$ there exists a nonincreasing sequence $(a_j)_j$, called the* bifurcation sequence*, with the following properties:*

(a) $a_j \geq 1$ *for every* $j \in \mathbb{N}$.

(b) $\sigma_j = 0$ *if and only if* $a_j = 1$ *for every* $j \in \mathbb{N}$.

(c) For any $j \in \mathbb{N}$, $a_{j+1} \leq a_j$ *with equality holding if and only if* $a_j = 1$.

(d) $\lim_{j\to\infty} a_j = 1$.

(e) $\{a_j\}$ *is finite if and only if* $\theta/\pi \in \mathbb{Q}$.

(f) The following statements hold for every $j \in \mathbb{N}$*:*

- *For every* $a_j \leq a < a_{j-1}$,

$$N(a,\theta) = N_j, \qquad n^+(a,\theta) = n_j^+, \qquad n^-(a,\theta) = n_j^-$$

Moreover,

$$V_{N+1,n^{\sigma_j}}(a_j) = V_0^{\sigma_j}(a_j) = V_{0,N+1}(a_j)$$

- *For every* $a_{j+1} < a \leq a_j$,

$$\ell^+(a,\theta) = \ell_j^+, \quad \ell^-(a,\theta) = \ell_j^-$$

Proof. The first five statements hold as we have already discussed (see also Remark 2.2.7). We prove the last one by induction:

The case $j = 1$ is true by the previous results. Assume that this theorem holds for $j = k$ and let us prove it for $j = k+1$. Assume without loss of generality that $\sigma_k = +1$. As we diminish the value of a from a_k to a_{k+1}, each point in the $\mathbf{A}_{a_k,\theta}$-orbit of $V_0^+(a_k)$ bifurcates into two new ones, one in the $\mathbf{A}_{a,\theta}$-orbit of $V_0^+(a)$ and the other in the $\mathbf{A}_{a,\theta}$-orbit

of $V_0^-(a)$, and this structure persists until the next contact takes place for $a = a_{k+1}$. It is easily deduced that for every $a_{k+1} \leq a < a_k$,

$$N(a,\theta) = N(a_k,\theta) + \ell^+(a_k,\theta) = N_k + \ell_k^+ = N_{k+1}$$

and

$$n^+(a,\theta) = N(a_k,\theta) + 1 = N_k + 1 = n_{k+1}^+$$

and

$$n^-(a,\theta) = n_k^- = n_{k+1}^-$$

Now, if $a_{k+1} < a$, then

$$\ell^+(a,\theta) = \ell^+(a_k,\theta) = \ell_k^+$$

and

$$\ell^-(a,\theta) = \ell^-(a_k,\theta) = N_k + 1 = \ell_k^-$$

Finally, if $\sigma_{k+1} \neq 0$, then

$$\ell^{\sigma_{k+1}}(a_{k+1},\theta) = \ell_k^{\sigma_{k+1}} = \ell_{k+1}^{\sigma_{k+1}}$$

and

$$\ell^{-\sigma_{k+1}}(a_{k+1},\theta) = N_{k+1} + 1 = \ell_{k+1}^{-\sigma_{k+1}}$$ □

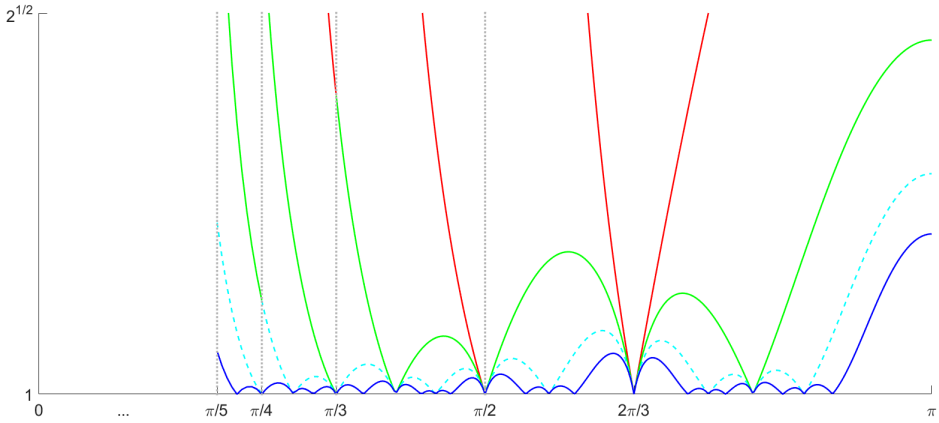

Figure 2.7: The curves of the bifurcation values $a_j(\theta)$ for $j = 1$ (red), 2 (green), 3 (cyan), 4 (blue) and $\theta \in (\pi/5, \pi)$

In Figure 2.7 we show a numerical approximation of the first bifurcation curves. The concatenation of some of them at certain points are justified by the following analytical results.

Proposition 2.2.17. *For every $j \in \mathbb{N}$ it holds that $\sigma_j \equiv -1$ on $(0, \pi/(j+1))$. In particular, for every $j \in \mathbb{N}$,*

$$\lim_{\theta \to (\frac{\pi}{k})^+} a_j(\theta) = a_{j-1}(\tfrac{\pi}{k})$$

for all $k > j$.

Proof. The result easily follows for $j = 1$. Assume that it holds for $j \leq k$ and let us prove it for $j = k + 1$. Fix $\theta \in (0, \pi/(k+2))$. Since

$$(0, \tfrac{\pi}{k+2}) \subseteq (0, \tfrac{\pi}{k+1}) \subseteq \cdots \subseteq (0, \tfrac{\pi}{2})$$

then $\sigma_n(\theta) = -1$ for $n = 1, 2, \ldots, k$ by the induction hypothesis, and therefore $N_{k+1} + 1 = N_\theta + k + 1$. Note that $N_\theta \geq k + 3$. Now, since $\pi/N_\theta < \theta \leq \pi/(N_\theta - 1)$ if $N_\theta > k + 3$ and $\pi/N_\theta < \theta < \pi/(N_\theta - 1)$ if $N_\theta = k + 3$, then

$$\pi < \pi + \frac{(k+1)\pi}{N_\theta} < (N_{k+1} + 1)\theta \leq \pi + \frac{(k+2)\pi}{N_\theta - 1} < 2\pi$$

and therefore $\sigma_{k+1}(\theta) = -1$. □

2.2.4 Existence of First-rate Strictly Invariant Sets

In Section 2.2.1, for each pair (a, θ) we constructed the $(N + 1)$-sided polygon $\mathcal{K}_N = \Pi_{N+1} \cap \Pi_N \cap \cdots \cap \Pi_1$ and proved that it is self-similar in Theorem 2.2.5. However, it may not be strictly invariant. Two particular cases are $\theta = \pi/2$ and $\theta = 2\pi/3$. For $\theta = \pi/2$, the rectangle $\mathcal{K}_3$ is strictly invariant if and only if $a \leq \sqrt{2}$. On the other hand, for $\theta = 2\pi/3$, the triangle $\mathcal{K}_2$ is strictly invariant if and only if $a = 1$. Recall that, for any (a, θ), if $\mathcal{K}_N$ is strictly invariant, then $a \leq \sqrt{2}$ because $\mathcal{K}_N$ is compact and has nonempty interior.

From the convexity of $\mathcal{R}_N$, it follows that $\mathcal{K}_N$ is strictly invariant if and only if $\mathcal{R}_N$ contains the images $\widetilde{V}^+_{N+1}$ and $\widetilde{V}^-_{N+1}$ under the fold of the proper vertices V^+_{N+1} and V^-_{N+1} of $\mathcal{K}_N$, respectively. Computing the coordinates (2.5) of these vertices and considering the equations (2.3) of the lines $\mathcal{L}_n$, we obtain the following result:

Proposition 2.2.18. *Let $0 < \theta < \pi$. For any $a > 1$, the self-similar polygon $\mathcal{K}_N$ is strictly $\Gamma_{a,\theta}$-invariant if and only if*

$$\begin{aligned} a^{N+1}\sin(n + n^+)\theta - a^{n^+}\sin(N + 1 + n)\theta - (a^n - 2\cos n\theta)\sin n^-\theta &\geq 0 \\ a^{N+1}\sin(n + n^-)\theta - a^{n^-}\sin(N + 1 + n)\theta - (a^n - 2\cos n\theta)\sin n^+\theta &\geq 0 \end{aligned}$$

for $n = 0, 1, \ldots, N$.

Proof. Since $\mathcal{R}_N = \Pi_N \cap \ldots \cap \Pi_1 \cap \Pi_0$, then the folded proper vertices $\widetilde{V}^\pm_{N+1}$ of $\mathcal{K}_N$ belong to $\mathcal{R}_N$ if and only if $\widetilde{V}^\pm_{N+1} \in \Pi_n$ for $n = 0, 1, ..., N$. That is, if and only if

$$\begin{aligned} (2 - x_{n^+,N+1})\cos n\theta + y_{n^+,N+1}\sin n\theta &\leq a^n \\ (2 - x_{n^-,N+1})\cos n\theta + y_{n^-,N+1}\sin n\theta &\leq a^n \end{aligned}$$

for $n = 0, 1, \ldots, N$, where

$$\begin{aligned} x_{n^\pm,N+1} &= (-a^{N+1}\sin n^\pm\theta + a^{n^\pm}\sin(N + 1)\theta)\csc n^\mp\theta \\ y_{n^\pm,N+1} &= (a^{N+1}\cos n^\pm\theta - a^{n^\pm}\cos(N + 1)\theta)\csc n^\mp\theta \end{aligned}$$

are the coordinates (2.5) of the proper vertices $V^\pm_{N+1}$ of $\mathcal{K}_N$. Since $\sin n^+\theta > 0$ and $\sin n^-\theta < 0$, we obtain the inequalities from the statement of this Proposition. □

Remark 2.2.19. It is sufficient to check the inequalities of Proposition 2.2.18 for those $n \in \{1, \ldots, N\}$ such that $\cos n\theta < 0$.

The characterization provided by Proposition 2.2.18 of the strict invariance of $\mathcal{K}_N$ has little practical value when N is large. However, the following corollary allows us to easily discard those which cannot be strictly invariant from a basic geometric remark.

Proposition 2.2.20. *Let $0 < \theta < \pi$. Assume that $\mathcal{K}_N$ is strictly $\Gamma_{a,\theta}$-invariant for some $a > 1$. Then, the following statements hold:*

(a) *If a is not a bifurcation value, then* $\min\{\cos n^+\theta, \cos n^-\theta\} \geq 0$.

(b) *If a is a bifurcation value, then*

$$\min\{\cos n^{-\sigma}\theta, \sigma \sin(2n^\sigma + n^{-\sigma})\theta\} \geq 0$$

where σ is the sign of $\sin(N+1)\theta$.

Proof.

(a) Assume that a is not a bifurcation value. Then, neither V_0^+ nor V_0^- is a vertex of $\mathcal{K}_N$ and the lines $\mathcal{L}_{n^+}$ and $\mathcal{L}_{n^-}$ must have non-positive and nonnegative slopes, respectively, because $\widetilde{V}_{N+1}^+ \in \Pi_{n^+}$ and $\widetilde{V}_{N+1}^- \in \Pi_{n^-}$. Since these slopes are equal to $-\cot n^{\pm}\theta$, and since $\sin n^+\theta > 0$ and $\sin n^-\theta < 0$, then that $\cos n^+\theta \geq 0$ and $\cos n^-\theta \geq 0$.

(b) Assume that a is a bifurcation value. Then, $\widetilde{V}_{N+1}^\sigma = V_{N+1}^\sigma = V_0^\sigma$ is a vertex of $\mathcal{K}_N$. In order that $\widetilde{V}_{N+1}^{-\sigma} \in \Pi_{n^{-\sigma}}$, the slope of $\mathcal{L}_{n^\sigma}$ must be no greater than the slope of $\mathcal{L}_{N+1}$ (both in absolute value), and line $\mathcal{L}_{n^{-\sigma}}$ must be in the same conditions as before. Therefore, $|\cot(N+1)\theta| \geq |\cot n^\sigma\theta|$ and $\cos n^{-\sigma}\theta \geq 0$.

Applying the fundamental identity of trigonometry, it follows that the first inequality is equivalent to

$$\sin^2 n^\sigma\theta \geq \sin^2(N+1)\theta$$

and

$$0 \leq \sin^2 n^\sigma\theta - \sin^2(N+1)\theta = -\sin(N + n^\sigma + 1)\theta \cdot \sin n^{-\sigma}\theta$$

Since $-\sigma$ is the sign of $\sin n^{-\sigma}\theta$, we conclude that

$$\sigma \sin(2n^\sigma + n^{-\sigma})\theta \geq 0$$ □

We just obtained a necessary condition for the strict invariance of $\mathcal{K}_N$. In this way, we say that the self-similar polygon $\mathcal{K}_N$ is a *possible strictly invariant polygon* if it verifies either of the conditions in Proposition 2.2.20.

Proposition 2.2.21. *Let $\theta \in (0,\pi) \setminus \{2\pi/3\}$. The following statements hold:*

(a) *There exists $\bar{a} > 1$ such that $\mathcal{K}_{N(\bar{a},\theta)}$ is a possible strictly $\Gamma_{\bar{a},\theta}$-invariant polygon.*

(b) *If $\mathcal{K}_{N(\bar{a},\theta)}$ is a possible strictly $\Gamma_{\bar{a},\theta}$-invariant polygon for some $\bar{a} > 1$, then $\mathcal{K}_{N(a,\theta)}$ is a possible strictly $\Gamma_{a,\theta}$-invariant polygon for all $a \in (1,\bar{a}]$.*

Proof.

(a) This statement easily follows from Remark 2.2.7. If β is an irrational number, then $n^+(a,\theta)\theta \to 0$ and $n^-(a,\theta)\theta \to 2\pi$ as $a \to 1$. Therefore, statement (a) of Proposition 2.2.20 is verified. On the other hand, assume that $\beta = p/q$ is a rational number. For $q = 4$, the rectangle $\mathcal{K}_3$ is strictly invariant for every $a \leq \sqrt{2}$. For $q \geq 5$, statement (a) of Proposition 2.2.20 also holds for a sufficiently close to 1 because the angles $n^+(a,\theta)\theta$ and $n^-(a,\theta)\theta$ lie in the first and fourth quadrants, respectively.

(b) Let $[a_j, a_{j-1})$ be the interval obtained in Theorem 2.2.16 containing $\bar{a}$. Since n^+ and n^- remain constant on $[a_j, a_{j-1})$, then $\cos n^+\theta \geq 0$ and $\cos n^-\theta \geq 0$ for every $a \in (a_j, a_{j-1})$. Assume first that $\bar{a} > a_j$. It is trivial that $\mathcal{K}_N$ is a possible strictly invariant polygon for every $a \in (a_j, \bar{a})$. On the other hand, if $a = a_j$ then

$$\sigma \sin(2n^\sigma + n^{-\sigma})\theta = \cos n^\sigma\theta|\sin(N+1)\theta| + |\sin n^\sigma\theta|\cos(N+1)\theta \geq 0$$

because $\cos n^+\theta \geq 0$ and $\cos n^-\theta \geq 0$ implies $\cos(N+1)\theta \geq 0$. Hence $\mathcal{K}_{N(a_j,\theta)}$ is a possible strictly invariant polygon.

By induction we only have to prove that $\mathcal{K}_{N(a,\theta)}$ is possibly strictly invariant for $a \in (a_{j+1}, a_j)$. This is straightforward since on that interval it holds that $n^\sigma = N_j + 1$ and $n^{-\sigma} = n_j^{-\sigma}$.

Assume now that $\bar{a} = a_j$ and $\cos n^\sigma\theta < 0$. Since $\sigma \sin(2n^\sigma + n^{-\sigma})\theta \geq 0$, then

$$|\sin n^\sigma\theta|\cos(N+1)\theta \geq -\cos n^\sigma\theta|\sin(N+1)\theta| \geq 0$$

Therefore, we have that $\cos(N+1)\theta \geq 0$ and $\mathcal{K}_{N(a,\theta)}$ is possibly strictly invariant for $a \in (a_{j+1}, a_j)$. □

Remark 2.2.22. For each $\theta \in (0,\pi) \setminus \{2\pi/3\}$, let $\bar{a} = \bar{a}(\theta)$ be the supremum of the a-values for which $\mathcal{K}_{N(a,\theta)}$ is a possible strictly $\Gamma_{a,\theta}$-invariant polygon. If $\bar{a} > 1$, then $\mathcal{K}_{N(a,\theta)}$ is a possible strictly $\Gamma_{a,\theta}$-invariant polygon for every $1 \leq a < \bar{a}$ by Proposition 2.2.21. In this case, note that $\bar{a}$ is a bifurcation value for θ. Note that the polygon $\mathcal{K}_{N(\bar{a},\theta)}$ may not be a possible strictly invariant polygon.

Now we prove Theorem 2 for $\theta \in (0,\pi) \setminus \{2\pi/3\}$.

Proof of Theorem 2. Let

$$B_a = \{(x,y) \in \mathbb{R}^2 : y_0^- < y < y_0^+\}$$

For every $a \in (1, \bar{a})$, since $\mathcal{K}_{N(a,\theta)}$ is a possible strictly $\Gamma_{a,\theta}$-invariant polygon by Remark 2.2.22, then both $V_{N+1}^\pm$ and $\widetilde{V}_{N+1}^\pm$ belong to B_a. On the other hand, the rectangle

$$C_a = \{(x,y) \in B_a : 0 \leq x \leq 1\}$$

is contained in $\mathcal{R}_{N(a,\theta)}$ by convexity. Therefore, since $x_{N+1}^\pm \to 1$ as $a \to 1$, then

$$\widetilde{V}_{N+1}^\pm \in C_a \subseteq \mathcal{R}_{N(a,\theta)}$$

for every a sufficiently close to 1. □

2.2.5 Existence of Second-rate Strictly Invariant Sets

In Section 2.2.4 we have seen that, for every $\theta \in (0,\pi) \setminus \{2\pi/3\}$, the self-similar polygons $\mathcal{K}_N$ are (first-rate) strictly invariant for every a sufficiently close to 1. For larger values of a, these polygons may not be strictly invariant. If not, then $\mathcal{K}_N$ is strictly contained in $\Gamma_{a,\theta}(\mathcal{K}_N)$. In that case, the consecutive images of $\mathcal{K}_N$ under $\Gamma_{a,\theta}$ form a nondecreasing sequence of sets that converge to a second-rate strictly invariant compact set, namely the closure of $\mathcal{K}_{a,\theta}$, provided that $\mathcal{K}_{a,\theta}$ is bounded. See Proposition 2.2.9 and formula (2.4).

Let us illustrate what we have said to the singular angle $\theta = 2\pi/3$. In this case, the self-similar triangle $\mathcal{K}_2$ is not even a possible strictly invariant polygon for any $a > 1$. However, we will see that there exist a-values in $(1, \sqrt{2}]$ for which $\mathcal{K}_{a,\theta}$ is a strictly invariant compact polygon.

A first example of a second-rate strictly invariant set is obtained by the union of the images of $\mathbb{R}^2$, which is in fact the maximal strictly invariant set. For $\theta = 2\pi/3$, it is easy to check that this union coincides with $\Gamma_{a,\theta}^2(\mathbb{R}^2)$ because

$$\mathcal{F}_{\mathcal{C},\mathcal{O}} \circ \Gamma_{a,\theta}(\mathbb{R}^2) = \mathcal{F}_{\mathcal{C},\mathcal{O}} \circ \Gamma_{a,\theta}^2(\mathbb{R}^2)$$

In Figure 2.8a we represent this unbounded strictly invariant set, which can be easily constructed from $\mathcal{L}_1$ and the vertical line through $V_{1,2}$. In Figure 2.8b we represent the polygon $\mathcal{K}_{a,\theta}$, which coincides with $\Gamma_{a,\theta}^5(\mathcal{K}_2)$ for every $a \in (1, a_\theta]$ for some $a_\theta > 1$.

In Figure 2.9 it is represented the construction of $\mathcal{K}_{a,\theta}$ for $a = 1.27$ from the first five iterates of $\mathcal{K}_2$. See in Figure 2.11a how the attractor numerically obtained for these values of the parameters adjusts to $\mathcal{K}_{a,\theta}$ thus showing that $\mathcal{K}_{a,\theta}$ is a second-rate strictly invariant minimal set.

In Figure 2.10 it is represented the construction of $\mathcal{K}_{a,\theta}$ for $a = 1.19$. However, in this case, see Figure 2.11b, the non-simply connected attractor is strictly contained in $\mathcal{K}_{a,\theta}$ and therefore $\mathcal{K}_{a,\theta}$ is not minimal.

Another attractor is numerically found for $a = 1.12$. In this case, as can be seen in Figure 2.11c, this attractor is formed by three connected components and is again strictly contained in $\mathcal{K}_{a,\theta}$.

2.2.6 Numerical Simulations

In Figure 2.12 is shown the region of parameters where attractors are numerically detected. For a pair of parameters (a, θ), we consider an initial point P_0 close to the origin and we perform 10^8 iterations. We set 10^{10} as an upper bound for the norm. If the norm of the iterated point is less than 10^{10}, then we paint (a, θ). Otherwise, we discard (a, θ) since the orbit of P_0 grows indefinitely and there cannot be an attractor. Recall that, for any $0 < \theta < \pi$, strictly $\Gamma_{a,\theta}$-invariant compact sets with nonempty interior can only exist for $a \leq \sqrt{2}$.

2.3 Existence of 2-D Strange Attractors: Proof of Theorem 3

Theorem 3 deals with the existence and characterization of the attractors exhibited by the Expanding Baker Map $\Gamma_{a,\theta}$ in the strictly invariant polygon $\mathcal{K}_{a,\theta}$ given in Theorem 2 and constructed in Section 2.2.1. It is a combination of various results obtained by placing $\Gamma_{a,\theta}$ in each one of the scenarios presented by Buzzi [10], Saussol [64], and Tsujii [68]. Before entering into details, let us give a sketch of the proof and explain how they are related to each other.

Proposition 2.3.15, based on Tsujii [68, Th. 3], provides a nonempty finite family of absolutely continuous invariant probability measures for $\Gamma_{a,\theta}$. As we will see later, the family announced in the theorem consists of the supports of such measures, from which statement (ii) obviously follows.

The fact that they are strange attractors follows from Lemma 2.3.22, which is proved using Proposition 2.3.21, based on several results from Saussol [64]. Lemma 2.3.22 is also used to prove statements (i), (iv) and (v).

From Proposition 2.3.18, based on Buzzi [10, Main Theorem], we obtain the decomposition and mixing properties of the attractors announced in statement (iii).

The proof of theorem is almost identical to the proof of Theorem 1.2 [59], and we reproduce it in this thesis for the sake of completeness. In fact, it would be the same if we restrict ourselves to the case in which θ/π is a rational number, since formula (2.16) is easily obtained in that case without using Buzzi's *geometric estimate* [10, p. 700]. See also

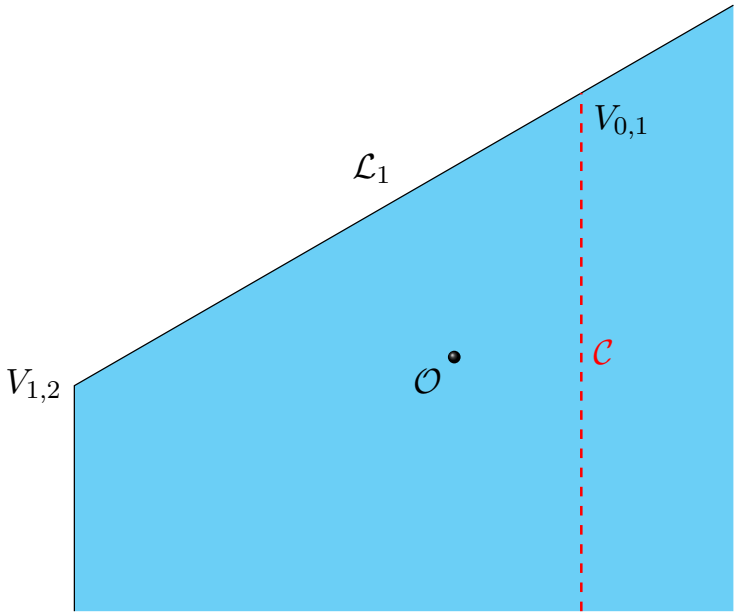

(a)

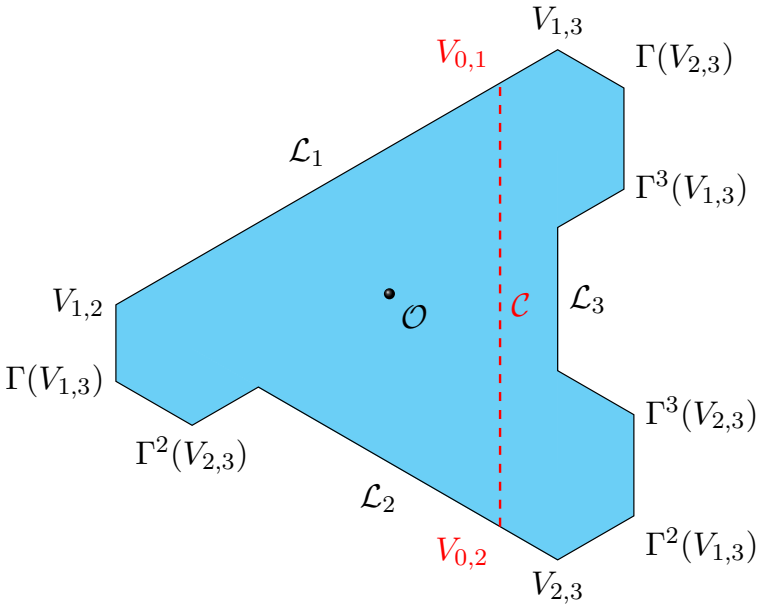

(b)

Figure 2.8: Two second-rate strictly invariant sets for $\theta = 2\pi/3$: (a) The maximal strictly $\Gamma_{a,2\pi/3}$-invariant set $\Gamma^2_{a,2\pi/3}(\mathbb{R}^2)$; (b) The strictly $\Gamma_{a,2\pi/3}$-invariant polygon $\Gamma^5_{a,2\pi/3}(\mathcal{K}_2)$

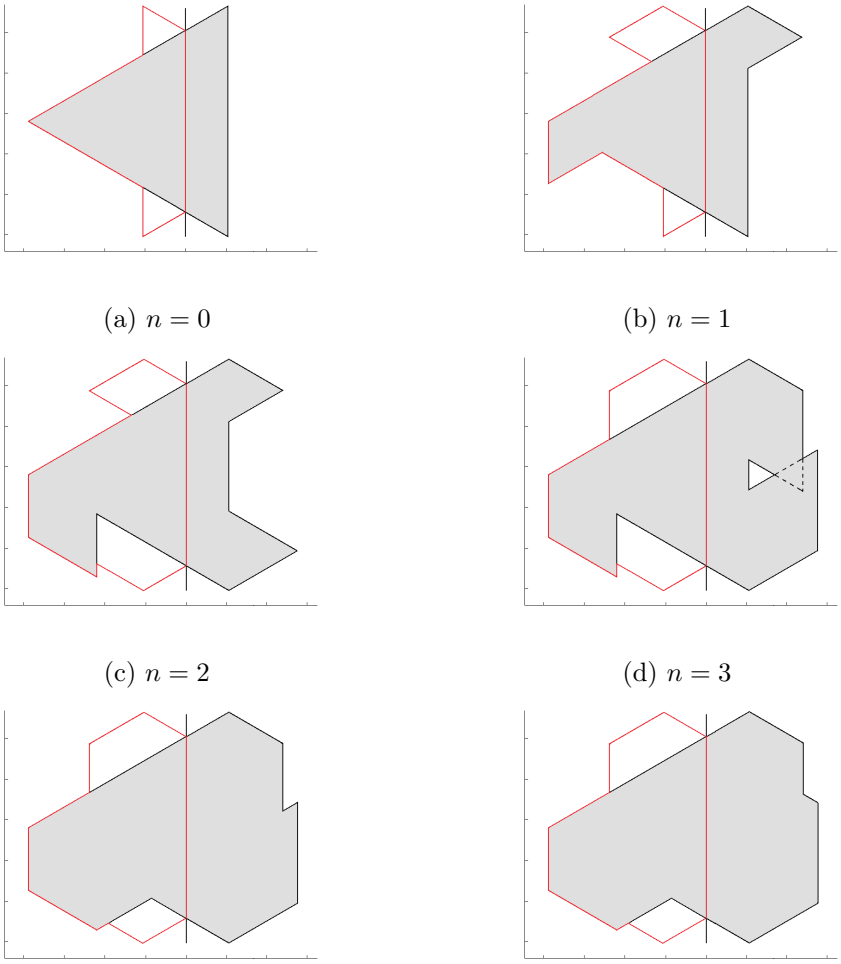

(a) $n = 0$ (b) $n = 1$

(c) $n = 2$ (d) $n = 3$

(e) $n = 4$ (f) $n = 5$

Figure 2.9: Construction of the second-rate strictly invariant compact set $\mathcal{K}_{a,\theta}$ for $a = 1.27$ and $\theta = 2\pi/3$. For $n = 0, 1, ..., 5$, the nth iterate of $\mathcal{K}_2$ painted in gray and the folded set $\mathcal{F}_{\mathcal{C},\mathcal{O}} \circ \Gamma^n_{a,\theta}(\mathcal{K}_2)$ drawn in red. Note that $\mathcal{F}_{\mathcal{C},\mathcal{O}} \circ \Gamma^4_{a,\theta}(\mathcal{K}_2) = \mathcal{F}_{\mathcal{C},\mathcal{O}} \circ \Gamma^5_{a,\theta}(\mathcal{K}_2)$.

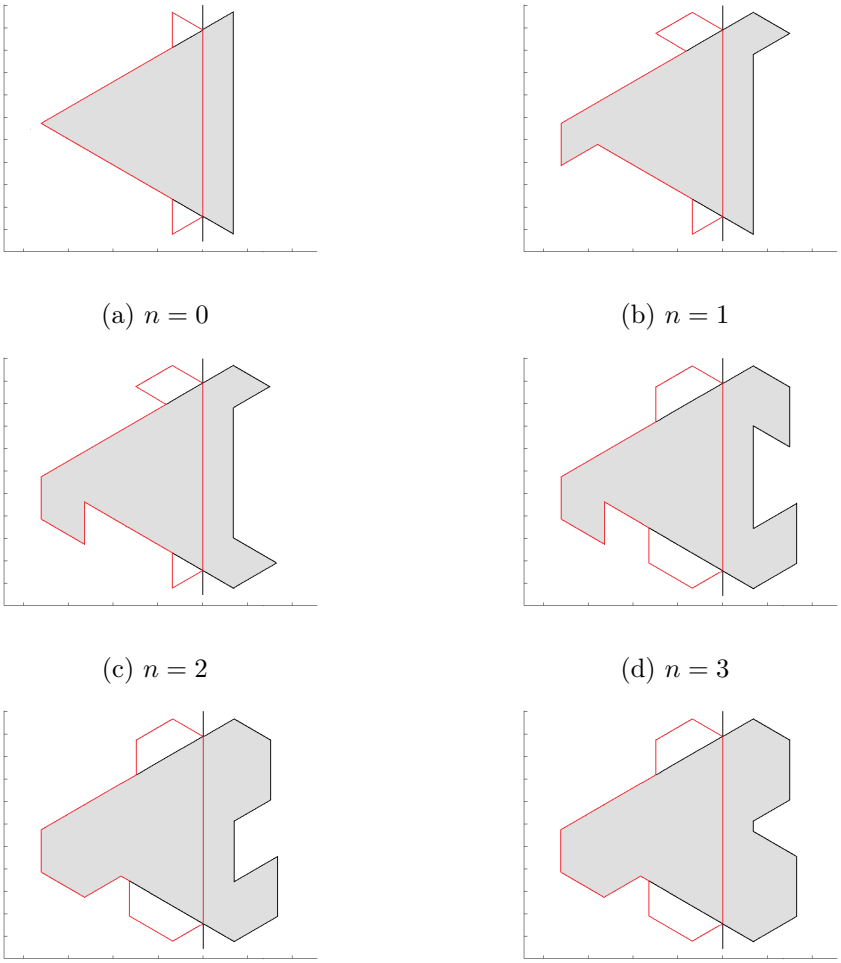

(a) $n = 0$ (b) $n = 1$

(c) $n = 2$ (d) $n = 3$

(e) $n = 4$ (f) $n = 5$

Figure 2.10: Construction of the second-rate strictly invariant compact set $\mathcal{K}_{a,\theta}$ for $a = 1.19$ and $\theta = 2\pi/3$. For $n = 0, 1, ..., 5$, the nth iterate of $\mathcal{K}_2$ painted in gray and the folded set $\mathcal{F}_{\mathcal{C},\mathcal{O}} \circ \Gamma^n_{a,\theta}(\mathcal{K}_2)$ drawn in red. Note that $\mathcal{F}_{\mathcal{C},\mathcal{O}} \circ \Gamma^4_{a,\theta}(\mathcal{K}_2) = \mathcal{F}_{\mathcal{C},\mathcal{O}} \circ \Gamma^5_{a,\theta}(\mathcal{K}_2)$.

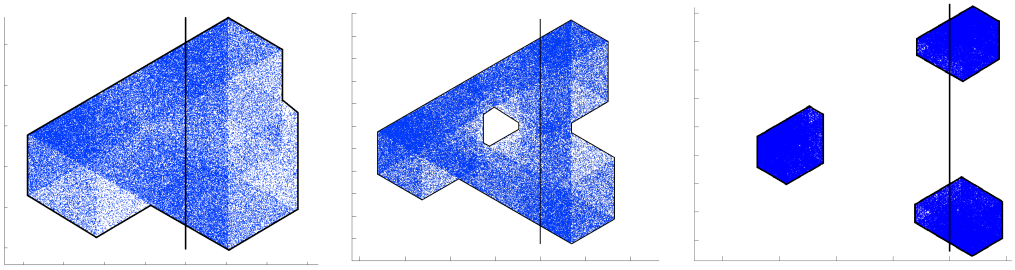

(a) (b) (c)

Figure 2.11: Numerical attractors for $\theta = 2\pi/3$: (a) $a = 1.27$; (b) $a = 1.19$; (c) $a = 1.12$. Note that the first attractor completely fills $\mathcal{K}_{a,\theta}$, which is therefore minimal, while the second and third one do not.

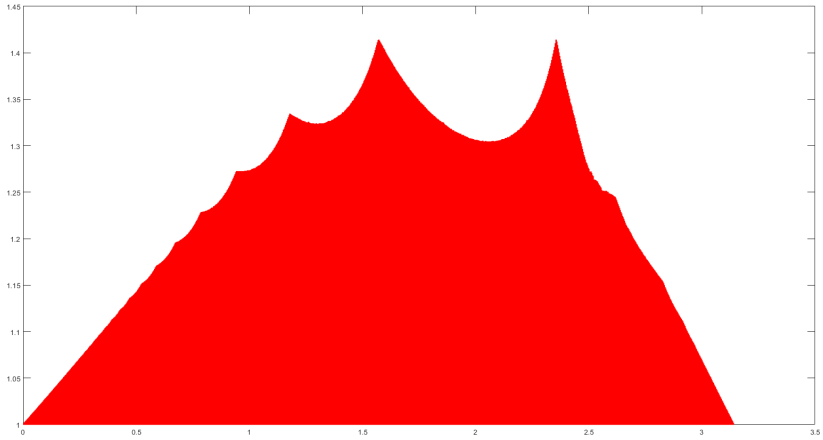

Figure 2.12: Numerical detection of attractors of $\Gamma_{a,\theta}$ for $a \leq \sqrt{2}$ and $0 < \theta < \pi$

Remark 2.3.20. Let us point out here that formula (2.16) is, as we will see soon, the key to applying Saussol's results [64].

2.3.1 Buzzi's Scenario

By controlling the accumulation of discontinuities under iteration, Buzzi [10] proves that any *expanding piecewise analytic map* of the plane, defined with respect to a partition made of finitely many bounded pieces with a sufficiently smooth piecewise boundary, admits absolutely continuous invariant probability measures.

Definition 2.3.1 (Analytic pieces)**.** An *arc* is a one-to-one map $\gamma\colon [0,1] \to \mathbb{R}^2$ of at least class C^1 such that $\|\gamma'(t)\| > 0$ for all $t \in [0,1]$. An *analytic piece* of the plane is a nonempty bounded open subset of $\mathbb{R}^2$ whose boundary is a finite union of real-analytic arcs.

Definition 2.3.2 (Piecewise analytic maps of the plane)**.** A *piecewise analytic map* of the plane is a map $\Phi\colon \mathcal{Y} \to \overline{\mathcal{Y}}$ verifying the following conditions:

(i) $\mathcal{Y} = \bigcup_{\mathcal{P}\in\mathtt{P}} \mathcal{P}$, being $\mathtt{P}$ a finite collection of pairwise disjoint analytic pieces $\mathcal{P}$ of $\mathbb{R}^2$

(ii) For each $\mathcal{P} \in \mathtt{P}$, the restriction $\Phi\colon \mathcal{P} \to \Phi(\mathcal{P})$ can be extended to $\Phi_{\mathcal{P}}\colon \mathcal{U} \to \mathcal{V}$, being $\Phi_{\mathcal{P}}$ an analytic diffeomorphism between neighborhoods $\mathcal{U}$ of $\overline{\mathcal{P}}$ and $\mathcal{V}$ of $\overline{\Phi(\mathcal{P})}$

The map Φ can also be referred to as the triple $(\mathcal{Y}, \mathtt{P}, \Phi)$.

Definition 2.3.3 (Expanding piecewise analytic maps of the plane)**.** A piecewise analytic map of the plane $\Phi\colon \mathcal{Y} \to \overline{\mathcal{Y}}$ is *expanding* if

$$\inf_{P\in\mathcal{Y}} \min_{v\in\mathbb{S}^1} \|\mathrm{D}\Phi(P)\cdot v\| > 1$$

In order to define the *weighted multiplicity* of a piecewise analytic map of the plane and state the geometric estimate, we introduce the notion of *circular sector*.

Definition 2.3.4 (Circular sectors)**.** A *circular sector* at a point $P \in \mathcal{Y}$ is the interior $\mathcal{S}_P$ of any bounded set whose boundary is formed by two different straight segments ℓ_1 and ℓ_2 starting at P and of equal length and the circular arc of the circle centered at P joining their extremes. Given a circular sector $\mathcal{S}_P$, let $\overrightarrow{\mathcal{S}}_P$ be the set of unit vectors which are in the cone generated by ℓ_1 and ℓ_2 at P.

The partition $\mathtt{P}$ defines at each point P the collection $\mathcal{S}_P(\mathtt{P})$ of sectors $\mathcal{S}_P$ at P with $\mathcal{S}$ ranging over the connected components of $\mathcal{B}(P,r)\cap\mathcal{P}$ for $\mathcal{P}\in\mathtt{P}$ and $r>0$ small enough. Note that these $\mathcal{S}_P$ are finitely many well defined sectors because of the analyticity of $\mathtt{P}$.

Definition 2.3.5 (Weighted multiplicity)**.** The *local weighted multiplicity* of a piecewise analytic map $(\mathcal{Y}, \mathtt{P}, \Phi)$ of the plane at a point $P \in \mathcal{Y}$ is

$$\mathtt{mult}(\mathtt{P}, \Phi; P) = \sum_{\mathcal{S}_P\in\mathcal{S}_P(\mathtt{P})} \frac{\Lambda_+(\Phi \mid \overrightarrow{\mathcal{S}}_P)}{\mathtt{jac}(\Phi_{\mathcal{P}})(P)}$$

where:

- $\mathcal{P}$ is the element of $\mathtt{P}$ containing $\mathcal{S}_P$
- $\mathtt{jac}(\Phi_{\mathcal{P}})(P) = |\det \mathrm{D}\Phi_{\mathcal{P}}(P)|$
- $\Lambda_+(\Phi \mid \overrightarrow{\mathcal{S}}_P) = \sup_{v\in\overrightarrow{\mathcal{S}}_P} \|\mathrm{D}\Phi_{\mathcal{P}}(P)\cdot v\|$

The *weighted multiplicity* of $(\mathcal{Y}, \mathtt{P}, \Phi)$ is

$$\mathtt{mult}(\mathtt{P}, \Phi) = \sup_{P\in\mathcal{Y}} \mathtt{mult}(\mathtt{P}, \Phi; P)$$

Definition 2.3.6 (Iterates of a partition)**.** The nth iterate of $\mathtt{P}$ is the partition $\mathtt{P}^{(n)}$ of $\mathcal{Y}$ made of the sets $\mathcal{P}$ which are given by a finite sequence of nonempty intersections

$$\mathcal{P}^0 \cap \Phi^{-1}(\mathcal{P}^1) \cap \cdots \cap \Phi^{-n+1}(\mathcal{P}^{n-1}), \qquad \mathcal{P}^0, \mathcal{P}^1, \ldots, \mathcal{P}^{n-1} \in \mathtt{P}$$

Remark 2.3.7. The partition $\mathtt{P}^{(n)}$ is dynamically related to the iterate Φ^n. In fact, the triple $(\mathcal{Y}, \mathtt{P}^{(n)}, \Phi^n)$ is a piecewise analytic map of the plane for every $n \in \mathbb{N}$. Therefore, we may consider the weighted multiplicity of every iterate. When computing Λ_+ and $\mathtt{jac}$, let us take the following notation:

$$\Phi^{\mathcal{P}} = \Phi_{\mathcal{P}^{n-1}} \circ \cdots \circ \Phi_{\mathcal{P}^1} \circ \Phi_{\mathcal{P}^0}, \qquad \mathcal{P} \in \mathtt{P}^{(n)}$$

Finally we can state Buzzi's geometric estimate [10, §3].

Geometric Estimate. *Let $(\mathcal{Y}, \mathtt{P}, \Phi)$ be an expanding piecewise real-analytic mapping of the plane. Then,*

$$\limsup_{n\to\infty} \tfrac{1}{n} \log \mathtt{mult}(\mathtt{P}^{(n)}, \Phi^n) \le -\log \Lambda_-(\Phi) < 0$$

where $\Lambda_-(\Phi) = \inf_{P\in\mathcal{Y}} \min_{v\in\mathbb{S}^1} \|\mathrm{D}\Phi(P)\cdot v\|$.

2.3.2 Saussol's Scenario

Saussol [64] works with a certain class of multidimensional piecewise expanding maps characterized by five properties, labelled as (PE1)–(PE5).

Definition 2.3.8 (Piecewise expanding maps)**.** Let $\mathcal{K} \subseteq \mathbb{R}^2$ be a compact set such that $\overline{\operatorname{int} \mathcal{K}} = \mathcal{K}$ and let $\Phi\colon \mathcal{K} \to \mathcal{K}$. Assume that there exist an at most countable family of disjoint open sets $\mathcal{U}_i \subseteq \mathcal{K}$ and $\mathcal{V}_i \subseteq \mathbb{R}^2$ such that $\mathcal{V}_i \supseteq \overline{\mathcal{U}}_i$, and maps $\Phi_i\colon \mathcal{V}_i \to \mathbb{R}^2$ such that $\Phi_i|_{\mathcal{U}_i} = \Phi|_{\mathcal{U}_i}$ for all i. We say that Φ is a *piecewise expanding map* if there exist constants $c, \varepsilon_0 > 0$ and $0 < \alpha \leq 1$ such that the following conditions hold:

(PE1) $\Phi_i(\mathcal{V}_i) \supseteq \mathcal{B}(\Phi(\mathcal{U}_i), \varepsilon_0)$ for all i.

(PE2) $\Phi_i \in C^1(\mathcal{V}_i)$, Φ_i is one-to-one and $\Phi_i^{-1} \in C^1(\Phi_i(\mathcal{V}_i))$ for all i. Moreover, for all i and every $\varepsilon \leq \varepsilon_0$ we have that

$$|\det \mathrm{D}\Phi_i^{-1}(P) - \det \mathrm{D}\Phi_i^{-1}(Q)| \leq c|\det \mathrm{D}\Phi_i^{-1}(R)|\varepsilon^\alpha$$

whenever $R \in \Phi_i(\mathcal{V}_i)$ and $P, Q \in \mathcal{B}(R, \varepsilon_0) \cap \Phi_i(\mathcal{V}_i)$.

(PE3) $m_2(\mathcal{K} \setminus \bigcup_i \mathcal{U}_i) = 0$, being m_2 the Lebesgue measure in $\mathbb{R}^2$.

(PE4) There exists $s = s(\Phi) < 1$ such that, for all $P, Q \in \Phi(\mathcal{V}_i)$ such that $\operatorname{dist}(P, Q) \leq \varepsilon_0$,

$$\operatorname{dist}(\Phi_i^{-1}(P), \Phi_i^{-1}(Q)) \leq s \cdot \operatorname{dist}(P, Q)$$

(PE5) Let $G(\varepsilon, \varepsilon_0) = \sup_P G(\varepsilon, \varepsilon_0; P)$, where

$$G(\varepsilon, \varepsilon_0; P) = \sum_i \frac{m_2(\Phi_i^{-1}(\mathcal{B}(\partial\Phi(\mathcal{U}_i), \varepsilon)) \cap \mathcal{B}(P, (1-s)\varepsilon_0))}{m_2(\mathcal{B}(P, (1-s)\varepsilon_0))}$$

and assume that η defined by

$$\eta(\varepsilon_0) = s^\alpha + 2 \sup_{\varepsilon \leq \varepsilon_0} \frac{G(\varepsilon, \varepsilon_0)}{\varepsilon^\alpha} \varepsilon_0^\alpha$$

satisfies $\sup_{\delta \leq \varepsilon_0} \eta(\delta) < 1$.

We introduce now the *multiplicity entropy* of a partition, as defined by Buzzi, and the *dilatation coefficient*.

Definition 2.3.9 (Multiplicity entropy)**.** The *multiplicity entropy* of a piecewise linear map $\Phi\colon \mathcal{K} \to \mathcal{K}$ is

$$h_{\mathrm{mult}}(\mathtt{P}, \Phi) = \lim_{n\to\infty} \tfrac{1}{n} \log \sup_{P \in \mathcal{K}} \operatorname{card}\{\mathcal{P} \in \mathtt{P}^{(n)} : P \in \overline{\mathcal{P}}\}$$

where $\mathtt{P} = \{\mathcal{U}_i\}$ and $\mathtt{P}^{(n)}$ is the nth iterate of $\mathtt{P}$.

Definition 2.3.10 (Dilatation coefficient)**.** The *dilatation coefficient* of a piecewise linear map $\Phi\colon \mathcal{K} \to \mathcal{K}$ is

$$\delta(\Phi) = \lim_{n\to\infty} \tfrac{1}{n} \log \sup_{P \in \Phi^n(\mathcal{K})} \|\mathrm{D}\Phi^{-n}(P)\|$$

where the norm of the derivative is taken along each smooth branch of Φ^{-n}.

In terms of both quantities, we may show that some iterate of a piecewise expanding map verifies condition (PE5) even though the map itself does not.

Proposition 2.3.11 ([64, Lem. 2.2])**.** *Let Φ be a piecewise invertible C^1 map with a partition $\mathtt{P}$ into smooth components such that (PE1)–(PE3) hold for some $0 < \alpha \leq 1$. Suppose that the boundary of the partition is included in a finite number of C^1 compact embedded submanifolds. If $h_{\mathrm{mult}}(\mathtt{P}, \Phi) + \delta(\Phi) < 0$, then some iterate of Φ satisfies (PE1)–(PE5).*

2.3.3 Tsujii's Scenario

Tsujii [68] proves the existence of absolutely continuous invariant measures for expanding piecewise linear maps defined on bounded polyhedra in arbitrary dimensions. We will put ourselves in the two-dimensional setting with the following definitions.

Definition 2.3.12 (Polyhedra)**.** A *half-plane* in $\mathbb{R}^2$ is each one of the two connected components of the complement of a straight line in $\mathbb{R}^2$. A *polyhedron* in $\mathbb{R}^2$ is a closed subset of $\mathbb{R}^2$ that is obtained from closures of half-planes by taking intersections and unions for finite times.

Definition 2.3.13 (Piecewise linear maps on a polyhedron)**.** Let $\mathbb{P}$ be a polyhedron in $\mathbb{R}^2$ with nonempty interior. A *piecewise linear map* on $\mathbb{P}$ is a pair $(\Phi, \overline{\mathtt{P}})$ of a map $\Phi\colon \mathbb{P} \to \mathbb{P}$ and a finite family $\overline{\mathtt{P}} = \{\mathbb{P}^k\}_{k=1}^{\ell}$ of polyhedra satisfying the following conditions:

(i) The interior sets of $\mathbb{P}^1, \dots, \mathbb{P}^\ell$ are mutually disjoint

(ii) $\mathbb{P} = \mathbb{P}^1 \cup \cdots \cup \mathbb{P}^\ell$

(iii) The restriction of Φ to the interior of $\mathbb{P}^k$ is an affine map for each k

Definition 2.3.14 (Expanding piecewise linear maps on a polyhedron)**.** A piecewise linear map $(\Phi, \overline{\mathtt{P}})$ on a polyhedron $\mathbb{P}$ in $\mathbb{R}^2$ is *expanding* if there exists $\rho > 1$ such that

$$\|\mathrm{D}\Phi(P) \cdot v\| \geq \rho \|v\|$$

for all $P \in \operatorname{int} \mathbb{P}^1 \cup \cdots \cup \operatorname{int} \mathbb{P}^\ell$ and all $v \in \mathrm{T}_P\mathbb{R}^2$.

2.3.4 Preliminaries: Buzzi, Saussol, and Tsujii's Works, and Some Lemmas

Fix $0 < \theta < \pi$. By Theorem 2 there exists an a-value a_θ such that the polygon $\mathcal{K}_{a,\theta}$ is (strictly) $\Gamma_{a,\theta}$-invariant for every $a \in (1, a_\theta]$. Let

$$\mathcal{K}_0 = \{(x,y) \in \mathcal{K}_{a,\theta} : x \leq 1\}, \quad \mathcal{K}_1 = \{(x,y) \in \mathcal{K}_{a,\theta} : x \geq 1\} \tag{2.12}$$

Taking $\mathbb{P} = \mathcal{K}_{a,\theta}$ and the family $\overline{\mathtt{P}} = \{\mathbb{P}^0, \mathbb{P}^1\}$ with $\mathbb{P}^0 = \mathcal{K}_0$ and $\mathbb{P}^1 = \mathcal{K}_1$, the map $\Gamma_{a,\theta}\colon \mathbb{P} \to \mathbb{P}$ is an expanding piecewise linear map on a polyhedron. Indeed, polygons are a particular case of polyhedra in $\mathbb{R}^2$. By definition, it is clear that $\operatorname{int} \mathbb{P}^0 \cap \operatorname{int} \mathbb{P}^1 = \varnothing$ and $\mathbb{P} = \mathbb{P}^0 \cup \mathbb{P}^1$. The restriction of $\Gamma_{a,\theta}$ to the interior of $\mathbb{P}^0$ and $\mathbb{P}^1$ are affine maps since

$$\Gamma_{a,\theta}(x,y) = \mathbf{A}_{a,\theta}(x,y)$$

for all $(x,y) \in \operatorname{int} \mathbb{P}^0$, and

$$\Gamma_{a,\theta}(x,y) = \mathbf{A}_{a,\theta}(-x,y) + (2a\cos\theta, 2a\sin\theta)$$

for all $(x,y) \in \operatorname{int} \mathbb{P}^1$. Finally, it holds that $\rho = a > 1$. Tsujii [68, Th. 3] provides the absolutely continuous invariant probability measures for $\Gamma_{a,\theta}$ whose supports will be 2-D strange attractors.

Proposition 2.3.15. *Let $0 < \theta < \pi$. For every $a \in (1, a_\theta]$, there exist finitely many absolutely continuous ergodic probability measures $\mu_1, \dots, \mu_{\mathtt{tsu}}$ for $\Gamma_{a,\theta}$. Moreover,*

$$\mathtt{basin}(\mu_i) = \left\{ P \in \mathcal{K}_{a,\theta} : \frac{1}{n} \sum_{j=0}^{n-1} \delta_{\Gamma_{a,\theta}^j(P)} \to \mu_i \text{ weakly} \right\}$$

is an open set modulo sets with null Lebesgue measure for $i = 1, \dots, \mathtt{tsu}$, and $\bigcup_{i=1}^{\mathtt{tsu}} \mathtt{basin}(\mu_i)$ has full Lebesgue measure in $\mathcal{K}_{a,\theta}$.

Remark 2.3.16. We may assume that the basin of each probability measure from Proposition 2.3.15 is a nonempty open set modulo sets with null Lebesgue measure.

Remark 2.3.17. By Proposition 2.3.15 it is clear that $\bigcup_{i=1}^{\mathtt{tsu}} \operatorname{int} \mathtt{basin}(\mu_i)$ has full Lebesgue measure in $\mathcal{K}_{a,\theta}$.

In order to prove that the supports of $\mu_1, \dots, \mu_{\mathtt{tsu}}$ are 2-D strange attractors, we will now place $\Gamma_{a,\theta}$ in Buzzi's and Saussol's settings.

Let $\mathcal{Y} = \mathcal{P}_0 \cup \mathcal{P}_1$ and $\mathtt{P} = \{\mathcal{P}_0, \mathcal{P}_1\}$ with $\mathcal{P}_0 = \operatorname{int} \mathcal{K}_0$ and $\mathcal{P}_1 = \operatorname{int} \mathcal{K}_1$. Note that $\overline{\mathcal{Y}} = \mathcal{K}_{a,\theta}$. Then, the map $\Gamma_{a,\theta} \colon \mathcal{Y} \to \overline{\mathcal{Y}}$ is an expanding piecewise analytic map of the plane in Buzzi's sense (see Definition 2.3.2). Indeed: the interior of polygonal domains are a particular case of analytic pieces of $\mathbb{R}^2$. By definition, it is clear that $\mathcal{P}_0 \cap \mathcal{P}_1 = \varnothing$. The restriction of $\Gamma_{a,\theta}$ to the interior of $\mathcal{P}^0$ and $\mathcal{P}^1$ are invertible affine maps since

$$\Gamma_{a,\theta}(x, y) = \mathbf{A}_{a,\theta}(x, y)$$

for all $(x, y) \in \operatorname{int} \mathcal{P}^0$, and

$$\Gamma_{a,\theta}(x, y) = \mathbf{A}_{a,\theta}(-x, y) + (2a \cos\theta, 2a \sin\theta)$$

for all $(x, y) \in \operatorname{int} \mathcal{P}^1$. Consequently, both restrictions can be extended to $\mathbb{R}^2$ as analytic diffeomorphisms. Moreover, the map $\Gamma_{a,\theta}$ is expanding as

$$\inf_{P \in \mathcal{Y}} \min_{v \in \mathbb{S}^1} \|\mathrm{D}\Gamma_{a,\theta}(P) \cdot v\| = a > 1$$

Therefore, according to Buzzi [10, Main Theorem], we have the following result.

Proposition 2.3.18. *For every $i \in \{1, \dots, \mathtt{tsu}\}$, there exist a constant $\kappa \in (0, 1)$, a natural number $\mathtt{b}$, and a decomposition*

$$\mathcal{A}^i = \mathcal{X}_0 \cup \mathcal{X}_1 \cup \cdots \cup \mathcal{X}_{\mathtt{b}-1}$$

of the support $\mathcal{A}^i$ of μ_i with $\Gamma_{a,\theta}(\mathcal{X}_j) = \mathcal{X}_{j+1 \bmod \mathtt{b}}$ for $j = 0, \dots, \mathtt{b} - 1$ such that, for all Lipschitz functions $h, g \colon \mathcal{A}^i \to \mathbb{R}$ and for all $n \geq 0$,

$$\left| \int_{\mathcal{X}_0} h \cdot g \circ \Gamma_{a,\theta}^{\mathtt{b}n} \, \mathrm{d}\mu - \int_{\mathcal{X}_0} h \, \mathrm{d}\mu \int_{\mathcal{X}_0} g \, \mathrm{d}\mu \right| \leq C\kappa^n$$

for some $C = C(h, g) < \infty$ independent of n.

Remark 2.3.19. It is well-known that Proposition 2.3.18 implies that every μ_i is mixing (up to the eventual period $\mathtt{b}$) and consequently the iterate $\Gamma_{a,\theta}^{\mathtt{b}}$ is topologically mixing on any $\mathcal{X}_j$.

Now, and here is where the differences between the proof of Theorem 3 and Theorem 1.2 [59] arise, the crucial argument is to control the weighted multiplicity of $\Gamma_{a,\theta}$ (see Definition 2.3.5).

For $\Gamma_{a,\theta}$, the partition $\mathtt{P}$ defines at each point $P \in \mathcal{K}_{a,\theta}$ a collection $\mathcal{S}_P(\mathtt{P})$ of at most two circular sectors: $\mathcal{B}(P, r) \cap \operatorname{int} \mathcal{K}_0$ and $\mathcal{B}(P, r) \cap \operatorname{int} \mathcal{K}_1$ for $r > 0$ small enough. (Here we also consider as a possible circular sector the whole ball $\mathcal{B}(P, r)$.) We have $\Lambda_+(\Gamma_{a,\theta} \mid \overrightarrow{\mathcal{S}}_P) = a$ and $\mathtt{jac}(\Gamma_{a,\theta})_{\mathcal{A}}(P) = a^2$. Therefore,

$$\mathtt{mult}(\mathtt{P}, \Gamma_{a,\theta}) = \frac{2}{a} \tag{2.13}$$

because the supremum is achieved at points in the critical set. Now, for each $n \in \mathbb{N}$, we have that $\Lambda_+(\Gamma_{a,\theta}^{\mathcal{P}} \mid \overrightarrow{\mathcal{S}}_P) = a^n$ and $\mathtt{jac}(\Gamma_{a,\theta}^{\mathcal{P}})(P) = a^{2n}$ for every $P \in \mathcal{K}_{a,\theta}$ and $\mathcal{P} \in \mathtt{P}^{(n)}$. Therefore, for every $n \in \mathbb{N}$, we obtain that

$$\mathtt{mult}(\mathtt{P}^{(n)}, \Gamma_{a,\theta}^n) = \frac{R_{n,a,\theta}}{a^n} \tag{2.14}$$

where we have introduced the sequence

$$R_{n,a,\theta} = \max_{P \in \mathcal{K}_{a,\theta}} \operatorname{card}\{\mathcal{P} \in \mathtt{P}^{(n)} : P \in \mathcal{P}\} \tag{2.15}$$

Observe that $R_{1,a,\theta} = 2$ and therefore equation (2.13) follows from equation (2.14). Following the Geometric Estimate, we may conclude that

$$\limsup_{n\to\infty} \tfrac{1}{n} \log R_{n,a,\theta} < \log a \tag{2.16}$$

Remark 2.3.20. If θ/π is a rational number, then $R_{n,a,\theta}$ remains bounded as n goes to infinity. This is because the slopes of the straight lines forming part of the boundary of any set in $\mathtt{P}^{(n)}$ belong to a finite set of real numbers. Therefore, inequality (2.16) easily follows without using the Geometric Estimate.

Now, we will check that some iterate of the map $\Gamma_{a,\theta}$ is an piecewise expanding map in Saussol's sense and obtain some results. Let $\mathcal{K} = \mathcal{K}_{a,\theta}$. It is clear that $\overline{\operatorname{int} \mathcal{K}} = \mathcal{K}$. Let $\mathtt{P} = \{\mathcal{U}_0, \mathcal{U}_1\}$ with $\mathcal{U}_0 = \operatorname{int} \mathcal{K}_0$ and $\mathcal{U}_1 = \operatorname{int} \mathcal{K}_1$, and let $\mathcal{V}_0$ and $\mathcal{V}_1$ be small open neighborhoods of $\mathcal{K}_0$ and $\mathcal{K}_1$, respectively. It is clear that $\mathcal{U}_0 \cap \mathcal{U}_1 = \varnothing$ and $\mathcal{V}_0 \supseteq \overline{\mathcal{U}}_0$ and $\mathcal{V}_1 \supseteq \overline{\mathcal{U}}_1$. Consider the maps

$$\Phi_0 \colon \mathcal{V}_0 \to \mathbb{R}^2, \quad \Phi_0(x,y) = \mathbf{A}_{a,\theta}(x,y)$$

and

$$\Phi_1 \colon \mathcal{V}_1 \to \mathbb{R}^2, \quad \Phi_1(x,y) = \mathbf{A}_{a,\theta}(-x,y) + (2a\cos\theta, 2a\sin\theta)$$

The existence of a sufficiently small $\varepsilon_0 > 0$ satisfying hypothesis (PE1) is evident. Hypothesis (PE2) is verified for any $c > 0$ and $0 < \alpha \leq 1$ because $\Phi_{0,1}$ are affine maps and $\mathbf{A}_{a,\theta}$ is invertible. Finally, hypothesis (PE3) obviously holds as $\mathcal{K} \setminus (\mathcal{U}_0 \cup \mathcal{U}_1)$ consists of a finite union of segments, namely the boundary of $\mathcal{K}_{a,\theta}$ and $\mathcal{K}_{a,\theta} \cap \mathcal{C}$. Therefore, the map $\Gamma_{a,\theta} \colon \mathcal{K} \to \mathcal{K}$ verifies conditions (PE1)–(PE3).

Let us now consider the dilatation coefficient of $\Gamma_{a,\theta}$ with $\mathcal{Y} = \mathcal{U}_0 \cup \mathcal{U}_1$. It is easy to check that $\delta(\Gamma_{a,\theta}) = -\log a$. Therefore, inequality (2.16) translates into

$$\lim_{n\to\infty} \tfrac{1}{n} \log R_{n,a,\theta} + \delta(\Gamma_{a,\theta}) < 0$$

This inequality allows us to apply Proposition 2.3.11 to assert that some iterate of the map $\Gamma_{a,\theta}$ satisfies conditions (PE1)–(PE5). Saussol [64, Prop. 3.4, Th. 5.1(ii), Prop. 5.1] provides then the following result.

Proposition 2.3.21. *For every $i \in \{1, \ldots, \mathtt{tsu}\}$, the interior of $\mathcal{A}^i$ has μ_i-measure 1. Moreover, the measure μ_i is finite.*

We finish this subsection presenting some lemmas that we will use in the proof of Theorem 3. Lemma 2.3.22 is crucial to prove that the supports $\mathcal{A}^i$ are attractors. Lemmas 2.3.23 and 2.3.24 will be used to prove that there exists a dense orbit in $\mathcal{K}_{a,\theta}$ exhibiting two positive Lyapunov exponents. Finally, Lemma 2.3.25 is auxiliary in the proof of statement (v).

Lemma 2.3.22 ([59, Lem. 6.1(i)])**.** *For every $i \in \{1, \ldots, \mathtt{tsu}\}$, the interior of $\mathcal{A}^i$ traps every point in $\mathtt{basin}(\mu_i)$, i.e. for every $P \in \mathtt{basin}(\mu_i)$ there exists $j \in \mathbb{N}$ such that $\Gamma^j_{a,\theta}(P) \in \operatorname{int} \mathcal{A}^i$.*

Proof. Let $P \in \mathtt{basin}(\mu_i)$. By definition, we have that $\nu_n \to \mu_i$ weakly, where $\nu_n = \frac{1}{n}\sum_{j=0}^{n-1} \delta_{\Gamma^j_{a,\theta}(P)}$ for each $n \in \mathbb{N}$. In order to apply Portmanteu's Theorem to the sequence $\{\nu_n\}_n$ and μ_i, we must check that μ_i is finite and the interior of $\mathcal{A}^i$ is a set of

continuity of μ_i, i.e. $\mu_i(\partial\mathcal{A}^i) = 0$. Indeed, from Proposition 2.3.21 we know that μ_i is finite and $\mu_i(\operatorname{int}\mathcal{A}^i) = 1$. Thus, by Portmanteau's Theorem,

$$\nu_n(\operatorname{int}\mathcal{A}^i) = \frac{1}{n}\sum_{j=0}^{n-1}\chi_{\operatorname{int}\mathcal{A}^i}(\Gamma_{a,\theta}^j(P))$$

converges to 1 as $n \to \infty$, from where it clearly follows that there exists $j \in \mathbb{N}$ such that $\Gamma_{a,\theta}^j(P) \in \operatorname{int}\mathcal{A}^i$. □

Lemma 2.3.23 ([60, Lem. 4, adapted]). *For every $i \in \{1,\dots,\mathtt{tsu}\}$, there exists $\mathcal{B} \subseteq \mathcal{K}_{a,\theta}$ such that $\mu_i(\mathcal{B}) = 1$ for which every point $P \in \mathcal{B}$ has a dense orbit in $\mathcal{K}_{a,\theta}$.*

Proof. First, we observe that if $\mathcal{U} \subseteq \mathcal{K}_{a,\theta}$ is open a nonempty, then $\mu_i(\bigcup_{n=0}^{\infty}\Gamma_{a,\theta}^{-n}(\mathcal{U})) > 0$. Let $\{\mathcal{U}^n\}$ be a countable open basis of open sets. For each $n \geq 0$, let $\mathcal{B}^n = \bigcap_{j=0}^{\infty}\mathcal{B}^{j,n}$, where $\mathcal{B}^{j,n} = \bigcup_{k=j}^{\infty}\Gamma_{a,\theta}^{-k}(\mathcal{U}^n)$. Then:

(i) $\mathcal{B}^{j,n} = \Gamma_{a,\theta}^{-1}(\mathcal{B}^{j-1,n}) \subseteq \mathcal{B}^{j-1,n}$ for all j

(ii) $\mu_i(\mathcal{B}^n) = \mu_i(\mathcal{B}^{j,n}) > 0$ for all $j, n \geq 0$ because the measure is invariant

(iii) $\mu_i(\mathcal{B}^n) = 1$ for all $n \geq 0$ because $\mathcal{B}^n$ is invariant and μ_i is ergodic

(iv) $\mathcal{B}^n$ is residual because $\mathcal{B}^{j,n}$ is open a dense for all $j, n \geq 0$ as $\Gamma_{a,\theta}$ is transitive

Now, if we define $\mathcal{B} = \bigcap_{n=0}^{\infty}\mathcal{B}^n$, then obviously $\mathcal{B}$ is residual. Moreover, the ω-limit set of every $P \in \mathcal{B}$ coincides with $\mathcal{K}_{a,\theta}$. Indeed, it is enough to prove that, for all $n \geq 0$, there are infinitely many values $m > 0$ for which $\Gamma_{a,\theta}^m(P) \in \mathcal{U}^n$. But, if $P \in \mathcal{S}$, then $P \in \mathcal{B}^n$, that is

$$P \in \bigcap_{j=0}^{\infty}\bigcup_{k=j}^{\infty}\Gamma_{a,\theta}^{-k}(\mathcal{U}^n)$$

which means that $P \in \Gamma_{a,\theta}^{-k}(\mathcal{U}^n)$ for infinitely many values k, and for these values $\Gamma_{a,\theta}^k(P) \in \mathcal{U}^n$. □

Lemma 2.3.24 ([59, Lem. 6.2, adapted]). *If an orbit $\{\Gamma_{a,\theta}^n(P) : n \geq 0\}$ does not visit the critical line, then*

$$\lim_{n\to\infty}\tfrac{1}{n}\log\|\mathrm{D}\Gamma_{a,\theta}^n(P)\cdot v\| = \log a > 0$$

for all $v \in \mathbb{S}^1$.

Lemma 2.3.25 ([59, Lem. 6.3, adapted]). *Let $\mathcal{U} \subseteq \mathcal{K}_{a,\theta}$ be a nonempty open set. Then, the interior of $\Gamma_{a,\theta}(\mathcal{U})$ is nonempty.*

2.3.5 Proof of Theorem 3

Fix $0 < \theta < \pi$, and then fix $a \in (1, a_\theta]$. By Proposition 2.3.15 there exists a finite number of absolutely continuous invariant ergodic probability measures $\mu_1,\dots,\mu_{\mathtt{tsu}}$ for $\Gamma_{a,\theta}$. For each $i = 1,\dots,\mathtt{tsu}$, let $\mathcal{A}^i$ be the support of μ_i. The family

$$\mathtt{A}_{a,\theta} = \{\mathcal{A}^i : i = 1,\dots,\mathtt{tsu}\} \tag{2.17}$$

is the one announced in Theorem 3. We will first prove that each $\mathcal{A}^i$ is a 2-D strange attractor with nonempty interior and then each one of the statements.

Let $i = 1,\dots,\mathtt{tsu}$. By definition, the support $\mathcal{A}^i$ of μ_i is compact. Moreover, since μ_i is $\Gamma_{a,\theta}$-invariant, then $\mathcal{A}^i$ is (forward) invariant for $\Gamma_{a,\theta}$. In order to show that $\Gamma_{a,\theta}$ is

transitive on $\mathcal{A}^i$, take two nonempty open subsets $\mathcal{U}$ and $\mathcal{V}$ in $\mathcal{A}^i$. It is clear by definition that $\mu_i(\mathcal{U}) > 0$ and $\mu_i(\mathcal{V}) > 0$. Thus, since μ_i is ergodic, Birkhoff's Theorem implies the existence of some point $P \in \mathcal{U}$ such that

$$\lim_{n\to\infty} \frac{1}{n} \sum_{j=0}^{n-1} \chi_{\mathcal{V}}(\Gamma_{a,\theta}^j(P)) = \mu_i(\mathcal{V}) > 0$$

Therefore, it is clear that $\Gamma_{a,\theta}^j(P) \in \mathcal{V}$ for some $j \in \mathbb{N}$ and consequently $\Gamma_{a,\theta}^j(\mathcal{U}) \cap \mathcal{V} = \varnothing$. On the other hand, Lemma 2.3.22 implies that $\texttt{basin}(\mu_i) \subseteq W^s(\mathcal{A}^i)$, and therefore $W^s(\mathcal{A}^i)$ has nonempty interior by Remark 2.3.16. Now, it remains to prove the existence of a dense orbit in $\mathcal{A}^i$ exhibiting two positive Lyapunov exponents. To this end, we begin by showing the existence of a dense orbit not visiting the critical segment $\mathcal{C} \cap \mathcal{K}_{a,\theta}$ of $\Gamma_{a,\theta}$. Let

$$\mathcal{C}_{a,\theta} = \{P \in \mathcal{K}_{a,\theta} : \Gamma_{a,\theta}^n(P) \in \mathcal{C} \text{ for some } n \in \mathbb{N}\}$$

Since the Lebesgue measure of $\mathcal{C}_{a,\theta}$ is zero and μ_i is absolutely continuous, it follows that $\mu_i(\mathcal{C}_{a,\theta}) = 0$. By Lemmas 2.3.23 and 2.3.24, there exists a dense orbit exhibiting two Lyapunov exponents, and therefore the attractor $\mathcal{A}^i$ is strange.

We will first prove statement (v) of Theorem 3. Let $\mathcal{K}$ be a compact $\Gamma_{a,\theta}$-invariant set with nonempty interior. By Remark 2.3.17 there exists a measure μ_i such that $\operatorname{int}\mathcal{K} \cap \operatorname{int}\texttt{basin}(\mu_i) \neq \varnothing$. Therefore, the set $\operatorname{int}\mathcal{K} \cap \texttt{basin}(\mu_i)$ must contain an nonempty open set $\mathcal{U}$. Let $P \in \mathcal{U}$. Since $\mathcal{U} \subseteq \texttt{basin}(\mu_i)$, by Lemma 2.3.22 there exists a natural number j such that $\Gamma_{a,\theta}^j(P) \in \operatorname{int}\mathcal{A}^i$. Let $\mathcal{V}$ be a neighborhood of $\Gamma_{a,\theta}^j$ in $\mathcal{A}^i$. Since $\Gamma_{a,\theta}^j$ is continuous, there exists an open neighborhood $\mathcal{V}_P$ of P such that $\Gamma_{a,\theta}^j(\mathcal{V}_P) \subseteq \mathcal{A}^i$. On the other hand, since $\mathcal{K}$ is invariant, we deduce that $\Gamma_{a,\theta}^j(\mathcal{V}_P) \subseteq \mathcal{K}$. By Lemma 2.3.25 there exists an open set $\mathcal{U}'$ contained in $\mathcal{K} \cap \mathcal{A}^i$. We claim that $\mathcal{A}^i \subseteq \mathcal{K}$. Indeed, assume for a contradiction that there exists $Q \in \mathcal{A}^i$ such that $Q \notin \mathcal{K}$. Since $\mathcal{K}$ is compact, there exists some open neighborhood $\mathcal{V}_Q$ of Q such that $\mathcal{V}_Q \cap \mathcal{K} = \varnothing$. From the fact that $\Gamma_{a,\theta}$ is transitive on $\mathcal{A}^i$, by Lemma 2.3.22 there must exist some natural number k such that $\Gamma_{a,\theta}^k(\mathcal{U}') \cap \mathcal{V}_Q \neq \varnothing$. This contradicts the invariance of $\mathcal{K}$, and therefore $\mathcal{A}^i \subseteq \mathcal{K}$. Now, take two compact $\Gamma_{a,\theta}$-invariant set $\mathcal{K}$ and $\mathcal{K}'$ with disjoint nonempty interiors. Following the previous arguments, it holds that there exist two 2-D strange attractors $\mathcal{A}^i$ and $\mathcal{A}_j$ with $\mathcal{A}^i \subseteq \mathcal{K}$ and $\mathcal{A}_j \subseteq \mathcal{K}'$. These attractors must be different because they have nonempty interior.

To prove statement (i), we observe that if $\mathcal{A}$ is an attractor for $\Gamma_{a,\theta}$, then from Remark 2.3.17 there exists $i \in \{1, \ldots, \texttt{tsu}\}$ such that $W^s(\mathcal{A}) \cap \texttt{basin}(\mu_i)$ has nonempty interior. From Lemma 2.3.22 it is evident that $\mathcal{A} = \mathcal{A}^i$.

Statement (ii) is obvious from the definition (2.17) of $\mathtt{A}_{a,\theta}$ and Proposition 2.3.15.

Statement (iii) is a direct consequence of the definition (2.17) of $\mathtt{A}_{a,\theta}$, Proposition 2.3.18 and Remark 2.3.19.

To prove statement (iv), let $i \in \{1, \ldots, \texttt{tsu}\}$. By Lemma 2.3.22, for each $P \in \texttt{basin}(\mu_i)$ there exists $j \in \mathbb{N}$ such that $\Gamma_{a,\theta}^j(P) \in \operatorname{int}\mathcal{A}^i$. Therefore, the basin of μ_i is contained in the stable set of $\mathcal{A}^i$. By Proposition 2.3.15, the difference $W^s(\mathcal{A}^i) \setminus \texttt{basin}(\mu_i)$ has null Lebesgue measure. Hence $\bigcup_{i=1}^{\texttt{tsu}} W^s(\mathcal{A}^i)$ covers a full Lebesgue measure set of $\mathcal{K}_{a,\theta}$.

2.4 Splitting of Attractors: Proof of Theorem 4

Recall that $\Gamma_{a,\theta}$ is the composition of the fold along the critical line $\mathcal{C} \equiv x = 1$ onto the origin $\mathcal{O}$ and the expanding linear map defined by matrix (2.1).

Let us assume that $\theta = 2\pi p/q \in (0, \pi)$ with $p, q \in \mathbb{N}$ and $\gcd(p, q) = 1$. It is clear that $q \geq 3$ and $2p < q$. Let $\theta_1 = 2\pi/q \in (0, 2\pi/3]$. Note that $\theta_1 = \theta$ if and only if $p = 1$.

For each $j \in \{0, 1, \ldots, q-1\}$, we will denote by Σ^j the ray that starts from $\mathcal{O}$ and extends indefinitely in the direction of the unit vector $(\cos j\theta_1, \sin j\theta_1)$. Thus, the plane is divided into q regions

$$\mathbb{R}^2 = \mathcal{R}^0 \cup \cdots \cup \mathcal{R}^{q-1}$$

where $\mathcal{R}^j$ is the region limited by Σ^j and Σ^{j+1} for $j = 0, 1, \ldots, q-1$, setting $\Sigma^q = \Sigma^0$. See Figure 2.13. The dynamics of $\Gamma_{a,\theta}$ on these regions depends on p and the following inclusion holds:

$$\Gamma_{a,\theta}(\mathcal{R}^j \cap \{x \leq 1\}) \subseteq \mathcal{R}^{j+p \bmod q} \qquad (j = 0, \ldots, q-1)$$

As a consequence, given a point $Q \in \mathcal{R}^j \cap \{x \leq 1\}$ for some $j \in \{0, 1, \ldots, q-1\}$, if $\Gamma^n_{a,\theta}(Q) \in \{x \leq 1\}$ for $n = 1, 2, \ldots, q-1$, then $\Gamma^q_{a,\theta}(Q) \in \mathcal{R}^j$. In order to define $\mathcal{D}$, first we will construct the set of points $Q \in \mathcal{R}^0 \cap \{x \leq 1\}$ such that $\Gamma^n_{a,\theta}(Q) \in \{x \leq 1\}$ for $n = 1, 2, \ldots, q-1$.

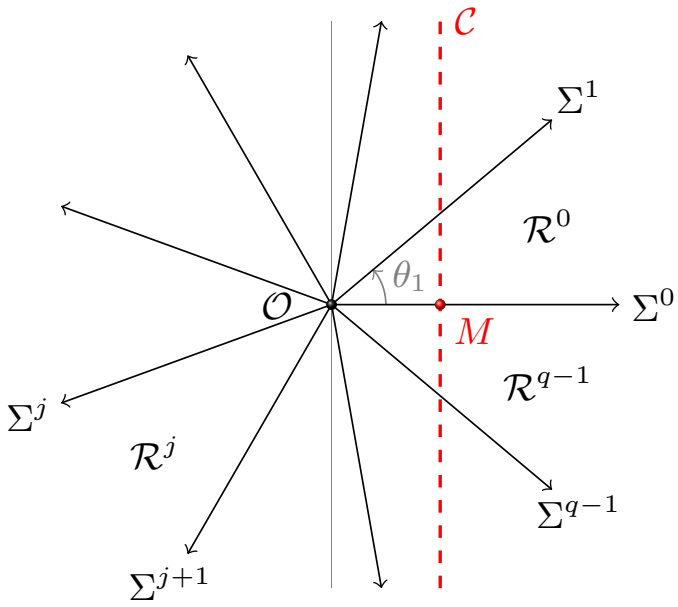

Figure 2.13: The regions $\mathcal{R}^j$ for $\theta = 2\pi p/q \in (0, \pi)$ with $p, q \in \mathbb{N}$ and $\gcd(p, q) = 1$

Let us now fix some notation for what follows. Given a point Q or a set $\mathcal{Q}$, for each $n \geq 0$ we will write $Q_n = \Gamma^n_{a,\theta}(Q)$ and $\mathcal{Q}_n = \Gamma^n_{a,\theta}(\mathcal{Q})$. We will denote by $\Omega(Q^1, Q^2, \ldots, Q^n)$ the polygon with consecutive vertices $Q^1, Q^2, \ldots, Q^n$. Also, the segment joining any pair of points Q, Q' is denoted by $\overline{QQ'}$.

We will divide the proof of Theorem 4 into three cases. First we will prove the result for $q \geq 5$ in order that $\cos\theta_1 > 0$ as in Figure 2.13. In this situation, the arguments of the proof hold regardless of the value of q. Then, we will consider the case $q = 4$, in which $\cos\theta_1 = 0$. Actually, this case was already studied previously and was collected separately in Lemma 2.1.11 because of its interest for the successive renormalizations given in Corollary 2. Finally, we will consider the special case $q = 3$ to which only statement (a) applies.

2.4.1 Case $q \geq 5$

Fix $q \geq 5$. In this case, the ray Σ^1 is contained in the first quadrant. We will construct a strictly $\Gamma^q_{a,\theta}$-invariant polygon from the iterates of $M = (1, 0)$.

Lemma 2.4.1. *There exists $a_M > 1$ such that $M_n \in \{x \leq 1\}$ for $n = 1, \ldots, q-1$ and every $a \in (1, a_M]$.*

Proof. Assuming that $\{M_1, \ldots, M_{n-1}\} \subseteq \{x \leq 1\}$ for any $2 \leq n < q$, then

$$M_n = (a^n \cos n\theta, a^n \sin n\theta)$$

Therefore, it suffices to find an a-value a_M such that

$$a^n \cos n\theta \leq 1 \tag{2.18}$$

for $n = 1, \ldots, q-1$ and every $a \in (1, a_M]$. If $\cos n\theta \leq 0$, then inequality (2.18) clearly holds for all $a > 1$. Otherwise, we have that $\cos n\theta < 1$ because $\gcd(p, q) = 1$. Let

$$a_M = \min_{\cos n\theta > 0} \sqrt[n]{\sec n\theta} \tag{2.19}$$

Then, we have that $a_M > 1$ and $a_M^n \cos n\theta \leq 1$, and therefore inequality (2.18) holds for every $a \in (1, a_M]$. □

We will only consider a-values in $(1, a_M]$. Denote by n_1 the smallest natural number such that $M_{n_1} \in \Sigma^1$. Note that $n_1 p \equiv 1 \mod q$. In particular, if $p = 1$, then $n_1 = 1$. It is straightforward to check that

$$\cos n_1\theta = \cos\theta_1, \quad \sin n_1\theta = \sin\theta_1 \tag{2.20}$$

and

$$\cos(q - n_1)\theta = \cos\theta_1, \quad \sin(q - n_1)\theta = -\sin\theta_1 \tag{2.21}$$

The point M_{n_1} belongs to the line $\mathcal{L}_{n_1}$, whose equation can be written by equalities (2.20) as

$$\mathcal{L}_{n_1} \equiv x \cos\theta_1 + y \sin\theta_1 = a^{n_1} \tag{2.22}$$

Since $q \geq 5$, then $\mathcal{L}_{n_1}$ intersects Σ^0 at the point

$$K = (a^{n_1} \sec\theta_1, 0) \tag{2.23}$$

In $\mathcal{R}^0$ we define the polygon

$$\Delta' = \Omega(\mathcal{O}, K, M_{n_1})$$

On the other hand, since $q\theta = 2\pi p$, then $\mathcal{L}_q \equiv x = a^q$ and $\mathcal{L}_q$ intersects Σ^0 at $M_q = (a^q, 0) \in \{x > 1\}$. Moreover, from equalities (2.21) we deduce that

$$a^q \cos\theta_1 \leq a^{n_1}$$

Hence M_q is on the left-hand side of K. Therefore, the line $\mathcal{L}_q$ intersects Δ^* at the segment of extremes M_q and

$$J = (a^q, a^{n_1} \csc\theta_1 - a^q \cot\theta_1) \tag{2.24}$$

We will prove that the polygon

$$\Delta = \Omega(\mathcal{O}, M_q, J, M_{n_1}) \tag{2.25}$$

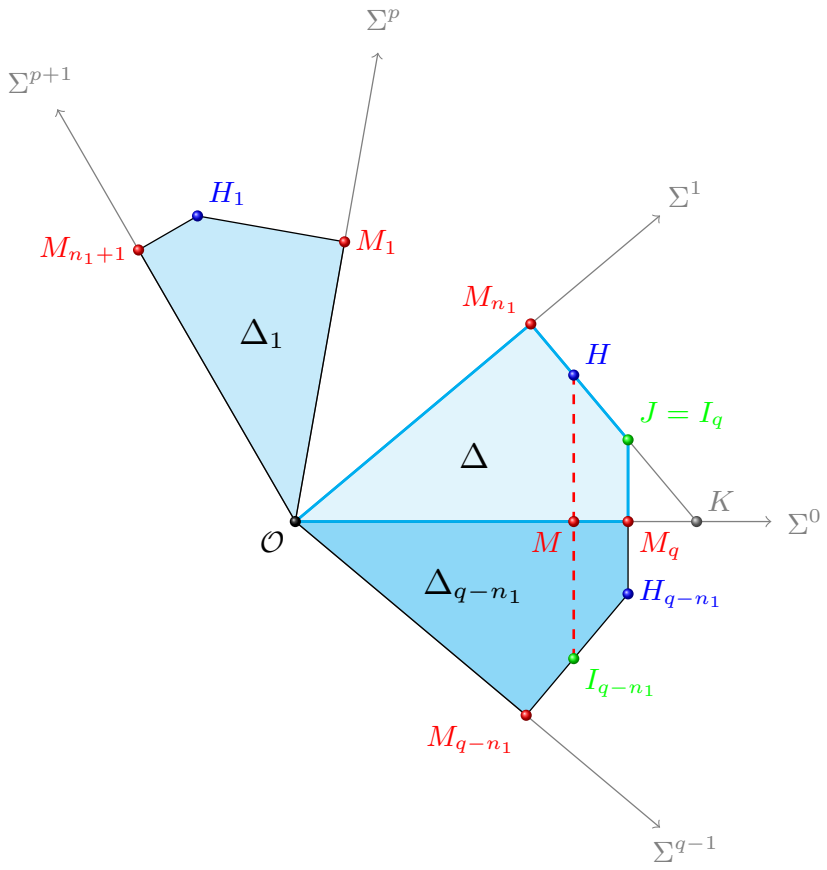

Figure 2.14: The strictly $\Gamma^q_{a,\theta}$-invariant polygon $\Delta = \Omega(\mathcal{O}, M_q, J, M_{n_1})$

is strictly $\Gamma^q_{a,\theta}$-invariant. If $\mathcal{F}_{\mathcal{C},\mathcal{O}}$ is a good fold for Δ, then

$$\mathcal{F}_{\mathcal{C},\mathcal{O}}(\Delta) = \Omega(\mathcal{O}, M, H, M_{n_1})$$

where

$$H = (1, a^{n_1} \csc\theta_1 - \cot\theta_1) \tag{2.26}$$

is the intersection point of $\mathcal{L}_{n_1}$ and $\mathcal{C}$. See Figure 2.14.

Lemma 2.4.2. *There exists $a_J > 1$ such that $\widetilde{J} \in \Delta$ for every $a \in (1, a_J]$.*

Proof. The symmetric point of J, see equation (2.24), with respect to $\mathcal{C}$ is

$$\widetilde{J} = (2 - a^q, a^{n_1} \csc\theta_1 - a^q \cot\theta_1)$$

In order to prove that $\widetilde{J} \in \Delta$, it is sufficient to show that $\widetilde{H}_{q-n_1}$ belongs to the triangle

$$\mathcal{R}^0 \cap \{x \leq 1\} = \{0 \leq x \leq 1, 0 \leq y \leq x \tan\theta_1\}$$

For all $a \in (1, a_M]$ sufficiently close to 1 it holds that $a^q < 2$. Therefore, it only remains to prove that

$$a^{n_1} \csc\theta_1 - a^q \cot\theta_1 \leq (2 - a^q) \tan\theta_1$$

or, equivalently,

$$a^q \cos^2\theta_1 - a^{n_1} \cos\theta_1 + (2 - a^q) \sin^2\theta_1 \geq 0 \tag{2.27}$$

since $\sin\theta_1$ and $\cos\theta_1$ are positive. For $a = 1$, inequality (2.27) is strictly satisfied:

$$\cos^2\theta_1 - \cos\theta_1 + \sin^2\theta_1 = 1 - \cos\theta_1 > 0$$

By continuity, there exists $a_J > 1$ such that inequality (2.27) holds and consequently $\widetilde{J} \in \Delta$ for every $a \in (1, a_J]$. □

Thus,

$$\Delta_1 = \Omega(\mathcal{O}, M_1, H_1, M_{n_1+1})$$

According to Lemma 2.4.1, since $n_1 + 1 < q$, then the points M_1 and M_{n_1+1}, and therefore H_1, belong to $\{x \leq 1\}$. In fact, this is also true for M_n and M_{n_1+n}, and therefore H_n, whenever $n_1 + n < q$. Therefore,

$$\Delta_n = \Omega(\mathcal{O}, M_n, H_n, M_{n_1+n})$$

is contained in $\{x \leq 1\}$ for $n = 1, \ldots, q - n_1 - 1$ and

$$\Delta_{q-n_1} = \Omega(\mathcal{O}, M_{q-n_1}, H_{q-n_1}, M_q)$$

is contained in $\mathcal{R}^{q-1}$. However, the iterate Δ_{q-n_1} is not contained in $\{x \leq 1\}$ since $M_q \in \{x > 1\}$ for all $a > 1$. Since $H_j \in \{x \leq 1\}$ for $j = 1, \ldots, q - n_1 - 1$, then

$$H_{q-n_1} = (a^q, a^q \cot\theta_1 - a^{q-n_1} \csc\theta_1) \tag{2.28}$$

Therefore, point (2.28) also belongs to the line $x = a^q$. Moreover, from equalities (2.20) and formula (2.19) it follows that $H_{q-n_1} \in \{y < 0\}$. Let I_{q-n_1} be the intersection point of $\mathcal{C}$ and $\overline{H_{q-n_1} M_{q-n_1}}$. See Figure 2.14. Note that this segment is contained in $\mathcal{L}_{q-n_1}$. If $\widetilde{H}_{q-n_1} \in \Delta_{q-n_1}$, then

$$\mathcal{F}_{\mathcal{C},\mathcal{O}}(\Delta_{q-n_1}) = \Omega(\mathcal{O}, M_{q-n_1}, I_{q-n_1}, M)$$

and

$$\Delta_{q-n_1+1} = \Omega(\mathcal{O}, M_{q-n_1+1}, I_{q-n_1+1}, M_1)$$

is contained in $\mathcal{R}^{p-1} \cap \{x \leq 1\}$. In the next lemma we prove that this is the case for all a sufficiently close to 1.

Lemma 2.4.3. *There exists $a_H > 1$ such that $\widetilde{H}_{q-n_1} \in \Delta_{q-n_1}$ for every $a \in (1, a_H]$.*

Proof. The symmetric point of H_{q-n_1}, see equation (2.28), with respect to $\mathcal{C}$ is

$$\widetilde{H}_{q-n_1} = (2 - a^q, a^q \cot\theta_1 - a^{q-n_1} \csc\theta_1)$$

In order to prove that $\widetilde{H}_{q-n_1} \in \Delta_{q-n_1}$, it is sufficient to show that $\widetilde{H}_{q-n_1}$ belongs to the triangle

$$\mathcal{R}^{q-1} \cap \{x \leq 1\} = \{0 \leq x \leq 1, -x\tan\theta_1 \leq y \leq 0\}$$

For all $a \in (1, a_M]$ sufficiently close to 1 it holds that $a^q < 2$. Therefore, it only remains to prove that

$$-(2 - a^q)\tan\theta_1 \leq a^q \cot\theta_1 - a^{q-n_1} \csc\theta_1$$

or, equivalently,

$$a^q \cos^2\theta_1 - a^{q-n_1} \cos\theta_1 + (2 - a^q)\sin^2\theta_1 \geq 0 \tag{2.29}$$

since $q \geq 5$ and both $\sin\theta_1$ and $\cos\theta_1$ are positive. For $a = 1$, inequality (2.29) is strictly satisfied:

$$\cos^2\theta_1 - \cos\theta_1 + \sin^2\theta_1 = 1 - \cos\theta_1 > 0$$

By continuity, there exists $a_H > 1$ such that inequality (2.29) holds and consequently $\widetilde{H}_{q-n_1} \in \Delta_{q-n_1}$ for every $a \in (1, a_H]$. □

Note that a_M, a_J, a_H depend on θ. Denote by a_θ the minimum of a_M, a_J, a_H.

Proposition 2.4.4. *Let $\theta = 2\pi p/q \in (0,\pi)$ with $p, q \in \mathbb{N}$ and $\gcd(p,q) = 1$. Assume that $q \geq 5$, and let $a_\theta = \min\{a_J, a_M, a_H\}$. Then, for every $1 < a \leq a_\theta$, the following hold:*

(i) $\Delta_q = \Delta$, *i.e.* Δ *is strictly* $\Gamma_{a,\theta}^q$*-invariant.*

(ii) $\Delta_n \cap \{x > 1\} = \varnothing$ *for every* $n \in \{1, \dots, q-1\} \setminus \{q - n_1\}$, *where* n_1 *is the smallest natural number such that* $M_{n_1} \in \Sigma^1$.

Proof. Let $a \in (1, a_\theta]$. From the previous discussion we know that the first $q-n_1-1$ iterates of Δ are contained in the half-plane $\{x \leq 1\}$, while $\Delta_{q-n_1} \cap \{x > 1\} \neq \varnothing$. Furthermore, since $a < a_\theta \leq a_H$, it follows from Lemma 2.4.3 that

$$\Delta_{q-n_1+1} = \Omega(\mathcal{O}, M_{q-n_1+1}, I_{q-n_1+1}, M_1)$$

Now, since $a < a_\theta \leq a_M$, then the points M_1 and M_{q-n_1+1}, and therefore I_{q-n_1+1}, belong to $\{x \leq 1\}$. This is also true for M_n and M_{q-n_1+n}, and therefore I_{q-n_1+n}, whenever $q - n_1 + n < q$. Thus,

$$\Delta_n = \Omega(\mathcal{O}, M_{n-(q-n_1)}, I_n, M_n)$$

is contained in $\{x \leq 1\}$ for $n = q-n_1+1, \dots, q-1$, which proves statement (ii). For $j = q$, it turns out that

$$\Delta_q = \Omega(\mathcal{O}, M_q, I_q, M_{n_1})$$

Note that I_q is the intersection point of $\mathcal{L}_{n_1}$ and $\mathcal{L}_q$, and therefore $I_q = J$. Hence $\Delta_q = \Delta$ and statement (i) is proved. □

Let us now study the dynamics of the qth power of $\Gamma_{a,\theta}$ on Δ. To that end, we introduce the line $\mathcal{L}_{-(q-n_1)} = \mathbf{A}_{a,\theta}^{-(q-n_1)}(\mathcal{C})$ given by

$$\mathcal{L}_{-(q-n_1)} \equiv x\cos(q-n_1)\theta - y\sin(q-n_1)\theta = a^{n_1-q} \tag{2.30}$$

We will prove that $\Gamma_{a,\theta}^q$ on Δ is the two-fold Expanding Baker Map associated to the folds $\mathcal{F}_{\mathcal{C},\mathcal{O}}$ and $\mathcal{F}_{\mathcal{L}_{-(q-n_1)},\mathcal{O}}$ and the (expanding) linear map $a^q\mathbf{I}$.

Proposition 2.4.5. *Let $\theta = 2\pi p/q \in (0,\pi)$ with $p, q \in \mathbb{N}$ and $\gcd(p,q) = 1$. Assume that $q \geq 5$, and let $a_\theta = \min\{a_J, a_M, a_H\}$. Then, there exists $1 < \bar{a}_\theta \leq a_\theta$ such that, for every $1 < a \leq \bar{a}_\theta$,*

$$\Gamma_{a,\theta}^q{\restriction_\Delta} = \mathrm{EBM}(\Delta, \mathcal{C}, \mathcal{L}_{-(q-n_1)}, \mathcal{O}, a^q\mathbf{I})$$

where n_1 is the smallest natural number such that $M_{n_1} \in \Sigma^1$.

Proof. From Proposition 2.4.4 it follows that

$$\Gamma_{a,\theta}^q = \mathbf{A}_{a,\theta}^{n_1} \circ \mathcal{F}_{\mathcal{C},\mathcal{O}} \circ \mathbf{A}_{a,\theta}^{q-n_1} \circ \mathcal{F}_{\mathcal{C},\mathcal{O}}$$

in Δ. We will check next that Lemma 2.1.6 can be applied to obtain

$$\mathcal{F}_{\mathcal{C},\mathcal{O}} \circ \mathbf{A}_{a,\theta}^{q-n_1} = \mathbf{A}_{a,\theta}^{q-n_1} \circ \mathcal{F}_{\mathcal{L}_{-(q-n_1)},\mathcal{O}}$$

in $\Delta \cap \{x \leq 1\}$, from which

$$\Gamma_{a,\theta}^q = a^q\mathbf{I} \circ \mathcal{F}_{\mathcal{L}_{-(q-n_1)},\mathcal{O}} \circ \mathcal{F}_{\mathcal{C},\mathcal{O}} \tag{2.31}$$

in Δ since $\mathbf{A}_{a,\theta}^q = a^q\mathbf{I}$ because $q\theta = 2\pi p$. That is, the restriction of $\Gamma_{a,\theta}^q$ to Δ is the Expanding Baker Map associated to $\mathcal{C}$ and $\mathcal{L}_{-(q-n_1)}$ and $a^q\mathbf{I}$.

In order to apply Lemma 2.1.6, we need to prove that $\mathcal{F}_{\mathcal{L}_{-(q-n_1)},\mathcal{O}}$ is a good fold for $\Delta \cap \{x \leq 1\}$. Indeed, line (2.30) can be written by equalities (2.21) as

$$\mathcal{L}_{-(q-n_1)} \equiv x\cos\theta_1 + y\sin\theta_1 = a^{n_1-q} \tag{2.32}$$

Hence $\mathcal{L}_{-(q-n_1)}$ is parallel to $\mathcal{L}_{n_1}$. Their slope is equal to $-\cot\theta_1 < 0$ and both lines are perpendicular to Σ^1. Moreover, since $0 < a^{n_1-q} < 1 < a^{n_1}$, the line $\mathcal{L}_{-(q-n_1)}$ has nonempty intersection with the interior of Δ_q and intersects $\mathcal{C}$ at the point

$$V = (1, a^{n_1-q}\csc\theta_1 - \cot\theta_1) \tag{2.33}$$

forming an angle θ_1. Then, the fold with respect to $\mathcal{L}_{-(q-n_1)}$ onto $\mathcal{O}$ is

$$\mathcal{F}_{\mathcal{L}_{-(q-n_1)},\mathcal{O}} = \mathbf{A}^{-1}_{a^{q-n_1},\theta_1} \circ \mathcal{F}_{\mathcal{C},\mathcal{O}} \circ \mathbf{A}_{a^{q-n_1},\theta_1} \tag{2.34}$$

As a consequence, it is directly verified that the reflection of $\mathcal{L}_{n_1}$ with respect to $\mathcal{L}_{-(q-n_1)}$, which is the line with equation

$$x\cos\theta_1 + y\sin\theta_1 = a^{n_1}(2a^{-q} - 1)$$

intersects $\mathcal{C}$ at the point

$$H'_{n_1} = (1, a^{n_1-q}(2-a^q)\csc\theta_1 - \cot\theta_1)$$

Hence $\mathcal{F}_{\mathcal{L}_{-(q-n_1)},\mathcal{O}}$ is a good fold for $\Delta \cap \{x \leq 1\}$ whenever

$$a^{n_1-q}(2-a^q) - \cos\theta_1 > 0 \tag{2.35}$$

Since inequality (2.35) trivially holds for $a = 1$, by continuity there exists $\bar{a}_\theta > 1$ such that inequality (2.35) holds for every $a \in (1, \bar{a}_\theta]$. □

Remark 2.4.6. The final argument of continuity in the proof of Proposition 2.4.5 also guarantees the existence of an a-value $a_1 \in (1, \bar{a}_\theta]$ for which

$$a^{n_1-q}(2-a^q) - \cos\theta_1 \geq \varepsilon \tag{2.36}$$

for some $\varepsilon > 0$ and every $a \in (1, a_1]$. Let $a_1 = a_1(\theta)$ be the supremum of such a-values and let $\varepsilon > 0$ be the supremum of the values for which inequality (2.36) holds for every $a \in (1, a_1]$.

Finally, we can prove Theorem 4. Let $1 < a_1 \leq \bar{a}_\theta$ and $\varepsilon > 0$ from Remark 2.4.6, and fix $1 < a < a_1$. Then,

$$\Gamma^q_{a,\theta} = a^q\mathbf{I} \circ \mathcal{F}_{\mathcal{L}_{-(q-n_1)},\mathcal{O}} \circ \mathcal{F}_{\mathcal{C},\mathcal{O}}$$

is well defined on Δ. In particular, it is well defined on $\Delta^\varepsilon = \Delta \cap \{y \geq \varepsilon\}$. Note that

$$\mathcal{F}_{\mathcal{L}_{-(q-n_1)},\mathcal{O}} \circ \mathcal{F}_{\mathcal{C},\mathcal{O}}(\Delta^\varepsilon) \subseteq \Delta^\varepsilon \cap \{x \leq 1\}$$

and

$$\Delta^\varepsilon_q \subseteq \Delta \cap \{y \geq a^q\varepsilon\} \subsetneq \Delta^\varepsilon$$

Hence $\Delta^\varepsilon \subsetneq \Delta$ is $\Gamma^q_{a,\theta}$-invariant. Moreover, the region Δ^ε traps the orbit of every point in $\Delta \cap \{y > 0\}$. Since $\Delta^\varepsilon \cap \Sigma^0 = \varnothing$, then Δ^ε and Δ^ε_1 are disjoint. Then, the set $\mathcal{D} = \Delta^\varepsilon$ verifies every statement of Theorem 4. The proof is complete for $q \geq 5$.

From the fact that $\mathcal{D} = \Delta^\varepsilon$ traps the orbit of every point in $\Delta \cap \{y > 0\}$, we can deduce Corollary 1 straightforwardly.

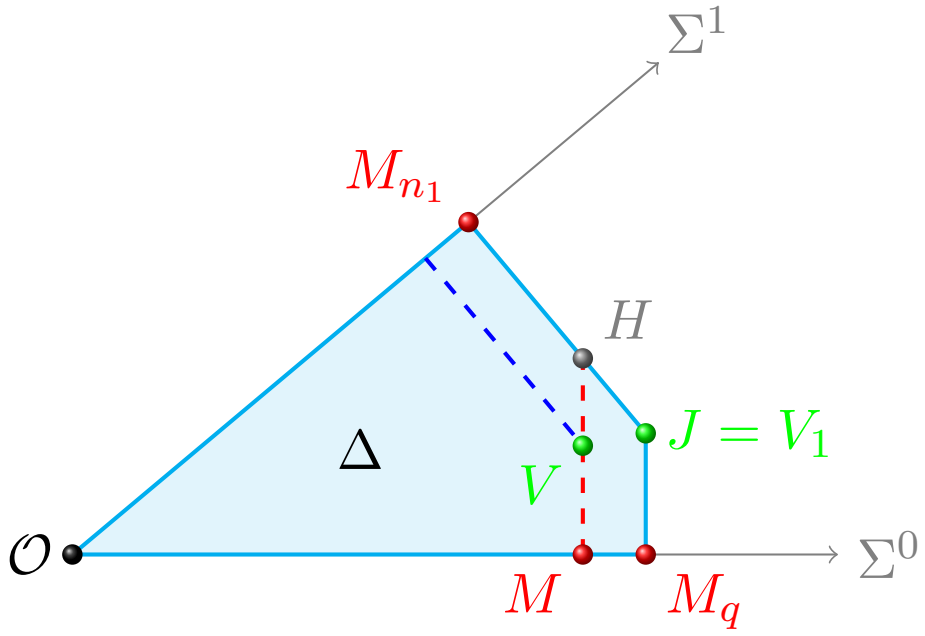

Figure 2.15: The strictly $\Gamma^q_{a,\theta}$-invariant polygon $\Delta = \Omega(\mathcal{O}, M_q, J, M_{n_1})$

2.4.2 Case $q = 4$

Since $2p < 4$, then $p = 1$ and $\theta = \pi/2$. Let

$$\Delta = [0, a^4] \times [0, a], \qquad 1 < a < \sqrt[4]{2}$$

It is clear that $\mathcal{F}_{\mathcal{C},\mathcal{O}}(\Delta) = [0, 1] \times [0, a]$. The iterates of Δ are easily obtained:

$$\Delta_1 = [-a^2, 0] \times [0, a], \qquad \Delta_2 = [-a^2, 0] \times [-a^3, 0], \qquad \Delta_3 = [0, a^4] \times [-a^3, 0]$$

Since $\mathcal{F}_{\mathcal{C},\mathcal{O}}(\Delta_3) = [0, 1] \times [-a^3, 0]$, then $\Delta_4 = \Delta$.

Another fold is necessary to express $\Gamma^4_{a,\theta}$ restricted to Δ as an Expanding Baker Map. Since

$$\Gamma^4_{a,\theta} = \mathbf{A}_{a,\theta} \circ \mathcal{F}_{\mathcal{C},\mathcal{O}} \circ \mathbf{A}^3_{a,\theta} \circ \mathcal{F}_{\mathcal{C},\mathcal{O}}$$

in Δ, from Lemma 2.1.6 it follows that

$$\Gamma^4_{a,\theta}\restriction_\Delta = \mathrm{EBM}(\Delta, \mathcal{C}, \mathcal{L}_{-3}, \mathcal{O}, a^4\mathbf{I})$$

where $\mathcal{L}_{-3} \equiv y = 1/a^3$. Indeed, the fold $\mathcal{F}_{\mathcal{L}_{-3},\mathcal{O}}$ is a good fold for $[0, 1] \times [0, a]$ as $2a^{-3} - a \geq 0$. Now, let

$$\Delta^\varepsilon = [0, a^4] \times [a^{-3}\varepsilon, a]$$

with $\varepsilon = 2 - a^4 \in (0, 1)$. It is straightforward to compute the iterates of Δ^ε from the iterates of Δ and conclude that Δ^ε is a $\Gamma^4_{a,\theta}$-invariant restrictive domain. See Figure 2.16. Moreover, the fold $\mathcal{F}_{\mathcal{L}_{-3},\mathcal{O}}$ is a good fold for $[0, 1] \times [a^{-3}\varepsilon, a]$ as $2a^{-3} - a = a^{-3}\varepsilon$. Thus, the rectangle $\mathcal{D} = \Delta^\varepsilon$ verifies Theorem 4 with $a_1 = \sqrt[4]{2}$.

Remark 2.4.7. From the expression of $\Gamma^4_{a,\theta}$ as an Expanding Baker Map on Δ^ε it is easy to check that the rectangle

$$\widehat{\Delta}^\varepsilon = [a^4\varepsilon, a^4] \times [a\varepsilon, a]$$

is strictly $\Gamma^4_{a,\theta}$-invariant. Moreover, numerical simulations show that $\widehat{\Delta}^\varepsilon \cup \widehat{\Delta}^\varepsilon_1 \cup \widehat{\Delta}^\varepsilon_2 \cup \widehat{\Delta}^\varepsilon_3$ is a 4-piece second-rate strange attractor for all $\sqrt[8]{2} \leq a < a_1$.

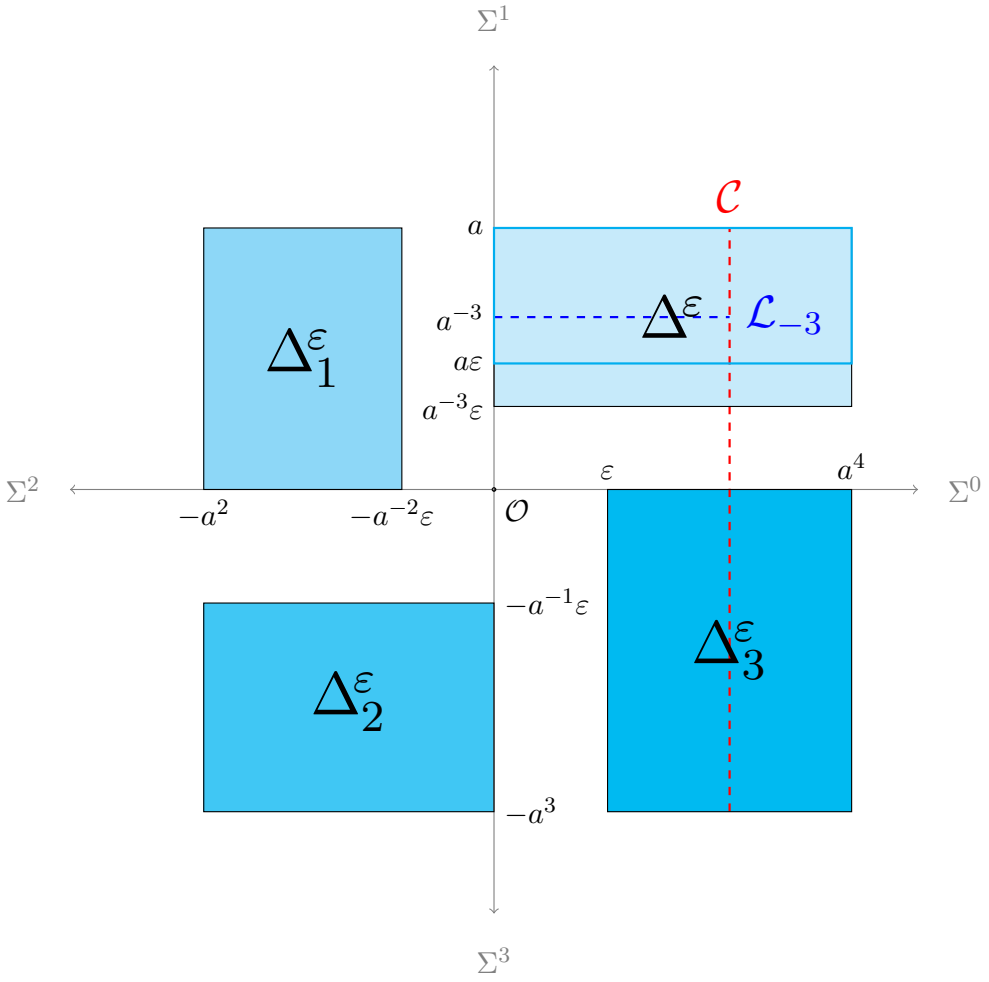

Figure 2.16: The $\Gamma^4_{a,\pi/2}$-invariant restrictive domain $\Delta^\varepsilon = [0, a^4] \times [a^{-3}\varepsilon, a]$ with $\varepsilon = 2 - a^4$

2.4.3 Case $q = 3$

Since $2p < 3$, then $p = 1$ and $\theta = 2\pi/3$. Let $M = (1, 0)$ and

$$A = (1, \tfrac{2\sqrt{3}}{3}a + \tfrac{\sqrt{3}}{3})$$

be the points of intersection between the critical line $\mathcal{C}$ and the ray Σ^0 and the line $\mathcal{L}_1 = \mathcal{C}_1$, respectively. Let

$$\Delta' = \Omega(\mathcal{O}, M, A, M_1)$$

Check Figure 2.17 along our next discussion.

Since $\Delta' \subseteq \{x \leq 1\}$ by construction, then $\Delta'_1 = \Omega(\mathcal{O}, M_1, A_1, M_2)$. It is clear that $\Delta'_1 \subseteq \{x \leq 0\}$, and therefore $\Delta'_2 = \Omega(\mathcal{O}, M_2, A_2, M_3)$, with

$$A_2 = (a^3, -\tfrac{\sqrt{3}}{3}a^3 - \tfrac{2\sqrt{3}}{3}a^2)$$

Since $a > 1$, then $\Delta'_2 \cap \{x > 1\} \neq \varnothing$. Thus, to obtain Δ'_3 we first need to obtain $\mathcal{F}_{\mathcal{C},\mathcal{O}}(\Delta'_2)$. Note that

$$\mathcal{F}_{\mathcal{C},\mathcal{O}}(\Delta'_2) \subseteq \Omega(\mathcal{O}, C_2, \widetilde{A}_2, B_2, M)$$

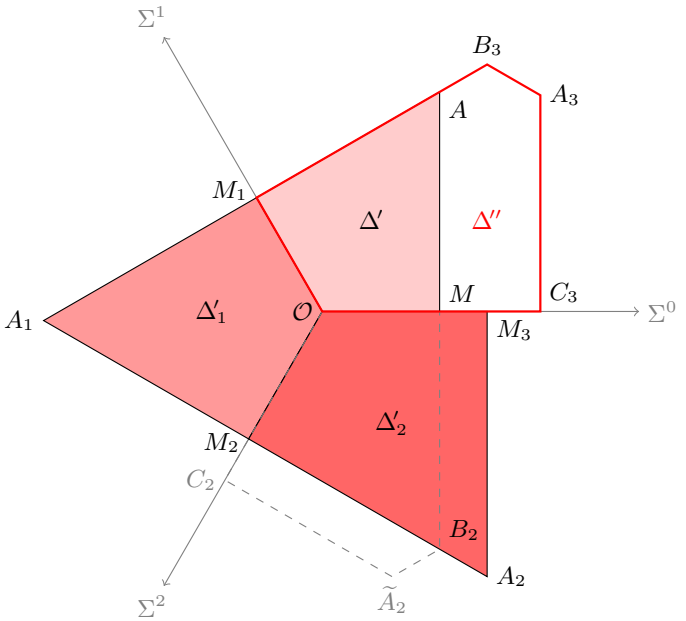

(a)

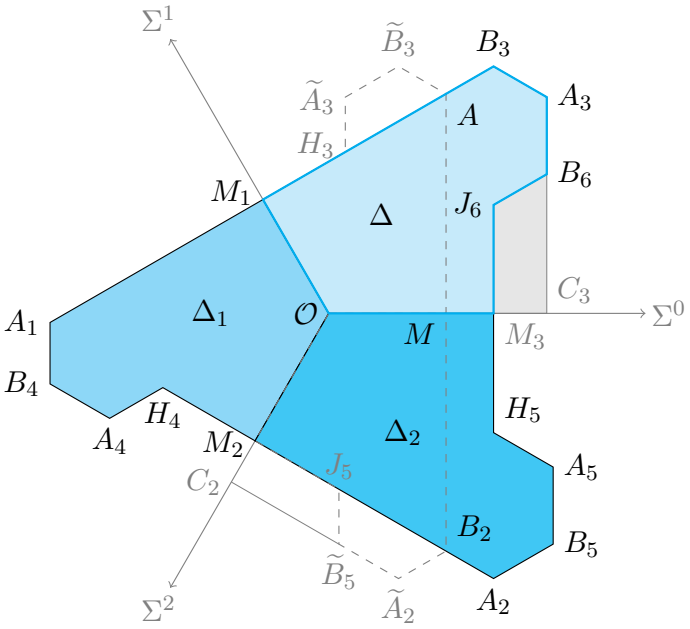

(b)

Figure 2.17: The strictly $\Gamma^3_{a,2\pi/3}$-invariant polygon $\Delta = \Omega(\mathcal{O}, M_3, J_6, B_6, A_3, B_3, M_1)$: (a) Orbit of Δ'; (b) Orbit of Δ'' and Δ

where $B_2 = (1, -2a^2\sqrt{3}/3 - \sqrt{3}/3)$ is the intersection point of $\mathcal{C}$ and $\mathcal{L}_2$, and C_2 is the intersection point of Σ^2 and the line parallel to $\mathcal{L}_2$ through the point $\widetilde{A}_2$. Therefore,

$$\Delta_3' \subseteq \Omega(\mathcal{O}, C_3, A_3, B_3, M_1)$$

where

$$A_3 = (a^4 + a^3 - a, -\tfrac{\sqrt{3}}{3}a^4 + \tfrac{\sqrt{3}}{3}a^3 + \sqrt{3}a)$$

Now, let $\Delta'' = \Omega(\mathcal{O}, C_3, A_3, B_3, M_1)$. We will prove that Δ'' is $\Gamma^3_{a,\theta}$-invariant. As a corollary, we deduce that $\Delta = \Delta_3''$ is strictly $\Gamma^3_{a,\theta}$-invariant since $\mathcal{F}_{\mathcal{C},\mathcal{O}}(\Delta) = \mathcal{F}_{\mathcal{C},\mathcal{O}}(\Delta'')$. In fact, it holds that $\mathcal{K}_{a,\theta} = \Delta \cup \Delta_1 \cup \Delta_2$.

Proposition 2.4.8. *Let $\theta = 2\pi/3$. Then, there exists $a_\theta > 1$ such that, for every $a \in (1, a_\theta)$, the following hold:*

(i) $\Delta_3'' \subseteq \Delta''$, *i.e.* Δ'' *is* $\Gamma^3_{a,\theta}$*-invariant.*

(ii) $\Delta_n'' \cap \{x > 1\} = \varnothing$ *for* $n = 1, 2$.

Proof. See Figure 2.17. Note that

$$\mathcal{F}_{\mathcal{C},\mathcal{O}}(\Delta'') = \Omega(\mathcal{O}, M, A, \widetilde{B}_3, \widetilde{A}_3, H_3, M_1)$$

where H_3 is the point of intersection between $\mathcal{C}_1$ and the vertical line through the point $\widetilde{A}_3$. Thus,

$$\Delta_1'' = \Omega(\mathcal{O}, M_1, A_1, B_4, A_4, H_4, M_2)$$

is contained in $\{x \leq 0\}$ and

$$\Delta_2'' = \Omega(\mathcal{O}, M_2, A_2, B_5, A_5, H_5, M_3)$$

where

$$A_5 = (a^5 + a^3 - a^2, \tfrac{2\sqrt{3}}{3}a^6 + \tfrac{\sqrt{3}}{3}a^5 - \sqrt{3}a^3 - \sqrt{3}a^2)$$

We claim that

$$\mathcal{F}_{\mathcal{C},\mathcal{O}}(\Delta_2'') \subseteq \Omega(\mathcal{O}, C_2, \widetilde{A}_2, B_2, M)$$

and hence $\Delta_3'' \subseteq \Delta''$. To prove the claim it suffices to show that $\widetilde{A}_5 \in \Delta_2$ or, equivalently, that $\widetilde{A}_5 \in \mathcal{R}^2$. This holds whenever $\widetilde{A}_5 \in \{y \leq \sqrt{3}x\}$, that is,

$$a^6 + 2a^5 - 3a^2 - 3 \leq 0$$

Thus, we have that $\Delta_3 \subseteq \Delta$ for all $1 < a < a_\theta$, where $a_\theta \approx 1.17621$ is the unique positive root of $a^6 + 2a^5 - 3a^2 - 3$. □

As in the previous cases, the proof of statement (a) for $q = 3$ concludes by taking $\mathcal{D} = \Delta \cap \{y \geq \varepsilon\}$ for $\varepsilon > 0$ sufficiently small. However, we cannot write $\Gamma^3_{a,\theta}$ as a two-fold Expanding Baker Map. In order to show that

$$\Gamma^3_{a,\theta}\restriction_\Delta = \mathbf{A}_{a,\theta} \circ \mathcal{F}_{\mathcal{C},\mathcal{O}} \circ \mathbf{A}^2_{a,\theta} \circ \mathcal{F}_{\mathcal{C},\mathcal{O}}$$

is the Expanding Baker Map associated to the lines $\mathcal{C}$ and

$$\mathcal{L}_{-2} \equiv -\tfrac{1}{2}x + \tfrac{\sqrt{3}}{2}y = a^{-2}$$

and the matrix $a^3\mathbf{I}$, we need that $\mathcal{F}_{\mathcal{C},\mathcal{O}} \circ \mathbf{A}^2_{a,\theta} = \mathbf{A}^2_{a,\theta} \circ \mathcal{F}_{\mathcal{L}_{-2},\mathcal{O}}$. But, unfortunately, Lemma 2.1.6 cannot be applied because $\mathcal{F}_{\mathcal{L}_{-2},\mathcal{O}}$ is not a good fold for $\mathcal{F}_{\mathcal{C},\mathcal{O}}(\Delta)$.

2.5 Renormalization and Coexistence of Attractors: Proof of Theorem 5 and Corollary 2

Throughout this section we will suppose that $\Gamma_{a,\theta}$ satisfies the assumptions in Theorem 4. In particular, we will assume that inequality (2.36) holds.

Since $\Gamma^2_{a,\pi/2}$ is the Cartesian product of two 1-D tent maps, the renormalization for the case $q = 4$ follows from Lemma 2.2 [58] and the results were already collected in Lemma 2.1.11. For $q \geq 5$ we cannot take advantage of this fact and we will see how the construction of the restrictive domains for the successive renormalizations gets more complicated, depending on whether q is odd or even. In the first case we will obtain a single restrictive domain as stated in statement (a). In the second case we have $q = 2\nu$. Then, when ν is odd, we also obtain a single restrictive domain for a first step in the renormalization, statement (i) of (b). When ν is even, two disjoint restrictive domains are obtained and the renormalization can be continued, at least one more step, in each of these domains, statement (ii) of (b). It is clear then that when q is a power of 2 there is a sequence of renormalizations leading to a sequence of doubling attractors, as stated in Corollary 2. We emphasize that the results obtained in previous publications [57, 58, 59] correspond to the case $q = 2^3$. For the general case $q \neq 2^m$, obstructions to the renormalization arise from the difficulty in defining good folds over the corresponding restrictive domain.

2.5.1 The Family $\Psi_{a,\theta}$ of Expanding Baker Maps

Let $\theta = 2\pi p/q \in (0, \pi)$ with $p, q \in \mathbb{N}$ and $\gcd(p, q) = 1$. Throughout this section we will assume that $q \geq 5$. As we have seen in Proposition 2.4.5, for a sufficiently close to 1, the restriction $G_{a,\theta}$ of $\Gamma^q_{a,\theta}$ to the polygon Δ given in (2.25) can be written as

$$G_{a,\theta} = a^q \mathbf{I} \circ \mathcal{F}_{\mathcal{L}_{-(q-n_1)},\mathcal{O}} \circ \mathcal{F}_{\mathcal{C},\mathcal{O}}$$

In other words, the map $G_{a,\theta}$ is the Expanding Baker Map that folds Δ first along the critical line $\mathcal{C}$ and then along line $\mathcal{L}_{-(q-n_1)}$, whose equation (2.32) is of the form $y = -\alpha x + \beta$ with $\alpha = \cot\theta_1 > 0$ and $\beta = a^{n_1-q}\csc\theta_1 > 0$. These lines cross each other at the angle θ_1, which means that the respective folds are conjugated by $\mathbf{A}_{a^{q-n_1},2\pi-\theta_1}$, that is,

$$\mathcal{F}_{\mathcal{L}_{-(q-n_1)},\mathcal{O}} = \mathbf{A}_{a^{n_1-q},\theta_1} \circ \mathcal{F}_{\mathcal{C},\mathcal{O}} \circ \mathbf{A}_{a^{q-n_1},2\pi-\theta_1}$$

Therefore, setting $\lambda = a^{n_1-q}$, we have (see Figure 2.18) that

$$G_{a,\theta} = \begin{cases} G^{0,0}_{a,\theta} = a^q \mathbf{I} & \text{in } \mathcal{K}_{00} \\ G^{0,1}_{a,\theta} = a^q \lambda e^{\theta_1 \mathrm{i}} \mathbf{I} \circ \mathcal{F}_{\mathcal{C},\mathcal{O}} \circ \lambda^{-1} e^{-\theta_1 \mathrm{i}} \mathbf{I} & \text{in } \mathcal{K}_{01} \\ G^{1,0}_{a,\theta} = a^q \mathbf{I} \circ \mathcal{F}_{\mathcal{C},\mathcal{O}} & \text{in } \mathcal{K}_{10} \\ G^{1,1}_{a,\theta} = a^q \lambda e^{\theta_1 \mathrm{i}} \mathbf{I} \circ \mathcal{F}_{\mathcal{C},\mathcal{O}} \circ \lambda^{-1} e^{-\theta_1 \mathrm{i}} \mathbf{I} \circ \mathcal{F}_{\mathcal{C},\mathcal{O}} & \text{in } \mathcal{K}_{11} \end{cases} \tag{2.37}$$

The differential map of $G_{a,\theta}$ is constant in its four smoothness domains, and we will see next that it has complex eigenvalues in $\mathcal{K}_{11}$. More concretely, in this case the differential map is given by the matrix $\mathbf{A}_{a^q,2\theta_1}$. In order to take advantage of this analogy, we will search for a fixed point P of $G_{a,\theta}$ in $\mathcal{K}_{11}$ and then perform a suitable change of variables in which P is the origin of coordinates.

In $\mathcal{K}_{11}$, the map $G_{a,\theta}$ can be written in the complex variable as

$$G_{a,\theta}(z) = a^q(2\lambda e^{\theta_1 \mathrm{i}} - 2e^{2\theta_1 \mathrm{i}} + e^{2\theta_1 \mathrm{i}} z)$$

Thus, the fixed point of $G_{a,\theta}$ is

$$z^* = x^* + \mathrm{i}y^* = \frac{2e^{2\theta_1 \mathrm{i}} - 2\lambda e^{\theta_1 \mathrm{i}}}{e^{2\theta_1 \mathrm{i}} - a^{-q}}$$

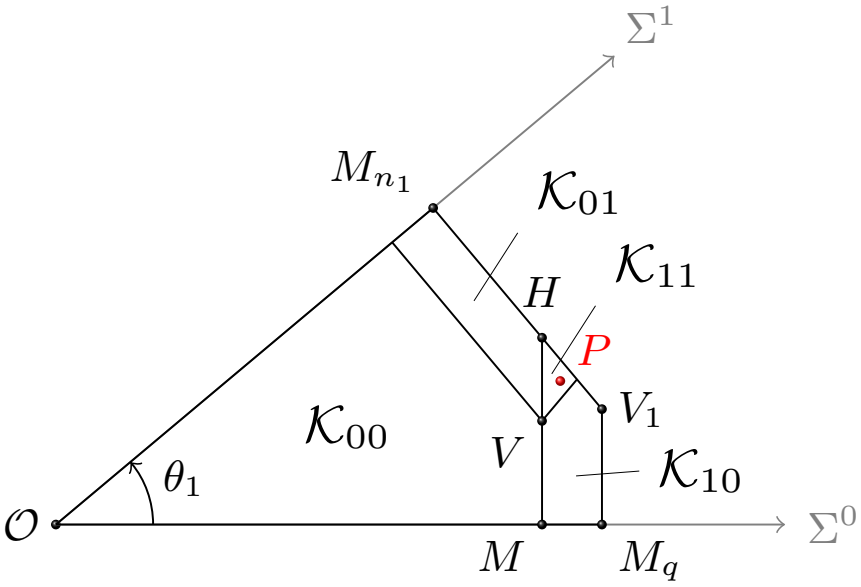

Figure 2.18: Smoothness domains of $G_{a,\theta}$ in $\Delta = \mathcal{K}_{00} \cup \mathcal{K}_{01} \cup \mathcal{K}_{10} \cup \mathcal{K}_{11}$

where

$$\begin{aligned} x^* &= 2\frac{a^{2q} - a^{n_1}(a^q - 1)\cos\theta_1 - a^q \cos 2\theta_1}{a^{2q} - 2a^q \cos 2\theta_1 + 1} \\ y^* &= 2\frac{a^{n_1}(1 + a^q)\sin\theta_1 - a^q \sin 2\theta_1}{a^{2q} - 2a^q \cos 2\theta_1 + 1} \end{aligned} \tag{2.38}$$

The subregion $\mathcal{K}_{11}$ of Δ is limited by $\mathcal{C}$, the reflection

$$\mathcal{L}^*_{-(q-n_1)} \equiv (2 - x)\cos\theta_1 + y \sin\theta_1 = a^{n_1 - q} \tag{2.39}$$

of $\mathcal{L}_{-(q-n_1)}$ with respect to $\mathcal{C}$, and $\mathcal{L}_{n_1}$. Therefore, the fixed point P is an interior point of $\mathcal{K}_{11}$ if and only if

$$\begin{aligned} \rho_1 &= x^* - 1 \\ \rho_2 &= (2 - x^*)\cos\theta_1 + y^* \sin\theta_1 - a^{n_1 - q} \\ \rho_3 &= a^{n_1} - x^* \cos\theta_1 - y^* \sin\theta_1 \end{aligned} \tag{2.40}$$

are positive. Their values are obtained by a straightforward substitution of coordinates (2.38) in formulas (2.40):

$$\begin{aligned} \rho_1 &= \frac{a^q - 2a^{n_1}\cos\theta_1 + 1}{a^{2q} - 2a^q \cos 2\theta_1 + 1}(a^q - 1) \\ \rho_2 &= \frac{a^{n_1} + a^{n_1 - q} - 2\cos\theta_1}{a^{2q} - 2a^q \cos 2\theta_1 + 1}(a^q - 1) \\ \rho_3 &= \frac{a^{n_1} + a^{q + n_1} - 2a^q \cos\theta_1}{a^{2q} - 2a^q \cos 2\theta_1 + 1}(a^q - 1) \end{aligned} \tag{2.41}$$

Since $a > 1$ and $\cos 2\theta_1 < 1$, we have the following lemma.

Lemma 2.5.1. *The Expanding Baker Map $G_{a,\theta}$ has a fixed point P in the interior of $\mathcal{K}_{11}$ if and only if the following inequalities hold:*

(i) $a^q - 2a^{n_1}\cos\theta_1 + 1 > 0$

(ii) $a^{n_1} + a^{n_1-q} - 2\cos\theta_1 > 0$

(iii) $a^{n_1} + a^{q+n_1} - 2a^q\cos\theta_1 > 0$

Remark 2.5.2. For any $q \geq 5$, the three inequalities of Lemma 2.5.1 hold for all a sufficiently close to 1. In particular, for all $a \in (1, \bar{a}_\theta]$, being $\bar{a}_\theta$ given in Proposition 2.4.5. Indeed, by inequality (2.35), and since $1 \leq n_1 \leq q-1$, we obtain

$$\begin{aligned} a^q - 2a^{n_1}\cos\theta_1 + 1 &> a^q + 2a^{2n_1}(1 - 2a^{-q}) + 1 \\ &\geq 1 + 2a^{2n_1} + a^{q-2}(a^2 - 4) \end{aligned}$$

where the latter term vanishes for $a = 1$ and increases as $a \to \infty$. On the other hand,

$$a^{n_1} + a^{n_1-q} - 2\cos\theta_1 > 3a^{n_1}(1 - a^{-q}) > 0$$

and

$$a^{n_1} + a^{q+n_1} - 2a^q\cos\theta_1 > 3a^{n_1}(a^q - 1) > 0$$

From Remark 2.5.2 we obtain the following result.

Proposition 2.5.3. *Let $\theta = 2\pi p/q \in (0, \pi)$ with $p, q \in \mathbb{N}$ and $\gcd(p, q) = 1$. Assume that $q \geq 5$ and let a_1 from Theorem 4. Then, for every $a \in (1, a_1)$, the Expanding Baker Map $G_{a,\theta}$ has a fixed point $P \in \operatorname{int}\mathcal{K}_{11}$. Moreover, the differential map of $G_{a,\theta}$ at P is the matrix $\mathbf{A}_{a^q,2\theta_1}$. In particular,*

$$G_{a,\theta}(Q) = P + \mathbf{A}_{a^q,2\theta_1}(Q - P)$$

for all $Q \in \mathcal{K}_{11}$.

Proof. The existence of the fixed point $P \in \mathcal{K}_{11}$ is an immediate consequence of Lemma 2.5.1 and Remark 2.5.2. To calculate the differential of $G_{a,\theta}$ at P, substitute expression (2.37) in $\mathcal{K}_{11}$ for its differential. Then, we obtain

$$\begin{pmatrix} a^q\cos\theta_1 & -a^q\sin\theta_1 \\ a^q\sin\theta_1 & a^q\cos\theta_1 \end{pmatrix}\begin{pmatrix} -1 & 0 \\ 0 & 1 \end{pmatrix}\begin{pmatrix} \cos\theta_1 & \sin\theta_1 \\ -\sin\theta_1 & \cos\theta_1 \end{pmatrix}\begin{pmatrix} -1 & 0 \\ 0 & 1 \end{pmatrix}$$

which is equal to

$$\begin{pmatrix} a^q\cos 2\theta_1 & -a^q\sin 2\theta_1 \\ a^q\sin 2\theta_1 & a^q\cos 2\theta_1 \end{pmatrix}$$

Finally, since $G_{a,\theta}^{1,1}$ is a composition of affine maps and fixes P, then it can be written as in the statement of this Proposition. □

Noting that $\mathcal{F}_{\mathcal{C},\mathcal{O}}$ and $\mathcal{F}_{\mathcal{C},P}$ are reversed folds (and so are $\mathcal{F}_{\mathcal{L}_{-(q-n_1)},\mathcal{O}}$ and $\mathcal{F}_{\mathcal{L}_{-(q-n_1)},P}$), the next lemma is directly obtained from definition of $G_{a,\theta}$. We will now consider the folds $\mathcal{F}_{\mathcal{C},P}$ and $\mathcal{F}_{\mathcal{L}^*_{-(q-n_1)},P}$. Both folds coincide with the identity on $\mathcal{K}_{11}$. It also holds that

$$\mathcal{F}_{\mathcal{L}^*_{-(q-n_1)},P} = \mathcal{F}_{\mathcal{C},P} \circ \mathcal{F}_{\mathcal{L}_{-(q-n_1)},P} \circ \mathcal{F}_{\mathcal{C},\mathcal{O}} \tag{2.42}$$

Lemma 2.5.4. *The following statements hold:*

(i) $G_{a,\theta} = G_{a,\theta}^{1,1} \circ \mathcal{F}_{\mathcal{C},P}$ *in* $\mathcal{K}_{01}^* = \{Q \in \mathcal{K}_{01} : \mathcal{F}_{\mathcal{C},P}(Q) \in \mathcal{K}_{11}\}$.

(ii) $G_{a,\theta} = G_{a,\theta}^{1,1} \circ \mathcal{F}_{\mathcal{L}^*_{-(q-n_1)},P}$ *in* $\mathcal{K}_{10}^* = \{Q \in \mathcal{K}_{10} : \mathcal{F}_{\mathcal{L}^*_{-(q-n_1)},P}(Q) \in \mathcal{K}_{11}\}$.

(iii) $G_{a,\theta} = G^{1,1}_{a,\theta} \circ \mathcal{F}_{\mathcal{L}^*_{-(q-n_1)},P} \circ \mathcal{F}_{\mathcal{C},P}$ *in* $\mathcal{K}^*_{00} = \{Q \in \mathcal{K}_{00} : \mathcal{F}_{\mathcal{C},P}(Q) \in \mathcal{K}^*_{10}\}$.

Proof.

(i) If $Q \in \mathcal{K}^*_{01}$, then

$$\begin{aligned} G^{1,1}_{a,\theta} \circ \mathcal{F}_{\mathcal{C},P}(Q) &= a^q \lambda \mathrm{e}^{\theta_1 \mathrm{i}} \mathbf{I} \circ \mathcal{F}_{\mathcal{C},\mathcal{O}} \circ \lambda^{-1} \mathrm{e}^{-\theta_1 \mathrm{i}} \mathbf{I} \circ \mathcal{F}_{\mathcal{C},\mathcal{O}} \circ \mathcal{F}_{\mathcal{C},P}(Q) \\ &= a^q \lambda \mathrm{e}^{\theta_1 \mathrm{i}} \mathbf{I} \circ \mathcal{F}_{\mathcal{C},\mathcal{O}} \circ \lambda^{-1} \mathrm{e}^{-\theta_1 \mathrm{i}} \mathbf{I}(Q) \\ &= G^{0,1}_{a,\theta}(Q) \end{aligned}$$

But $G^{0,1}_{a,\theta}(Q) = G_{a,\theta}(Q)$ because $Q \in \mathcal{K}_{01}$.

(ii) If $Q \in \mathcal{K}^*_{10}$, then $\mathcal{F}_{\mathcal{L}^*_{-(q-n_1)},P}(Q) \in \mathcal{K}_{11}$. Therefore, by equality (2.42),

$$\begin{aligned} G^{1,1}_{a,\theta} \circ \mathcal{F}_{\mathcal{L}^*_{-(q-n_1)},P}(Q) &= a^q \mathbf{I} \circ \mathcal{F}_{\mathcal{L}_{-(q-n_1)},\mathcal{O}} \circ \mathcal{F}_{\mathcal{C},\mathcal{O}} \circ \mathcal{F}_{\mathcal{L}^*_{-(q-n_1)},P}(Q) \\ &= a^q \mathbf{I} \circ \mathcal{F}_{\mathcal{C},\mathcal{O}}(Q) \\ &= G^{1,0}_{a,\theta}(Q) \end{aligned}$$

with $G^{1,0}_{a,\theta}(Q) = G_{a,\theta}(Q)$ because $Q \in \mathcal{K}_{10}$.

(iii) If $Q \in \mathcal{K}^*_{00}$, then $\mathcal{F}_{\mathcal{C},P}(Q) \in \mathcal{K}^*_{10}$ and, according to statement (ii),

$$\begin{aligned} G^{1,1}_{a,\theta} \circ \mathcal{F}_{\mathcal{L}^*_{q-n_1},P} \circ \mathcal{F}_{\mathcal{C},P}(Q) &= G_{a,\theta} \circ \mathcal{F}_{\mathcal{C},P}(Q) \\ &= G^{1,0}_{a,\theta} \circ \mathcal{F}_{\mathcal{C},P}(Q) \\ &= G^{0,0}_{a,\theta}(Q) \end{aligned}$$

but $G^{0,0}_{a,\theta}(Q) = G_{a,\theta}(Q)$ because $Q \in \mathcal{K}_{00}$. □

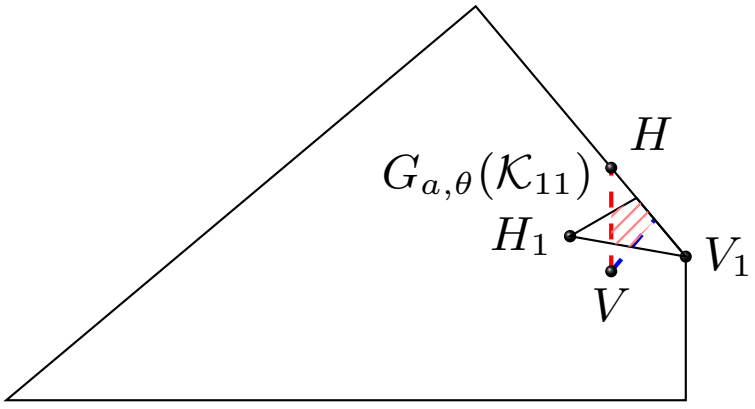

Figure 2.19: Intersection of $\mathcal{K}_{11}$ and $G_{a,\theta}(\mathcal{K}_{11})$

Going back to Lemma 2.5.4 to define $\mathcal{K}^* = \mathcal{K}^*_{00} \cup \mathcal{K}^*_{01} \cup \mathcal{K}_{11} \cup \mathcal{K}^*_{10}$. Then, we obtain the following result:

Proposition 2.5.5. *For all $Q \in \mathcal{K}^*$,*

$$G_{a,\theta}(Q) = G_{a,\theta}^{1,1} \circ \mathcal{F}_{\mathcal{L}^*_{-(q-n_1)},P} \circ \mathcal{F}_{\mathcal{C},P}(Q)$$

Proof. The first equality is trivially verified in $\mathcal{K}_{11}$ because both $\mathcal{F}_{\mathcal{L}^*_{-(q-n_1)},P}$ and $\mathcal{F}_{\mathcal{C},P}$ are the identity map. In $\mathcal{F}_{\mathcal{C},P}(\mathcal{K}^*_{01})$, the fold $\mathcal{F}_{\mathcal{L}^*_{-(q-n_1)},P}$ coincides with the identity map. Therefore, by statement (i) of Lemma 2.5.4,

$$G_{a,\theta} = G_{a,\theta}^{1,1} \circ \mathcal{F}_{\mathcal{C},P} = G_{a,\theta}^{1,1} \circ \mathcal{F}_{\mathcal{L}^*_{-(q-n_1)},P} \circ \mathcal{F}_{\mathcal{C},P}$$

In $\mathcal{K}^*_{10}$, the fold $\mathcal{F}_{\mathcal{C},P}$ is the identity map. Therefore, by statement (ii) of Lemma 2.5.4,

$$G_{a,\theta} = G_{a,\theta}^{1,1} \circ \mathcal{F}_{\mathcal{L}^*_{-(q-n_1)},P} = G_{a,\theta}^{1,1} \circ \mathcal{F}_{\mathcal{L}^*_{-(q-n_1)},P} \circ \mathcal{F}_{\mathcal{C},P}$$

Finally, in $\mathcal{K}^*_{00}$ we directly obtain the expression from the statement of this Proposition by statement (iii) of Lemma 2.5.4. □

Remark 2.5.6. It is clear that the line $y = 0$ is invariant for $G_{a,\theta}$ and that every line of the form $y = \varepsilon > 0$ is moved upwards by $G_{a,\theta}$. Also, every line forming an angle θ_1 with $y = 0$ located at the right of the origin is moved rightwards. Therefore, it easily follows that the possible attractors for $\Gamma^q_{a,\theta}$ on Δ must be in $\mathcal{K}^*$.

Since Δ is an invariant set for $G_{a,\theta}$, according to Remark 2.5.6, the study of the dynamics of $\Gamma^q_{a,\theta}$ on Δ reduces to that on $\mathcal{K}^*$. We will use the expression of $G_{a,\theta}$ given in Proposition 2.5.5. The composition of $\mathcal{F}_{\mathcal{L}^*_{-(q-n_1)},P}$ with $\mathcal{F}_{\mathcal{C},P}$ takes all $\mathcal{K}^*$ on $\mathcal{K}_{11}$, which is the region limited by the lines $\mathcal{C}$ and $\mathcal{L}^*_{-(q-n_1)}$. These lines intersect at point (2.33) and cross each other at an angle θ_1. The image of V is obtained after rotating around P an angle $2\theta_1$ and multiplying by a, or directly from $G_{a,\theta}(V) = G^{0,0}_{a,\theta}(V)$ to obtain $V_1 = J$. Then, the image $G_{a,\theta}(\mathcal{K}_{11})$ of $\mathcal{K}_{11}$ intersects $\mathcal{K}_{11}$ according to Figure 2.19.

Let $\mathcal{A} = G_{a,\theta}(\mathcal{A}) \subseteq \mathcal{K}^*$ be a strictly $G_{a,\theta}$-invariant set. Then,

$$G_{a,\theta}(\mathcal{A}) \subseteq G_{a,\theta}(\mathcal{K}^*) = G_{a,\theta}(\mathcal{K}_{11})$$

and therefore $\mathcal{A} \subseteq \mathcal{K}^* \cap G_{a,\theta}(\mathcal{K}_{11}) = \mathcal{R}_1$. Repeating this process iteratively we have that $\mathcal{A} \subseteq \mathcal{K}^* \cap G_{a,\theta}(\mathcal{R}_1) = \mathcal{R}_2$ and in general $\mathcal{A} \subseteq \mathcal{R}_n$ with $\mathcal{R}_n = \mathcal{K}^* \cap G_{a,\theta}(\mathcal{R}_{n-1})$. Hence $\mathcal{A} \subseteq \cap_{n=1}^{\infty} \mathcal{R}_n$. Following the arguments in Section 2.2.1 we can prove that there exists a natural number N such that $\mathcal{R}_n = \mathcal{R}_{n+1}$ for all $n \geq N$, and therefore $\mathcal{R} = \cap_{n=1}^{N} \mathcal{R}_n$ is an strictly invariant set. However, we are interested in studying next how this strictly invariant set can split into several pieces.

We will translate $\mathcal{O}$ onto the fixed point $P = (x^*, y^*)$ of the map $G_{a,\theta}$ given in (2.38). Afterwards, the change of variables $(x, y) \to (\frac{x}{1-x^*}, \frac{y}{1-x^*})$ turns $\mathcal{C}$ into another critical line whose equation is $x = 1$ in the new coordinates and which will be still denoted by $\mathcal{C}$. The line $\mathcal{L}^*_{-(q-n_1)}$ is turned into the line

$$\mathcal{L}_{a,\theta} \equiv y = x \cot\theta_1 + \rho(a,\theta) \csc\theta_1$$

that crosses $\mathcal{C}$ at an angle θ_1 and whose distance to the origin is

$$\rho(a,\theta) = \frac{\rho_2(a,\theta)}{\rho_1(a,\theta)} = \frac{a^{n_1}(a^q - 2a^{q-n_1}\cos\theta_1 + 1)}{a^q(a^q - 2a^{n_1}\cos\theta_1 + 1)}$$

As usual, we will denote by $\mathcal{K}_{00}$ the region limited by $\mathcal{C}$ and $\mathcal{L}_{a,\theta}$ that contains the new origin. Note that $\lim_{a\to 1} \rho(a,\theta) = 1$ and $\lim_{a\to\infty} \rho(a,\theta) = 0$.

After performing these changes of variables, according to Propositions 2.5.3 and 2.5.5, the dynamics of the restriction of $\Gamma^q_{a,\theta}$ to Δ for $a \in (1, a_1)$ is equivalent to that of the family of Expanding Baker Maps

$$\Psi_{a,\theta} = \mathbf{A}_{a^q,2\theta_1} \circ \mathcal{F}_{\mathcal{L}_{a,\theta},\mathcal{O}} \circ \mathcal{F}_{\mathcal{C},\mathcal{O}} \tag{2.43}$$

Proposition 2.5.7. *Let $\theta = 2\pi p/q \in (0,\pi)$ with $p, q \in \mathbb{N}$ and $\gcd(p,q) = 1$. Assume that $q \geq 5$. Then, under an affine change of coordinates, the map $\Gamma^q_{a,\theta}$ restricted to Δ transforms into the map $\Psi_{a,\theta}$ for all $a \in (1, a_1)$. In other words, the map $\Gamma_{a,\theta}$ is a renormalizable Expanding Baker Map.*

2.5.2 Proof of Theorem 5

As at the beginning of Section 2.4, for each $j = 0, \dots, q-1$ let us denote by Σ^j the ray that starts from $\mathcal{O}$ and extends indefinitely in the direction of $(\cos j\theta_1, \sin j\theta_1)$, and by $\mathcal{R}^j$ the region between Σ^j and Σ^{j+1}, setting $\Sigma^q = \Sigma^0$. It is clear that

$$\Psi_{a,\theta}(\mathcal{R}^j \cap \mathcal{K}_{00}) \subseteq \mathcal{R}^{j+2 \bmod q}$$

In this section, for each $n \geq 1$, we will write $B_n = \Psi^n_{a,\theta}(B)$ for a given point B and $\mathcal{B}_n = \Psi^n_{a,\theta}(\mathcal{B})$ for a given set $\mathcal{B}$. Note that $M_n \in \Sigma^{2n \bmod q}$ whenever $M_n \in \mathcal{K}_{00}$. In Figure 2.20 we represent the position of the line $\mathcal{L}_{a,\theta}$ with respect to the regions $\mathcal{R}^j$, depending on whether q is odd (Figure 2.20a) or even (Figure 2.20b). We will study each case separately.

2.5.2.1 Case $q = 2\nu + 1$

The angle $\theta' = 2\theta_1 \in (0, 4\pi/5]$ verifies the hypotheses of Theorem 4. Note that $\theta'_1 = \theta_1$ since $\gcd(2, q) = 1$. We will revisit its proof with $\delta = a^q > 1$ instead of a. It is immediate to check that $n_1 = \nu + 1$.

Since the angle formed by $\mathcal{L}_{a,\theta}$ and $\mathcal{C}$ is θ_1, the line $\mathcal{L}_{a,\theta}$ is orthogonal to the bisector of the region $\mathcal{R}^{\nu-1}$, which is limited by $\Sigma^{\nu-1}$ and Σ^ν (see Figure 2.20a). Let $r \in \mathbb{N}$ be such that $\mathcal{R}^{\nu-1} = \mathbf{A}^r_{1,2\theta_1}(\mathcal{R}^0)$. If ν is odd, then $r = (\nu-1)/2$, otherwise $r = 3\nu/2$. Note that in the latter case the iterates $\mathbf{A}^j_{1,2\theta_1}(\mathcal{R}^0)$ with $j = 0, \dots, r$ describe a full rotation.

Lemma 2.5.8. *There exists $\delta_M > 1$ such that for all $1 < \delta = a^q < \delta_M$ it holds that:*

(i) $M_n, H_n \in \{x \leq 1\}$ *for* $n = 1, \dots, q-1$

(ii) $\mathcal{F}_{\mathcal{L}_{a,\theta},\mathcal{O}}(M_n) = M_n$ *for* $n = 1, \dots, q-1$

(iii) $\mathcal{F}_{\mathcal{L}_{a,\theta},\mathcal{O}}(H_n) = H_n$ *for all* $n \in \{1, \dots, q-1\} \setminus \{r\}$ *and* $\mathcal{F}_{\mathcal{L}_{a,\theta},\mathcal{O}}(H_r) \neq H_r$

Proof. Assuming that $\{M_1, \dots, M_{n-1}\} \subseteq \mathcal{K}_{00}$ for any $2 \leq n < q$, then

$$M_n = (\delta^n \cos 2n\theta_1, \delta^n \sin 2n\theta_1)$$

Therefore, it suffices to find a δ-value δ_M such that

$$\delta^n \cos 2n\theta_1 \leq 1 \tag{2.44}$$

and

$$-\delta^n \cos(2n+1)\theta_1 \leq \rho(\delta) \tag{2.45}$$

for $n = 1, \dots, q-1$ and every $\delta \in (1, \delta_M]$. If $\cos 2n\theta_1 \leq 0$, then inequality (2.44) clearly holds for all $\delta > 1$. Otherwise, we have that $\cos 2n\theta_1 < 1$ because $\gcd(2, q) = 1$. Let

$$\delta'_M = \min_{\cos 2n\theta_1 > 0} \sqrt[n]{\sec 2n\theta_1}$$

On the other hand, if $\cos(2n+1)\theta_1 \geq 0$, then inequality (2.45) clearly holds for all $\delta > 0$. Otherwise, we have that $\cos(2n+1)\theta_1 > -1$ because $\gcd(2, q) = 1$. Since $\delta^n/\rho(\delta) \to 1$ as $\delta \to 1$, then there exists $\delta_n > 1$ such that inequality (2.45) holds for all $\delta \in (1, \delta_n]$.

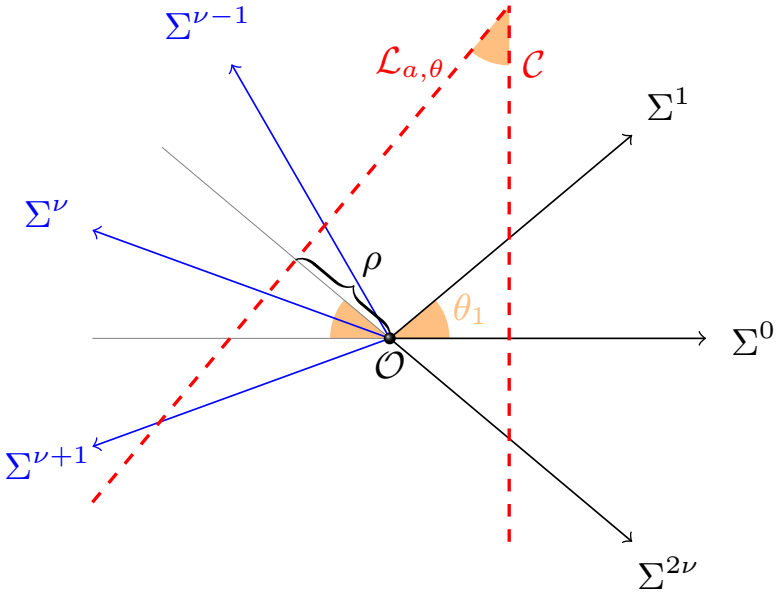

(a)

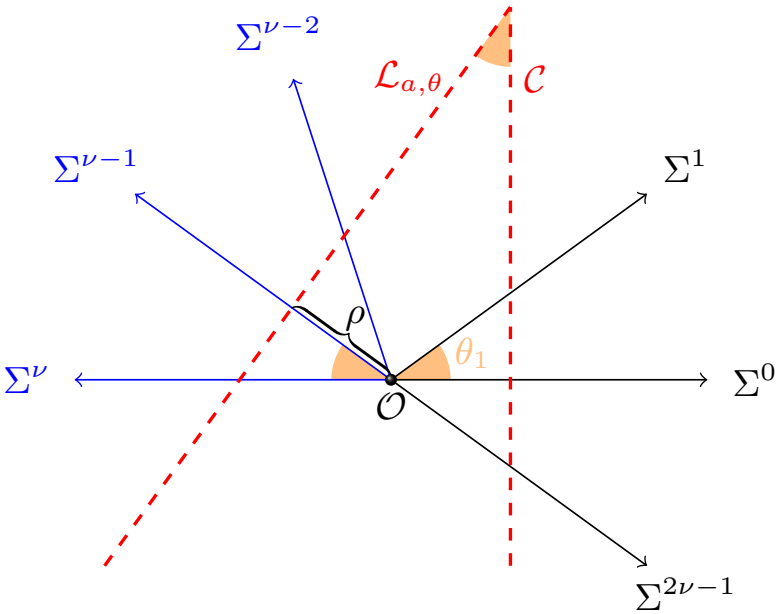

(b)

Figure 2.20: Relative position of $\mathcal{L}_{a,\theta}$ with $\theta = 2\pi p/q \in (0, \pi)$: (a) Case $q = 2\nu + 1$; (b) Case $q = 2\nu$

Therefore, it suffices to take δ_M the minimum of those values δ_n and δ'_M. Then, we have that $\delta_M > 1$ and inequalities (2.44) and (2.45) hold for every $\delta \in (1, \delta_M]$. This proves statement (i). Statement (ii) is a consequence of statement (i). Statement (iii) is proved proceeding as in statement 2.5.8. It holds that $H_n \in \mathcal{K}_{00}$ if and only if

$$\delta^{n+\nu+1} \sin(2n+1)\theta_1 \leq \delta^n \sin(2n+2)\theta_1 + \rho(\delta) \sin\theta_1 \tag{2.46}$$

Up to reducing δ_M if necessary, inequality (2.46) holds for all $n \neq r$. For $n = r$, inequality (2.46) does not hold for any $\delta > 1$ because $\cos\theta_1/2 < 1$. □

Let us take the points $M_r \in \Sigma^{\nu-1}$ and $M_{r+n_1} \in \Sigma^{\nu}$, respectively. Whether ν is even or odd, the distance from these points to the origin is less than δ^q. The orthogonal lines through M_r and M_{r+n_1} to the respective rays $\Sigma^{\nu-1}$ and Σ^{ν} intersect each other at the point H_r. According to Lemma 2.5.8, the line $\mathcal{L}_{a,\theta}$ intersects the polygon

$$\Omega(\mathcal{O}, M_r, H_r, M_{r+n_1})$$

at two points $H_r^- \in \overline{M_{r+n_1} H_r}$ and $H_r^+ \in \overline{H_r M_r}$. See Figure 2.21.

Before proving statement (a), note that, if the fold $\mathcal{F}_{\mathcal{L}_{a,\theta},\mathcal{O}}$ does not intervene, the map $\Psi_{a,\theta}$ behaves as $\Gamma_{a^q,2\theta_1}$. Therefore, we will try to construct the set $\mathcal{D}'$ from another polygon Δ as in (2.25). Then,

$$\mathcal{F}_{\mathcal{C},\mathcal{O}}(\Delta) = \Omega(\mathcal{O}, M, H, M_{n_1})$$

as in Figure 2.14, and

$$\Delta_1 = \Omega(\mathcal{O}, M_1, H_1, M_{n_1+1})$$

In the case $r = (\nu-1)/2$, we obtain

$$\Delta_r = \Omega(\mathcal{O}, M_{n_1+r}, H_r, M_r)$$

Now, in order to obtain Δ_{r+1}, it is necessary to consider the fold $\mathcal{F}_{\mathcal{L}_{a,\theta},\mathcal{O}}$ that leads to

$$\mathcal{F}_{\mathcal{L}_{a,\theta},\mathcal{O}}(\Delta_r) = \Omega(\mathcal{O}, M_r, H_r^+, H_r^-, M_{n_1+r})$$

where H_r^+ and H_r^- are the points given in Lemma 2.5.8. Then,

$$\Delta_{r+1} = \Omega(\mathcal{O}, M_{n_1+1}, H_{r+1}^+, H_{r+1}^-, M_{n_1+r+1})$$

and

$$\Delta_\nu = \Omega(\mathcal{O}, M_q, H_\nu^+, H_\nu^-, M_\nu)$$

See Figure 2.21a and compare with Figure 2.14. Of course, the iterate Δ_ν is contained in

$$\Gamma_{\delta,\theta}^{\nu}(\Delta) = \Omega(\mathcal{O}, M_\nu, H_\nu, M_q)$$

Note that Δ_ν would coincide with $\Gamma_{\delta,\theta}^{\nu}(\Delta)$ if the fold $\mathcal{F}_{\mathcal{L}_{a,\theta},\mathcal{O}}$ had not intervened. After applying to both Δ_ν and $\Gamma_{\delta,\theta}^{\nu}(\Delta)$ the fold $\mathcal{F}_{\mathcal{C},\mathcal{O}}$ and the iteration $\Psi_{a,\theta}^{\nu+1}$, we obtain

$$\Delta_q \subseteq \Gamma_{\delta,\theta}^{q}(\Delta) = \Delta$$

In the case $r = 3\nu/2$, the fold $\mathcal{F}_{\mathcal{L}_{a,\theta},\mathcal{O}}$ does not intervene before the νth iterate and therefore $\Delta_\nu = \Gamma_{\delta,\theta}^{\nu}(\Delta)$. See Figure 2.21b. In fact,

$$\Delta_{\nu+j} = \Gamma_{\delta,\theta}^{\nu+n}(\Delta), \qquad n = 0, 1, \ldots, \tfrac{\nu}{2}$$

We have that $\mathcal{F}_{\mathcal{L}_{a,\theta},\mathcal{O}}(\Delta_r) \subseteq \Gamma_{\delta,\theta}^{r}(\Delta)$, and therefore

$$\Delta_{\nu+n} \subseteq \Gamma_{\delta,\theta}^{\nu+n}(\Delta), \qquad n = 0, 1, \ldots, n_1$$

In conclusion, we obtain for the map $\Psi_{a,\theta}$ given in (2.43) the following result, which is similar to Proposition 2.4.4.

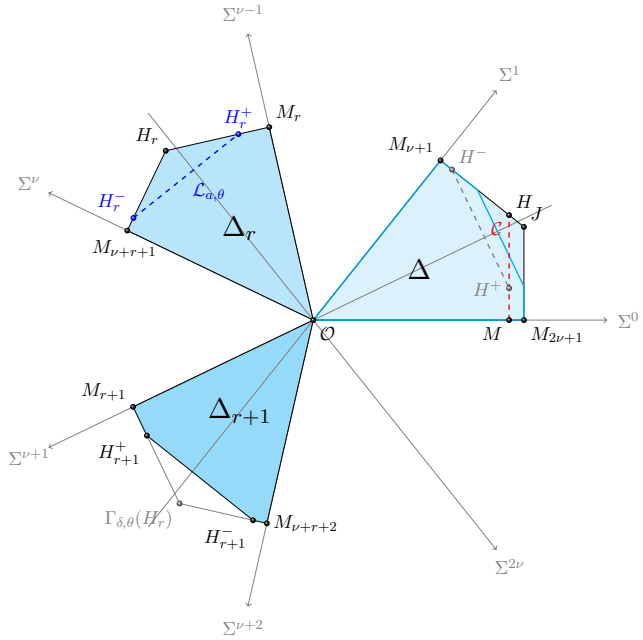

(a)

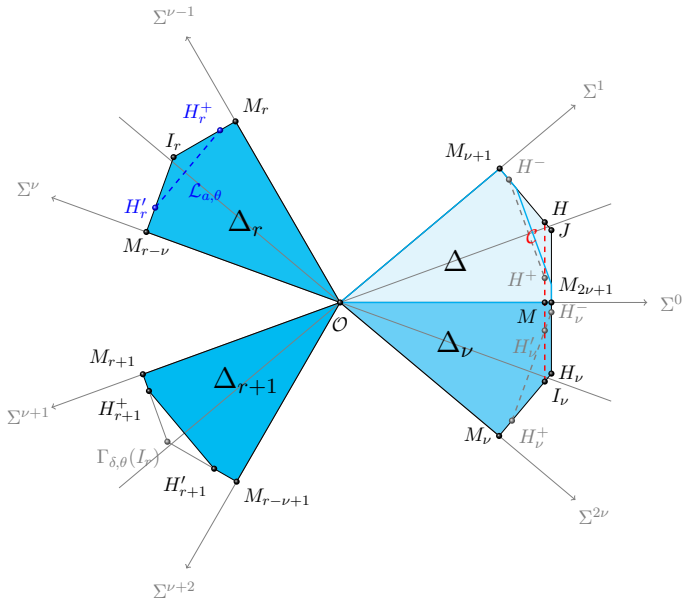

(b)

Figure 2.21: Case $q = 2\nu + 1$: (a) $r = (\nu - 1)/2$ if ν odd; (b) $r = 3\nu/2$ if ν even

Proposition 2.5.9. *Let $\theta = 2\pi p/q \in (0,\pi)$ with $p,q \in \mathbb{N}$ and $\gcd(p,q) = 1$. Assume that $q \geq 5$. If q is odd, then there exists $1 < \delta_1 < \delta_M$ such that, for all $1 < \delta = a^q < \delta_1$, the following hold:*

(i) $\Delta_q \subseteq \Delta$, *i.e.* Δ *is* $\Psi_{a,\theta}^q$*-invariant.*

(ii) $\Delta_n \cap \{x > 1\} = \varnothing$ *for every* $n \in \{1,\dots,q-1\} \setminus \{(q-1)/2\}$.

(iii) $\mathcal{F}_{\mathcal{L}_{a,\theta},\mathcal{O}}(\Delta_n) = \Delta_n$ *for every* $n \in \{1,\dots,q-1\} \setminus \{r\}$.

As in the proof of Theorem 4, we construct the set

$$\widehat{\mathcal{D}} = \Delta^{\varepsilon} = \Delta \cap \{y \geq \varepsilon\} \tag{2.47}$$

verifying statement (a) of Theorem 4 for $\Psi_{a,\theta}$, which proves statement (a) of Theorem 5.

Remark 2.5.10. We have seen that each one of the q disjoint pieces $\mathcal{D}_j$ that contain the strange attractor for $\Gamma_{a,\theta}$ for $1 < a < a_1$ splits itself into another q pieces $\widehat{\mathcal{D}}_i$ when $1 < a < a_2 < a_1$, thus giving rise to q^2 disjoint pieces that contain the strange attractor for $\Gamma_{a,\theta}$. When considering the restriction of $\Gamma_{a,\theta}^{q^2}$ on each one of these q^2 pieces, it is necessary to take into account the fold $\mathcal{F}_{\mathcal{L}_{a,\theta},\mathcal{O}}$. Then, by applying Lemma 2.1.6 we obtain the restriction of $\Gamma_{a,\theta}^{q^2}$ as a three-fold Expanding Baker Map.

2.5.2.2 Case $q = 2\nu$

In this case, the line $\mathcal{L}_{a,\theta}$ is orthogonal to the ray $\Sigma^{\nu-1}$ limiting the regions $\mathcal{R}^{\nu-2}$ and $\mathcal{R}^{\nu-1}$. See Figure 2.20b. We will distinguish two cases: ν odd or even, according to statements (i) and (ii) of (b) of Theorem 5. If ν is odd, by merging two consecutive regions $\mathcal{R}^j$ into ν pairs we can proceed similarly to the case q odd. If ν is even, we will find two different restrictive domains whose iterates are contained in the regions of odd and even indices, respectively.

Case ν odd. Assume first that ν is odd. Then, we will follow the steps in the proof of Theorem 4 for map (2.43). Let us take the domains

$$\widehat{\mathcal{R}}^j = \mathcal{R}^{2j} \cup \mathcal{R}^{2j+1}, \qquad j = 0,\dots,\nu-1$$

and $\widehat{\mathcal{R}}^{\nu} = \widehat{\mathcal{R}}^0$. Since $\theta' = 2\pi/\nu$, then $n_1 = 1$. Therefore,

$$\Psi_{a,\theta}(\widehat{\mathcal{R}}^j \cap \mathcal{K}_{00}) \subseteq \widehat{\mathcal{R}}^{j+1}, \qquad j = 0,\dots,\nu-1$$

We will consider two cases: $q \geq 10$ and $q = 6$, depending on whether Σ^2 is contained in the first or second quadrant, respectively.

Case $\nu \geq 5$. In $\widehat{\mathcal{R}}^0$ let us take the strictly $\Gamma_{\delta,\theta}$-invariant polygon

$$\Delta = \Omega(\mathcal{O}, (\delta^{\nu}, 0), J, M_1)$$

for all $1 < \delta \leq \delta_\theta$. We will find $1 < \delta_1 \leq \delta_\theta$ such that $\Delta_\nu \subseteq \Delta$ for all $1 < \delta \leq \delta_1$.

Lemma 2.5.11. *There exists $\delta_M > 1$ such that for all $1 < \delta = a^q < \delta_M$ it holds that:*

(i) $M_n, H_n \in \{x \leq 1\}$ *for all* $n = 1,\dots,q/2-1$

(ii) $\mathcal{F}_{\mathcal{L}_{a,\theta},\mathcal{O}}(M_n) = M_n$ *for all* $n \in \{1,\dots,q/2-1\} \setminus \{(q-2)/4\}$

(iii) $\mathcal{F}_{\mathcal{L}_{a,\theta},\mathcal{O}}(H_n) = H_n$ *for all* $n \in \{1,\dots,q/2-1\} \setminus \{(q-6)/4, (q-2)/4\}$

According to Lemma 2.5.11, we can proceed as in the proof of Theorem 4 to obtain

$$\Delta_n = \Gamma_{\delta,\theta}^n(\Delta), \qquad n = 1, \dots, \tfrac{\nu-3}{2}$$

Since the line $\mathcal{L}_{a,\theta}$ intersects the interior of $\Delta_{(\nu-3)/2}$, we have to consider the fold $\mathcal{F}_{\mathcal{L}_{a,\theta},\mathcal{O}}$ to obtain $\Delta_{(\nu-1)/2}$. If $\mathcal{F}_{\mathcal{L}_{a,\theta},\mathcal{O}}$ is a good fold for $\Delta_{(\nu-3)/2}$, then

$$\mathcal{F}_{\mathcal{L}_{a,\theta},\mathcal{O}}(\Delta_{\frac{\nu-3}{2}}) = \Omega(\mathcal{O}, M_{\frac{\nu-3}{2}}, H'_{\frac{\nu-3}{2}}, M'_{\frac{\nu-1}{2}})$$

where $H'_{(\nu-3)/2}$ and $M'_{(\nu-1)/2}$ are the intersection points of $\mathcal{L}_{a,\theta}$ with $\mathcal{L}_{(\nu-3)/2}$ and $\mathcal{L}_{(\nu-1)/2}$, respectively. Thus,

$$\Delta_{(\nu-1)/2} = \Omega(\mathcal{O}, M_{\frac{\nu-1}{2}}, H'_{\frac{\nu-1}{2}}, M'_{\frac{\nu+1}{2}})$$

The line $\mathcal{L}_{a,\theta}$ also intersects the interior of $\Delta_{(\nu-1)/2}$ and consequently we have to consider the fold $\mathcal{F}_{\mathcal{L}_{a,\theta},\mathcal{O}}$ to obtain $\Delta_{(\nu+1)/2}$. If $\mathcal{F}_{\mathcal{L}_{a,\theta},\mathcal{O}}$ is a good fold for $\Delta_{(\nu-1)/2}$, then

$$\mathcal{F}_{\mathcal{L}_{a,\theta},\mathcal{O}}(\Delta_{\frac{\nu-1}{2}}) = \Omega(\mathcal{O}, M'_{\frac{\nu-1}{2}}, H''_{\frac{\nu-1}{2}}, M'_{\frac{\nu+1}{2}})$$

where $H''_{(\nu-1)/2}$ is the intersection point of $\mathcal{L}_{a,\theta}$ and $\mathbf{A}_{\delta,\theta}(\mathcal{L}_{a,\theta})$. Thus,

$$\Delta_{(\nu+1)/2} = \Omega(\mathcal{O}, M_{\frac{\nu+1}{2}}, H''_{\frac{\nu+1}{2}}, M'_{\frac{\nu+3}{2}})$$

In the next lemma we prove that this is the case for all δ sufficiently close to 1.

Lemma 2.5.12. *There exists $\delta_H > 1$ such that*

$$\mathcal{F}_{\mathcal{L}_{a,\theta},\mathcal{O}}(H_{\frac{\nu-3}{2}}) \in \Delta_{\frac{\nu-3}{2}}$$

and

$$\mathcal{F}_{\mathcal{L}_{a,\theta},\mathcal{O}}(H'_{\frac{\nu-1}{2}}) \in \Delta_{\frac{\nu-1}{2}}$$

for every $\delta \in (1, \delta_H]$.

Hence $\Delta_{(\nu+1)/2} \subseteq \Gamma_{\delta,\theta}^{(\nu+1)/2}(\Delta)$. Since the fold $\mathcal{F}_{\mathcal{L}_{a,\theta},\mathcal{O}}$ does not intervene in the rest of the iterates of Δ, we can proceed as in the proof of Theorem 4 to obtain

$$\Delta_n \subseteq \Gamma_{\delta,\theta}^n(\Delta), \qquad n = \tfrac{\nu+1}{2}, \dots, \nu$$

In particular, since $\Gamma_{\delta,\theta}^{\nu}(\Delta) = \Delta$, then $\Delta_\nu \subseteq \Delta$.

Theorem 2.5.13. *Let $\theta = 2\pi p/q \in (0, \pi)$ with $p, q \in \mathbb{N}$ and $\gcd(p, q) = 1$. Assume that q is even and $q \geq 10$. If $q/2$ is odd, then there exists $\delta_\theta > 1$ such that for every $\delta \in (1, \delta_\theta]$, the following hold:*

(i) $\Delta_{q/2} \subseteq \Delta$, *i.e.* Δ *is* $\Psi_{a,\theta}^{q/2}$*-invariant.*

(ii) $\Delta_n \cap \{x > 1\} = \varnothing$ *for every* $n \in \{1, \dots, q/2 - 2\}$

(iii) $\mathcal{F}_{\mathcal{L}_{a,\theta},\mathcal{O}}(\Delta_n) = \Delta_n$ *for every* $n \in \{1, \dots, q/2 - 1\} \setminus \{(q-6)/4, (q-2)/4\}$

Therefore, taking again $\widehat{\mathcal{D}}$ as in (2.47) we obtain statement (a) of Theorem 4 for $\Psi_{a,\theta}$ or, equivalently, statement (b) of Theorem 5.

Remark 2.5.14. In this case, each one of the q disjoint pieces $\mathcal{D}_j$ that contain the strange attractor of $\Gamma_{a,\theta}$ for $1 < a < a_1$ splits now into $q/2$ new pieces $\widehat{\mathcal{D}}_i$ when $1 < a < a_2 < a_1$, thus giving rise to $q^2/2$ disjoint pieces in which the strange attractor of $\Gamma_{a,\theta}$ is contained. When considering the restriction of $\Gamma_{a,\theta}^{q^2/2}$ on each one of these $q^2/2$ pieces, it is necessary to take into account the fold along the line $\mathcal{F}_{\mathcal{L}_{a,\theta},\mathcal{O}}$. If this fold intervenes in the dynamics, then again by Lemma 2.1.6 we know that this restriction $\Gamma_{a,\theta}^{q^2/2}$ is a three-fold Expanding Baker Map.

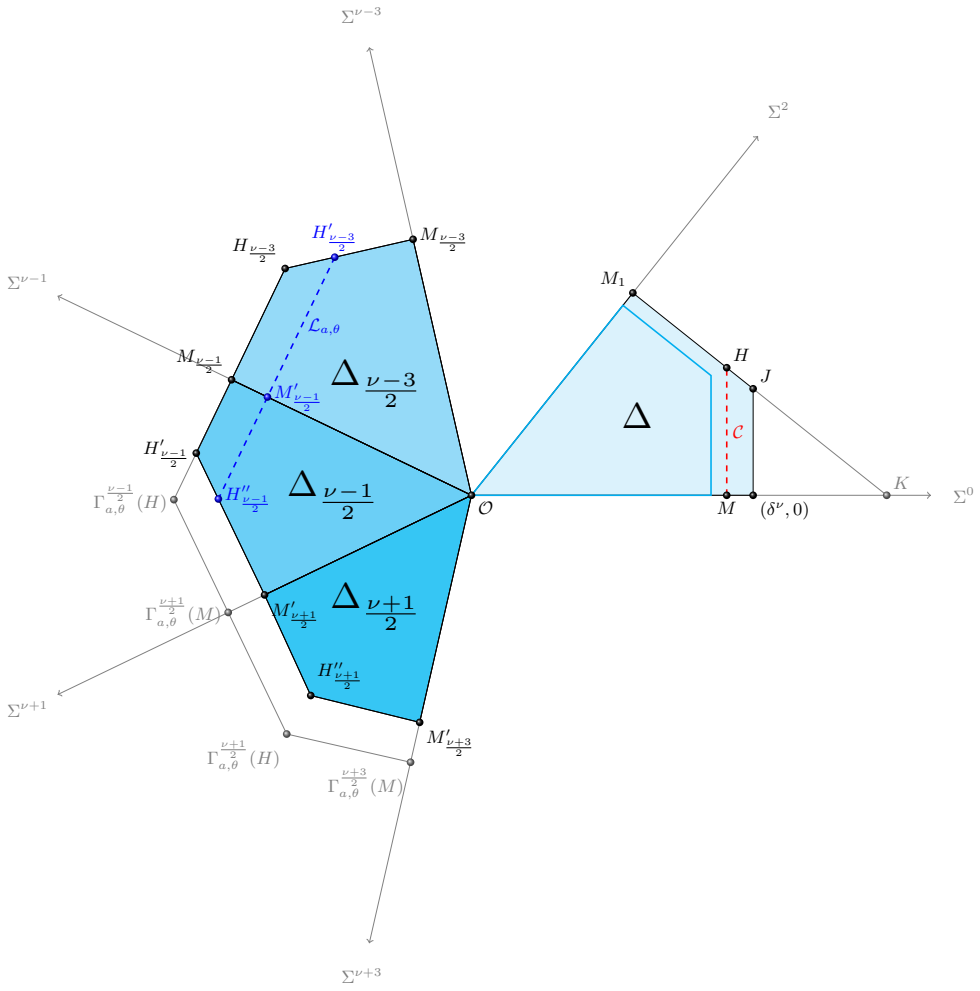

Figure 2.22: Case $q = 2\nu$ with ν odd: The $\Psi^{\nu}_{a,\theta}$-invariant polygon $\Delta = \Omega(\mathcal{O}, (\delta^\nu, 0), J, M_1)$

Case $\nu = 3$. Since $2p < 6$ and $\gcd(p, 6) = 1$, then $p = 1$ and $\theta = \pi/3$. In this case, the line $\mathcal{L}_{a,\theta}$ is orthogonal to the ray Σ^2 and parallel to

$$\mathcal{C}_1 \equiv -\tfrac{1}{2}x + \tfrac{\sqrt{3}}{2}y = \delta = a^6$$

It is easy to check that $\delta > \rho$ for all $\delta > 1$. Proceeding as in Subsection 2.4, we will construct a strictly $\Psi^3_{a,\theta}$-invariant set Δ from

$$\Delta' = \Omega(\mathcal{O}, M, A, M_1)$$

In this case, the fold $\mathcal{F}_{\mathcal{L}_{a,\theta},\mathcal{O}}$ will intervene in the first and second iterates of both Δ' and Δ. Check Figure 2.23 along our next discussion. Given a point Q, we will write $\widehat{Q}$ for $\mathcal{F}_{\mathcal{L}_{a,\theta},\mathcal{O}} \circ \mathcal{F}_{\mathcal{C},\mathcal{O}}(Q)$.

By construction, the set Δ' is contained in $\{x \leq 1\}$. In order that $\mathcal{F}_{\mathcal{L}_{a,\theta},\mathcal{O}}(\Delta') \subseteq \mathcal{R}^0$, we need to impose that $\widehat{M_1} \in \Sigma^1$, which is equivalent to $\delta \leq 2\rho$. Then,

$$\mathcal{F}_{\mathcal{L}_{a,\theta},\mathcal{O}}(\Delta') = \Omega(\mathcal{O}, M, C, \widehat{A}, B, D)$$

where:

- C is the intersection point of $\mathcal{C}$ and the symmetric line of $\mathcal{C}_1$ with respect to $\mathcal{L}_{a,\theta}$

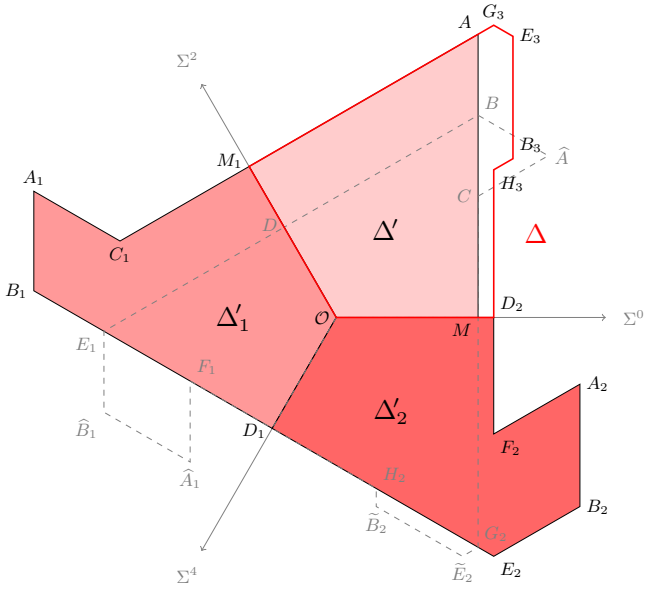

(a)

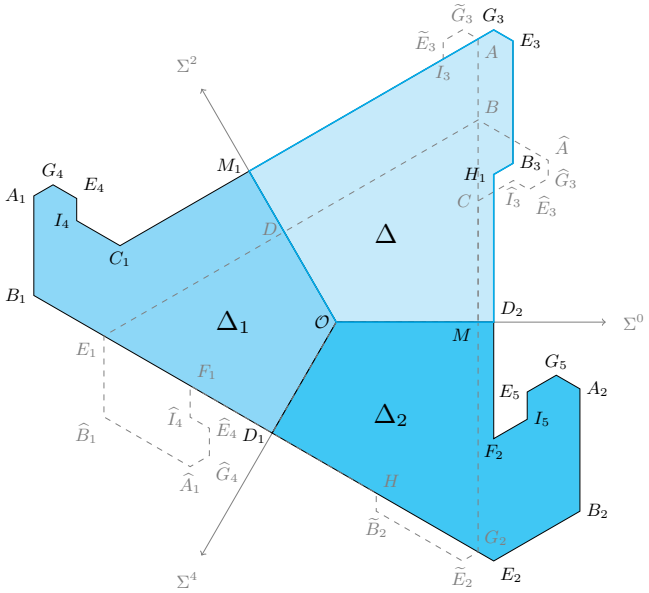

(b)

Figure 2.23: The strictly $\Psi^3_{a,\pi/3}$-invariant polygon $\Delta = \Omega(\mathcal{O}, D_2, H_1, B_3, E_2, G_1, M_1)$: (a) Orbit of Δ'; (b) Orbit of Δ

- B is the intersection point of $\mathcal{C}$ and $\mathcal{L}_{a,\theta}$
- D is the intersection point of Σ^1 and $\mathcal{L}_{a,\theta}$

Now,

$$\Delta'_1 = \Omega(\mathcal{O}, M_1, C_1, A_1, B_1, D_1)$$

It is clear that $\Delta'_1 \subseteq \{x \leq 0\}$. Folding Δ'_1 with respect to $\mathcal{L}_{a,\theta}$, we obtain

$$\mathcal{F}_{\mathcal{L}_{a,\theta},\mathcal{O}}(\Delta'_1) = \Omega(\mathcal{O}, D, E_1, \widehat{B}_1, \widehat{A}_1), F_1, D_1)$$

where:

- E_1 is the intersection point of $\mathcal{L}_{a,\theta}$ and $\mathbf{A}_{a,\theta}(\mathcal{L}_{a,\theta})$
- F_1 is the intersection point of $\mathbf{A}_{a,\theta}(\mathcal{L}_{a,\theta})$ and the symmetric line of $\mathcal{C}_1$ with respect to $\mathcal{L}_{a,\theta}$

Thus,

$$\Delta'_2 = \Omega(\mathcal{O}, D_1, E_2, B_2, A_2, F_2, D_2)$$

Now, the iterate Δ'_2 is not contained in $\{x \leq 1\}$. In order that $\mathcal{F}_{\mathcal{C},\mathcal{O}}(\Delta'_2) \subseteq \mathcal{R}^2$, we need to impose that $\widetilde{A}_2 \in \mathcal{R}^2$. In that case,

$$\mathcal{F}_{\mathcal{C},\mathcal{O}}(\Delta'_2) = \Omega(\mathcal{O}, D_1, H_2, \widetilde{B}_2, \widetilde{E}_2, G_2, M)$$

where H_2 is the intersection point of $\mathbf{A}_{a,\theta}(\mathcal{L}_{a,\theta})$ and the symmetric line of $\mathbf{A}^2_{a,\theta}(\mathcal{L}_{a,\theta})$ with respect to $\mathcal{C}$. Therefore,

$$\Delta'_3 = \Omega(\mathcal{O}, D_2, H_3, B_3, E_3, G_3, M_1)$$

The following lemma guarantees that this reasoning applies for all δ sufficiently close to 1.

Lemma 2.5.15. *There exists $\delta_H > 1$ such that*

$$\widehat{M}_1 \in \Delta', \qquad \widehat{C}_1 \in \Delta'_1, \qquad \widetilde{A}_2 \in \Delta'_2$$

for every $\delta \in (1, \delta_H]$.

In the following proposition we will prove that the set $\Delta = \Delta'_3$ is strictly $\Psi^3_{a,\theta}$-invariant.

Proposition 2.5.16. *Let $\theta = \pi/3$. Then, there exists $\delta_\theta > 1$ such that, for every $\delta \in (1, \delta_\theta)$, the following hold:*

(i) $\Delta_3 = \Delta$, *i.e.* Δ *is strictly* $\Psi^3_{a,\theta}$*-invariant.*

(ii) $\Delta_2 \cap \{x > 1\} = \varnothing$.

Proof. Note that $\mathcal{F}_{\mathcal{C},\mathcal{O}}$ is a bad fold for Δ and

$$\mathcal{F}_{\mathcal{C},\mathcal{O}}(\Delta) = \Omega(\mathcal{O}, M, A, \widetilde{G}_3, \widetilde{E}_3, I_3, M_1)$$

where I_3 is the intersection point of $\mathcal{L}_1$ and the vertical line through $\widetilde{E}_3$. The fold $\mathcal{F}_{\mathcal{L}_{a,\theta},\mathcal{O}}$ is a bad fold for $\mathcal{F}_{\mathcal{C},\mathcal{O}}(\Delta)$ and

$$\mathcal{F}_{\mathcal{L}_{a,\theta},\mathcal{O}} \circ \mathcal{F}_{\mathcal{C},\mathcal{O}}(\Delta) = \Omega(\mathcal{O}, M, C, \widehat{I}_3, \widehat{E}_3, \widehat{G}_3, \widehat{A}, B, D)$$

Thus,

$$\Delta_1 = \Omega(\mathcal{O}, M_1, C_1, I_4, E_4, G_4, A_1, B_1, D_1)$$

It is clear that $\Delta_1 \subseteq \{x \leq 0\}$. Hence $\mathcal{F}_{\mathcal{C},\mathcal{O}}(\Delta_1) = \Delta_1$. Now, the fold $\mathcal{F}_{\mathcal{L}_{a,\theta},\mathcal{O}}$ is a bad fold for Δ_1 and

$$\mathcal{F}_{\mathcal{L}_{a,\theta},\mathcal{O}}(\Delta_1) = \Omega(\mathcal{O}, D, E, \widehat{B}_4, \widehat{A}_1, \widehat{G}_2, \widehat{E}_4, \widehat{I}_4, F_1, D_1)$$

Then,

$$\Delta_2 = \Omega(\mathcal{O}, D_1, E_1, B_5, A_2, G_3, E_5, I_5, F_2, D_2)$$

Since $\mathcal{F}_{\mathcal{C},\mathcal{O}}(\Delta_2) = \mathcal{F}_{\mathcal{C},\mathcal{O}}(\Delta_2')$, then $\Delta_3 = \Delta_3' = \Delta$. □

As in the previous cases, the proof of statement (a) of Theorem 4 for $\nu = 3$ concludes by taking $\widehat{\mathcal{D}} = \Delta \cap \{y \geq \varepsilon\}$ for $\varepsilon > 0$ sufficiently small.

Case ν even. Finally, let us suppose that ν is even. In this case, we construct the triangles

$$\Delta^+ = \Omega(\mathcal{O}, K, M^+), \quad \Delta^- = \Omega(\mathcal{O}, M^-, K)$$

where

$$M^\pm = (l\cos\theta_1, \pm l\sin\theta_1)$$

with $1 < l < \sec\theta_1$ and $K = (l\sec\theta_1, 0)$. Note that $l\cos\theta_1 < 1$ and $l\sec\theta_1 > 1$. The orthogonal lines to the rays Σ^1 and $\Sigma^{2\nu-1}$ through M^+ and M^-, respectively, intersect Σ^0 at K. The critical line $\mathcal{C}$ intersects $\Delta^\pm$ at $M = (1, 0)$ and

$$H^\pm = (1, \pm l\csc\theta_1 \mp \cot\theta_1)$$

respectively. See Figure 2.24.

Arguments as in the proofs of Lemma 2.4.1 and Lemma 2.5.8 allows to prove the next result.

Lemma 2.5.17. *There exists $\delta_M > 1$ such that for all $1 < \delta = a^q < \delta_M$ the following statements hold:*

(i) For $j = 0, 1, \ldots, q/2 - 1$, the points M_j and $M_j^\pm$ belong to the half-plane $\{x \leq 1\}$

(ii) $\mathcal{F}_{\mathcal{L}_{a,\theta},\mathcal{O}}(M_j^+) = M_j^+$ for all $j \neq q/4 - 1$ and $\mathcal{F}_{\mathcal{L}_{a,\theta},\mathcal{O}}(M_{q/4-1}^+) \neq M_{q/4-1}^+$

(iii) $\mathcal{F}_{\mathcal{L}_{a,\theta},\mathcal{O}}(M_j^-) = M_j^-$ for all $j \neq q/4 - 1$ and $\mathcal{F}_{\mathcal{L}_{a,\theta},\mathcal{O}}(M_{q/4}^-) \neq M_{q/4}^-$

It is clear that $M_{\nu/2} \in \Sigma^\nu$, while $M_{\nu/2}^- \in \Sigma^{\nu-1}$ and $M_{\nu/2-1}^+ \in \Sigma^{\nu-1}$. The respective distances from these points to the origin are $\delta^{\nu/2}$, $l\delta^{\nu/2}$, and $l\delta^{\nu/2-1}$.

Theorem 2.5.18. *Let $\theta = 2\pi p/q \in (0, \pi)$ with $p, q \in \mathbb{N}$ and $\gcd(p, q) = 1$. Assume that q is even and $q \geq 8$. If $q/2$ is even, then there exists $\delta_1 > 1$ such that for every $\delta \in (1, \delta_1]$, the following hold:*

(i) $\Delta_{q/2}^\pm \subseteq \Delta^\pm$, i.e. $\Delta^\pm$ are $\Psi_{a,\theta}^{q/2}$-invariant.

(ii) $\Delta_n^\pm \cap \{x > 1\} = \varnothing$ for every $n \in \{1, \ldots, q/2 - 1\}$

(iii) $\mathcal{F}_{\mathcal{L}_{a,\theta},\mathcal{O}}(\Delta_n^+) = \Delta_n^+$ for every $n \in \{1, \ldots, q/2 - 1\} \setminus \{q/4\}$ and $\mathcal{F}_{\mathcal{L}_{a,\theta},\mathcal{O}}(\Delta_n^-) = \Delta_n^-$ for every $n \in \{1, \ldots, q/2 - 1\} \setminus \{q/4 + 1\}$.

Proof. Let us first consider the triangle Δ^+ to analyse the different iterates Δ_n^+ under $\Psi_{a,\theta}$. The segment $\overline{\mathcal{O}M}$ returns into Σ^0 after ν iterates. According to Lemma 2.5.17, in each of these iterates it does not undergo any fold and thus returns with a length of $\delta^\nu > 1$. On the other hand, the segment $\overline{\mathcal{O}M^+}$ also returns into Σ^1 after ν iterates, but it is folded by $\mathcal{F}_{\mathcal{L}_{a,\theta},\mathcal{O}}$ in its $\nu/2$th iterate. Therefore, the segment $\overline{\mathcal{O}M^+}$ returns into Σ^1 with

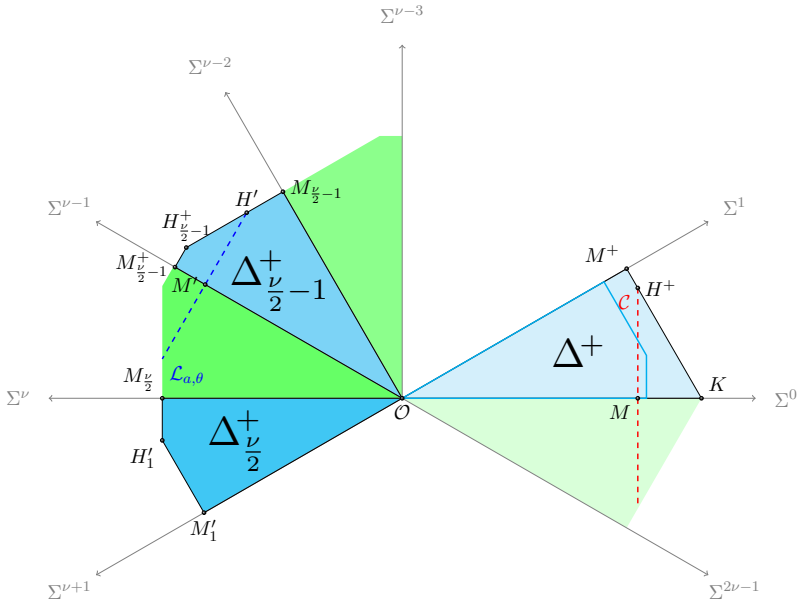

(a)

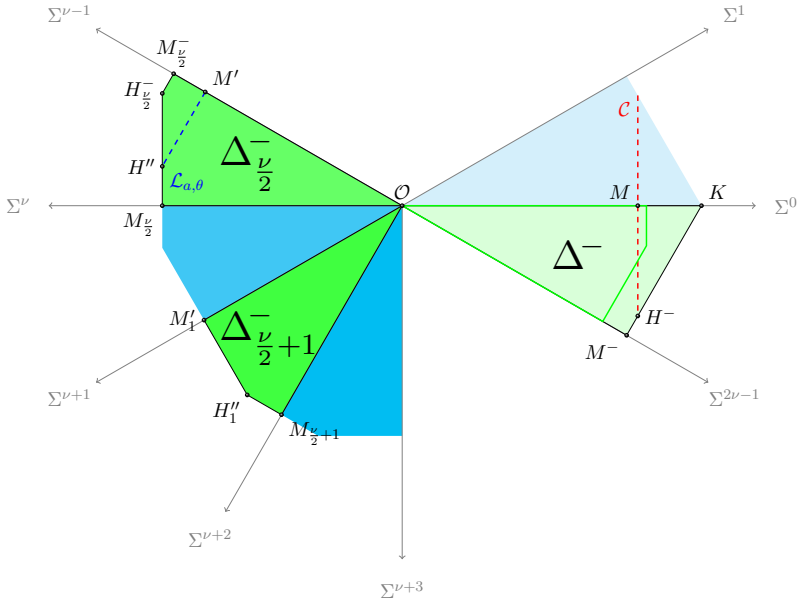

(b)

Figure 2.24: Case $q = 2\nu$ with ν even: There exist two disjoint restrictive domains respectively contained in Δ^+ and Δ^-

a length of $\rho(a)\delta^{\nu/2+1}$. Therefore, in order that Δ_ν^+ is contained in Δ^+, it is enough to take $\delta^\nu < l\sec\theta_1$ and $\rho\delta^{\nu/2+1} < l$. Since

$$\lim_{a\to 1}\delta^\nu = \lim_{a\to 1}\rho\delta^{\frac{\nu}{2}+1} = 1$$

we conclude that there exists $\delta_1 \leq \delta_M$ such that $\Delta_\nu^+ \subseteq \Delta^+$ for all $1 < \delta = a^q < \delta_1$.

Let us now consider the triangle Δ^-. The segment $\overline{\mathcal{O}M^-}$ returns into $\Sigma^{2\nu-1}$ after ν iterates, but it is folded by $\mathcal{F}_{\mathcal{L}_{a,\theta},\mathcal{O}}$ in its $(\nu/2+1)$th iterate. Therefore, the segment $\overline{\mathcal{O}M^-}$ returns into $\Sigma^{2\nu-1}$ with a length of $\rho\delta^\nu$. Therefore, the same value δ_1 in the previous case is valid to guarantee that $\Delta_\nu^- \subseteq \Delta^-$ for all $1 < \delta = a^n < \delta_1$. □

Moreover, the restriction of $\Psi_{a,\theta}^\nu$ to Δ_ν^+ is again an Expanding Baker Map of at most two folds. Taking $\mathcal{D}' = \Delta_\nu^+ \cap \{y \geq \varepsilon\}$ as in (2.47), we conclude that $\mathcal{D}'$ verifies the first three statements of Theorem 4, and the restriction of $\Psi_{a,\theta}^\nu$ to $\mathcal{D}'$ belongs to the set $\mathbb{F}_{a,\theta}$. Then again, the restriction of $\Psi_{a,\theta}^\nu$ to Δ_ν^- is an Expanding Baker Map of at most two folds. Taking $\mathcal{D}' = \Delta_\nu^- \cap \{y \leq -\varepsilon\}$ as in (2.47), we conclude that $\mathcal{D}'$ verifies the first three statements of Theorem 4, and the restriction of $\Psi_{a,\theta}^\nu$ to $\mathcal{D}'$ belongs to the set $\mathbb{F}_{a,\theta}$. The proof of statement (ii) of (b) of Theorem 5 is complete.

2.6 Statistical Properties of the 2-D Tent Maps

In this section we study the statistical properties of one-parameter families of *piecewise expanding maps* with *bounded distortion* and *long branches*, such as the tent maps family from Example 2.1.5. We include two improvements for Alves, Pumariño, and Vigil's theorems about the continuity of the densities and the entropies of the absolutely continuous invariant measures of such type of maps.

2.6.1 Preliminaries

We start by giving a brief introduction to measure theory including some elementary definitions.

Definition 2.6.1 (Measurable spaces)**.** A *σ-algebra* on a set $\mathcal{K}$ is a collection $\mathtt{B}$ of subsets of $\mathcal{K}$ with the following properties:

- The set $\mathcal{K}$ belongs to $\mathtt{B}$.
- If $\mathcal{B} \in \mathtt{B}$, then $\mathcal{K} \setminus \mathcal{B} \in \mathtt{B}$.
- If $\mathcal{B}_n \in \mathtt{B}$ for all $n \in \mathbb{N}$, then $\bigcup_n \mathcal{B}_n \in \mathtt{B}$.

A *measurable space* is a pair $(\mathcal{K}, \mathtt{B})$ of a set $\mathcal{K}$ and a σ-algebra $\mathtt{B}$ on $\mathcal{K}$.

Definition 2.6.2 (Measures)**.** A *measure* on a measurable space $(\mathcal{K}, \mathtt{B})$ is function $\mu\colon \mathtt{B} \to [0, +\infty]$ with the following properties:

- $\mu(\varnothing) = 0$
- If $\{\mathcal{B}_n\}_n$ is a family of pairwise disjoint elements of $\mathtt{B}$, then

$$\mu\Big(\bigcup_n \mathcal{B}_n\Big) = \sum_n \mu(\mathcal{B}_n)$$

The measure μ is a *probability measure* if $\mu(\mathcal{K}) = 1$.

Definition 2.6.3 (Measure spaces)**.** A *measure space* is a triple $(\mathcal{K}, \mathtt{B}, \mu)$ of a measurable space $(\mathcal{K}, \mathtt{B})$ and a measure μ on $\mathtt{B}$. If μ is a probability measure, then the triple $(\mathcal{K}, \mathtt{B}, \mu)$ is a *probability space*.

Before defining some properties associated to any measure, first we introduce the notion of *measurable map*.

Definition 2.6.4 (Measurable maps)**.** Let $(\mathcal{K}_1, \mathtt{B}_1)$ and $(\mathcal{K}_2, \mathtt{B}_2)$ two measurable spaces. A map $f\colon \mathcal{K}_1 \to \mathcal{K}_2$ is *measurable* if $f^{-1}(\mathcal{B}_2) \in \mathtt{B}_1$ for all $\mathcal{B}_2 \in \mathtt{B}_2$.

Definition 2.6.5 (Invariant measures)**.** Let $(\mathcal{K}, \mathtt{B})$ be a measurable space, and let $f\colon \mathcal{K} \to \mathcal{K}$ be a measurable map. A measure μ on $(\mathcal{K}, \mathtt{B})$ is *f-invariant* if $\mu(f^{-1}(\mathcal{B})) = \mu(\mathcal{B})$ for all $\mathcal{B} \in \mathtt{B}$.

Definition 2.6.6 (Absolutely continuous measures)**.** Let μ_1 and μ_2 be two measures on measurable space $(\mathcal{K}, \mathtt{B})$. The measure μ_1 is *absolutely continuous* with respect to μ_2 if $\mu_1(\mathcal{B}) = 0$ whenever $\mu_2(\mathcal{B}) = 0$.

We will usually take μ_2 as the Lebesgue measure m_d on $\mathbb{R}^d$ and simply say that a measure μ is *absolutely continuous* if it is absolutely continuous with respect to m_d. In such case, there exists a m_d-integrable nonnegative function ρ, called the *density* of μ with respect to m_d and denoted by $\mathrm{d}\mu/\mathrm{d}m_d$, such that $\mu(\mathcal{B}) = \int_{\mathcal{B}} \rho \, \mathrm{d}m_d$ for all Borel $\mathcal{B}$.

Definition 2.6.7 (Ergodicity)**.** Let $(\mathcal{K}, \mathtt{B})$ be a measurable space, and let $f\colon \mathcal{K} \to \mathcal{K}$ be a measurable map. An f-invariant probability measure μ is *ergodic* if either $\mu(\mathcal{B}) = 0$ or $\mu(\mathcal{B}) = 1$ whenever $f^{-1}(\mathcal{B}) = \mathcal{B}$.

Now, we will define the concept of *statistical stability* for families of maps. Since we will work with discrete-time dynamical systems defined in a compact regions of $\mathbb{R}^d$ for some $d \geq 1$, we will restrict the following definitions to this condition in order to simplify the notation. From now on, we will denote by m_d the Lebesgue measure on the Borel sets of $\mathbb{R}^d$ and $\mathcal{K}$ will be a compact set in $\mathbb{R}^d$. For each $1 \leq p \leq \infty$, we denote by $L^p(\mathcal{K})$ the Banach space of functions in $L^p(m_d)$ with support contained in $\mathcal{K}$, endowed with the usual norm $\|\cdot\|_p$. We also denote by $\angle(v, w)$ the angle between v and w.

Definition 2.6.8 (Statistical stability)**.** Let $\{\Phi_t\}_{t \in I}$ a family of maps $\Phi_t\colon \mathcal{K} \to \mathcal{K}$ indexed by a metric space I. The family $\{\Phi_t\}_{t \in I}$ is *statistically stable* if the following conditions hold:

(1) For each $t \in I$, the map Φ_t has an absolutely continuous Φ_t-invariant probability measure.

(2) For any $t' \in I$, any choice of a sequence $(t_n)_{n \in \mathbb{N}} \subseteq I$ converging to t' and any choice of a sequence of absolutely continuous Φ_{t_n}-invariant probability measures $(\mu_{t_n})_{n \in \mathbb{N}}$, then any accumulation point of the sequence of densities $\mathrm{d}\mu_{t_n}/\mathrm{d}m_d$ converges in the L^1-norm to the density of an absolutely continuous $\Phi_{t'}$-invariant probability measure.

Of course, when each Φ_t has a unique absolutely continuous invariant measure μ_t, then statistical stability means that $\mathrm{d}\mu_t/\mathrm{d}m_d \to \mathrm{d}\mu_{t'}/\mathrm{d}m_d$ as $t \to t'$ in the L^1-norm. This is precisely the case for the one-parameter 2-D tent maps with $I = (\tau, 1]$. A strictly weaker notion of statistical stability may be given if we assume only weak* convergence of the measures μ_t to $\mu_{t'}$ when $t \to t'$.

2.6.2 Piecewise Expansion, Bounded Variation, and Long Branches

Sufficient conditions for the existence of an absolutely continuous invariant probability measure for *piecewise expanding maps* with *bounded distortion* are given not only for finitely many domains of smoothness [29], but also for infinitely many domains [1, §5]. In the latter case, these conditions include the *long branches*.

Definition 2.6.9 (Piecewise expansion, bounded distortion, long branches)**.** Let $\Phi\colon \mathcal{K} \to \mathcal{K}$ be a map for which there is a (Lebesgue mod 0) partition $\{\mathcal{K}_i\}$ such that:

1. Each $\mathcal{K}_i$ is a closed domain with piecewise C^2 boundary of finite $(d-1)$-dimensional measure.
2. The restriction Φ_i of Φ to $\mathcal{K}_i$ is a C^2 bijection from the interior of $\mathcal{K}_i$ onto its image with a C^2 extension to $\mathcal{K}_i$.

We say that:

(P_1) The map Φ is *piecewise expanding* if there exists $0 < \sigma < 1$ such that, for every i and $P \in \operatorname{int}\Phi(\mathcal{K}_i)$,

$$\|\mathrm{D}\Phi_i^{-1}(P)\| \le \sigma$$

(P_2) The map Φ has *bounded distortion* if there exists $D \ge 0$ such that for every i and for all $P, Q \in \operatorname{int}\mathcal{K}_i$

$$\log \frac{J_\Phi(P)}{J_\Phi(Q)} \le D\|\Phi(P) - \Phi(Q)\|$$

where J_Φ denotes the Jacobian of Φ.

(P_3) The map Φ has *long branches* if there exist $\beta, \rho > 0$ and, for each $i \ge 1$, there exist a C^1 unitary vector field X_i in $\partial\Phi(\mathcal{K}_i)$ such that:

(a) the segments joining each $P \in \partial\Phi(\mathcal{K}_i)$ to $P + \rho X_i(P)$ are pairwise disjoint and contained in $\Phi(\mathcal{K}_i)$, and their union forms a neighborhood of $\partial\Phi(\mathcal{K}_i)$ in $\Phi(\mathcal{K}_i)$

(b) for every $P \in \partial\Phi(\mathcal{K}_i)$ and $v \in \mathrm{T}_P\partial\Phi(\mathcal{K}_i)\setminus\{0\}$, the angle $\angle(v, X_i(P))$ between v and $X_i(P)$ satisfies $|\sin\angle(v, X_i(P))| \ge \beta$.

Here we assume that, at the singular points $P \in \partial\Phi(\mathcal{K}_i)$ where $\partial\Phi(\mathcal{K}_i)$ is not smooth, the vector $X_i(P)$ is a common C^1 extension of X_i restricted to each $(d-1)$-dimensional smooth component of $\partial\Phi(\mathcal{K}_i)$ having P in its boundary. We also assume that the tangent space of any such singular point P is the union of the tangent spaces to the $(d-1)$-dimensional smooth components it belongs to.

For $d = 1$, condition (a) of (P_3) is clearly satisfied by taking the sets in the partition as intervals whose images have sizes uniformly bounded away from zero. Additionally, condition (b) of (P_3) always holds since $\partial\Phi(\mathcal{K}_i)$ is a zero-dimensional manifold and therefore $\mathrm{T}_P\partial\Phi(\mathcal{K}_i) = \{0\}$ for any $P \in \Phi(\mathcal{K}_i)$. In this case, we can even take the optimal value $\beta = 1$.

2.6.3 The Entropy Formula

In this subsection we state the *entropy formula* obtained for an absolutely continuous invariant probability measure of a C^1 piecewise expanding map $\Phi\colon \mathcal{K} \to \mathcal{K}$.

Definition 2.6.10 (Entropy of a partition)**.** The *entropy* of a partition $\mathtt{P}$ of $\mathcal{K}$ with respect to a measure μ is

$$H_\mu(\mathtt{P}) = -\sum_{\mathcal{P}\in\mathtt{P}} \mu(\mathcal{P}) \log \mu(\mathcal{P})$$

Definition 2.6.11 (Entropy of a map)**.** The *entropy* of Φ with respect to μ and a partition $\mathtt{P}$ is

$$h_\mu(\Phi, \mathtt{P}) = \lim_{n\to\infty} \tfrac{1}{n} H_\mu(\mathtt{P}^{(n)})$$

The *entropy* of Φ with respect to μ is

$$h_\mu(\Phi) = \sup_{\mathtt{P}} h_\mu(\Phi, \mathtt{P})$$

Definition 2.6.12 (Entropy formula)**.** Let $\Phi\colon \mathcal{K} \to \mathcal{K}$ be a C^1 piecewise expanding map. An absolutely continuous invariant measure μ with respect to Φ satisfies the *entropy formula* if

$$h_\mu(\Phi) = \int \log J_\Phi \, \mathrm{d}\mu$$

where $J_\Phi = |\det \mathrm{D}\Phi|$.

Some results that guarantee that a measure satisfies the entropy formula assume that the corresponding partition is *quasi-Markovian*.

Definition 2.6.13 (Quasi-Markovian partitions)**.** A $\mu \mod 0$ partition $\mathtt{P}_\Phi$ of $\mathcal{K}$ is *quasi-Markovian* with respect to a measure μ if there exists $\eta > 0$ such that, for μ-almost every $P \in \mathcal{K}$,

$$\mu(\Phi^n(\mathcal{P}^n(P))) \geq \eta$$

for infinitely many values of n, where $\mathcal{P}^n(P)$ is the element in $\mathtt{P}_\Phi^{(n)}$ containing P.

Remark 2.6.14. In Definition 2.6.13 we are implicitly assuming that $\mathtt{P}_\Phi^{(n)}$ is a $\mu \mod 0$ partition of $\mathcal{K}$ for all $n \in \mathbb{N}$.

In order to verify thet quasi-Markovian property, we introduce now the concept of *singular set*.

Definition 2.6.15 (The singular set)**.** The *singular set* of a piecewise expanding map $\Phi\colon \mathcal{K} \to \mathcal{K}$ is

$$\mathtt{S}_\Phi = \overline{\bigcup_{\mathcal{P}\in\mathtt{P}_\Phi} \partial\mathcal{P}}$$

Note that when the partition $\mathtt{P}_\Phi$ is finite, then the singular set $\mathtt{S}_\Phi$ is a finite union of $(d-1)$-dimensional submanifolds of $\mathbb{R}^d$.

Proposition 3.4 [2] provides a useful criterium for the quasi-Markovian property of the partition associated to a piecewise expanding map *behaving as a power of the distance* close the singular set.

Definition 2.6.16 (Behavior as a power of the distance)**.** A piecewise expanding map $\Phi\colon \mathcal{K} \to \mathcal{K}$ *behaves as a power of the distance* close to the singular set $\mathtt{S}_\Phi$ if there exist $B, \beta > 0$ such that, for every $P, Q \in \mathcal{K} \setminus \mathtt{S}_\Phi$ with $\mathrm{dist}(P, Q) < \mathrm{dist}(P, \mathtt{S}_\Phi)/2$, the following conditions hold:

(S_1) $\|\mathrm{D}\Phi(P)\| \leq B \cdot \mathrm{dist}(P, \mathtt{S}_\Phi)^{-\beta}$

(S_2) $\log \frac{\|\mathrm{D}\Phi(P)^{-1}\|}{\|\mathrm{D}\Phi(Q)^{-1}\|} \leq B \frac{\mathrm{dist}(P,Q)}{\mathrm{dist}(P,\mathtt{S}_\Phi)^\beta}$

2.6.4 Functions of Bounded Variation

The main ingredient for the proof of Alves, Pumariño, and Vigil's theorems [1, 3, 2] is the notion of *variation* for functions in multidimensional spaces. We adopt the definition presented by Giusti [24].

Definition 2.6.17 (Variation)**.** The *variation* of a function $f \in L^1(\mathbb{R}^d)$ with compact support is

$$V(f) = \sup \left\{ \int_{\mathbb{R}^d} f \operatorname{div} g \, \mathrm{d}m_d : g \in C_0^1(\mathbb{R}^d, \mathbb{R}^d) \text{ and } \|g\| \leq 1 \right\}$$

where $C_0^1(\mathbb{R}^d, \mathbb{R}^d)$ is the set of C^1 functions from $\mathbb{R}^d$ to $\mathbb{R}^d$ with compact support and $\|\cdot\|$ is the supremum norm in $C_0^1(\mathbb{R}^d, \mathbb{R}^d)$.

Remark 2.6.18. If $f \in C^1(\mathbb{R}^d)$, then $V(f) = \int_{\mathbb{R}^d} \|\nabla f\| \, \mathrm{d}m_d$.

The *space of bounded variation functions* on a bounded set $\mathcal{K} \subseteq \mathbb{R}^d$ is

$$\mathrm{BV}(\mathcal{K}) = \{f \in L^1(\mathcal{K}) : V(f) < +\infty\}$$

Contrary to the classical one-dimensional definition of bounded variation, a multidimensional bounded variation function need not be bounded. However, by Sobolev's Inequality, there is some constant $C > 0$, only depending on the dimension d, such that, for every $f \in \mathrm{BV}(\mathcal{K})$,

$$\left(\int |f|^p \, \mathrm{d}m_d \right)^{\frac{1}{p}} \leq C \cdot V(f), \qquad p = \frac{d}{d-1}$$

This in particular gives $\mathrm{BV}(\mathcal{K}) \subseteq L^p(\mathcal{K})$. We shall use the following properties of bounded variation functions [24]:

(B_1) $\mathrm{BV}(\mathcal{K})$ is dense in $L^1(\mathcal{K})$.

(B_2) If $(f_n)_{n\in\mathbb{N}}$ is a sequence in $\mathrm{BV}(\mathcal{K})$ converging to f in the L^1-norm, then

$$V(f) \leq \liminf_{n\to\infty} V(f_n)$$

(B_3) If $(f_n)_{n\in\mathbb{N}}$ is a sequence in $\mathrm{BV}(\mathcal{K})$ such that $(\|f_n\|_1)_{n\in\mathbb{N}}$ and $(V(f_n))_{n\in\mathbb{N}}$ are bounded, then $(f_n)_{n\in\mathbb{N}}$ has some subsequence converging in the L^1-norm to a function in $\mathrm{BV}(\mathcal{K})$.

(B_4) Given $f \in \mathrm{BV}(\mathbb{R}^d)$, there is a sequence $(f_n)_{n\in\mathbb{N}}$ of C^∞ maps such that

$$\lim_{n\to\infty} \int |f - f_n| \, \mathrm{d}m = 0, \quad \lim_{n\to\infty} \int \|\mathrm{D}f_n\| \, \mathrm{d}m = V(f)$$

Let $\{\mathcal{K}_i^t\}_{i=1}^\infty$ be the domains of smoothness of Φ_t with $t \in I$ satisfying the assumptions of Theorem 10, and let $\Phi_{t,i}$ be the restriction of Φ_t to $\mathcal{K}_i^t$ for all $i \geq 1$. For each $t \in I$, we consider the *Perron-Frobenius operator*

$$\mathrm{P}_t \colon L^1(\mathcal{K}) \to L^1(\mathcal{K})$$

defined for $f \in L^1(\mathcal{K})$ as

$$\mathrm{P}_t f = \sum_{i=1}^{\infty} \frac{f \circ \Phi_{t,i}^{-1}}{|J \circ \Phi_{t,i}^{-1}|} \chi_{\Phi_t(\mathcal{K}_i^t)}$$

It is well known that the following two properties hold for each P_t:

(P_1) $\|\mathrm{P}_t f\|_1 \leq \|f\|_1$ for every $f \in L^1(\mathcal{K})$.

(P_2) $P_t f = f$ if and only if f is the density of an absolutely continuous Φ_t-invariant probability measure.

The following lemma provides a uniform Lasota–Yorke inequality.

Lemma 2.6.19 ([1, Lem. 5.4]). *Let $\Phi\colon \mathcal{K} \to \mathcal{K}$ be a C^2 piecewise expanding map with bounded distortion and long branches. If $\sigma(1+1/\beta) < 1$, then there exists a constant $K_0 > 0$ such that*

$$V(P_t f) \le \sigma(1 + \tfrac{1}{\beta})V(f) + K_0\|f\|_1$$

for all $f \in \mathrm{BV}(\mathcal{K})$.

2.6.5 Alves, Pumariño, and Vigil's Works

Alves, Pumariño, and Vigil [3] gave sufficient conditions for the statistical stability of piecewise expanding maps with bounded distortion and long branches and, as a corollary, they proved the statistical stability of the one-parameter two-dimensional tent maps Λ_t from Example 2.1.5.

Theorem ([3, Th. A, adapted]). *Let I be a metric space and $(\Phi_t)_{t\in I}$ a family of C^2 piecewise expanding maps $\Phi_t\colon \mathcal{K} \to \mathcal{K}$ with bounded distortion and long branches. Assume that there exist $0 < \lambda < 1$ and $K > 0$ such that for each $t \in I$ the following hold:*

(1) for each continuous $f\colon \mathcal{K} \to \mathbb{R}$ we have $\|f \circ \Phi_t - f \circ \Phi_{t'}\|_d \to 0$ when $t \to t'$.

(2) $\sigma_t(1+\frac{1}{\beta_t}) \le \lambda$ and $\Delta_t + \frac{1}{\alpha_t\beta_t} + \frac{\Delta_t}{\beta_t} \le K$ where $\sigma_t, \Delta_t, \alpha_t, \beta_t$ are the constants in (P_1)–(P_3) associated with Φ_t.

Then, the family $(\Phi_t)_{t\in I}$ is statistically stable.

Theorem ([3, Th. B]). *The family $\{\Lambda_t\}_{t\in[\tau,1]}$ is statistically stable.*

Then, Alves and Pumariño [2] proved the continuity of the entropy of certain multidimensional piecewise expanding maps which admit ergodic absolutely continuous invariant probability measures, and deduced it for Λ_t. In order to verify that the entropy formula holds, the following result is used.

Theorem ([2, Cor. E, adapted]). *Let $\Phi\colon \mathcal{K} \to \mathcal{K}$ be a C^1 piecewise expanding map with bounded distortion and large branches that behaves as a power of the distance close to $\mathtt{S}_\Phi$ such that*

$$\sigma\left(1 + \frac{1}{\beta}\right) < 1$$

where σ and β are the constants given in properties (P_1) and (P_3). If $\log \mathrm{dist}(\cdot, \mathtt{S}_\Phi) \in L^d(m)$ and μ is an ergodic absolutely continuous invariant probability measure for Φ such that $H_\mu(\mathtt{P}_\Phi) < \infty$, then the entropy formula holds.

Theorem ([2, Th. F, adapted]). *Let $(\Phi_t)_{t\in I}$ be a family of C^2 piecewise expanding maps with bounded distortion and large branches such that each Φ_t has a unique absolutely continuous invariant probability measure μ_t for which $H_{\mu_t}(\mathtt{P}_t) < \infty$ and the entropy formula holds. Assume that:*

(1) There are $0 < \lambda < 1$ and $K > 0$ such that, for each $t \in I$,

$$\sigma_t\left(1 + \frac{1}{\beta_t}\right) \le \lambda, \quad \Delta_t + \frac{1}{\alpha_t\beta_t} + \frac{\Delta_t}{\beta_t} \le K$$

where $\sigma_{t,\ell}, \Delta_{t,\ell}, \alpha_{t,\ell}, \beta_{t,\ell}$ are the constants such that (P_1)–(P_3) hold for Φ_t.

(2) $f \circ \Phi_t$ *depends continuously on* $t \in I$ *in* $L^d(m)$ *for each continuous* $f \colon \mathcal{K} \to \mathbb{R}$.

(3) $\log J_{\Phi_t} \in L^q(m)$ *for some* $q > d$ *and* $\log J_{\Phi_t}$ *depends continuously on* $t \in I$ *in* $L^1(m)$.

Then, the entropy $h_{\mu_t}(\Phi_t)$ *depends continuously on* $t \in I$.

Theorem ([2, Th. G])**.** *Each* Λ_t *has a unique absolutely continuous invariant probability measure* μ_t *depending continuously on* $t \in [\tau, 1]$. *Moreover, the entropy formula holds for* μ_t *and* $h_{\mu_t}(\Lambda_t)$ *depends continuously on* $t \in [\tau, 1]$.

2.6.6 Hölder Continuity of The Densities and The Entropy

Here we consider the one-parameter family of tent maps from Example 2.1.5. We include two theorems from a preprint by Alves and Bahsoun that generalize the statistical stability and the continuity of the entropy of the family Λ_t in a Hölder-like way.

Theorem 10. *Let* $\{\Phi_t\}_{t \in I}$ *be a family of* C^2 *piecewise expanding maps such that each* Φ_t *has a unique absolutely continuous invariant probability measure* μ_t, *which is mixing. Assume that the following hold:*

(1) There exist $\ell \in \mathbb{N}$ *such that every* Φ_t^ℓ *has bounded distortion and large branches. Moreover, there exist* $0 < \theta < 1$ *and* $K > 0$ *such that*

$$\sigma_{t,\ell}\Big(1 + \frac{1}{\beta_{t,\ell}}\Big) \le \theta, \quad \Delta_{t,\ell} + \frac{1}{\alpha_{t,\ell}\beta_{t,\ell}} + \frac{\Delta_{t,\ell}}{\beta_{t,\ell}} \le K$$

for every $t \in I$, *where* $\sigma_{t,\ell}, \Delta_{t,\ell}, \alpha_{t,\ell}, \beta_{t,\ell}$ *are the constants in* (P_1), (P_2), *and* (P_3) *associated to* Φ_t^ℓ.

(2) There exists a nonnegative function $\mathcal{E} \colon U \to \mathbb{R}$ *such that, for all* $s, t \in I$ *and all* i, *the following hold:*

(a) For all $P \in \mathcal{K}_i^s$ *and* $Q \in \mathcal{K}_i^t$ *with* $\Phi_s(P) = \Phi_t(Q)$,

$$\left| \frac{J_s(P)}{J_t(Q)} - 1 \right| \le \mathcal{E}(t - s)$$

(b) $m(\Phi_{s,i}^{-1}(\Phi_s(\mathcal{K}_i^s) \setminus \Phi_t(\mathcal{K}_i^t)))^{1/d} \le \mathcal{E}(t - s)$

Then, there exist $C > 0$ *and* $0 < \eta < 1$ *such that*

$$\left\| \frac{\mathrm{d}\mu_t}{\mathrm{d}m} - \frac{\mathrm{d}\mu_s}{\mathrm{d}m} \right\|_1 \le C\mathcal{E}(t - s)^\eta$$

for all $s, t \in I$.

Remark 2.6.20. The existence of the measure μ_t follows from hypothesis (1). Here we additionally assume uniqueness and mixing.

Theorem 11. *Let* $\{\Phi_t\}_{t \in I}$ *be a family of* C^2 *piecewise expanding maps such that each* Φ_t *has a unique absolutely continuous invariant probability measure* μ_t *for which the entropy formula holds. Assume that the following hold:*

(1) There exists $\ell \in \mathbb{N}$ *such that every* Φ_t^ℓ *has bounded distortion and large branches. Moreover, there exist* $0 < \theta < 1$ *and* $K > 0$ *such that*

$$\sigma_{t,\ell}\Big(1 + \frac{1}{\beta_{t,\ell}}\Big) \le \theta, \quad \Delta_{t,\ell} + \frac{1}{\alpha_{t,\ell}\beta_{t,\ell}} + \frac{\Delta_{t,\ell}}{\beta_{t,\ell}} \le K$$

for every $t \in I$, *where* $\sigma_{t,\ell}, \Delta_{t,\ell}, \alpha_{t,\ell}, \beta_{t,\ell}$ *are the constants in* (P_1), (P_2), *and* (P_3) *associated to* Φ_t^ℓ.

(2) There exists a nonnegative function $\mathcal{E}\colon U \to \mathbb{R}$ *such that*

$$\left\| \log \frac{J_s}{J_t} \right\|_d \leq \mathcal{E}(t-s), \quad \left\| \frac{\mathrm{d}\mu_t}{\mathrm{d}m} - \frac{\mathrm{d}\mu_s}{\mathrm{d}m} \right\|_1 \leq \mathcal{E}(t-s)$$

for all $s, t \in I$.

Then, there exists $C > 0$ *such that*

$$\|h_{\mu_t}(\Phi_t) - h_{\mu_s}(\Phi_s)\|_1 \leq C\mathcal{E}(t-s)$$

for all $s, t \in I$.

For all $t \in [\tau, 1]$, from the definition of Λ_t we have that the domains of smoothness are $\mathcal{K}_0^t = \mathcal{T}_0$ and $\mathcal{K}_1^t = \mathcal{T}_1$. On the other hand, hypotheses (1) of Theorems 10 and (1) of Theorem 11 are satisfied for $\ell = 6$ [3]. With the next lemma, we will check both hypotheses (2) of Theorem 10 and (2) of Theorem 11.

Lemma 2.6.21. *There exists a nonnegative function* $\mathcal{E}\colon U \to \mathbb{R}$ *such that, for all* $s, t \in [\tau, 1]$ *and for* $i = 0, 1$, *the following hold:*

(1) For all $P, Q \in \mathcal{T}_i$ *with* $\Lambda_s(P) = \Lambda_t(Q)$,

$$\left| \frac{J_s(P)}{J_t(Q)} - 1 \right| \leq \mathcal{E}(t-s)$$

(2) $m(\Lambda_{s,i}^{-1}(\Lambda_s(\mathcal{T}_i) \setminus \Lambda_t(\mathcal{T}_i)))^{\frac{1}{2}} \leq \mathcal{E}(t-s)$

(3) $\|\log J_s - \log J_t\|_2 \leq \mathcal{E}(t-s)$

Proof. The tent map Λ_t is piecewise linear with

$$\mathrm{D}\Lambda_t(P) = \begin{pmatrix} t & t \\ t & -t \end{pmatrix}$$

for $P \in \mathcal{T}_0 \setminus \mathcal{C}$, and

$$\mathrm{D}\Lambda_t(P) = \begin{pmatrix} -t & -t \\ t & -t \end{pmatrix}$$

for $P \in \mathcal{T}_1 \setminus \mathcal{C}$. From here we deduce that, for all $P \in \mathcal{T} \setminus \mathcal{C}$ and all $\tau \leq t \leq 1$, we have $J_t(P) = 2t^2$. This gives, for all $\tau \leq s, t \leq 1$,

$$\left| \frac{J_s(P)}{J_t(Q)} - 1 \right| = \left| \frac{s^2}{t^2} - 1 \right| = \tfrac{1}{t^2}(s+t)|s-t| \leq \tfrac{2}{\tau^2}|s-t|$$

On the other hand, for all $t \in I$,

$$\Lambda_t(\mathcal{T}_0) = \Lambda_t(\mathcal{T}_1) = \Omega(\mathcal{O}, (2t, 0), (t, t))$$

and therefore

$$m(\Lambda_t(\mathcal{T}_0)) = m(\Lambda_t(\mathcal{T}_1)) = t^2$$

Thus, for every $\tau \leq t < s \leq 1$,

$$m(\Lambda_s(\mathcal{T}_i) \setminus \Lambda_t(\mathcal{T}_i)) = (s+t)(s-t)$$

As the Jacobian of $\Lambda_{s,i}$ is constant and bigger than 1, we easily deduce that

$$m(\Lambda_{s,i}^{-1}(\Lambda_s(\mathcal{T}_i) \setminus \Lambda_t(\mathcal{T}_i))^{\frac{1}{2}} \leq \sqrt{2}(s-t)^{\frac{1}{2}}$$

Now, since the area of $\mathcal{T}$ is equal to 1, then

$$\int \left| \log \frac{J_s}{J_t} \right|^2 \, \mathrm{d}m_2 = 4(\log s - \log t)^2$$

By the Mean Value Theorem,

$$\|\log J_s - \log J_t\|_2 \leq \tfrac{2}{\tau}(s-t)$$

for all $\tau \leq t < s \leq 1$. Therefore, it suffices to take $\mathcal{E}(u) = 2/\tau^2|u|$. □

Chapter 3

Dynamics of the 2-D Quadratic Family: Existence of 1-D and 2-D Strange Attractors

This chapter is devoted to the 2-D quadratic family

$$T_{a,b}(x,y) = (a + y^2, x + by) \tag{3.1}$$

In Section 3.1 we study the existence and the stability of the fixed points and the periodic points of periods two and three, paying special attention to the loss of hyperbolicity, and prove Theorems 6 and 7. In Section 3.2 we prove Theorem 8. In the first part of Section 3.3 we prove Theorem 9, while in the second part we numerically check the persistence of 2-D strange attractors for random parameter values in the sharp regions of Theorem 8 for both $(-2,0)$ and $(-4,-2)$. Moreover, we numerically find out that $T_{a,b}$ for parameter values along the curve $2a = b^3$ reproduces the same behavior as $\Gamma_{a,\theta}$: splitting of attractors in several pieces, for example.

3.1 Local Dynamics: Proof of Theorems 6 and 7

We will first search for other expressions of family (3.1) that could be useful to explain its dynamics from a simple study of the fixed points.

The fixed points of family (3.1) are of the form $P^{(1)} = ((1-b)c, c)$ with c verifying

$$c^2 + (b-1)c + a = 0 \tag{3.2}$$

These fixed points exist if and only if $(b-1)^2 - 4a \geq 0$. In the region of parameters

$$\{(a,b) \in \mathbb{R}^2 : (b-1)^2 - 4a < 0\}$$

the dynamics of family (3.1) is trivial: there is no bounded orbit and, consequently, there are no attractors.

Proposition 3.1.1. *If $4a > (b-1)^2$, then every $T_{a,b}$-orbit is unbounded.*

Proof. Immediate from the fact that

$$L(T_{a,b}(\mathbf{x},\mathbf{y})) - L(\mathbf{x},\mathbf{y}) = \mathbf{y}^2 + (b-1)\mathbf{y} + a \geq a - \tfrac{1}{4}(b-1)^2 > 0$$

for all $(\mathbf{x},\mathbf{y}) \in \mathbb{R}^2$, where $L(\mathbf{x},\mathbf{y}) = \mathbf{x} + \mathbf{y}$. □

In what follows, we will only consider parameter values in

$$\{(a,b) \in \mathbb{R}^2 : (b-1)^2 - 4a \geq 0\}$$

In this region, the solutions of equation (3.2) are

$$c^{\pm} = \tfrac{1}{2}(1-b \pm \delta), \qquad \delta = \sqrt{(b-1)^2 - 4a} \tag{3.3}$$

Note that $c^+ = c^-$ if and only if $\delta = 0$, in which case

$$P^{(1)} = (\tfrac{1}{2}(1-b)^2, \tfrac{1}{2}(1-b))$$

is the unique fixed point. If $\delta > 0$, then map (3.1) has two different fixed points

$$P^{(1),\pm} = ((1-b)c^{\pm}, c^{\pm})$$

After performing the change of variables

$$x = 1 - \tfrac{1}{c^{\pm}}\mathbf{y}, \quad y = 1 - \tfrac{1}{c^{\pm}}(\mathbf{x} + b\mathbf{y}) \qquad (c^{\pm} \neq 0) \tag{3.4}$$

family (3.1) is transformed into

$$F^{\pm}_{c,b}(x,y) = (y, 2c^{\pm}x - c^{\pm}x^2 + by) \tag{3.5}$$

Remark 3.1.2. Maps (3.5) can be written as

$$F^{\pm}_{c,b}(x,y) = \begin{pmatrix} 0 & 1 \\ c^{\pm} & b \end{pmatrix} \begin{pmatrix} 2x - x^2 \\ y \end{pmatrix}$$

These maps can also be written as the composition of the diffeomorphism

$$\Phi^{\pm}_{c,b}(x,y) = \begin{pmatrix} 0 & 1 \\ c^{\pm} & b \end{pmatrix} \begin{pmatrix} 2x - x^2 \\ y \end{pmatrix}$$

defined on $\{x \leq 1\}$ with the fold

$$\mathcal{F}_{\mathcal{C},\mathcal{O}}(x,y) = \begin{cases} (x,y) & \text{if } x \leq 1 \\ (2-x,y) & \text{if } x \geq 1 \end{cases}$$

Remark 3.1.3. All the results obtained for family (3.5) can be translated for family (3.1) by means of the change of variables (3.4) and the change of parameters (3.3). Thus, the origin is always a fixed point of $F^{\pm}_{c,b}$ and corresponds to the fixed point $P^{(1),\pm}$ of $T_{a,b}$, respectively. A straightforward relation of the variables $a, b, c^{\pm}$ is given by equation (3.2).

3.1.1 Fixed Point Stability

The first information on the dynamics of family (3.1) is obtained by the study of the stability of its fixed points. After performing the changes of variables (3.4) and parameters (3.3), it is sufficient to study the eigenvalues of the differential of $F^+_{c,b}$ and $F^-_{c,b}$ at $\mathcal{O}$, which are

$$\lambda^+_{1,2} = \tfrac{b}{2} \pm \tfrac{1}{2}\sqrt{(b-2)^2 + 4\delta} \tag{3.6}$$

and

$$\lambda^-_{1,2} = \tfrac{b}{2} \pm \tfrac{1}{2}\sqrt{(b-2)^2 - 4\delta} \tag{3.7}$$

respectively. Since $\delta \geq 0$, then $\mathcal{O}$ may have complex eigenvalues only for $F^-_{c,b}$. For that reason, we will take $c = c^-$. Now we prove a result on the stability of the fixed points of $F_{c,b} = F^-_{c,b}$ that is equivalent to Theorem 6 for $T_{a,b}$. See Figure 3.1. Let us previously recall the notion of *unipotent singularity*.

Definition 3.1.4 (Unipotent singularities)**.** A fixed point of an analytic 2-D diffeomorphism f is a *unipotent singularity* if there exists a smooth change of variables that transforms the fixed point into $\mathcal{O}$ for which there exists a neighborhood of $\mathcal{O}$ where f can be expressed as

$$f(\xi,\eta) = (\xi + \eta + q_1(\xi,\eta), \eta + q_2(\xi,\eta)), \qquad q_{1,2}(\xi,\eta) = O(\xi^2+\eta^2)$$

A *Bogdanov–Takens singularity* is a unipotent singularity that satisfies the following generic condition:

$$\frac{\partial^2 q_2}{\partial \xi^2}(0,0) \neq 0, \quad \frac{\partial^2 q_2}{\partial \xi \partial \eta}(0,0) + \frac{\partial^2 q_1}{\partial \xi^2}(0,0) - \frac{\partial^2 q_2}{\partial \xi^2}(0,0) \neq 0$$

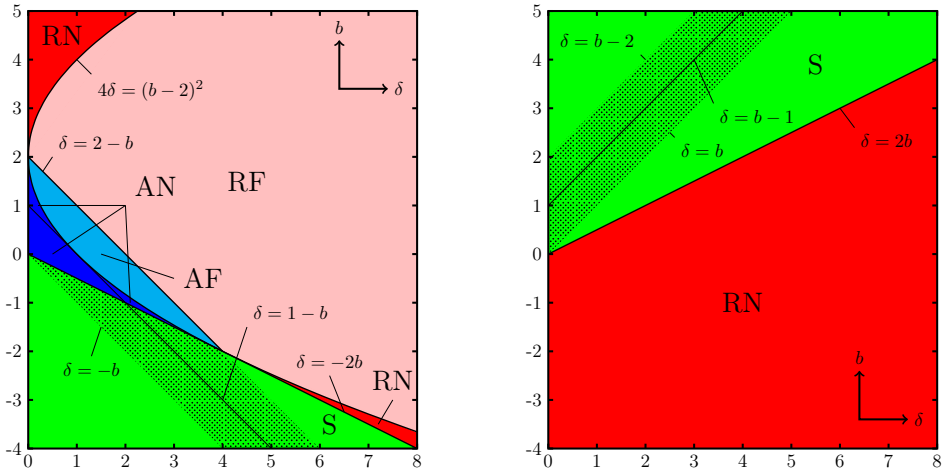

(a) (b)

Figure 3.1: (a) Stability configuration of the fixed point $\mathcal{O}$ in (δ, b): AN (blue): attracting node; RN (red): repelling node; AF (cyan): attracting focus; RF (pink): repelling focus; S (green): saddle fixed point, dashed: dissipative. Along $\delta = 1-b$, one eigenvalue is zero. (b) Stability configuration of the fixed point $Q^{(1),+}$ in (δ, b): RN (red): repelling node; S (green): saddle fixed point, dashed: dissipative. Along $\delta = b-1$, one eigenvalue is zero.

Theorem 3.1.5 (cf. Th. 6)**.** *The fixed points of*

$$F_{c,b}(x,y) = (y, 2cx - cx^2 + by)$$

verify the following statements:

b) If $\delta = 0$, then $F_{c,b}$ has the origin as the unique fixed point with eigenvalues $b-1$ and 1. In particular, for $(c,b) = (-1/2, 2)$, a Bogdanov–Takens bifurcations occurs at the origin.

c) If $\delta > 0$, then $F_{c,b}$ has two fixed points:

$$\mathcal{O} = (0,0), \quad Q^{(1),+} = (-\tfrac{\delta}{c}, -\tfrac{\delta}{c})$$

i) The origin is a focus if and only if

$$4\delta > (b-2)^2, \quad \delta \neq 2-b$$

This focus is attracting if $\delta < 2-b$ and repelling otherwise. Along the segment

$$\delta = 2-b, \qquad -2 < b < 2$$

the origin is a center. Moreover, a Hopf–Neimark–Sacker bifurcation occurs at the origin for $b \neq -1, 0$. The parabola $4\delta = (b-2)^2$ intersects the line $\delta = 2-b$ at the points $B^* = (0,2)$ and $D^* = (4,-2)$. For $(\delta, b) = D^*$, the origin has double eigenvalue equal to -1. It is a unipotent singularity of $F^2_{-1/2,-2}$, but not Bogdanov–Takens.

If $4\delta \leq (b-2)^2$, then the origin is a node if $\delta > -2b$. This node is attracting if $-2 < b < 2$ and repelling otherwise. If $\delta < -2b$, then the origin is a saddle fixed point that is dissipative if and only if $-\delta < b < 2-\delta$.

ii) The fixed point $Q^{(1),+}$ is a repelling node if $\delta > 2b$. If $\delta < 2b$, then $Q^{(1),+}$ is a saddle fixed point that is dissipative if and only if $\delta < b < 2+\delta$.

Proof. We perform the proof item by item:

b) It is straightforward to check that for $\delta = 0$ the unique fixed point $\mathcal{O}$ of $F_{c,b}$ has eigenvalues $b-1$ and 1. In particular, if $b = 2$, then $c = -1/2$ and

$$\mathrm{D}F_{-\frac{1}{2},2}(\mathcal{O}) = \begin{pmatrix} 0 & 1 \\ -1 & 2 \end{pmatrix}$$

has double eigenvalue $\lambda^-_{1,2} = 1$. The change of variables $x = \xi + \eta$, $y = \xi + 2\eta$ allows to write $F_{-1/2,2}$ as

$$(\xi, \eta) \mapsto \left(\xi + \eta - \tfrac{1}{2}(\xi+\eta)^2, \eta + \tfrac{1}{2}(\xi+\eta)^2\right)$$

Taking $q_1(\xi,\eta) = -(\xi+\eta)^2/2$ and $q_2(\xi,\eta) = (\xi+\eta)^2/2$ in Definition 3.1.4, it then follows that $\mathcal{O}$ is a Bogdanov–Takens singularity for the diffeomorphism $\Phi_{-1/2,2}$.

c) Suppose now that $\delta > 0$. It is immediate to obtain the two fixed points $\mathcal{O}$ and $Q^{(1),+}$. The eigenvalues of $\mathcal{O}$ are given in formula (3.7), and it is also immediate to check that the eigenvalues of $Q^{(1),+}$ are the ones given in formula (3.6).

i) The eigenvalues $\lambda^-_{1,2}$ of $\mathcal{O}$ are complex if and only if $4\delta > (b-2)^2$. In such case, it holds that $|\lambda^-_{1,2}| = 1$ if and only if $\delta = 2-b$. If $\delta < 2-b$, then $|\lambda^-_{1,2}| < 1$ and $\mathcal{O}$ is an attracting focus. If $\delta > 2-b$, then $|\lambda^-_{1,2}| > 1$ and $\mathcal{O}$ is a repelling focus. The line $\delta = 2-b$ intersects the region $4\delta > (b-2)^2$ at the segment of extremes $B^* = (0,2)$ and $D^* = (4,-2)$. Along this segment, we can write

$$\lambda^-_{1,2} = \mathrm{e}^{\pm \mathrm{i}\theta} = \tfrac{b}{2} \pm \tfrac{\mathrm{i}}{2}\sqrt{4-b^2}$$

Therefore, a Hopf–Neimark–Sacker bifurcation takes place (see [36]), which consists of the birth of attracting closed curves towards the half-plane $\delta > 2-b$, whenever $\theta \neq 2\pi/k$ for $k = 1,2,3,4$. Since $\tan^2\theta = (4-b^2)/b^2$, this condition is equivalent to $b \neq -2, -1, 0, 2$. For $B^* = (0,2)$ it was proved above that $\mathcal{O}$ is a Bogdanov–Takens singularity. For $D^* = (4,-2)$, which corresponds to $(c,b) = (-1/2, -2)$, it holds that

$$\mathrm{D}F_{-\frac{1}{2},-2}(\mathcal{O}) = \begin{pmatrix} 0 & 1 \\ -1 & -2 \end{pmatrix}, \quad \mathrm{D}F^2_{-\frac{1}{2},-2}(\mathcal{O}) = \begin{pmatrix} -1 & -2 \\ 2 & 3 \end{pmatrix}$$

The change of variables $x = 2\xi$, $y = -2\xi - \eta$ allows to express $F^2_{-1/2,-2}$ as

$$(\xi, \eta) \mapsto (\xi + \eta + \xi^2, \eta - 2\xi\eta - \tfrac{\eta^2}{2})$$

Therefore, the origin is a unipotent singularity, but not Bogdanov–Takens because, taking $q_1(\xi,\eta)=\xi^2$ and $q_2(\xi,\eta)=-2\xi\eta-\eta^2/2$ in Definition 3.1.4, we have that $\partial^2 q_2/\partial\xi^2\equiv 0$ and

$$\frac{\partial^2 q_2}{\partial\xi\partial\eta}+\frac{\partial^2 q_1}{\partial\xi^2}-\frac{\partial^2 q_2}{\partial\xi^2}\equiv 0$$

If $4\delta\leq(b-2)^2$, then $\lambda^-_{1,2}$ are real and satisfy

$$\tfrac{b}{2}-\tfrac{1}{2}|b-2|<\lambda_2^-\leq\lambda_1^-<\tfrac{b}{2}+\tfrac{1}{2}|b-2| \tag{3.8}$$

If $b>2$, then $\lambda_2^->1$ by inequality (3.8), and therefore $\mathcal{O}$ is a repelling node. Assume that $b<2$. Then, from inequality (3.8) it follows that

$$b-1<\lambda_2^-\leq\lambda_1^-<1$$

Therefore, if $b\geq 0$, then $\mathcal{O}$ is an attracting node. By formula (3.7), it holds that

$$\operatorname{sgn}(\lambda^-_{1,2}+1)=\operatorname{sgn}(b+2\pm\sqrt{(b-2)^2-4\delta}) \tag{3.9}$$

From equivalences (3.9) we deduce that $\lambda_2^->-1$ only if $b>-2$, and $\lambda_1^-<-1$ only if $b<-2$. Moreover, from equivalences (3.9) it follows that $\lambda_2^->-1$ and $\lambda_1^-<-1$ if and only if $\delta+2b>0$. Therefore, the origin is a node if $\delta+2b>0$, which is attracting if $-2<b<2$ and repelling if $b<-2$. On the other hand, the origin is a saddle fixed point if $\delta+2b<0$. Since

$$\lambda_1^-\lambda_2^-=b+\delta-1$$

then $\mathcal{O}$ is dissipative if and only if $0<b+\delta<2$.

ii) Since $\delta>0$, it readily follows that $\lambda^+_{1,2}$ are real and $\lambda_2^+<1<\lambda_1^+$. It is immediate to check that $\lambda_2^+<-1$ if and only if $\delta-2b>0$. In that case, the fixed point $Q^{(1),+}$ is a repelling node. If $\delta-2b>0$, then $Q^{(1),+}$ is a saddle fixed point. Since

$$\lambda_1^+\lambda_2^+=b-\delta-1$$

then $Q^{(1),+}$ is dissipative if and only if $0<b-\delta<2$. □

The equivalence between Theorem 3.1.5 and Theorem 6 is straightforwardly checked by applying the changes of variables and parameters (3.4) and (3.3) from Remark 3.1.3.

Compare Figures 16 and 3.1. The fixed points $\mathcal{O}$ and $Q^{(1),+}$ are in correspondence with $P^{(1),-}$ and $P^{(1),+}$, respectively.

3.1.2 Periodic Orbits

The Hopf–Neimark–Sacker bifurcation given in Theorem 3.1.5 justifies the birth of the attracting closed curves for parameter regions on the left-hand side of the segment $\overline{BD}$, represented in green in Figure 15. These regions alternate with other ones in blue, such as $\mathcal{P}_0$, for which the periodic attractor must have a period greater than or equal to two, since for such parameters there are no attracting fixed points.

On the other hand, the existence of periodic orbits can explain the origin of 1-D strange attractors that appear for parameter values in the regions in red limiting with the ones in blue and/or green. As already mentioned, these attractors appear generically when a homoclinic tangency of a dissipative saddle periodic point is unfolded [44]. This homoclinic tangency can be produced, for instance, when the invariant curve collides with such saddle periodic point.

Let us study, therefore, the existence of periodic points of period $n \geq 2$, as well as their possible dissipative and/or attracting nature. To that end, let us operate with the expression

$$F_{c,b}(x,y) = (y, \varphi_c(x) + by)$$

where $\varphi_c(x) = cx(2-x)$. Recall that $c < 0$ for all $a < 0$. Let (x,y) be a n-periodic point with $n \geq 2$. Set $s_1 = x$ and $s_2 = y$, and

$$s_j = \varphi_c(s_{j-2}) + bs_{j-1}, \qquad j = 3, \ldots, n+2 \tag{3.10}$$

Then, it holds that $F^j_{c,b}(x,y) = (s_{j+1}, s_{j+2})$ for $j = 1, \ldots, n$. Note that $s_{n+1} = s_1$ and $s_{n+2} = s_2$. As a consequence of the next proposition, we will prove that all the periodic orbits of $F_{c,b}$ of any given period greater than or equal to two, provided that they exist, are contained in a closed disk passing through the origin.

Proposition 3.1.6. *Let (x,y) be a n-periodic point of $F_{c,b}$ with $n \geq 2$. Then, the point*

$$(s_1, s_2, \ldots, s_n) \in \mathbb{R}^n$$

belongs to the sphere of centre $(-\delta/2c, \ldots, -\delta/2c) \in \mathbb{R}^n$ passing through the origin, i.e.

$$\sum_{j=1}^{n} (s_j + \tfrac{\delta}{2c})^2 = \frac{n\delta^2}{4c^2}$$

Moreover,

$$\det \mathrm{D}F^n_{c,b}(x,y) = 2^n c^n (s_1 - 1)(s_2 - 1) \cdots (s_n - 1)$$

Proof. Adding up all the members from both sides of the n equations (3.10), we have that

$$c(s_1^2 + s_2^2 + \cdots + s_n^2) + (1 - b - 2c)(s_1 + s_2 + \cdots + s_n) = 0$$

Since $\delta = 1 - b - 2c$, we have that

$$s_1^2 + s_2^2 + \cdots + s_n^2 + \tfrac{\delta}{c}(s_1 + s_2 + \cdots + s_n) = 0$$

is the equation of a sphere in $\mathbb{R}^n$ of centre $(-\delta/2c, \ldots, -\delta/2c) \in \mathbb{R}^n$ that goes through the origin. Therefore, such sphere has radius equal to $-\delta\sqrt{n}/2c$. On the other hand, note that

$$\mathrm{D}F^n_{c,b}(x,y) = \mathrm{D}F_{c,b}(s_n, s_{n+1}) \circ \cdots \circ \mathrm{D}F_{c,b}(s_2, s_3) \circ \mathrm{D}F_{c,b}(s_1, s_2)$$

In order to conclude this proof, it is enough to observe that the matrix

$$\mathrm{D}F_{c,b}(s_j, s_{j+1}) = \begin{pmatrix} 0 & 1 \\ 2c(1 - s_j) & b \end{pmatrix}$$

has determinant equal to $2c(s_j - 1)$ for $j = 1, \ldots, n$. □

Now we will state a result on the existence of periodic orbits for family $F_{c,b}$ which is equivalent to Theorem 7 by means of the change of variables from Remark 3.1.3. See Figure 3.2.

Theorem 3.1.7 (cf. Th. 7)**.** *The following statements on the periodic orbits of*

$$F_{c,b}(x,y) = (y, 2cx - cx^2 + by)$$

hold:

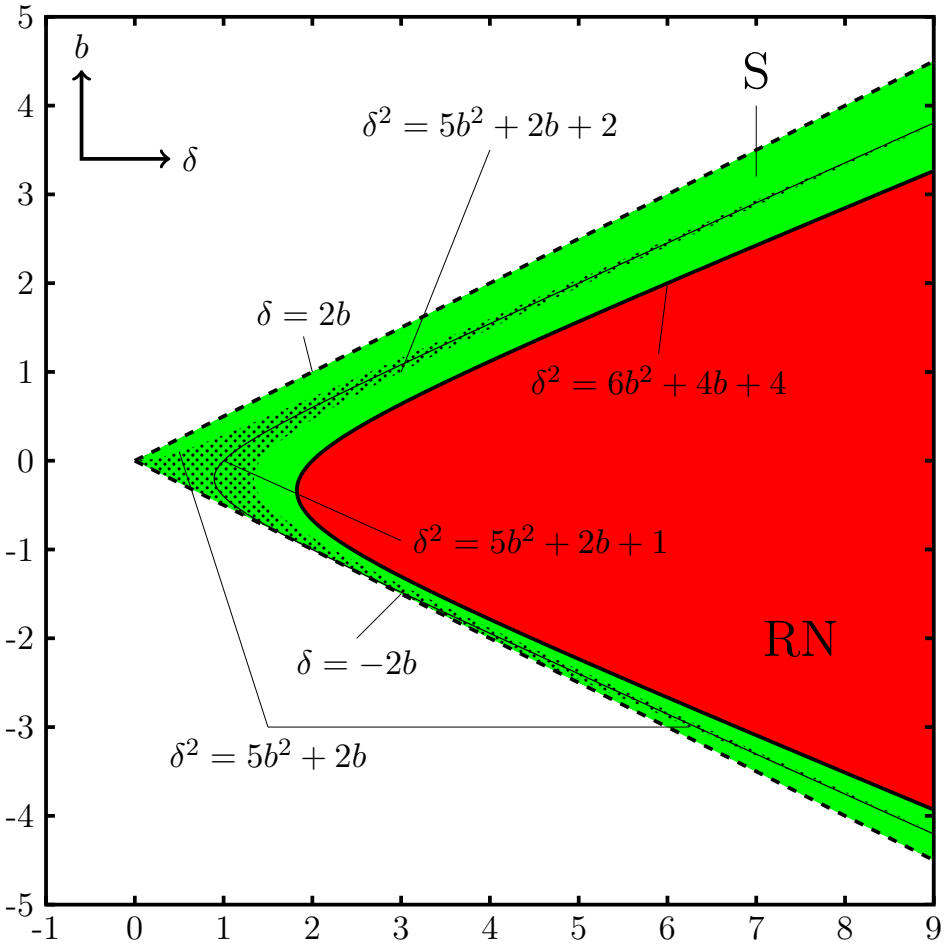

(a)

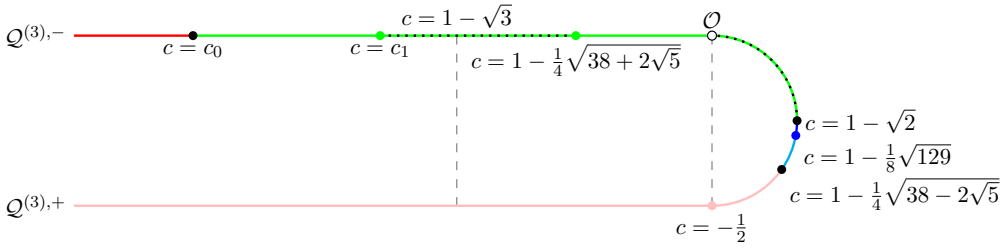

(b)

Figure 3.2: (a) Stability configuration of the unique 2-periodic orbit of $F_{c,b}$: RN (red): repelling node; S (green): saddle fixed point, dotted: dissipative. Along $\delta^2 = 5b^2 + 2b + 1$, one eigenvalue is zero. (b) Stability configuration of the two 3-periodic orbits $\mathcal{Q}^{(3),\pm}$ of $F_{c,b}$ for $b = -1$: attracting node (blue); repelling node (red); attracting focus (cyan); repelling focus (pink); saddle fixed point (green), dotted: dissipative. For $c = -1/2$, the orbit $\mathcal{Q}^{(3),-}$ collapses to $\mathcal{O}$, which is a fixed point.

1. *There exists a 2-periodic orbit if and only if* $|b| < \delta/2$. *In such case, it is unique. Moreover, it is a repelling node if*

$$\delta^2 > 4 + 4b + 6b^2$$

If $\delta^2 < 4 + 4b + 6b^2$, *then it is a saddle periodic orbit that is dissipative if and only if*

$$\delta^2 < 2 + 2b + 5b^2$$

and either $-2 < b < 0$ *or* $2b + 5b^2 < \delta^2$.

2. *Let* $b = 0$. *There exists a decreasing sequence*

$$-1 < \cdots < c_{n+1} < c_n < \cdots < c_3 < c_2 = -\tfrac{1}{2}$$

of c-values such that there exists an attracting 2^n*-periodic orbit for every* $c_{n+1} < c < c_n$ *and* $n \geq 2$.

3. *Let* $b = -1$. *There exists a 3-periodic orbit if and only if* $c \leq 1 - \sqrt{2}$. *Moreover:*

   a) *If* $c = 1 - \sqrt{2}$ *or* $c = -1/2$, *then there exists a unique 3-periodic orbit* $\mathcal{Q}^{(3)}$. *If* $c = 1 - \sqrt{2}$, *then*

   $$\mathcal{Q}^{(3)} = \{(1, 1), (1, -\sqrt{2}), (-\sqrt{2}, 1)\}$$

   with eigenvalues 0 *and* 1. *If* $c = -1/2$, *then*

   $$\mathcal{Q}^{(3)} = \{(2, 2), (2, -2), (-2, 2)\}$$

   with eigenvalues $\pm \mathrm{i}\sqrt{3}$.

   b) *If* $c \in (-\infty, 1 - \sqrt{2}) \setminus \{-1/2\}$, *there exist two different 3-periodic orbits* $\mathcal{Q}^{(3),\pm}$.

      i) *The orbit* $\mathcal{Q}^{(3),-}$ *is a dissipative saddle periodic orbit if* $c > -1/2$. *There exists* $c_0 < 1 - \sqrt{3}$ *such that* $\mathcal{Q}^{(3),-}$ *is a repelling node if* $c < c_0$ *and a saddle periodic orbit if* $c_0 < c < -1/2$, *which is dissipative if and only if* $c_1 < c < 1 - \sqrt{38 + 2\sqrt{5}}/4$ *for some* $c_0 < c_1 < 1 - \sqrt{3}$. *For* $c = c_0$, *the orbit* $\mathcal{Q}^{(3),-}$ *has one eigenvalue equal to* -1.

      ii) *The orbit* $\mathcal{Q}^{(3),+}$ *is an attracting node if and only if* $c \geq 1 - \sqrt{129}/8$. *Otherwise, the orbit* $\mathcal{Q}^{(3),+}$ *is a focus if and only if* $c \neq 1 - \sqrt{38 - 2\sqrt{5}}/4$. *This focus is attracting if and only if* $c > 1 - \sqrt{38 - 2\sqrt{5}}/4$ *and repelling otherwise. For* $c = 1 - \sqrt{38 - 2\sqrt{5}}/4$, *a Hopf–Neimark–Sacker bifurcation occurs.*

4. *For each* $n \in \mathbb{N}$, *the closed disk of centre* $(-\delta/2c, -\delta/2c)$ *and radius* $-\delta\sqrt{n}/2c$ *contains all the n-periodic points.*

Proof. Statement 4 is a direct consequence of Proposition 3.1.6 by projecting the n sphere onto the plane (x, y). In the following sections we prove the other three statements of Theorem 3.1.7.

Period 2: Proof of Statement 1. Any 2-periodic point $Q^{(2)} = (x^{(2)}, y^{(2)})$ of $F_{c,b}$ must satisfy the following equations:

$$\begin{aligned} x &= \varphi_c(x) + by \\ y &= \varphi_c(y) + bx \end{aligned} \tag{3.11}$$

If $x = y$, we obtain the fixed points $\mathcal{O}$ and $Q^{(1),+}$ from Theorem 3.1.5. Otherwise, substracting both equations we obtain

$$x + y = -\tfrac{1}{c}(2b + \delta) \tag{3.12}$$

Therefore, any 2-periodic orbit must be of the form $\{(x^{(2)}, y^{(2)}), (y^{(2)}, x^{(2)})\}$ with $x^{(2)} \neq y^{(2)}$ verifying equation (3.12). Combining equations (3.12) and (3.11), we obtain

$$x^{(2),\pm} = \tfrac{1}{2c}(-2b - \delta) \pm \tfrac{1}{2c}\sqrt{\delta^2 - 4b^2}$$

and $y^{(2),\pm} = x^{(2),\mp}$. Therefore, there exists a 2-periodic orbit $\mathcal{Q}^{(2)}$, which is unique, with points $Q^{(2),\pm} = (x^{(2),\pm}, x^{(2),\mp})$ if and only if $\delta^2 > 4b^2$. The differential of $F_{c,b}$ at each one of these points is

$$\mathrm{D}F_{c,b}(Q^{(2),\pm}) = \begin{pmatrix} 0 & 1 \\ \sigma^{\pm} & b \end{pmatrix}$$

with $\sigma^{\pm} = 2c(1 - x^{(2),\pm})$, respectively. Then,

$$\mathrm{D}F^2_{c,b}(Q^{(2),+}) = \begin{pmatrix} \sigma^{+} & b \\ b\sigma^{+} & \sigma^{-} + b^2 \end{pmatrix}$$

The eigenvalues of $\mathcal{Q}^{(2)}$ are the roots of the characteristic equation

$$\lambda^2 - (2 + 2b + b^2)\lambda + (1 + 2b + 5b^2 - \delta^2) = 0$$

whose discriminant is

$$\Delta^{(2)} = 4\delta^2 - 12b^2 + 4b^3 + b^4$$

Since $\delta^2 > 4b^2$, then $\Delta^{(2)} > b^2(2 + b)^2 \geq 0$. Therefore, the two eigenvalues

$$\lambda_{1,2} = \tfrac{1}{2}(2 + 2b + b^2) \pm \tfrac{1}{2}\sqrt{\Delta^{(2)}}$$

are real. Moreover, since $\sqrt{\Delta^{(2)}} > |b(2 + b)|$, then it is clear that $\lambda_2 < 1 < \lambda_1$. On the other hand, it is easily checked that

$$\mathrm{sgn}(\lambda_2 + 1) = \mathrm{sgn}(3 + (1 + b)^2 - \sqrt{\Delta^{(2)}}) = \mathrm{sgn}(4 + 4b + 6b^2 - \delta^2) \tag{3.13}$$

Therefore, from equation (3.13) we deduce that $\mathcal{Q}^{(2)}$ is a repelling orbit if $\delta^2 > 4 + 4b + 6b^2$, and a saddle periodic orbit if $\delta^2 < 4 + 4b + 6b^2$. In the latter case, since

$$\lambda_1\lambda_2 = 1 + 2b + 5b^2 - \delta^2$$

then $\mathcal{Q}^{(2)}$ is dissipative if and only if

$$2b + 5b^2 < \delta^2 < 2 + 2b + 5b^2$$

Period-doubling Cascade: Proof of Statement 2. From statement 1 of Theorem 3.1.7 it follows that family (3.5) does not have 2-periodic attractors, and consequently neither does family (3.1). The proof of the existence of periodic attractors of greater period complicates excessively the calculations for $b \neq 0$. However, for $b = 0$, we have that

$$F_{c,0}(x, y) = (y, \varphi_c(x)), \quad T_{a,0}(\mathbf{x}, \mathbf{y}) = (a + \mathbf{y}^2, \mathbf{x})$$

Then, we can easily deduce for both families the existence of a period-doubling cascade of periodic attractors.

Let $f_a(\mathbf{y}) = a + \mathbf{y}^2$. The following period-doubling process is well-known: for $a < 1/4$, the map f_a has two fixed points $\mathbf{y}^{\pm}$ with derivatives $f_a'(\mathbf{y}^{\pm}) = 1 \pm \sqrt{1-4a}$. The point $\mathbf{y}^+$ is always repelling as $f_a'(\mathbf{y}^+) > 1$ for all $a < 1/4$. However, for $a > -3/4$, the point $\mathbf{y}^-$ is attracting. For $a < -3/4$, the point $\mathbf{y}^-$ becomes repelling, and a 2-periodic orbit appears. Let $a_2 = -3/4$. The 2-periodic orbit is attracting for $a_3 < a < a_2$ for some $a_3 < a_2$, loses its stability for $a < a_3$, and an attracting 4-periodic orbit appears. By means of a renormalization process, we obtain a bounded decreasing sequence $\{a_n\}_{n\geq 2}$ of a-values in $(-2, -3/4]$ such that f_a has an attracting 2^{n-1}-periodic orbit for all $a_{n+1} < a < a_n$. The existence of attracting 2^n-periodic orbits for $T_{a,0}$ on the left-hand side of $\overline{BD}$ is a consequence of the next result.

Lemma 3.1.8. *If $\{f_a^j(\mathbf{y}_0) : j = 0, 1, \ldots, m-1\}$ is an attracting m-periodic orbit of f_a with $m \geq 2$, then $\{T_{a,0}^j(\mathbf{y}_0, \mathbf{y}_0) : j = 0, 1, \ldots, 2m-1\}$ is an attracting $2m$-periodic orbit of $T_{a,0}$.*

Proof. The point $(\mathbf{y}_0, \mathbf{y}_0)$ is $2m$-periodic for $T_{a,0}$ because

$$T_{a,0}^{2m}(\mathbf{y}_0, \mathbf{y}_0) = (f_a^m(\mathbf{y}_0), f_a^m(\mathbf{y}_0))$$

and $f_a^m(\mathbf{y}_0) = \mathbf{y}_0$. Moreover, the point $(\mathbf{y}_0, \mathbf{y}_0)$ is attracting for $T_{a,0}$ because the differential of $T_{a,0}^{2m}$ at $(\mathbf{y}_0, \mathbf{y}_0)$ is the diagonal matrix with coefficients equal to the derivative of f_a^m at $\mathbf{y}_0$, which has modulus less than 1 as $\mathbf{y}_0$ is attracting for f_a. □

According to our previous discussion, the map $T_{a,0}$ has attracting 2^k-periodic orbits with $k \geq 2$ for $a \leq -3/4$, that is, on the left-hand side of $\overline{BD}$. The attracting nature persists for small perturbations of b and explains the existence of the blue region $\mathcal{P}_0$ from Figure 15 with vertex R_0.

The same arguments employed for f_a can be used for φ_c. Since the value $a = -3/4$ corresponds to the value $c = -1/2$, we obtain the sequence of c-values from statement 2.

Remark 3.1.9. It is very important to observe that the attracting orbit $\mathcal{A}^{(n)}$ of period 2^n appears for $a = a_{n-1}$ when an orbit $\mathcal{A}^{(n-1)}$ of period 2^{n-1} loses its stability. The orbit $\mathcal{A}^{(n-1)}$ has -1 as a double eigenvalue (flip bifurcation, Bogdanov–Takens bifurcation for the double composition) for $a = a_{n-1}$, and persists as a repelling orbit for $a < a_{n-1}$. Therefore, for $a_n < a < a_{n-1}$, the attracting orbit $\mathcal{A}^{(n)}$ of period 2^n coexists with repelling orbits of period 2^k with $k = 1, \ldots, n-1$.

Period 3: Proof of Statement 3. Any 3-periodic point $Q^{(3)} = (x^{(3)}, y^{(3)})$ of $F_{c,b}$ must satisfy the following equations:

$$\begin{aligned} x &= \varphi_c(y) + b\varphi_c(x) + b^2 y \\ y &= \varphi_c(\varphi_c(x) + by) + bx \end{aligned}$$

Operating in these expressions, we obtain

$$bcx^2 + cy^2 + (1-2bc)x - (2c + b^2)y = 0 \tag{3.14}$$

and

$$\begin{aligned} c^3x^4 - 4c^3x^3 - 2bc^2x^2y + (2c^2 + 4c^3)x^2 \\ + 4bc^2xy + b^2cy^2 - (4c^2 + b)x + (1-2bc)y = 0 \end{aligned} \tag{3.15}$$

For $b = -1$, equation (3.14) represents a pair of lines. In this subsection, we take advantage of this simplification and compute the 3-periodic orbits of $F_{c,-1}$, thus proving statement 3 of Theorem 3.1.7.

Lemma 3.1.10. *Let $b = -1$. For all $c \leq 1 - \sqrt{2}$, the map $F_{c,b}$ has two 3-periodic orbits $\mathcal{Q}^{(3),\pm}$:*

$$Q_0^{(3),-} = (1+\sigma, 1+\sigma), \quad Q_1^{(3),-} = (1+\sigma, 1+\tfrac{1}{c}-\sigma), \quad Q_2^{(3),-} = (1+\tfrac{1}{c}-\sigma, 1+\sigma)$$

with eigenvalues

$$\lambda_{1,2}^{-} = \tfrac{1}{2}(1+\kappa) \pm \tfrac{1}{2}(\kappa-1)\sqrt{4\kappa+1}$$

and

$$Q_0^{(3),+} = (1-\sigma, 1-\sigma), \quad Q_1^{(3),+} = (1-\sigma, 1+\tfrac{1}{c}+\sigma), \quad Q_2^{(3),+} = (1+\tfrac{1}{c}+\sigma, 1-\sigma)$$

with eigenvalues

$$\lambda_{1,2}^{+} = \tfrac{1}{2}(1-\kappa) \pm \tfrac{1}{2}(\kappa+1)\sqrt{1-4\kappa}$$

where $\sigma = \sqrt{(1-c)^2-2}/c$ and $\kappa = 2c\sigma$.

Remark 3.1.11. Both orbits coincide when $\sigma = 0$, that is, when $c = 1 - \sqrt{2}$. In that case, the unique 3-periodic orbit for $b = -1$ is $\{(1,1), (1, -\sqrt{2}), (-\sqrt{2}, 1)\}$, and its eigenvalues are 0 and 1.

Remark 3.1.12. As $c \to -1/2$, it holds that $\sigma \to -1$ and therefore $\mathcal{Q}^{(3),-}$ approaches $\mathcal{O}$, which is a fixed point of $F_{c,-1}$, until they collapse for $c = -1/2$. Thus, the only 3-periodic orbit for $c = -1/2$ is

$$\mathcal{Q}^{(3),+} = \{(2,2), (2,-2), (-2,2)\}$$

and has eigenvalues $\pm i\sqrt{3}$.

Proof. For $b = -1$, equations (3.14) and (3.15) are

$$(c(x+y) - (1+2c))(y-x) = 0 \tag{3.16}$$

and

$$c^3x^4 - 4c^3x^3 + 2c^2x^2y + (2c^2+4c^3)x^2 - 4c^2xy + cy^2 - (4c^2-1)x + (1+2c)y = 0 \tag{3.17}$$

respectively. Substituting $y = x$ in equation (3.17), we obtain

$$c^3x^4 + 2c^2(1-2c)x^3 + (4c^3 - 2c^2 + c)x^2 + (2 + 2c - 4c^2)x = 0 \tag{3.18}$$

The fixed points provide two solutions: $x = 0$ and $x = 2 - 2/c$. The other two solutions are provided by

$$c^2x^2 - 2c^2x + 2c + 1 = 0$$

which are

$$x_0^{(3),\pm} = 1 \mp \sigma, \qquad \sigma = \tfrac{1}{c}\sqrt{(1-c)^2-2} \tag{3.19}$$

as long as $c \leq 1 - \sqrt{2}$. Substituting $y = -x + 2 + 1/c$ in equation (3.17), we obtain

$$c^3x^4 - (4c^3+2c^2)x^3 + (4c^3+10c^2+3c)x^2 - (12c^2+10c+2)x + \tfrac{2}{c}(1+2c)^2 = 0 \tag{3.20}$$

Equation (3.20) can be written as

$$(c^2x^2 - 2c^2x + 2c + 1)(cx^2 - 2(1+c)x + 4 + \tfrac{2}{c}) = 0$$

Thus, the abscissa of the 3-periodic points for $b = -1$ are given by points (3.19) and

$$x_2^{(3),\pm} = 1 + \tfrac{1}{c} \pm \sigma \tag{3.21}$$

as long as $c \leq 1-\sqrt{2}$. In conclusion, there exist six 3-periodic points for $b=-1$ divided into the two periodic orbits from the statement of this Lemma. On the other hand, it is straightforward to check that

$$\mathrm{D}F^3_{c,b}(Q_0^{(3),-}) = \begin{pmatrix} \kappa & 1-\kappa \\ \kappa(1-\kappa) & 1 \end{pmatrix}, \quad \mathrm{D}F^3_{c,b}(Q_0^{(3),+}) = \begin{pmatrix} -\kappa & 1+\kappa \\ -\kappa(1+\kappa) & 1 \end{pmatrix}$$

Thus, the respective characteristic equations are

$$\lambda^2 - (1+\kappa)\lambda + 2\kappa^2 - \kappa^3 = 0$$

for $\mathcal{Q}^{(3),-}$, and

$$\lambda^2 - (1-\kappa)\lambda + 2\kappa^2 + \kappa^3 = 0$$

for $\mathcal{Q}^{(3),+}$. By solving those equations, we obtain the announced eigenvalues $\lambda^-_{1,2}$ and $\lambda^+_{1,2}$ of $\mathcal{Q}^{(3),-}$ and $\mathcal{Q}^{(3),+}$, respectively. □

Since $\kappa \geq 0$, the eigenvalues of $\mathcal{Q}^{(3),-}$ are always real, while those of $\mathcal{Q}^{(3),+}$ are real if and only if $\kappa \leq 1/4$. When $\kappa > 1/4$, they are complex with modulus $\kappa\sqrt{\kappa+2}$. In the following lemmas, we study the nature of the 3-periodic orbits $\mathcal{Q}^{(3),-}$ and $\mathcal{Q}^{(3),+}$.

Lemma 3.1.13. *For all $\kappa > 0$, the eigenvalues $\lambda^-_{1,2}$ of $\mathcal{Q}^{(3),-}$ are real and $\lambda^-_1 > -1$. Moreover:*

i) $\lambda^-_1 \leq 1$ if and only if $\kappa \leq 1$, with equality holding if and only if $\kappa = 1$.

ii) $\lambda^-_2 \leq 1$ if and only if $\kappa \geq 1$, with equality holding if and only if $\kappa = 1$.

iii) $\lambda^-_2 \geq -1$ if and only if $\kappa \leq \kappa_0$, being κ_0 the unique root of

$$\kappa^3 - 2\kappa^2 - \kappa - 2 = 0$$

in $(2,3)$, with equality holding if and only if $\kappa = \kappa_0$.

In particular:

1. *The orbit $\mathcal{Q}^{(3),-}$ is a hyperbolic saddle periodic point if $\kappa \in (0,\kappa_0)\setminus\{1\}$. This saddle is dissipative if and only if either $\kappa < 1$ or $\kappa \in ((1+\sqrt{5})/2, \kappa_1)$, where $\kappa_1 \in (2,\kappa_0)$ is the unique positive root of $\kappa^3 - 2\kappa^2 - 1$.*

2. *If $\kappa \in \{1, \kappa_0\}$, then $\mathcal{Q}^{(3),-}$ is nonhyperbolic. In particular, if $\kappa = 1$, then $F_{c,-1}$ displays a Bogdanov–Takens singularity at $\mathcal{Q}^{(3),-}$, which collapses to the origin.*

3. *If $\kappa > \kappa_0$, then $\mathcal{Q}^{(3),-}$ is a repelling node.*

Proof. The eigenvalues of $\mathcal{Q}^{(3),-}$ are given in Lemma 3.1.10. It is clear that $\lambda^-_{1,2} \in \mathbb{R}$. Moreover, it holds that $\lambda^-_1 > -1$ is equivalent to $3+\kappa \geq (1-\kappa)\sqrt{4\kappa+1}$, which holds for all $\kappa \geq 0$.

i) $\lambda^-_1 \leq 1$ is equivalent to $(1-\kappa)(1+\sqrt{4\kappa+1}) \geq 0$. Since $1+\sqrt{4\kappa+1} > 0$, then $\lambda^-_1 \leq 1$ if and only if $1-\kappa \geq 0$, and equality holds if and only if $1-\kappa = 0$.

ii) $\lambda^-_2 \leq 1$ is equivalent to $(1-\kappa)(1-\sqrt{4\kappa+1}) \geq 0$. Since $\sqrt{4\kappa+1} > 1$, then $\lambda^-_2 \leq 1$ if and only if $1-\kappa \leq 0$, and equality holds if and only if $1-\kappa = 0$.

iii) $\lambda^-_2 \geq -1$ is equivalent to $3+\kappa \geq (\kappa-1)\sqrt{4\kappa+1}$. It is straightforward to check that the latter inequality holds if and only if $\kappa \leq \kappa_0$, and equality holds if and only if $\kappa = \kappa_0$. □

Lemma 3.1.14. *The eigenvalues $\lambda_{1,2}^+$ of $\mathcal{Q}^{(3),+}$ are complex with modulus $\kappa\sqrt{\kappa+2}$ if and only if $\kappa > 1/4$. Otherwise, it holds that $-1 < \lambda_2^+ \leq \lambda_1^+ < 1$, with equality holding if and only if $\kappa = 1/4$, for which $\lambda_1^+ = \lambda_2^+ = 3/8$. In particular:*

1. *If $0 < \kappa \leq 1/4$, then $\mathcal{Q}^{(3),+}$ is an attracting node.*
2. *If $\kappa > 1/4$, then $\mathcal{Q}^{(3),+}$ is a focus if and only if $\kappa \neq (\sqrt{5}-1)/2$. This focus is attracting if $\kappa < (\sqrt{5}-1)/2$ and repelling otherwise.*
3. *If $\kappa = (\sqrt{5}-1)/2$, then $\mathcal{Q}^{(3),+}$ is a center.*

Proof. The eigenvalues of $\mathcal{Q}^{(3),+}$ are given in Lemma 3.1.10. It is clear that $\lambda_{1,2}^+$ are complex if and only if $\kappa > 1/4$, and their modulus is equal to $\kappa\sqrt{\kappa+2}$. It is immediate to check that $|\lambda_{1,2}^+| = 1$ if and only if $\kappa = (\sqrt{5}-1)/2$. Otherwise, it is trivial that $\lambda_2^+ \leq \lambda_1^+$, and equality holds if and only if $1 - 4\kappa = 0$. Moreover:

i) $\lambda_1^+ < 1$ is equivalent to $\sqrt{1-4\kappa} < 1$, which trivially holds for all $0 < \kappa \leq 1/4$.

ii) $\lambda_2^+ > -1$ is equivalent to $\kappa^3 + 2\kappa^2 - \kappa + 2 > 0$, which holds for all $0 < \kappa \leq 1/4$. □

Remark 3.1.15. If $b = -1$, then $c = 1 - \sqrt{1-a}$ for all $a \leq 1$. Thus, it holds that $c \leq 1 - \sqrt{2}$ if and only if $a \leq -1$. In that case, we have that $\kappa = 2\sqrt{-1-a}$ and the following correspondences:

κ	a	c
1	$-5/4$	$-1/2$
$1/4$	$-65/64$	$1 - \sqrt{129}/8$
$(1+\sqrt{5})/2$	$-(11+\sqrt{5})/8$	$1 - \sqrt{38+2\sqrt{5}}/4$
$(\sqrt{5}-1)/2$	$(\sqrt{5}-11)/8$	$1 - \sqrt{38-2\sqrt{5}}/4$
$\kappa_{0,1}$	$-1 - \kappa_{0,1}^2/4$	$1 - \sqrt{\kappa_{0,1}^2+8}/2$

With the aid of Remark 3.1.15 and Lemmas 3.1.13 and 3.1.14 we prove statement 3 of Theorem 3.1.7 straightforwardly: The existence of the 3-periodic orbits of $F_{c,-1}$ is proved in Lemma 3.1.10, providing their expressions and their eigenvalues. Statement a) is proved in Remarks 3.1.11 and 3.1.12. Statement b) is a direct consequence of the eigenvalue discussion from Lemmas 3.1.13 and 3.1.14. □

Remark 3.1.16. For $-1/2 < c < 1 - \sqrt{2}$, the orbit $\mathcal{Q}^{(3),-}$ is a dissipative saddle periodic orbit that coexists with $\mathcal{Q}^{(3),+}$, which exhibits a Hopf–Neimark–Sacker bifurcation for $c = 1 - \sqrt{38-2\sqrt{5}}/4 \approx -0.4476$. This bifurcation generates closed orbits that collide with $\mathcal{Q}^{(3),-}$ to give place to a homoclinic cycle. See Figure 3.3. The generation and/or destruction of this cycle justifies [44] the existence of strange attractors numerically obtained for the parameter values in red from Figure 20.

3.2 Global Dynamics: Proof of Theorem 8

This section is devoted to the proof of the existence of the invariant compact sets with nonempty interior provided by Theorem 8 for sharp regions of parameter values whose vertice is either $(-2, 0)$ or $(-4, -2)$. Although we could translate our results to the original plane of parameters (a, b) from Figure 14, we will work with family (3.5) from Remark 3.1.2. It will be useful to observe that these maps transforms horizontal lines $y = h$ into vertical lines $x = h$, and these ones into non-vertical lines of slope b.

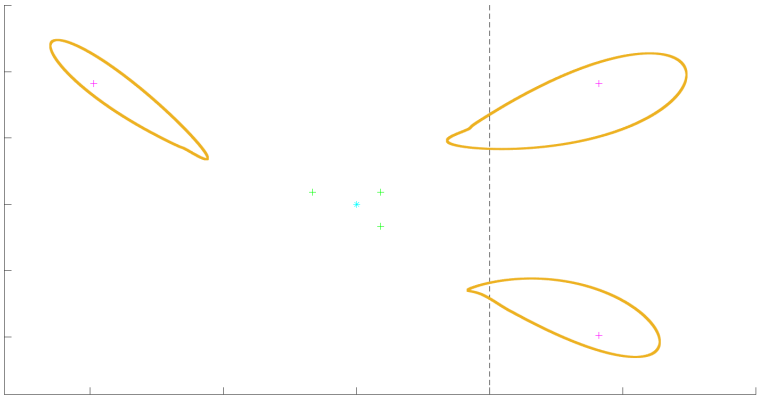

Figure 3.3: The repelling 3-periodic focus in magenta for $(c, b) = (-0.464581, -1)$ gives rise to three limit cycles that get closer to the dissipative saddle 3-periodic orbit in green, closer itself to the origin in cyan, which is an attracting fixed focus

3.2.1 A Sharp Parameter Region With Vertex at $(-2, 0)$

We will first consider parameter values (a, b) close to the point C_1. We will construct invariant squares for $F_{c,b}$ that transform into invariant quadrilaterals for $T_{a,b}$.

Lemma 3.2.1. *Let $0 \leq b < 1$. The square*

$$R^+_{c,b} = [h^+_1, h^+_2] \times [h^+_1, h^+_2], \qquad -1 \leq h^+_1 \leq c < 0 < h^+_2$$

where

$$h^+_1 = \frac{c}{1-b}, \quad h^+_2 = (h^+_1)^2(2 - h^+_1)$$

is $F_{c,b}$-invariant whenever $0 > a \geq -2(b-1)^2$.

Proof. If $a \geq -2(b-1)^2$, then $\delta^2 = (b-1)^2 - 4a \leq 9(b-1)^2$. Therefore, we have that $c \geq -(1-b)$ and, consequently, that $h^+_1 \geq -1$. We will prove next that $R^+_{c,b}$ is $F_{c,b}$-invariant. In Figure 3.4 we represent the square $R^+_{c,b}$ of vertices

$$E = (h^+_1, h^+_1), \qquad F = (h^+_2, h^+_1), \qquad G = (h^+_2, h^+_2), \qquad H = (h^+_1, h^+_2)$$

If $h^+_2 \geq 1$, then $\mathcal{L}_0$ intersects $R^+_{c,b}$ at the points $S_0 = (1, h^+_2)$ and $Q_0 = (1, h^+_1)$. Note that $\mathcal{L}_0$ is a good fold for $R^+_{c,b}$ since $h^+_1 + h^+_2 \leq 2$ as $(h^+_1)^2 \leq 1$. The images of S_0 and Q_0 are $S_1 = (h^+_2, c + bh^+_2)$ and $Q_1 = E$, respectively. Since $h^+_2 > 0 > h^+_1$ and $0 \leq b < 1$, then $S_1 \in \overline{FG}$. The images of Q_1 and H are

$$Q_2 = (h^+_1, (1-b)h^+_2 + bh^+_1)$$

and $H_1 = G$, respectively. Since $0 \leq b < 1$, it follows that $Q_2 \in \overline{EH}$. Thus,

$$F_{c,b}(R^+_{c,b}) = \Omega(E, S_1, G, Q_2)$$

is contained in $R^+_{c,b}$.

On the other hand, if $h^+_2 < 1$, then $\mathcal{L}_0$ does not intersect $R^+_{c,b}$. It still holds that $E_1 \in \overline{EH}$ and $H_1 = G$. We have to check that $G_1 \in \overline{FG}$ and $F_1 \in \overline{EH}$. Indeed, the images of F and G are

$$F_1 = (h^+_1, ch^+_2(2 - h^+_2) + bh^+_1) \tag{3.22}$$

and

$$G_1 = (h_2^+, ch_2^+(2 - h_2^+) + bh_2^+) \tag{3.23}$$

Since $1 > h_2^+ > 0 > h_1^+$ and $c < 0$, then F_1 is clearly below E_1, and above E because

$$ch_2^+(2 - h_2^+) + bh_1^+ > h_1^+$$

is equivalent to $(h_2^+ - 1)^2 > 0$, which trivially holds. Since $1 > h_2^+ > 0 > h_1^+$ and $0 \leq b < 1$, then G_1 is clearly below G, and above F because the ordinate of G_1 is greater than that of F_1. Thus,

$$F_{c,b}(R_{c,b}^+) = \Omega(F_1, G_1, G, E_1)$$

is contained in $R_{c,b}^+$. □

Remark 3.2.2. The square $R_{c,b}^+$ is symmetric with respect to $\mathcal{L}_0$ if and only if $a = -2(b-1)^2$, in which case $h_1^+ = 2 - h_2^+ = -1$ and $(h_2^+, h_2^+) = (3, 3)$ is a fixed point. The square $R_{c,b}^+$ is strictly invariant if and only if $b = 0$ and $a \leq -1$. By applying the changes of variables and parameters from Remark 3.1.3, the square $R_{c,b}^+$ is transformed into the $T_{a,b}$-invariant quadrilateral $R_{a,b}^+$ of vertices

$$\left(a, \tfrac{a}{1-b}\right), \quad \left(a - \tfrac{a^2 b}{(1-b)^3}, \tfrac{a^2+a(1-b)^2}{(1-b)^3}\right), \quad \left(a + \tfrac{a^2}{(1-b)^2}, \tfrac{a^2+a(1-b)^2}{(1-b)^3}\right), \quad \left(\tfrac{a^2+a(1-b)(1-2b)}{(1-b)^3}, \tfrac{a}{1-b}\right)$$

Note that $R_{a,0}^+ = [a, a+a^2] \times [a, a+a^2]$. Also, it is easy to check that $h_2^+ \geq 1$ whenever $b \geq (1+\sqrt{5})(1+a)/2$. In particular, this case holds for all parameter values sufficiently close to $(-2, 0)$.

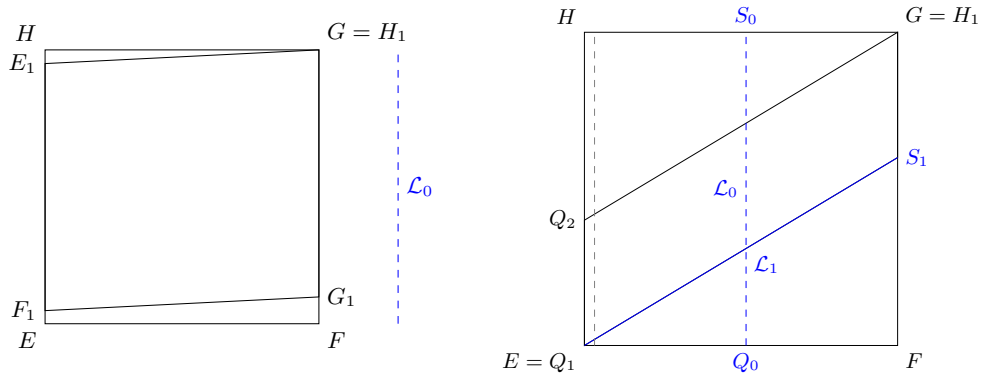

Figure 3.4: The $F_{c,b}$-invariant square $[h_1^+, h_2^+] \times [h_1^+, h_2^+]$ for $0 \leq b < 1$: (a) $h_2^+ < 1$; (b) $h_2^+ \geq 1$

We will now prove a result analogous to Lemma 3.2.1 for $-1 < b \leq 0$.

Lemma 3.2.3. *Let* $-1 < b \leq 0$. *The square*

$$R_{c,b}^- = [h_1^-, h_2^-] \times [h_1^-, h_2^-], \qquad h_1^- < 0 < 2 < h_2^-$$

where

$$h_1^- = \frac{c+2b}{1+b}, \quad h_2^- = \frac{2-c}{1+b}$$

is $F_{c,b}$*-invariant whenever* $-2(b+1)^2 \leq a < 0$.

Remark 3.2.4. Any square $[h_1', h_2'] \times [h_1', h_2']$ with $h_1' \leq h_1^-$ and $h_2' = 2 - h_1'$ is $F_{c,b}$-invariant.

Proof. In Figure 3.5 we represent the square $R_{c,b}^-$ with vertices

$$E = (h_1^-, h_1^-), \qquad F = (h_2^-, h_1^-), \qquad G = (h_2^-, h_2^-), \qquad H = (h_1^-, h_2^-)$$

The critical line $\mathcal{L}_0$ intersects the boundary of $R_{c,b}^-$ at the points $S_0 = (1, h_2^-)$ and $Q_0 = (1, h_1^-)$. Since $h_1^- + h_2^- = 2$, then $\mathcal{L}_0$ is a good fold for $R_{c,b}^-$. The image of the segment $\overline{Q_0 S_0}$ is the segment $\overline{Q_1 S_1}$ with $Q_1 = (h_1^-, c + bh_1^-)$ and $S_1 = F$, and the image of the side $\overline{EH}$ is the segment $\overline{E_1 H_1}$ with

$$E_1 = (h_1^-, ch_1^- h_2^- + bh_1^-)$$

and

$$H_1 = (h_2^-, ch_1^- h_2^- + bh_2^-)$$

Since $h_1^- < h_2^-$ and $b < 0$, then $H_1 \in \overline{FG}$, and the square $R_{c,b}^-$ is invariant if and only if E_1 is below H, that is,

$$ch_1^- h_2^- + bh_1^- \leq h_2^- \tag{3.24}$$

Inequality (3.24) is equivalent to

$$c(2-c)(c+2b) + b(1+b)(c+2b) \leq (1+b)(2-c) \tag{3.25}$$

Since $c^2 + bc = c - a$, inequality (3.25) transforms into

$$(1+b)\big((2-c)(c-1) + b(c+2b)\big) \leq (2-c)a \tag{3.26}$$

From a direct substitution of

$$(2-c)(c-1) + b(c+2b) = 2c(1+b) + 2(b^2-1) + a$$

into equation (3.26), we arrive at

$$(1+b)\big(2c(1+b) + 2(b^2-1)\big) \leq (2-c-1-b)a \tag{3.27}$$

The left-hand side of inequality (3.27) is equal to

$$(1+b)\big(2c(1+b) + 2(b^2-1)\big) = (1+b)^2(b-1-\delta)$$

while the right-hand side is equal to

$$(2-c-1-b)a = \tfrac{a}{2}(1-b-\delta)$$

Therefore,

$$(1+b)^2(b-1-\delta) \leq \tfrac{a}{2}(1-b+\delta)$$

Since $1 - b + \delta > 0$, we conclude that $a \geq -2(b+1)^2$. □

Remark 3.2.5. The square $R_{c,b}^-$ is always symmetric with respect to the $\mathcal{L}_0$, and is strictly invariant if and only if $(a, b) = (-2, 0)$. For $a = -2(b+1)^2$, we have that $F_{c,b}((h_1^-, h_1^-)) = (h_1^-, h_2^-)$.

Proposition 3.2.6. *Let $(a^*, b^*) = (-2, 0)$. The curves*

$$\gamma^+(a) = 1 - \sqrt{-\tfrac{a}{2}}, \quad \gamma^-(a) = -1 + \sqrt{-\tfrac{a}{2}}$$

intersect at (a^*, b^*) and define a sharp region

$$\mathcal{V} = \{\gamma^-(a) \leq b \leq \gamma^+(a) : a^* \leq a < 0\}$$

such that, for every $(a, b) \in \mathcal{V}$, there exists a $T_{a,b}$-invariant quadrilateral.

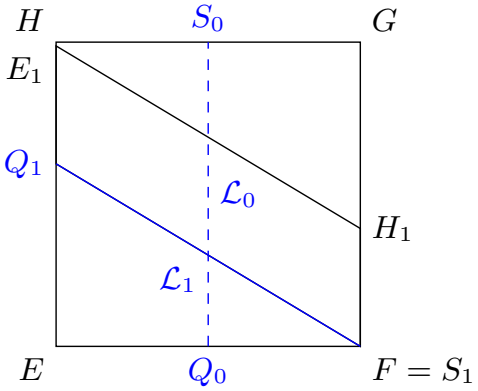

Figure 3.5: The $F_{c,b}$-invariant square $[h_1^-, h_2^-] \times [h_1^-, h_2^-]$ for $-1 < b \leq 0$

The sharp region $\mathcal{V}$ for $(a^*, b^*) = (-2, 0)$ intersects the line $b = 0$. It was proved [60] that, for the points in $\mathcal{V}$ along this line, the square $R^+_{a,0}$, see Remark 3.2.2, contains a 2-D strange attractor for a-values in a subset of $[-2, -2 + \delta]$, for $\delta > 0$ arbitrarily small, with positive Lebesgue measure [60]. Since the measure of E is null in the plane of parameters, the persistence of the 2-D strange attractors is still an open problem.

3.2.2 A Sharp Parameter Region With Vertex at $(-4, -2)$

We will now search for invariant compact sets for parameter values close to $C_2 = (-4, -2)$. We will work with family (3.5), for which the critical line is $\mathcal{L}_0 \equiv x = 1$. The first and second images of $\mathcal{L}_0$ are

$$\mathcal{L}_1 \equiv y = c + bx \tag{3.28}$$

and

$$\mathcal{L}_2 \equiv b^2 y = -cx^2 + (b^3 + 2bc + 2c^2)x - c^2(2b + c) \tag{3.29}$$

respectively. If $b < 0$, then $\mathcal{L}_1$ is a line with negative slope and $\mathcal{L}_2$ is an upwards parabola. In Figure 3.6 we represent all these curves. The intersection point of $\mathcal{L}_0$ and $\mathcal{L}_1$ is $V_{0,1} = (1, c + b)$, and its first and second images are $V_{1,2} = (c + b, c + b(c + b))$, and

$$V_{2,3} = (c, b(c + b), c(c + b)(2 - c - b) + b(c + bc + b^2))$$

respectively. The construction of the invariant domain will involve the symmetric line

$$\widetilde{\mathcal{L}}_1 \equiv y = c + 2b - bx$$

of $\mathcal{L}_1$ with respect to the critical line $\mathcal{L}_0$, whose preimage

$$\widetilde{\mathcal{L}}_{-1} \equiv y = \tfrac{c}{2b}(x - 1)^2 + 1 \tag{3.30}$$

is a parabola symmetric with respect to $\mathcal{L}_0$ with vertex at $(1, 1)$ that intersects the lines $\mathcal{L}_1$ and $\widetilde{\mathcal{L}}_1$ if and only if $2a \geq b^3$. In such case, the respective intersection points are

$$Q^{\pm} = (x^{\pm}, c + bx^-), \qquad x^{\pm} = 1 \pm \tfrac{b^2}{c} \mp \tfrac{1}{c}\sqrt{b^4 - 2ab}$$

The image of both points is

$$Q_1^- = Q_1^+ = (x, c + 2b - bx), \qquad x = c + b + \tfrac{b^3}{c} - \tfrac{b}{c}\sqrt{b^4 - 2ab}$$

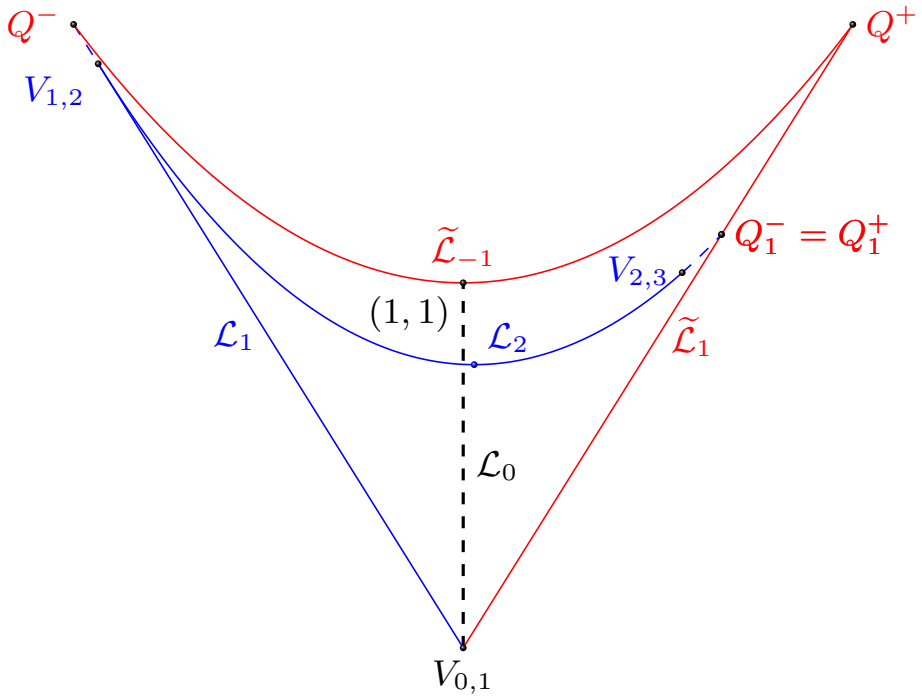

Figure 3.6: The $F_{c,b}$-invariant curvilinear triangle $\langle V_{0,1}, Q^+, Q^- \rangle$

Lemma 3.2.7. *Let $-2 \leq b < 0$. If $0 > a \geq b^3/2$, then the following hold:*

a) The point $Q_1^- = Q_1^+$ is below Q^+ and both coincide if and only if $(a,b) = (-4,-2)$. In such case, the points $Q_1^- = Q_1^+$ and Q^+ are equal to $(5,5)$, the fixed point of $F_{-1,-2}$.

b) The point $V_{1,2}$ is below the point Q^- if and only if $a \leq -2b - 2b^2$, and both coincide if and only if $a = -2b - 2b^2$.

Proof.

a) Since $b < 0$, the point $Q_1^- = Q_1^+$ is below Q^+ if and only if

$$c + b + \tfrac{b^3}{c} - \tfrac{b}{c}\sqrt{b^4 - 2ab} \leq 1 - \tfrac{b^2}{c} + \tfrac{1}{c}\sqrt{b^4 - 2ab} \tag{3.31}$$

Since $c < 0$, inequality (3.31) is equivalent to

$$c^2 + (b-1)c + (b+1)(b^2 - \sqrt{b^4 - 2ab}) \geq 0$$

By equation (3.2), the equivalent inequality

$$a \leq (b+1)(b^2 - \sqrt{b^4 - 2ab})$$

transforms, by multiplying by $b^2 + \sqrt{b^4 - 2ab} > 0$, into

$$a(b^2 + \sqrt{b^4 - 2ab}) \leq 2ab(b+1)$$

It is sufficient to divide by $a < 0$ to arrive at

$$\sqrt{b^4 - 2ab} \geq b(b+2) \tag{3.32}$$

which is equivalent to inequality (3.31). Note that inequality (3.32) always holds as $\sqrt{b^4-2ab} \geq 0$ and $b(b+2) \leq 0$. Equality holds if and only if $a=-4$ and $b=-2$. In this case, both points coincide with the fixed point $(5,5)$ of $F_{c,b}$ with $c=-1$.

b) Since $b<0$, the point $V_{1,2}$ is below Q^- if and only if

$$c+b \geq 1+\tfrac{b^2}{c}-\tfrac{1}{c}\sqrt{b^4-2ab} \tag{3.33}$$

Since $c<0$, inequality (3.33) is equivalent to

$$c^2+(b-1)c \leq b^2-\sqrt{b^4-2ab}$$

By equation (3.2), we obtain

$$\sqrt{b^4-2ab} \leq -b(b+2) \tag{3.34}$$

which is equivalent to inequality (3.33). Since $\sqrt{b^4-2ab} \geq 0$, squaring both sides, we have that inequality (3.34) is equivalent to $a \leq -2b-2b^2$. Equality holds if and only if $V_{1,2}=Q^-$. □

Lemma 3.2.8. *Let $-2<b<0$. If $b^3/2 \leq a < 0$, then the arc Q^-Q^+ of the parabola $\widetilde{\mathcal{L}}_{-1}$ does not intersect the arc $V_{1,2}Q_1^+$ of the parabola $\mathcal{L}_2$ whenever $a<-2b-2b^2$.*

Remark 3.2.9. If $a=-2b-2b^2$, from Lemma 3.2.8 it follows that both arcs intersect only at $V_{1,2}=Q^-$. For $b=-2$, then $a=-4$ and both arcs coincide.

Proof. Since $b>-2$, then $b/2>-1$, and since $c<0$, it follows that $bc/2<-c$. Dividing by b^2, we conclude that $c/2b<-c/b^2$. Therefore, the parabola $\widetilde{\mathcal{L}}_{-1}$ is wider than $\mathcal{L}_2$. Substracting equation (3.29) from equation (3.30) we obtain the distance

$$d(x)=\tfrac{1}{2b^2}\big(c(b+2)x^2-(2b^3+4c^2+6bc)x+(2b+c)(2c^2+b)\big)$$

between both parabolas. Since $a<-2b-2b^2$, it follows from Lemma 3.2.7 that the relative positions of the points Q^- and $V_{1,2}$, and Q^+ and Q_1^+, are as represented in Figure 3.6. Therefore, at the extremes of the interval

$$I=\big[c+b, c+b+b\big(b^2-\sqrt{b^4-2ab}\big)\big]$$

determined by the abscissas of $V_{1,2}$ and Q_1^+ the parabola d is positive. Moreover, since $d'' \equiv c(b+2)/b^2<0$, then d is positive on all I, and therefore the arc $V_{1,2}Q_1^+$ is strictly below the arc Q^-Q^+. □

From Figure 3.6, we obtain the next result.

Proposition 3.2.10. *Let $-2 \leq b < 0$. If $b^3/2 \leq a < 0$, then the curvilinear triangle $\langle V_{0,1}, Q^-, Q^+\rangle$ is $F_{c,b}$-invariant whenever $a \leq -2b-2b^2$.*

Remark 3.2.11. It is strictly $F_{c,b}$ invariant if and only if $(c,b)=(-1,-2)$, in which case

$$\langle V_{0,1}, Q^-, Q^+\rangle = \langle (1,-3),(-3,5),(5,5)\rangle$$

Proof. The lines $\mathcal{L}_1$ and $\widetilde{\mathcal{L}}_1$ and the parabola $\widetilde{\mathcal{L}}_{-1}$ intersect forming a curvilinear triangle $R_{c,b}$ of vertices $V_{0,1}$, Q^-, and Q^+, which is symmetric with respect to the critical line $\mathcal{L}_0$. Therefore, the fold of $R_{c,b}$ with respect to $\mathcal{L}_0$ is the curvilinear triangle of vertices $V_{0,1}$, P_0, and Q^-. The image of $R_{c,b}$ under $F_{c,b}$ is another curvilinear triangle, limited by the lines $\mathcal{L}_1$ and $\widetilde{\mathcal{L}}_1$ and the parabola $\mathcal{L}_2$, which intersect at the points $V_{0,1}$, $V_{1,2}$, and Q_1^+, respectively. From Lemma 3.2.8 we deduce that $F_{c,b}(R_{c,b}) \subseteq R_{c,b}$. □

By applying the changes of variables and parameters from Remark 3.1.3 to the $F_{c,b}$-invariant curvilinear triangle from Proposition 3.2.10, we obtain a $T_{a,b}$-invariant curvilinear triangle and straighforwardly prove the next result, from which Theorem 8 follows.

Proposition 3.2.12. *Let* $(a^*, b^*) = (-4, -2)$. *The curves*

$$\gamma^+(a) = \sqrt[3]{2a}, \quad \gamma^-(a) = -\tfrac{1}{2} - \tfrac{1}{2}\sqrt{1-2a}$$

intersect at (a^*, b^*) *and define a sharp region*

$$\mathcal{V} = \{\gamma^-(a) \leq b \leq \gamma^+(a) : a^* \leq a < 0\}$$

such that, for every $(a, b) \in \mathcal{V}$, *there exists a* $T_{a,b}$*-invariant curvilinear triangle.*

The existence of 2-D strange attractors was numerically proved [61] for parameter values (a, b) along the curve G. It can be checked that G, on the right-hand side of $a = -4$, is between the curves $2a = b^3$ and $a = -2b - 2b^2$. The three of them go through the point $(-4, -2)$ with equal tangent. See Figure 3.7.

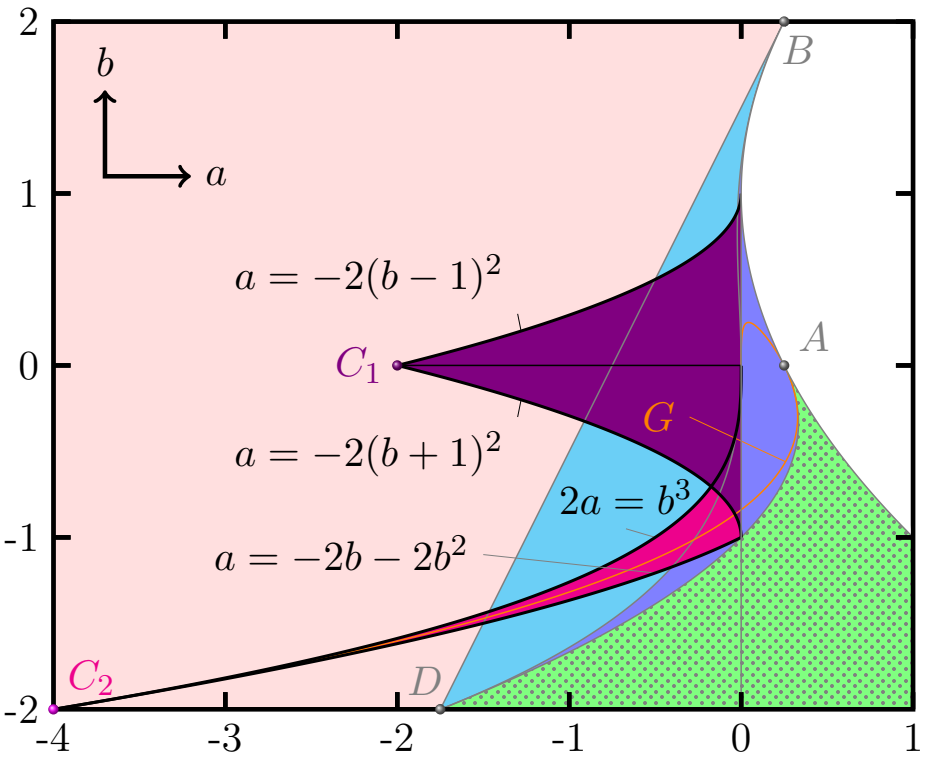

Figure 3.7: The sharp regions $\mathcal{V}(-2, 0)$ and $\mathcal{V}(-4, -2)$ and the curve G plotted over the stability configuration of $P^{(1),-}$ from Figure 16a

3.3 Strictly Invariant Sets and Numerical Results

In Section 3.2 we proved the existence of invariant compact sets with nonempty interior for parameter values (a, b) in sharp regions $\mathcal{V}$ whose boundary contains either $(-2, 0)$ or $(-4, -2)$. For the latter point, the sharp region $\mathcal{V}$ is limited by the curve $2a = b^3$. Along

this curve, the second iterate of the critical line is a parabola symmetric with respect to it, and the third one is a straight line. This property will make easier the construction in this section of compact sets $R_{a,b}$ with non-empty interior that will be strictly invariant. Thus, the sets $R_{a,b}$ will be 2-D strange attractors as long as they are minimal (transitive). Although we will not analytically prove such minimality here, we will numerically show that they contain attractors seemingly strange. Also, we will show that these attractors present processes of splitting and doubling that had been proved for $\Gamma_{a,\theta}$ in Chapter 2.

Possible 2-D strange attractors will also be numerically simulated for random parameter values in the sharp region $\mathcal{V}$ for both $(-2,0)$ and $(-4,-2)$, thus strongly supporting the conjecture that they are points of density.

3.3.1 Strictly Invariant Sets Along $2a = b^3$: Proof of Theorem 9

Let us first fix some notation. The image of a given curve $\mathcal{C}_j$ under $F_{c,b}$ (or $T_{a,b}$) is denoted by $\mathcal{C}_{j+1}$. The intersection point of two given curves $\mathcal{C}_i$ and $\mathcal{C}_j$ is denoted by $V_{i,j}$ for $F_{c,b}$ and by $Q_{i,j}$ for $T_{a,b}$. The segment of extremes P and Q is written as $\overline{PQ}$. A curvilinear polygon of consecutive vertices $V^1, V^2, \ldots, V^n$ is denoted by $\langle V^1, V^2, \ldots, V^n\rangle$.

Recall that the second iterate (3.29) of the critical line $\mathcal{L}_0$ is a parabola. The third iterate of $\mathcal{L}_0$ is

$$\mathcal{L}_3 = \{(\zeta, b\zeta + 2cx - cx^2) : x \in \mathbb{R}\} \tag{3.35}$$

where

$$b^2\zeta = -cx^2 + (b^3 + 2c(c+b))x - c^2(2b+c)$$

Therefore, the curve $\mathcal{L}_3$ is a line if and only if

$$b^3 + 2cb + 2c^2 = 2c \tag{3.36}$$

In such case,

$$\mathcal{L}_3 \equiv y = b(1+b)x + 2bc^2 + c^3 \tag{3.37}$$

and

$$\mathcal{L}_2 \equiv b^2 y = -cx^2 + 2cx - c^2(2b+c)$$

is symmetric with respect to $\mathcal{L}_0$. It is easy to check that equation (3.36) is equivalent to $2a = b^3$.

Let us take parameter values along the curve $2a = b^3$. In particular, for $(a,b) = (-4,-2)$, the point $V_{1,2}$ coincide with Q^-, and $V_{2,3}$ coincide with Q^+ and $Q_1^- = Q_1^+$ (see Figure 3.6), from which it follows that the curvilinear triangle $\mathcal{K}$ of vertices $V_{0,1} = (1,-3)$, $V_{1,2} = (-3,5)$, and $V_{2,3} = (5,5)$, represented in Figure 3.8a, is strictly invariant. Moreover, this triangle is self-similar: it coincides with the image of the triangle $\mathcal{K}_0$ of vertices $V_{0,1}$, $V_{1,2}$, and $V_{0,2}$, which is itself the image of $\mathcal{K}$ under the fold $\mathcal{F}_{\mathcal{L}_0}$. The critical line intersects the parabola $\mathcal{L}_2$ at its vertex $V_{0,2} = (1,1)$. The preimages of the critical line define a partition of the triangle $\mathcal{K}$. By performing the changes of variables and parameters from Remark 3.1.3, the curvilinear triangle $\mathcal{K}$ is transformed into $\langle Q_{0,1}, Q_{1,2}, Q_{2,3}\rangle$, the curvilinear triangle represented in Figure 3.8b. This triangle is strictly $T_{-4,-2}$-invariant and it was constructed a topological conjugation between $T_{-4,-2}$ and a certain Expanding Baker Map on it [60]. By means of this conjugation, it was also proved that such triangle is a 2-D strange attractor that supports an ergodic absolutely continuous invariant measure.

For parameter values (a,b) along $2a = b^3$ with $b > -2$, the point $V_{2,3}$ does not belong to the line $\widetilde{\mathcal{L}}_1$. According to Figure 3.9a, we obtain another curvilinear triangle, limited by $\mathcal{L}_1$, $\mathcal{L}_2$, and $\mathcal{L}_3$, which is invariant, but not in a strict sense. Note that, for instance, the point $V_{0,1}$, whose image is $V_{1,2}$, does not belong to $\langle V_{1,3}, V_{1,2}, V_{2,3}\rangle$. In order to construct a possible strictly invariant compact set contained in such curvilinear triangle, we will study

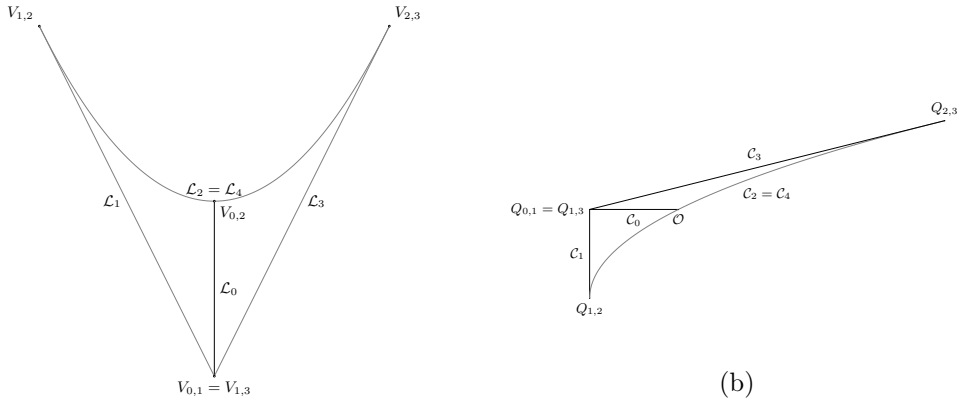

(a) (b)

Figure 3.8: (a) Strictly $F_{c,b}$-invariant curvilinear triangle for $(c, b) = (-1, 2)$; (b) Strictly $T_{a,b}$-invariant curvilinear triangle for $(a, b) = (-4, -2)$

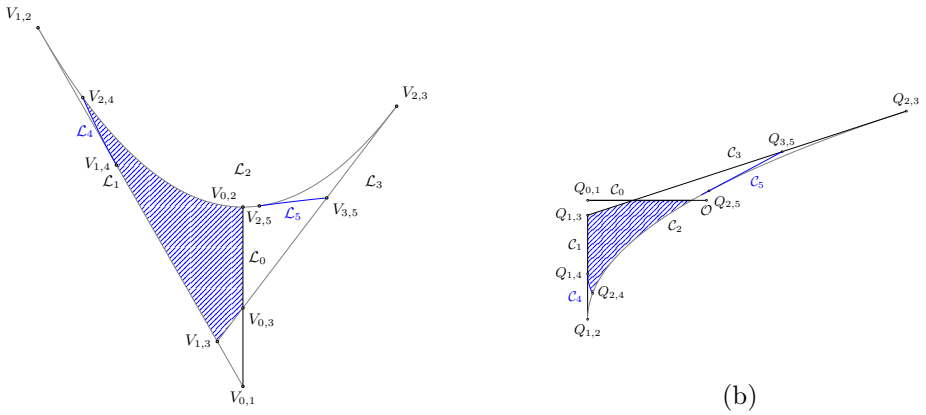

(a) (b)

Figure 3.9: (a) Strictly $F_{c,b}$-invariant curvilinear pentagon; (b) Strictly $T_{a,b}$-invariant curvilinear pentagon

the position of the successive images $\mathcal{L}_4$, $\mathcal{L}_5$, and $\mathcal{L}_6$. We will prove that $\mathcal{L}_4$ intersects $\mathcal{L}_1$ and $\mathcal{L}_2$ at $V_{1,4}$ and $V_{2,4}$, and that $\mathcal{L}_5$ intersects $\mathcal{L}_2$ and $\mathcal{L}_3$ at $V_{2,5}$ and $V_{3,5}$ for certain b-values. Then, the pentagon

$$\mathcal{K} = \langle V_{1,3}, V_{1,4}, V_{2,4}, V_{2,5}, V_{3,5} \rangle$$

represented in Figure 3.9a is strictly invariant as long as $\mathcal{L}_6$ does not intersects it. Moreover, the pentagon $\mathcal{K}$ is $F_{c,b}$ self-similar because $F_{c,b}(\mathcal{K}_0) = \mathcal{K}$, being

$$\mathcal{K}_0 = \langle V_{1,3}, V_{1,4}, V_{2,4}, V_{0,2}, V_{0,3} \rangle$$

The respective curvilinear pentagon for $T_{a,b}$ is represented in Figure 3.9b.

On the other hand, for parameter values (a, b) along the curve $2a = b^3$ with $b < -2$, the line $\mathcal{L}_3$ intersects $\mathcal{L}_0$ at the point $V_{0,3}$ below $V_{0,1}$ and there exists no invariant compact set with nonempty interior. See Figure 3.12.

Remark 3.3.1. Each vertex $V_{i,j}$ is the intersection point between $\mathcal{L}_i$ and $\mathcal{L}_j$, and can be obtained from the equations of those curves. However, since the expressions of the iterates of the critical line $\mathcal{L}_0$ of $F_{c,b}$ are generally more complicated than those of the iterates of the critical line $\mathcal{C}_0$ of $T_{a,b}$, it is more convenient to calculate $V_{i,j}$ as the images of the points $Q_{i,j}$ by the change of variables (3.4). For $(a, b) = (-4, -2)$, we have that $c = -1$ and each vertex $Q_{i,j}$ is transformed into $V_{i,j}$.

We will search for parameter values (a, b) along the curve $2a = b^3$ for which the curvilinear pentagon $\mathcal{K}$ is a $T_{a,b}$ self-similar set. Then, we will prove that $\mathcal{K}$ is strictly invariant for all those values. We will frequently do all the computations for family (3.1). See Remark 3.3.1.

Proposition 3.3.2. *Let b' and b'' the lesser roots of the polynomials $2+2b-2b^3-b^4$ and $8+8b+8b^3+4b^4+b^5$ in the interval $(-2,-1)$, respectively. Let $b_1 = \min\{b', b''\}$. Then, the curvilinear pentagon limited by the first five iterates of $\mathcal{C}_0$ is $T_{a,b}$-self-similar for all (a, b) along the curve $2a = b^3$ with $-2 < b < b_1$.*

Remark 3.3.3. Since

$$(8 + 8b + 8b^2 + 8b^3 + 4b^4 + b^5) - 4(2 + 2b - 2b^3 - b^4) = b^2(8 + 16b + 8b^2 + b^3)$$

is negative for $-2 < b < -1$, then $b' < b''$ and therefore $b_1 = b'$. Actually, it can be numerically checked that $b' \approx -1.7167$ and $b'' \approx -1.4619$.

Proof. If $b \leq -1$, then the arc

$$\mathcal{C}_2 = \{(a + s^2, a + bs) : a \leq s \leq 0\}$$

intersects $\mathcal{C}_0$ for $s = s_1 = -a/b \in [a, 0]$ at the point

$$Q_{0,2} = (a + \tfrac{a^2}{b^2}, 0) = (\tfrac{b^3}{2} + \tfrac{b^4}{4}, 0)$$

with $b^3/2 + b^4/4 < 0$. This implies that the line $\mathcal{C}_3$ intersects $\mathcal{C}_1$ for $s = s_1$ at the point

$$Q_{1,3} = (a, a + \tfrac{a^2}{b^2}) = (\tfrac{b^3}{2}, \tfrac{b^3}{2} + \tfrac{b^4}{4})$$

and $\mathcal{C}_0$ at the point

$$Q_{0,3} = (\tfrac{b^3}{2} - \tfrac{b^5}{2} - \tfrac{b^6}{4}, 0)$$

The image $\mathcal{C}_4$ of the line $\mathcal{C}_3$ is a parabola intersecting $\mathcal{C}_1$ and $\mathcal{C}_2$ at the points

$$Q_{1,4} = (a, \tfrac{b^3}{2} - \tfrac{b^5}{2} - \tfrac{b^6}{4}) = (\tfrac{b^3}{2}, \tfrac{b^3}{2} - \tfrac{b^5}{2} - \tfrac{b^6}{4})$$

and

$$Q_{2,4} = (\tfrac{b^3}{2} + (\tfrac{b^3}{2} + \tfrac{b^4}{4})^2, \tfrac{b^3}{2} + \tfrac{b^4}{2} + \tfrac{b^5}{4})$$

respectively. At the same time, we obtain the points

$$\begin{aligned} Q_{2,5} &= (\tfrac{b^3}{2} + (\tfrac{b^3}{2} - \tfrac{b^5}{2} - \tfrac{b^6}{4})^2, \tfrac{b^3}{2} + \tfrac{b^4}{2} - \tfrac{b^6}{2} - \tfrac{b^7}{4}) \\ Q_{3,5} &= (\tfrac{b^3}{2} + (\tfrac{b^3}{2} + \tfrac{b^4}{2} + \tfrac{b^5}{4})^2, \tfrac{b^3}{2} + (\tfrac{b^3}{2} + \tfrac{b^4}{4})^2 + \tfrac{b^4}{2} + \tfrac{b^5}{2} + \tfrac{b^6}{4}) \end{aligned}$$

as the images of the points $Q_{1,4}$ and $Q_{2,4}$, respectively. In order to conclude that the points $Q_{1,3}$, $Q_{1,4}$, $Q_{2,4}$, $Q_{2,5}$ and $Q_{3,5}$ are the vertices of a curvilinear pentagon $\mathcal{K}$ like the one shown in Figure 3.9b, we have to check the relative position of these vertices with respect to the critical line:

- The point $Q_{1,3}$ is above $Q_{1,4}$, and both belong to the half plane $\{\mathbf{y} < 0\}$ for all $-2 < b < -1$. Indeed,
$$0 > \tfrac{b^3}{2} + \tfrac{b^4}{4} > \tfrac{b^3}{2} - \tfrac{b^5}{2} - \tfrac{b^6}{4}$$
trivially holds.

- For all $-2 < b < -1$, then the ordinate $b^3/2 + b^4/2 - b^6/2 - b^7/4$ of $Q_{2,5}$ is greater than the ordinate $b^3/2 + b^4/2 + b^5/4$ of $Q_{2,4}$, which is negative. Indeed,
$$\tfrac{b^3}{2} + \tfrac{b^4}{2} - \tfrac{b^6}{2} - \tfrac{b^7}{4} - (\tfrac{b^3}{2} + \tfrac{b^4}{2} + \tfrac{b^5}{4}) = -\tfrac{b^5}{4}(1 + 2b + b^2) > 0$$
and
$$\tfrac{b^3}{2} + \tfrac{b^4}{2} + \tfrac{b^5}{4} = \tfrac{b^3}{4}(1 + (1 + b)^2) < 0$$
Moreover, since $b^3/2 + b^4/2 - b^6/2 - b^7/4 > 0$ is equivalent to $2 + 2b - 2b^3 - b^4 < 0$, we have that $Q_{2,5} \in \{\mathbf{y} > 0\}$ for all $-2 < b < b'$.

- The point $Q_{3,5}$ belongs to the half-plane $y > 0$. Indeed,
$$\tfrac{b^3}{2} + (\tfrac{b^3}{2} + \tfrac{b^4}{4})^2 + \tfrac{b^4}{2} + \tfrac{b^5}{2} + \tfrac{b^6}{4} > 0$$
is equivalent to
$$8 + 8b + 8b^2 + 8b^3 + 4b^4 + b^5 < 0$$
which is verified for $-2 < b < b''$.

Let $\mathcal{K}_0 = \langle Q_{0,2}, Q_{0,3}, Q_{1,3}, Q_{1,4}, Q_{2,4} \rangle$. Then, we have that $T_{a,b}(\mathcal{K}_0) = \mathcal{K}$, and therefore $\mathcal{K}$ is self-similar. □

The change of variables (3.4) transforms $\mathcal{K}$ and $\mathcal{K}_0$ from the proof of Proposition 3.3.2 into the curvilinear pentagons

$$\mathcal{K} = \langle V_{1,3}, V_{1,4}, V_{2,4}, V_{2,5}, V_{3,5} \rangle, \quad \mathcal{K}_0 = \langle V_{0,2}, V_{0,3}, V_{1,3}, V_{1,4}, V_{2,4} \rangle$$

respectively, verifying $F_{c,b}(\mathcal{K}_0) = \mathcal{K}$. See Figure 3.9a. In order to conclude that $\mathcal{K}$ and its folded image $\mathcal{F}_{\mathcal{L}_0,\mathcal{O}}(\mathcal{K})$ are as shown in Figure 3.9a, and consequently, $F_{c,b}(\mathcal{K}) = \mathcal{K}$, we need some previous results.

Lemma 3.3.4. *Let $2a = b^3$. For all $-2 < b < b_1$, the line $\mathcal{L}_3$ intersects the lines $\mathcal{L}_0$ and $\mathcal{L}_1$ at the points*

$$V_{0,3} = (1, b + b^2 + 2bc^2 + c^3), \quad V_{1,3} = \left(\tfrac{1}{b^2}(c - 2bc^2 - c^3), \tfrac{1}{b}(c - 2bc^2 - c^3) + c\right)$$

respectively. The image under $F_{c,b}$ of the segment $V_{0,3}V_{1,3}$ is the arc

$$V_{1,4}V_{2,4} = \{(s, \alpha s^2 + \beta s + \gamma) : s_1 \leq s \leq s_0\}$$

with

$$\alpha = -\frac{c}{(b+b^2)^2}$$
$$\beta = \frac{2c(2bc^2+c^3)}{(b+b^2)^2} + \frac{2c}{b+b^2} + b$$
$$\gamma = -2c\frac{2bc^2+c^3}{b+b^2} - c\frac{(2bc^2+c^3)^2}{(b+b^2)^2}$$

and

$$s_1 = \tfrac{1}{b}(c(1+b) - 2bc^2 - c^3)$$
$$s_0 = b + b^2 + 2bc^2 + c^3$$

The arc $V_{1,4}V_{2,4}$ is tangent to the line $\mathcal{L}_1$ for $s = (b-\beta)/2\alpha$ at the point

$$V_{1,4} = \big(1 - \tfrac{1}{4c}(2b^3 - 2b^5 - b^6), 1 - \tfrac{1}{4c}(2b^3 + 2b^4 - 2b^6 - b^7)\big)$$

and transversal to $\mathcal{L}_2$ at the point

$$V_{2,4} = \big(1 - \tfrac{1}{4c}(2b^3 + 2b^4 + b^5), 1 - \tfrac{1}{4c}(2b^3 + (b^3 + b^4/2)^2 + 2b^4 + 2b^5 + b^6)\big)$$

Remark 3.3.5. It holds that $\gamma = c(1 - s_0^2/(b+b^2)^2)$.

Proof. The points $V_{0,3}$ and $V_{1,3}$ are obtained directly from equations (3.28) and (3.37). The arc $V_{1,4}V_{2,4}$ is an arc of the parabola

$$\mathcal{L}_4 \equiv y = \alpha s^2 + \beta s + \gamma \tag{3.38}$$

whose equation is obtained directly as the image under $F_{c,b}$ of equation (3.37). The slope of its tangent line is equal to $2\alpha s+\beta$, which coincides with the slope b of $\mathcal{L}_1$ for $s = (b-\beta)/2\alpha$. For this value of s, we obtain the point $V_{1,4}$, whose coordinates are obtained directly by performing the change of variables (3.4) to $Q_{1,4}$. Likewise, we obtain the coordinates of $V_{2,4}$ from those of $Q_{2,4}$. □

Lemma 3.3.6. *The image under $F_{c,b}$ of the arc $V_{1,4}V_{2,4}$ is*

$$V_{2,5}V_{3,5} = \{(\alpha s^2 + \beta s + \gamma, 2cs - cs^2 + b(\alpha s^2 + \beta s + \gamma)) : s_1 \le s \le s_0\}$$

The arc $V_{2,5}V_{3,5}$ is tangent to $\mathcal{L}_2$ at the point $V_{2,5} = (x_{2,5}, y_{2,5})$ with

$$x_{2,5} = 1 - \tfrac{1}{c}(\tfrac{b^3}{2} + \tfrac{b^4}{2} - \tfrac{b^6}{2} - \tfrac{b^7}{4})$$
$$y_{2,5} = 1 - \tfrac{1}{c}\big(\tfrac{b^3}{2} + (\tfrac{b^3}{2} - \tfrac{b^5}{2} - \tfrac{b^6}{4})^2 + \tfrac{b^4}{2} + \tfrac{b^5}{2} - \tfrac{b^7}{2} - \tfrac{b^8}{4}\big)$$

and the folded arc

$$\widetilde{V_{2,5}V_{3,5}} = \{(2 - (\alpha s^2 + \beta s + \gamma), 2cs - cs^2 + b(\alpha s^2 + \beta s + \gamma)) : s_1 \le s \le s_0\}$$

is tangent to $\mathcal{L}_2$ at the point $\widetilde{V}_{2,5}$.

Proof. The arc $V_{2,5}V_{3,5}$ is an arc of the curve $\mathcal{L}_5$, whose parametrization is obtained directly from equation (3.38). The coordinates of $V_{2,5}$ are obtained from those of $Q_{2,5}$ by means of the change of variables (3.4). Since $\mathcal{L}_4$ and $\mathcal{L}_1$ are tangent at $V_{1,4}$, the lines $\mathcal{L}_5$ and $\mathcal{L}_2$ are tangent at $V_{2,5}$. Since $\mathcal{L}_2$ is symmetric with respect to $\mathcal{L}_0$, then the folded arc $\widetilde{V_{2,5}V_{3,5}}$ is tangent to $\mathcal{L}_2$ at $\widetilde{V}_{2,5}$. □

Lemma 3.3.7. *For all $-2 < b < -1$, the points $\widetilde{V}_{2,3}$ and $\widetilde{V}_{2,5}$ belong to the parabola $\mathcal{L}_2$. Moreover: $x_{1,2} < x_{2,4} < 2 - x_{2,3} < 2 - x_{2,5}$.*

Proof. The points $V_{2,3}$ and $V_{2,5}$ are found on the parabola $\mathcal{L}_2$ by construction. Since $\mathcal{L}_2$ is symmetric with respect to $\mathcal{L}_0$, then both $\widetilde{V}_{2,3}$ and $\widetilde{V}_{2,5}$ also belong to $\mathcal{L}_2$. We compute directly the abscissas of all theses points:

$$\begin{aligned} x_{1,2} &= 1 - \tfrac{b^3}{2c} \\ x_{2,4} &= 1 - \tfrac{1}{2c}(b^3 + b^4 + \tfrac{b^5}{2}) \\ \tilde{x}_{2,3} &= 1 + \tfrac{b^3+b^4}{2c} \\ \tilde{x}_{2,5} &= 1 + \tfrac{1}{2c}(b^3 + b^4 - b^6 - \tfrac{b^7}{2}) \end{aligned}$$

Thus, the point $V_{1,2}$ is on the left of $V_{2,4}$ if and only if $b^3 > b^3 + b^4 + b^5/2$, which holds whenever $-2 < b < -1$. On the other hand, the point $V_{2,4}$ is on the left of $\widetilde{V}_{2,3}$ if and only if $b^3(2+b)^2 < 0$, which holds whenever $b < 0$. Finally, it is straightforward that $\widetilde{V}_{2,3}$ is on the left of $\widetilde{V}_{2,5}$, since $\tilde{x}_{2,3} < \tilde{x}_{2,5}$ is equivalent to $0 < 2 + b$. □

Proposition 3.3.8. *For all $-2 < b < b_1$, the $F_{c,b}$-self-similar curvilinear pentagon $\widetilde{\mathcal{K}}$ is strictly $F_{c,b}$-invariant.*

Proof. Let $\mathcal{K}_1 = \mathcal{K} \cap \{x \geq 1\}$. It is clear that $\widetilde{\mathcal{K}}_1$ is contained in $\langle V_{0,2}, V_{0,3}, \widetilde{V}_{2,3}\rangle$. In order to conclude that $\mathcal{F}_{\mathcal{L}}(\mathcal{K}) = \mathcal{K}_0$, it is sufficient to notice that the arc $V_{1,4}V_{2,4}$ does not intersect the previous curvilinear triangle. This is straightforward from the inequality $x_{2,4} < \tilde{x}_{2,3}$ from Lemma 3.3.7 and the fact that the arc $V_{1,4}V_{2,4}$ is a parabolic arc tangent to $\mathcal{L}_1$ at $V_{1,4}$. □

From the proof of Proposition 3.3.2 we see that no $T_{a,b}$-self-similar pentagon is obtained for $b' < b < b''$. The curve $\mathcal{C}_5$ intersects the pentagon $\mathcal{K}_0$, and so will the curves $\mathcal{C}_6$ and $\mathcal{C}_7$. If the points $Q_{5,8}$ and $Q_{3,8}$, where $\mathcal{C}_8$ intersects the curves $\mathcal{C}_5$ and $\mathcal{C}_3$, respectively, have positive ordinates, then a certain $T_{a,b}$-self-similar curvilinear octogon appears. See Figure 3.11.

The following result proves that there are no strictly invariant compact sets with nonempty interior for $b < -2$.

Proposition 3.3.9. *Along the parameter curve $2a = b^3$, the map $T_{a,b}$ has no strictly invariant compact set with nonempty interior if $b < -2$.*

Proof. In Figure 3.12a, respectively in Figure 3.12b, we show the relative position of the curves $\mathcal{L}_j$, respectively $\mathcal{C}_j$, for $j = 0, 1, 2, 3$, when $2a = b^3$ and $b < -2$. We check that, indeed, the curve $\mathcal{C}_3$, respectively $\mathcal{L}_3$, does not intersect $\langle Q_{0,1}, Q_{1,2}, Q_{0,2}\rangle$, respectively $\langle V_{0,1}, V_{1,2}, V_{0,2}\rangle$. Since $Q_{2,0} = (a + a^2/b^2, 0)$, it is sufficient to observe that if $2a = b^3$ and $b < -2$, then $a + a^2/b^2 > 0$. If $\mathcal{C}_3$ does not intersect $\langle Q_{0,1}, Q_{1,2}, Q_{0,2}\rangle$, then $T_{a,b}$ does not display any strictly invariant set with non-empty interior intersecting the critical line. We next prove this property holds for any line $\mathcal{C}_{0,\varepsilon} \equiv y = -\varepsilon$ parallel to the critical line with $0 < \varepsilon < -c$.

Indeed, the line $\mathcal{C}_{0,\varepsilon}$ and its image $\mathcal{C}_{1,\varepsilon} \equiv x = a + \varepsilon^2$ intersect at the point $Q^{\varepsilon}_{0,1} = (a + \varepsilon^2, -\varepsilon)$, whose preimage is $Q^{\varepsilon}_{-1,0} = ((b-1)\varepsilon, -\varepsilon)$. The image of $\mathcal{C}_{1,\varepsilon}$ is

$$\mathcal{C}_{2,\varepsilon} = \{(a + s^2, a + \varepsilon^2 + bs) \in \mathbb{R}^2 : s \in \mathbb{R}\}$$

which intersects $\mathcal{C}_{0,\varepsilon}$ at the point $Q^{\varepsilon}_{0,2} = (a + (\varepsilon^2 + \varepsilon + a)^2/b^2, -\varepsilon)$. If $2a = b^3$ with $b < -2$, then it is straightforward to check that

$$a + \tfrac{1}{b^2}(\varepsilon^2 + \varepsilon + a)^2 > a + \varepsilon^2$$

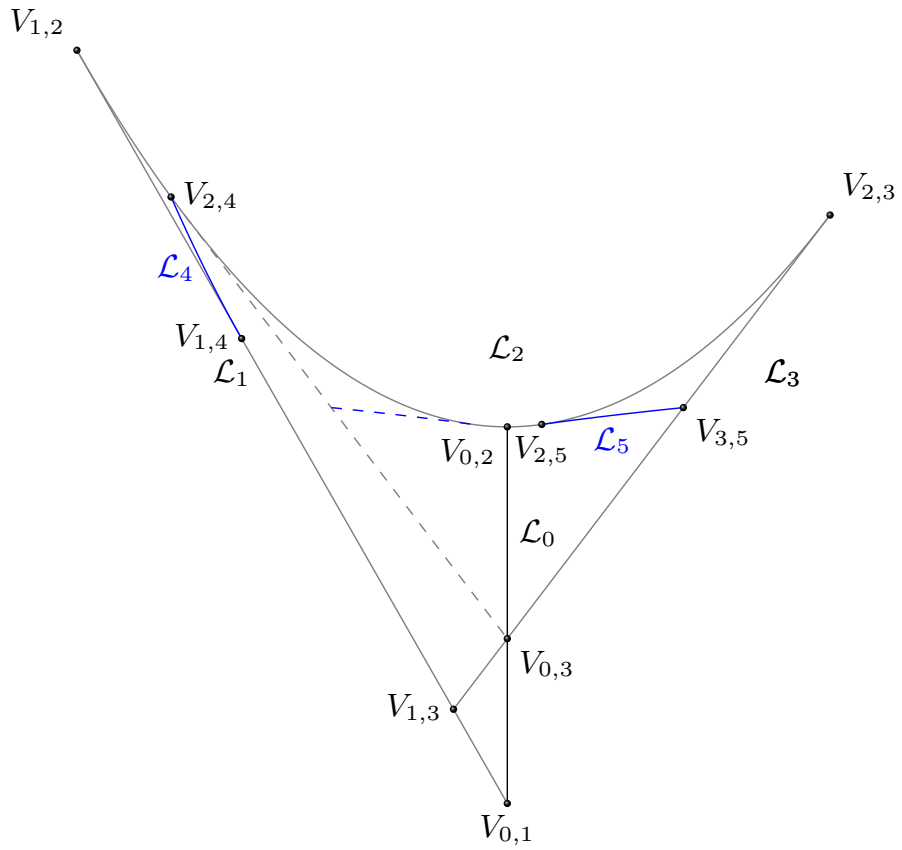

Figure 3.10: The $F_{c,b}$ self-similar curvilinear pentagon $\langle V_{1,3}, V_{3,5}, V_{2,5}, V_{2,4}, V_{1,4}\rangle$ is strictly $F_{c,b}$-invariant

for all $0 < \varepsilon < -c$. This means that $\mathcal{C}_{3,\varepsilon}$ does not intersect $\langle Q^{\varepsilon}_{0,1}, Q^{\varepsilon}_{1,2}, Q^{\varepsilon}_{0,2}\rangle$ and, therefore, there exists no strictly invariant set with nonempty interior intersecting $\mathcal{C}_{0,\varepsilon}$ with $0 < \varepsilon < -c$. Since $\langle Q^{\varepsilon}_{0,1}, Q^{\varepsilon}_{1,2}, Q^{\varepsilon}_{0,2}\rangle$ reduces to the fixed point Q^{-} for $\varepsilon = -c$, the proof is complete. □

Proof of Theorem 9. Statement 1) is an immediate consequence of [60, Prop. 3]. The existence of a strictly invariant pentagon for $-2 < b < b_1$ follows from Propositions 3.3.2 and 3.3.8. Statement 3) is equivalent to Proposition 3.1.1. □

3.3.2 Numerical Attractors Along $2a = b^3$

In this subsection we find numerical attractors along the parameter curve $2a = b^3$ for $-2 < b < -1.4$ and show similarities between the dynamical behavior of the quadratic family and the 2-D tent maps, namely the splitting and doubling of attractors analytically proved for the latter in Chapter 2.

We start our numerical study by recalling that the fixed point $P^{(1),-}$ of $T_{a,b}$ is an attracting focus for all $b_N < b < -1.4$, where $b_N \approx -1.4311$ is the Hopf–Neimark–Sacker bifurcation value. Past $b = b_N$, an invariant circle springs and persists for b-values sufficiently close to b_N. When this invariant circle reaches the critical line for some value $b \approx -1.52805$, a 8-periodic orbit appears. This periodic orbit persists until one of its points is above a critical line for some value $b \approx -1.54473$, and an attracting

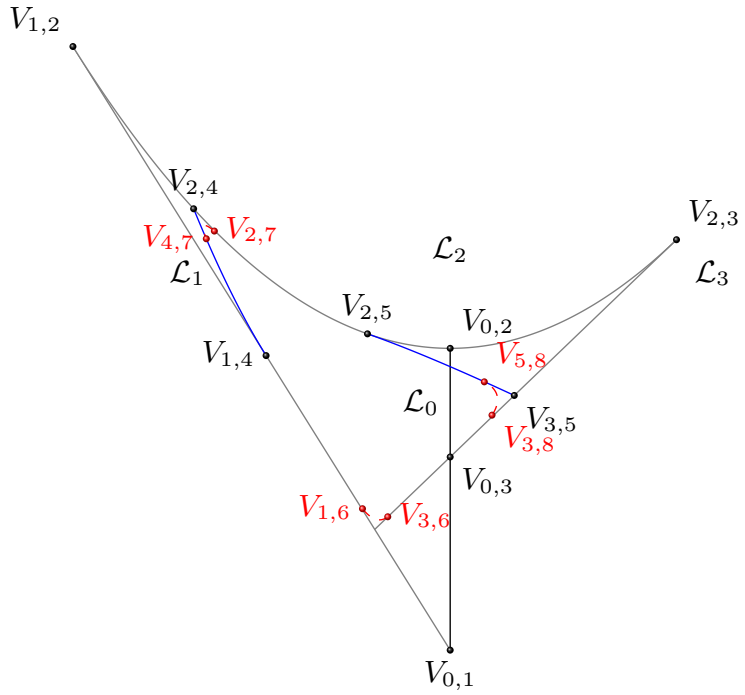

Figure 3.11: When the iterate $\mathcal{L}_6$ intersects $\langle V_{1,3}, V_{1,4}, V_{2,4}, V_{2,5}, V_{3,5}\rangle$ from Figure 3.9a, a curvilinear octogon appears

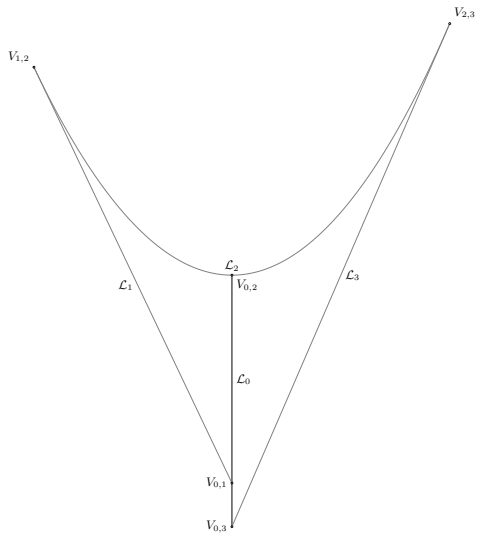

(a)

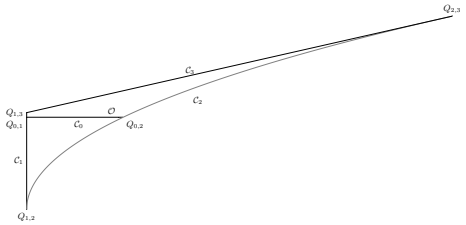

(b)

Figure 3.12: (a) When $b < -2$, the point $Q_{0,3}$ is below $Q_{0,1} = F_{c,b}(1,1)$, and $\mathcal{L}_0$ gets farther away not allowing the existence of a strictly compact set with nonempty interior; (b) The analogous situation of (a) for $T_{a,b}$

invariant circle intersecting the critical line appears. This invariant circle persists in the interval $[-1.55, -1.6]$, showing sharper features as b diminishes. See Figure 3.13.

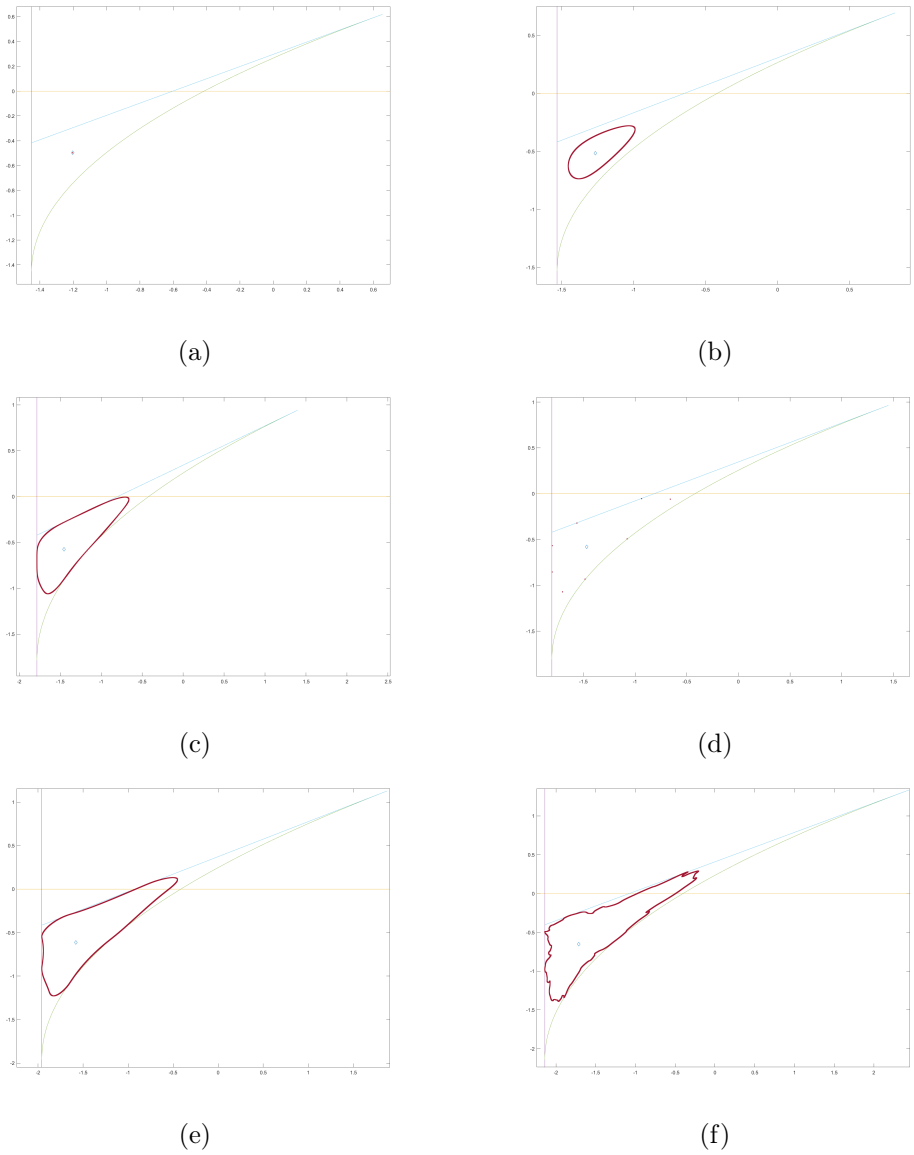

Figure 3.13: From an attracting fixed point to an invariant circle through the Hopf–Neimark–Sacker bifurcation segment: (a) the attracting fixed point for $b = -1.4263$; (b) the attracting invariant circle sprung when $b = b_N$ for $b = -1.4526$; (c) the invariant circle of (b) grows until reaching the critical line for $b \approx -1.5281$; (d) the invariant circle disintegrates into a 8-periodic orbit for $b \approx -1.5342$; (e) the invariant circle reappears for $b \approx -1.5762$; (f) the invariant circle keeps growing and has sharper features for $b = -1.6237$.

In the interval $[-1.7, -1.6]$ we find our first 1-D strange attractor. Let us explain how it is formed. First, the invariant curve from Figure 3.13f continues developing sharper features as b diminishes, until a 35-periodic attractor appears for $b \approx -1.62895$. Then, a Hopf bifurcation occurs and 35 invariant circles spring from this periodic orbit. Afterwards, a period-doubling occurs: a 27-periodic attractor becomes a 2×27-periodic attractor for $b \approx -1.64211$. For $b \approx -1.64474$, a 27-piece 1-D attractor appears. As b diminishes, the pieces of this attractor sligthly change their form and become closer to each other until they merge forming our first 2-D strange attractor for $b \approx -1.66579$. See Figure 3.14.

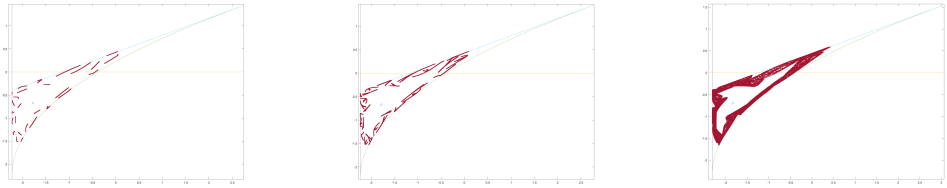

(a) (b) (c)

Figure 3.14: The 27 pieces of a 1-D strange attractor merge into a 1-piece 2-D strange attractor with one hole: (a) $b = -1.64472$; (b) $b = -1.64737$; (c) $b = -1.6658$

The attractor from Figure 3.14c is a 1-piece 2-D attractor with one hole, formed by the merging of the 27 pieces of the former 1-D strange attractor. This 2-D strange attractor disappears for $b \approx -1.6789$ with the appearence of a 2×11-periodic attractor, which halves its period for $b \approx -1.67632$. Then, a Hopf bifurcation occurs and 11 invariant circle spring from the previous periodic attractor. For $b \approx -1.69211$ we find a 11-piece 1-D strange attractor. As b diminishes, the pieces of this attractor become closer until merging into a 1-piece 1-D strange attractor with one hole, which becomes 2-D after several periodic bifurcations. See Figure 3.15.

As b continues diminishing, the hole of the 1-piece 2-D strange attractor from Figure 3.15f is filled. For $b \approx -1.7868$, a 15-periodic attractor appears which becomes a 2×15-piece 1-D strange attractor for $b \approx -1.78947$. These pieces become closer until merging in a 3-piece 1-D strange attractor for $b \approx -1.7921$. See Figure 3.16a. This attractor persists and its pieces become thicker as b diminishes, until a 9-periodic attractor appears for $b \approx -1.82105$, which transforms into a 9×4-piece 1-D strange attractor for $b \approx -1.82368$. Then, the 3-piece 1-D strange attractor from Figure 3.16a reappears and its pieces become closer until merging into a 1-piece 2-D strange attractor without hole, which seems to fill the curvilinear pentagon from Proposition 3.3.2. See Figure 3.16.

For $b \approx -1.85$, a 3-periodic attractor appears and persists until it undergoes a Hopf bifurcation for $b \approx -1.85263$. Then, the curvilinear pentagon from Figure 3.16d reappears as a 1-piece 2-D strange attractor without hole and persists for almost all $b \in (-2, -1.860526)$. The most remarkable exception is the appearence of a 4-periodic attractor for $b \approx -1.93878106$. This periodic orbit undergoes a Hopf bifurcation for $b \approx -1.942105$ and a 16-periodic attractor appears later, which transforms into a 4-piece 2-D strange attractor for $b \approx -1.94072$. See Figure 3.17.

3.3.3 Numerical Attractors in the Sharp Parameter Regions

Here we show some examples of numerical attractors for $F_{c,b}$ in the invariant domains from Propositions 3.2.6 and 3.2.12.

Let us begin with $(a^*, b^*) = (-2, 0)$. Figure 3.18 supports the conjecture that this point is a point of density of strange attractors as the majority of the parameter values around (a^*, b^*) are coloured in black. Recall that for $b = 0$ the square $R^+_{a,0} = [a, a + a^2] \times$

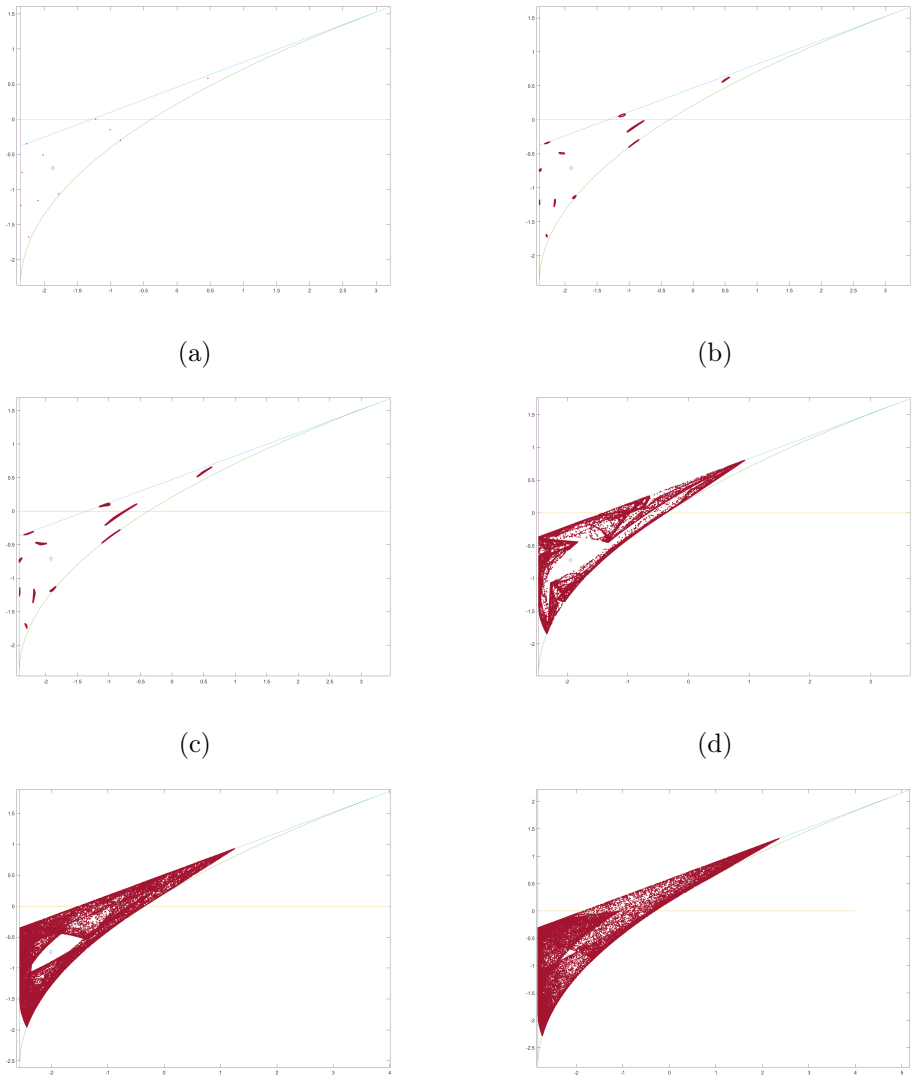

Figure 3.15: From an 11-periodic attractor to a holed 1-piece 2-D strange attractor: (a) an attracting 11-periodic orbit for $b \approx -1.6763$; (b) 11 invariant circle spring after a Hopf bifurcation for $b \approx -1.6868$; (c) a 11-piece 1-D strange attractor is formed for $b \approx -1.6921$; (d) the 11- pieces in (c) get closer until they merge into a hole 1-piece 1-D strange attractor for $b \approx -1.7026$; (e) a holed 1-piece 2-D strange attractor is created from the attractor of (d) for $b \approx -1.7237$; (f) the hole of the attractor of (e) almost filled for $b \approx -1.7816$.

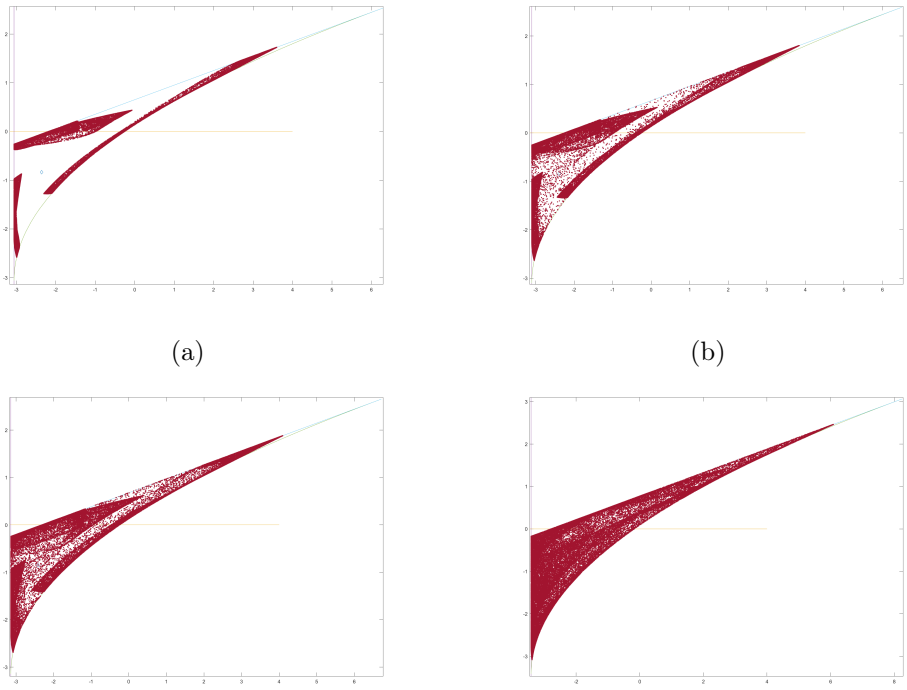

(a) (b)

(c) (d)

Figure 3.16: From a 3-piece 1-D strange attractor to a 1-piece 2-D strange attractor without hole: (a) a 3-piece 1-D attractor for $b = -1.82895$; (b) the 3 pieces of (a) start merging for $b = -1.83684$; (c) the merging continues for $b = -1.84474$; (d) a 2-D strange attractor that fills the curvilinear pentagon $b = -1.89737$

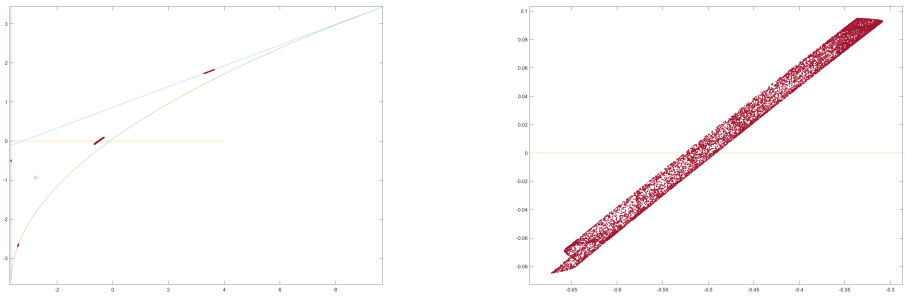

(a) (b)

Figure 3.17: A 4-piece 2-D strange attractor for $b = -1.94082$: (a) the 4 pieces of the attractor; (b) Amplification of a piece in (a)

$[a, a + a^2]$ is strictly invariant for all $-2 \leq a \leq -1$ and contains a 2-D strange attractor for all a sufficiently close to -2.

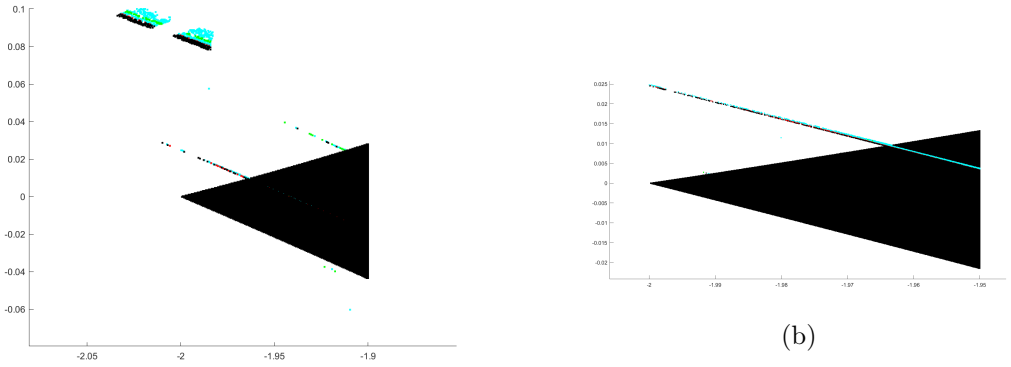

(a) (b)

Figure 3.18: The black region predominates around $(a^*, b^*) = (-2, 0)$: (a) Amplification of Figure 14b around (a^*, b^*); (b) Amplification of (a)

The evolution of the general 2-D strange attractor for $b > 0$ is shown in Figure 3.19. In Figures 3.20 and 3.21 we show other 1-D and 2-D strange attractors numerically found for parameter values in the sharp region.

For $b < 0$, the attractors seem to show a symmetry with respect to those found for $b > 0$. Compare Figures 3.19 and 3.22.

For the case $(a^*, b^*) = (-4, -2)$, very close to (a^*, b^*) we find the curvilinear pentagon from Figure 3.9a and a similar evolution. See Figure 3.24. Figure 3.23 also supports the conjecture that this point is a point of density of strange attractors. In Figures 3.25 and 3.26 we show other numerical strange attractors.

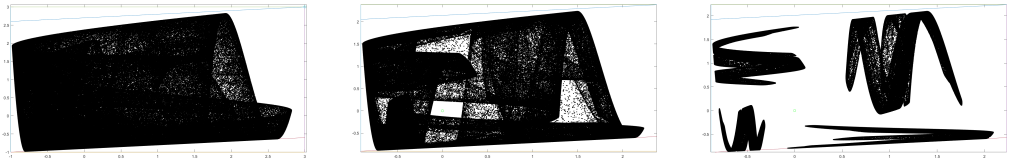

(a) (b) (c)

Figure 3.19: Evolution of the general 2-D strange attractor near $(a^*, b^*) = (-2, 0)$ for $b > 0$: (a) $(a, b) = (-1.62, 0.01)$; (b) $(a, b) = (-1.397, 0.01)$; (c) $(a, b) = (-1.3412, 0.01)$

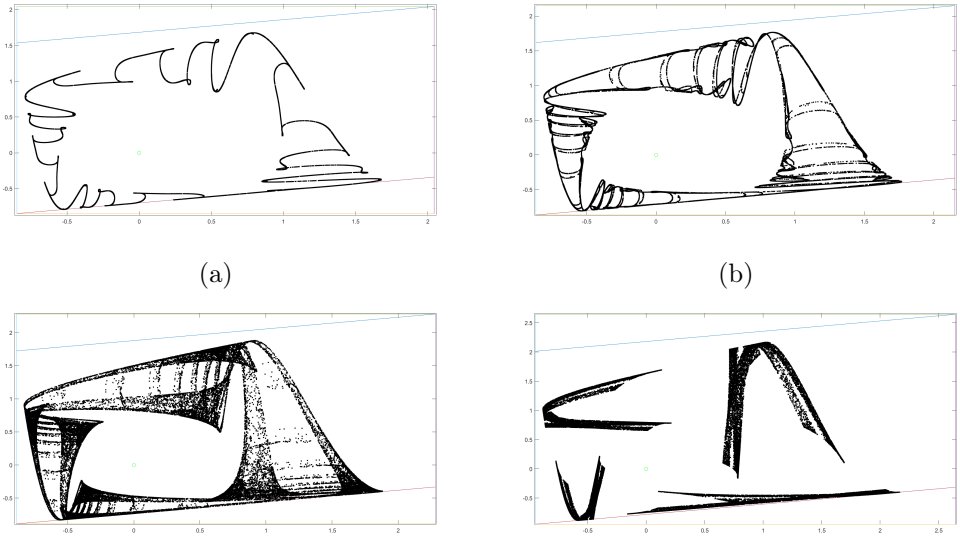

(a) (b) (c) (d)

Figure 3.20: From a 1-piece 1-D strange attractor to a 4-piece 2-D strange attractor for $b = 0.176$: (a) $a = -1.0626$; (b) $a = -1.0978$; (c) $a = -1.1400$; (d) $a = -1.2525$

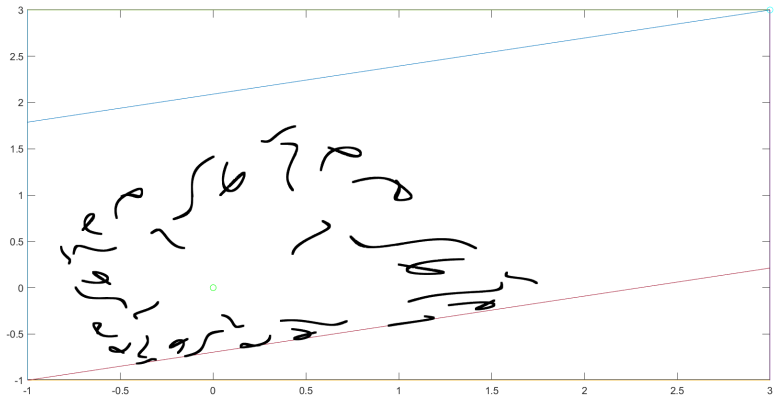

(a)

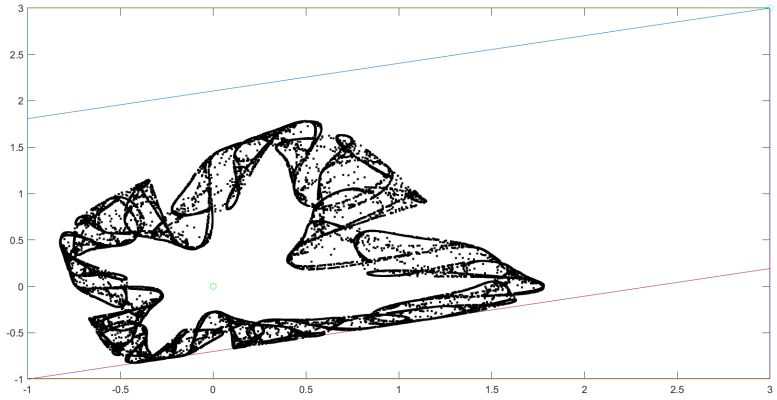

(b)

Figure 3.21: The 31 pieces of a 1-D strange attractor merge into a 1-piece 2-D strange attractor with one hole: (a) $(a, b) = (0.303, -0.97153352)$; (b) $(a, b) = (0.297, -0.98566473)$

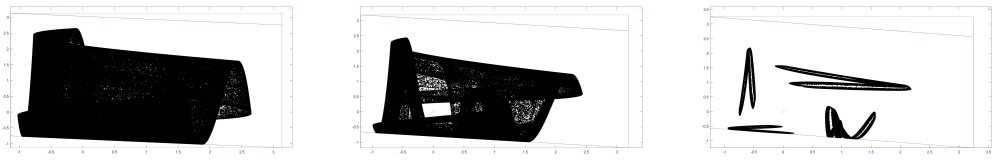

(a) (b) (c)

Figure 3.22: Evolution of the general 2-D strange attractor near $(a^*, b^*) = (-2, 0)$ for $b < 0$: (a) $(a, b) = (-1.662088, -0.08838)$; (b) $(a, b) = (-1.548977, -0.11994)$; (c) $(a, b) = (-1.439853, -0.1515)$

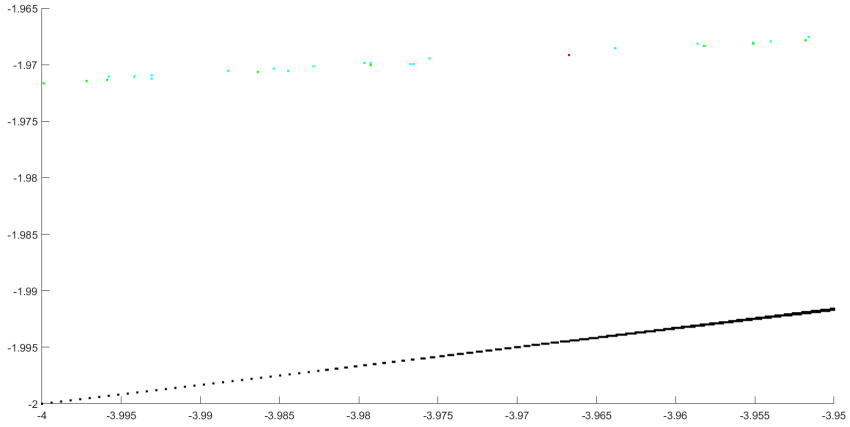

Figure 3.23: Amplification of Figure 14b around $(a^*, b^*) = (-4, -2)$

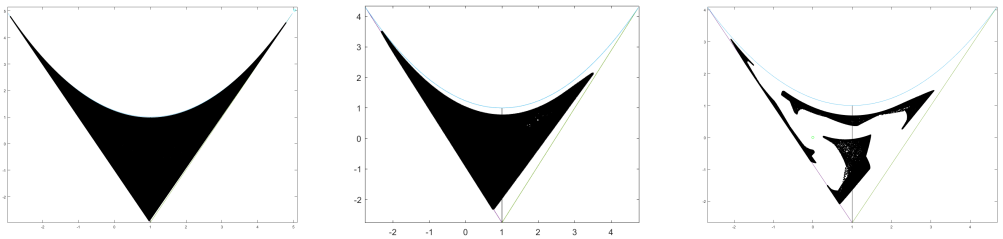

(a) (b) (c)

Figure 3.24: Evolution of the general 2-D strange attractor near $(a^*, b^*) = (-4, -2)$: (a) $(a, b) = (-3.9093, -1.948)$; (b) $(a, b) = (-3.3022, -1.8788)$; (c) $(a, b) = (-3.8026, -1.8384)$

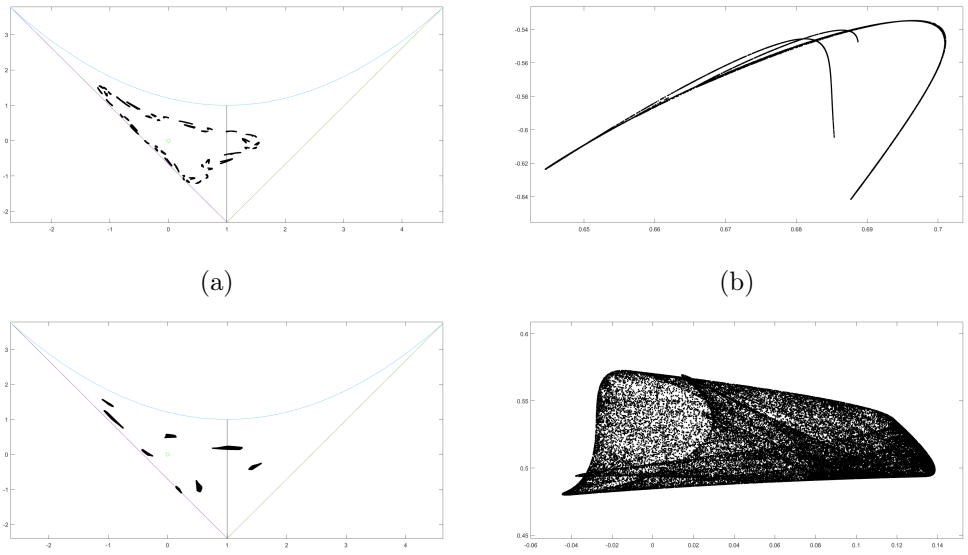

(a) (b)

(c) (d)

Figure 3.25: Strange attractors of several pieces for $\mathcal{V}(a^*, b^*)$ with $(a^*, b^*) = (-4, -2)$: (a) A 1-D strange attractor for $(a, b) = (-2.2, -1.6431)$; (b) Amplification of a piece in (a); (c) A 2-D strange attractor for $(a, b) = (-2.4, -1.6932)$; (d) Amplification of a piece in (c)

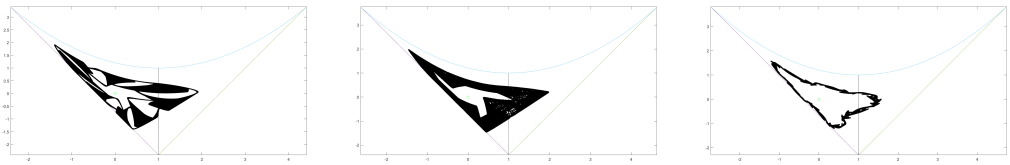

(a) (b) (c)

Figure 3.26: Strange attractors of one piece for $\mathcal{V}(a^*, b^*)$ with $(a^*, b^*) = (-4, -2)$: (a) $(a, b) = (-2.389, -1.702)$; (b) $(a, b) = (-2.4, -1.6937)$; (c) $(a, b) = (-2.2, -1.6422)$

Conclusiones

En esta memoria hemos iniciado el estudio de una familia biparamétrica $\Gamma_{a,\theta}$ de *Expanding Baker Map*, dada por una expansividad $a > 1$ y un ángulo de rotación $0 < \theta < \pi$, que parece ser una buena aproximación de la familia cuadrática bidimensional $T_{a,b}$. Primero, la familia $\Gamma_{a,\theta}$ generaliza la familia uniparamétrica Λ_t de *tiendas* bidimensionales, correspondiente al ángulo $\theta = 3\pi/4$, que se demostró que es la mejor elección dentro del marco de las aplicaciones lineales a trozos para describir la dinámica de $T_{a,b}$ a lo largo de cierta curva de parámetros [55]. Segundo, para rotaciones de ángulos múltiplos racionales de π, hemos extendido la mayoría de los resultados previamente probados [57, 58, 59] para Λ_t. Y tercero, la familia $\Gamma_{a,\theta}$ presenta los mismos tipos topológicos de atractores extraños que $T_{a,b}$. Más concretamente, estos son los principales resultados analíticos:

1. Para todo $0 < \theta < \pi$, existe $a_\theta > 1$ tal que $\Gamma_{a,\theta}$ tiene un polígono estrictamente invariante $\mathcal{K}_{a,\theta}$ para todo $1 < a \leq a_\theta$. Más aún, existe una sucesión no creciente de valores de a en $(1, a_\theta]$ en los que el número de lados de $\mathcal{K}_{a,\theta}$ aumenta. Esta sucesión es finita (eventualmente constante e igual a 1) si y solo si θ/π es un número racional.

2. Para todo $0 < \theta < \pi$, la aplicación $\Gamma_{a,\theta} \colon \mathcal{K}_{a,\theta} \to \mathcal{K}_{a,\theta}$ presenta un número finito de atractores extraños bidimensionales persistentes.

3. Sea $\theta = 2\pi p/q \in (0, \pi)$ con $p, q \in \mathbb{N}$ y $\mathrm{mcd}(p, q) = 1$. Si $q \geq 4$, entonces $\Gamma_{a,\theta}$ es una *Expanding Baker Map* renormalizable para todo a suficientemente próximo a 1.

4. Sea $\theta = 2\pi p/q \in (0, \pi)$ con p un número natural impar y q una potencia de 2. Entonces, la aplicación $\Gamma_{a,\theta} \colon \mathcal{K}_{a,\theta} \to \mathcal{K}_{a,\theta}$ presenta una cascada de duplicación de atractores.

En cuanto a la familia cuadrática bidimensional, hemos llevado a cabo un análisis de sus puntos fijos y órbitas periódicas de periodo dos, así como uno parcial de las de periodo tres. Hemos descubierto que no existen órbitas periódicas atrayentes de periodo dos, y algunos atractores extraños unidimensionales surgen de la colisión entre una órbita periódica de periodo tres de tipo silla disipativa y los tres ciclos límite originados a partir de otra órbita periódica de periodo tres a través de una bifurcación de Hopf-Neimark-Sacker. Finalmente, hemos encontrado numéricamente coexistencia de atractores.

Conclusions

In this memoir we have initiated the study of a two-parameter family $\Gamma_{a,\theta}$ of Expanding Baker Maps, given by an expansion rate $a > 1$ and a rotation angle $0 < \theta < \pi$, that seems to be a good approximation of the 2-D quadratic family $T_{a,b}$. First, the family $\Gamma_{a,\theta}$ generalizes the one-parameter family Λ_t of 2-D tent maps, which corresponds to the angle $\theta = 3\pi/4$, that was proved to be the best choice in the piecewise linear setting to describe the dynamics of $T_{a,b}$ along a certain parameter curve [55]. Second, for rotations of angles that are rational multiples of π, we have extended most of the results previously proved [57, 58, 59] for Λ_t. And third, the family $\Gamma_{a,\theta}$ displays the same topological types of numerical strange attractors as $T_{a,b}$. More concretely, these are the main analytical results:

1. For every $0 < \theta < \pi$, there exists $a_\theta > 1$ such that $\Gamma_{a,\theta}$ has a strictly invariant polygon $\mathcal{K}_{a,\theta}$ for every $1 < a \leq a_\theta$. Moreover, there exists a nonincreasing sequence of a-values in $(1, a_\theta]$ at which the number of sides of $\mathcal{K}_{a,\theta}$ increases. This sequence is finite (eventually constant and equal to 1) if and only if θ/π is a rational number.

2. For all $0 < \theta < \pi$, the map $\Gamma_{a,\theta} \colon \mathcal{K}_{a,\theta} \to \mathcal{K}_{a,\theta}$ displays a finite number of persistent 2-D strange attractors.

3. Let $\theta = 2\pi p/q \in (0, \pi)$ with $p, q \in \mathbb{N}$ and $\gcd(p, q) = 1$. If $q \geq 4$, then $\Gamma_{a,\theta}$ is a renormalizable Expanding Baker Map for every a sufficiently close to 1.

4. Let $\theta = 2\pi p/q \in (0, \pi)$ with p an odd natural number and q a power of 2. Then, the map $\Gamma_{a,\theta} \colon \mathcal{K}_{a,\theta} \to \mathcal{K}_{a,\theta}$ displays a cascade of doubling of attractors.

As for the 2-D quadratic family, we have carried out a full analysis of the fixed points and the 2-periodic orbits, and a partial one of the 3-periodic orbits. We have found out that there are no attracting 2-periodic orbits, and some 1-D strange attractors arise from the collision between a 3-periodic orbit of dissipative saddle type and the three limit cycles originated by another 3-periodic orbit through a Hopf–Neimark–Sacker bifurcation. Finally, we have numerically found coexistence of attractors.

List of Symbols

$\mathbf{A}_{a,\theta}$	the counterclowise rotation of angle θ by a factor of a
$\mathtt{basin}(\mu)$	the basin of an invariant measure μ
$\mathcal{B}(P,r)$	the open ball centered at P with radius r
$\mathcal{C}$	the critical line $x=1$
$\mathrm{D}f(P)$	the differential of a map f at a point P
$\delta(\Phi)$	the dilatation coefficient
$\mathrm{EBM}(\mathcal{L}^0,\ldots,\mathcal{L}^n,P,\mathbf{A})$	an Expanding Baker Map
$f\restriction_{\mathcal{K}}$	the restriction of a map f to a set $\mathcal{K}$
$\mathcal{F}_{\mathcal{L},P}$	the fold with respect to a line $\mathcal{L}$ onto a point $P\notin\mathcal{L}$
$G_{a,\theta}$	the restriction of $\Gamma_{a,\theta}^q$ to Δ for $q\geq 5$
$\Gamma_{a,\theta}$	the Expanding Baker Map associated to $\mathcal{C}$ and $\mathbf{A}_{a,\theta}$
$h_{\mathrm{mult}}(\mathtt{P},\Phi)$	the multiplicity entropy
$\operatorname{int}\mathcal{K}$	the interior of a set $\mathcal{K}$
$\mathcal{K}_{a,\theta}$	the strictly $\Gamma_{a,\theta}$-invariant set $\bigcup_{n=1}^{\infty}\Gamma_{a,\theta}^n(\mathcal{K}_N)$
$\mathcal{K}_N$	the self-similar N-sided polygon $\bigcap_{n=1}^{\infty}\Pi_n$
$\langle Q^1,Q^2,\ldots,Q^n\rangle$	a curvilinear polygon of consecutive vertices $Q^1,Q^2,\ldots,Q^n$
$\mathcal{L}_{a,\theta}$	the line $-x\cos\theta_1+y\sin\theta_1=\rho$
$\mathcal{L}_n$	the nth iterate of $\mathcal{C}$ under $\mathbf{A}_{a,\theta}$ or $F_{c,b}$
Λ_t	the 2-D tent maps family
M	the point $(1,0)$
$\mathtt{mult}(\mathtt{P},\Phi)$	the weighted multiplicity
m_2	the Lebesgue measure in $\mathbb{R}^2$
N_θ	the natural number $1+\lfloor\pi/\theta\rfloor$
n_1	the smallest natural number such that $M_{n_1}\in\Sigma^1$
$\mathcal{O}$	the origin $(0,0)$
$\Omega(Q^1,Q^2,\ldots,Q^n)$	the polygon of consecutive vertices $Q^1,Q^2,\ldots,Q^n$
$\mathtt{P}^{(n)}$	the nth iterate of a partition $\mathtt{P}$
$\partial\mathcal{K}$	the boundary of a set $\mathcal{K}$
Π_n	the half-plane limited by $\mathcal{L}_n$ containing $\mathcal{O}$
$\Psi_{a,\theta}$	the Expanding Baker Map associated to $\mathcal{C}$ and $\mathcal{L}_{a,\theta}$ and $\mathbf{A}_{a^q,2\theta_1}$
Q_n	the nth iterate of a point Q under $\Gamma_{a,\theta}$ or $\Psi_{a,\theta}$
$\mathcal{Q}_n$	the nth iterate of a set $\mathcal{Q}$ under $\Gamma_{a,\theta}$ or $\Psi_{a,\theta}$
$\overline{QQ'}$	the segment joining a pair of points Q and Q'
$\widetilde{Q}$	the symmetric point of Q with respect to a line $\mathcal{L}$
$\mathcal{R}_N$	the compact and convex N-sided polygon $\bigcap_{n=0}^{\infty}\Pi_n$
$\mathcal{R}^j$	the sector limited by Σ^j and Σ^{j+1}
Σ^j	the ray $\{(s\cos j\theta_1, s\sin j\theta_1) : s\geq 0\}$ with $j=0,\ldots,q-1$
$T_{a,b}$	the 2-D quadratic family $T_{a,b}(x,y)=(a+y^2,x+by)$
θ_1	the angle $2\pi/q$ if $\theta=2\pi p/q\in(0,\pi)$ with $p,q\in\mathbb{N}$ and $\gcd(p,q)=1$
$V_{n,m}$	the intersection point of $\mathcal{L}_n$ and $\mathcal{L}_m$
$W^{\mathrm{s}}(\mathcal{A})$	the stable set of an attractor $\mathcal{A}$

Bibliography

[1] Alves, J. F. SRB measures for non-hyperbolic systems with multidimensional expansion. *Ann. Sci. École Norm. Sup. 33*, 4 (200), 1–32.

[2] Alves, J. F., and Pumariño, A. Entropy formula and continuity of entropy for piecewise expanding maps. *Ann. Inst. Henri Poincaré (C) Anal. Non Linéaire 38*, 1 (2021), 91–108.

[3] Alves, J. F., Pumariño, A., and Vigil, E. Statistical stability for multidimensional piecewise expanding maps. *Proc. Amer. Math. Soc. 145* (2017), 3057–3068.

[4] Baladi, V., Rockmore, D., Tongring, N., and Tresser, C. Renormalization on the n-dimensional torus. *Nonlinearity 5*, 5 (Sep. 1992), 1111–1136.

[5] Benedicks, M., and Carleson, L. On iterations of $1-ax^2$ on $(-1,1)$. *Ann. Math. 122*, 1 (Jul. 1985), 1–25.

[6] Benedicks, M., and Carleson, L. The dynamics of the Hénon map. *Ann. Math. 133*, 1 (1991), 73–169.

[7] Birkhoff, G. D. Nouvelles recherches sur les systèmes dynamiques. *Mem. Pont. Acad. Sci. Novi. Lyncaei 1* (1935), 85–216.

[8] Broer, H., Roussarie, R., and Simó, C. Invariant circles in the Bogdanov-Takens bifurcation for diffeomorphisms. *Ergod. Theory Dyn. Syst. 16* (1996), 1147–1172.

[9] Brucks, K. M., and Bruin, H. *Topics from One-Dimensional Dynamics*, vol. 62 of *London Mathematical Society Student Texts*. Cambridge University Press, 2004.

[10] Buzzi, J. Absolutely continuous invariant probability measures for arbitrary expanding piecewise $\mathbb{R}$-analytic maps of the plane. *Ergod. Theory Dyn. Syst. 20*, 3 (2000), 697–708.

[11] Collet, P., and Eckmann, J. P. *Iterated maps of the interval as dynamical systems*. Birkhäuser, 1980.

[12] Collet, P., and Tresser, C. Itération d'endomorphismes et group de renormalisation. *J. de Physique 39*, C5, 25–28.

[13] Colli, E. Infinitely many coexisting strange attractors. *Ann. Inst. Henri Poincaré 15*, 5 (1998), 539–579.

[14] De Melo, W. Renormalization in one-dimensional dynamics. *J. Differ. Equ. Appl. 17*, 8 (2011), 1185–1197.

[15] De Melo, W., and Van Strien, S. *One-Dimensional Dynamics*, vol. 3 of *Ergebnisse der Mathematik und ihrer Grenzgebiete/ A Series of Modern Surveys in Mathematics*. Springer-Verlag, 1993.

[16] Drubi, F., Ibáñez, S., and Rodríguez, J. Á. Coupling leads to chaos. *J. Diff. Eq. 239* (2007), 371–385.

[17] Dumortier, F., and Ibáñez, S. Nilpotent singularities in generic 4-parameter families of 3-dimensional vector fields. *J. Diff. Eq. 127*, 2 (1996), 590–647.

[18] Dumortier, F., Ibáñez, S., Kokubo, H., and Simó, C. About the unfolding of a Hopf-zero singularity. *Discrete Continuous Dyn. Syst. 33* (2013), 4435–4471.

[19] Feigembaum, M. J. Quantitative universality for a class of nonlinear transformations. *J. Stat. Phys. 19* (1978), 25–52.

[20] Feigembaum, M. J. The universal metric properties of nonlinear transformations. *J. Stat. Phys. 21* (1979), 669–706.

[21] Fowler, A. C., and Sparrow, C. T. Bifocal homoclinic orbits in four dimensions. *Nonlinearity 4* (1991), 1159–1182.

[22] G.-Barrientos, P., Ibáñez, S., and Rodríguez, J. Á. Heteroclinic cycles arising in generic unfoldings of nilpotent singularities. *J. Diff. Eq. 239* (2011), 999–1028.

[23] Gambaudo, J. M., van Strein, S., and Tresser, C. Hénon-like maps with strange attractors: there exist C^∞ Kupka-Smale diffeomorphisms on S^2 with neither sinks nor sources. *Nonlinearity 2*, 2 (May 1989), 187–304.

[24] Giusti, E. *Minimal surfaces and functions of bounded variation.* Birkhauser Verlag, 1984.

[25] Gonchenko, S. V., Shilnikov, L. P., and Turaev, D. V. Dynamical phenomena in multidimensional systems with a nonrough Poincaré homoclinic curve. *Russ. Acad. Sci. Dokl. Math. 47* (1993), 410–415.

[26] Gonchenko, S. V., Shilnikov, L. P., and Turaev, D. V. On the existence of Newhouse regions near systems with a nonrough Poincaré homoclinic curve (multidimensional case). *Russ. Acad. Sci. Dokl. Math. 47* (1993), 268–273.

[27] Gonchenko, S. V., Shilnikov, L. P., and Turaev, D. V. On dynamical properties of diffeomorphisms with homoclinic tangencies. *J. Math. Sci. 126* (2005), 1317–1343.

[28] Gonchenko, S. V., Shilnikov, L. P., and Turaev, D. V. On dynamical properties of multidimensional diffeomorphisms from Newhouse regions. *Nonlinearity 21* (2008), 923–972.

[29] Góra, P., and Boyarsky, A. Absolutely continuous invariant measures for piecewise expanding C^2 transformation in $\mathbb{R}^n$. *Israel J. Math. 67*, 3 (1989), 272–286.

[30] Guckenheimer, J., and Holmes, P. *Nonlinear Oscillations, Dynamical Systems and Bifurcations of Vector Fields.* Springer-Verlag, 1983.

[31] Hénon, M. A two-dimensional mapping with a strange attractor. *Commun. Math. Phys. 50* (1976), 69–77.

[32] Ibáñez, S., and Rodríguez, J. Á. Sil'nikov bifurcations in generic 4-unfoldings of a codimension-4 singularity. *J. Diff. Eq. 120* (1995), 411–428.

[33] Ibáñez, S., and Rodríguez, J. Á. Shil'nikov configurations in any generic unfolding of the nilpotent singularity of codimension three on $\mathbb{R}^3$. *J. Diff. Eq. 208* (2005), 147–175.

[34] Jakobson, M. Absolutely continuous invariant measures for one-parameter families of one-dimensional maps. *Commun. Math. Phys. 81* (1981), 39–88.

[35] Kiriki, S., Nakano, Y., and Soma, T. Non-trivial wandering domains for heterodimensional cycles. *Nonlinearity 30* (2017), 3255–3270.

[36] Kuznetsov, Y. A. *Elements of Applied Bifurcation Theory*, vol. 112. Springer, 2004.

[37] Landau, L. D., and Lifshitz, E. M. *Fluid mechanics*, vol. 6. Pergamon, 1959.

[38] Lasota, A., and Yorke, J. A. On the existence of invariant measures for piecewise monotonic transformations. *Trans. Amer. Math. Soc. 186* (1973), 481–488.

[39] Lorenz, E. N. Deterministic nonperiodic flow. *J. Atmos. Sci. 20*, 2 (1963), 130–141.

[40] Lyubich, M., and Martens, M. *Renormalization of Hénon Maps*. Springer Berlin Heidelberg, 2011, pp. 597–618. DYNA 2008, in Honor of Maurício Peixoto and David Rand, University of Minho, Braga, Portugal, September 8-12, 2008.

[41] Mañé, R. A proof of the C^1 stability conjecture. *Publications Mathématiques de l'IHÉS 66* (1987), 161–210.

[42] Marqués-Lobeiras, A., Pumariño, A., Rodríguez, J. Á., and Vigil, E. Strictly invariant sets for 2-D tent maps: 2-D strange attractors. *Bulletin of the Brazilian Mathematical Society, New Series 54*, 10 (Mar. 2022).

[43] Marqués-Lobeiras, A., Pumariño, A., Rodríguez, J. Á., and Vigil, E. Splitting and coexistence of 2-D strange attractors in a general family of expanding baker maps. *Nonlinearity 36*, 8 (2023).

[44] Mora, L., and Viana, M. Abundance of strange attractors. *Acta Math. 171*, 1 (1993), 1–71.

[45] Newhouse, S. Diffeomorphisms with infinitely many sinks. *Topology 13*, 1 (1974), 9–18.

[46] Newhouse, S. The abundance of wild hyperbolic sets and non-smooth stable sets for diffeomorphisms. *Publications Mathématiques de l'IHÉS 50* (1979), 101–151.

[47] Palis, J., and De Melo, W. *Geometric theory of dynamical systems: an introduction*. Cambridge University Press, 1993.

[48] Palis, J., and Takens, F. *Hyperbolicity and sensitive chaotic dynamics at homoclinic bifurcations*. Cambridge University Press, 1993.

[49] Palis, J., and Yoccoz, J.-C. Homoclinic tangencies for hyperbolic sets of large Hausdorff dimension. *Acta Math. 172*, 1 (Mar. 1994), 91–136.

[50] Parry, W. Symbolic dynamics and transformations of the unit interval. *Trans. AMS 122* (1966), 368–378.

[51] Poincaré, H. Sur le problème des trois corps et les équations de la dynamique. *Acta Math. 13* (1890), 1–270.

[52] Pumariño, A., and Rodríguez, J. Á. *Coexistence and persistence of strange attractors*, vol. 1658 of *Lecture notes in mathematics*. Springer-Verlag, 1997.

[53] Pumariño, A., and Rodríguez, J. Á. Coexistence and persistence of infinitely many strange attractors. *Ergod. Theory Dyn. Syst. 21*, 5 (Oct. 2001), 1511–1523.

[54] Pumariño, A., Rodríguez, J. Á., Tatjer, J. C., and Vigil, E. Piecewise Linear Bidimensional Maps as Models of Return Maps for 3D Diffeomorphisms. In *Progress and Challenges in Dynamical Systems* (2013), Springer Proceedings in Mathematics & Statistics, Springer Berlin Heidelberg, pp. 351–366. Proceedings of the International Conference Dynamical Systems: 100 Years after Poincaré, September 2012, Gijón, Spain.

[55] Pumariño, A., Rodríguez, J. Á., Tatjer, J. C., and Vigil, E. Expanding baker maps as models for the dynamics emerging from 3D-homoclinic bifurcations. *Discrete Continuous Dyn. Syst. Ser. B 19*, 2 (Mar. 2014), 523–541.

[56] Pumariño, A., Rodríguez, J. Á., Tatjer, J. C., and Vigil, E. Chaotic dynamics for two-dimensional tent maps. *Nonlinearity 28*, 2 (Jan. 2015), 407–434.

[57] Pumariño, A., Rodríguez, J. Á., and Vigil, E. Renormalizable expanding baker maps: coexistence of strange attractors. *Discrete Continuous Dyn. Syst. Ser. A 37*, 3 (Mar. 2017), 523–550.

[58] Pumariño, A., Rodríguez, J. Á., and Vigil, E. Renormalization of two-dimensional piecewise linear maps: abundance of 2D strange attractors. *Discrete Continuous Dyn. Syst. Ser. A 38*, 2 (Feb. 2018), 941–966.

[59] Pumariño, A., Rodríguez, J. Á., and Vigil, E. Persistent two-dimensional strange attractors for a two-parameter family of Expanding Baker Maps. *Discrete Continuous Dyn. Syst. Ser. B 24*, 2 (Feb. 2019), 657–670.

[60] Pumariño, A., and Tatjer, J. C. Dynamics near homoclinic bifurcations of three-dimensional dissipative diffeomorphisms. *Nonlinearity 19*, 12 (Nov. 2006), 2833–2852.

[61] Pumariño, A., and Tatjer, J. C. Attractors for return maps near homoclinic tangencies of three-dimensional dissipative diffeomorphisms. *Discrete Continuous Dyn. Syst. Ser. B 8*, 4 (Nov. 2007), 971–1005.

[62] Rodrigues, A. Strange attractors and wandering domains near a homoclinic cycle to a bifocus. *J. Diff. Eq. 269*, 4 (2020), 3221–3258.

[63] Ruelle, D., and Takens, F. On the nature of turbulence. *Comm. Math. Phys. 20* (1971), 167–192.

[64] Saussol, B. Absolutely continuous invariant measures for multidimensional expanding maps. *Isr. J. Math. 116* (2000), 223–248.

[65] Smale, S. Diffeomorphisms with many periodic points. In *Differential and Combinatorial Topology: A Symposium in Honor of Marston Morse*, S. S. Cairns, Ed. Princeton University Press, 1965, pp. 63–80.

[66] Smale, S. Differentiable dynamical systems. *Bull. Am. Math. Soc. 73*, 6 (1967), 747–817.

[67] Tatjer, J. C. Three-dimensional dissipative diffeomorphisms with homoclinic tangencies. *Ergod. Theory Dyn. Syst. 21*, 1 (Feb. 2001), 249–302.

[68] Tsujii, M. Absolutely continuous invariant measures for expanding piecewise linear maps. *Invent. Math. 143* (2001), 349–373.

[69] Viana, M. Strange attractors in higher dimensions. *Bull. Braz. Math. Soc. 24* (1993), 13–62.

[70] Yorke, J. A., and Alligood, K. T. Cascades of period-doubling bifurcations: A prerequisite for horseshoes. *Bull. Am. Math. Soc. 9*, 3 (Nov. 1983), 319–322.